Symposium on Magnetism and Spintronics

SMS-2021

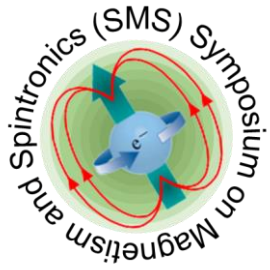

November 25-27, 2021

Abstract Book

Organized by

National Institute of Science Education and Research (NISER), Bhubaneswar

COMMITTE

Patrons

- Prof. Sudhakar Panda, Director, NISER, India
- Prof. Karuna Kar Nanda, Director, IOP, India

Convener

- Dr. Subhankar Bedanta, NISER, India

Core Committee

- Dr. Perumal Alagarsamy, IIT Guwahati, India
- Prof. Anjan Barman, SNBNCBS, India
- Dr. Subhankar Bedanta, NISER, India
- Prof. P. S. Anil Kumar, IISc, India
- Prof. Pranaba Kishor Muduli, IIT Delhi, India
- Dr. Chandrasekhar Murapaka, IIT Hyderabad, India
- Prof. Ashwin Tulapurkar, IIT Bombay, India

Local Organizing committee

- Dr. V. Ravi Chandra, NISER, India
- Dr. Ashok Mohapatra, NISER, India
- Dr. Niharika Mohapatra, IIT Bhubaneswar, India
- Dr. Ashis Kumar Nandy, NISER, India
- Dr. Ajaya Kumar Nayak, NISER, India
- Dr. Shovon Pal, NISER, India
- Dr. Kush Saha, NISER, India
- Dr. Pratap Kumar Sahoo, NISER, India
- Dr. Debakanta Samal, IOP, India
- Dr. Satyaprasad P Senanayak, NISER, India
- Dr. Kartikeswar Senapati, NISER, India
- Dr. Braj Bhusan Singh, NISER, India

Program at a glance

Time slot (IST)	25.11.2021 (Thursday)		26.11.2021 (Friday)		27.11.2021 (Saturday)	
2.00 pm	Inauguration		**Session IV** Session chair Debakanta Samal	Thomas Brueckel	**Session VIII** Session chair Sanjay Singh	Takeshi Seki
2.30pm	**Session I** Session chair Saurav Giri	Wolfgang Kleemann		Tanusri Saha Dasgupta		Susana Cardoso
3.00pm		Anjan Barman		Kalobaran Maiti		V. Chandrasekhar
3.30pm		Del Atkinson		Kalpataru Pradhan		J. Arout Chelvane
4.00pm		Haifeng Ding		E. V. Sampathkumaran		Yixi Su
4.30pm	BREAK		BREAK		BREAK	
5.00pm	**Session II** Session chair Indranil Sarkar	Niru Chowdhury	**Session V** Session chair Chandrasekhar Murapaka	Poster session-I	**Session IX** Session chairs Vivek Mallick Ashis Nandy	Poster Session-II
		Sagarika Nayak				
5.30pm		Mona M M Bhukta				
		Gajanan Pradhan				
6.00pm		Bandapelli Ravi Kumar	**Session VI** Session chair Suvankar Chakraverty	Andrzej Maziewski	**Session X** Session chair Saswati Barman	P.S. Anil Kumar
		V. Thiruvengadam				
6.30pm		Debajyoti De		Stanislas Rohart		Perumal Alagarsamy
		Adyashakti Dash				
7.00pm		Aditya Kumar		Sabine Puetter		Saibal Basu
7.30pm	BREAK		BREAK		BREAK	
8.00pm	**Session III** Session chair Bedangadas Mohanty	Sougata Mallick	**Session VII** Session chair Subham Majumdar	Antonio Azevedo	**Session XI** Session chair Subhankar Bedanta	Ashwin Tulapurkar
		Srijani Mallik				
8.30pm		Aroop K. Behera		Dipankar Das Sarma		General Discussion and Concluding session
		Swapna Sindhu Mishra				
9.00pm		Biswajit Sahoo		Pranaba K. Muduli		

N.B: Program starts at 2.00 PM IST i.e. 9.30 AM CET

Inauguration details

- Welcome address by Dr. Subhankar Bedanta, Convenor, Symposium on Magnetism and Spintronics (SMS-2021).
- Address by Prof. Sudhakar Panda, Director, National Institute of Science Education and Research, Bhubaneswar.
- Address by Prof. Karuna Kar Nanda, Director, Institute of Physics, Bhubaneswar.
- Address by Prof. Bedangadas Mohanty, Dean of Faculty Affairs, National Institute of Science Education and Research, Bhubaneswar.
- Address by Prof. Wolfgang Kleemann, Emeritus Professor, University of Duisburg-Essen, Germany.
- Vote of thanks by Prof. Anjan Barman, Core-committee member SMS-1, S N Bose National Centre for Basic Sciences, India.

Invited Speakers

S. No.	Speaker Name	Address	Abstract Title
1	Prof. Wolfgang Kleemann	Univ. Dui.-Essen, Germany	Universal domain wall dynamics in disorderedferroic materials
2	Prof. Anjan Barman	SNBNCBS, India	Emergent Phenomena in Nanoscale Magnonics
3	Prof. Del Atkinson	Durham Univ., UK	Ferromagnetic/non-magnetic multi-layered systems: Understanding damping, spin transport and the roleof proximity induced magnetism
4	Prof. Haifeng Ding	Nanjing Univ., China	Evidence of the inverse Rashba-Edelstein effect inheavy metal/Cu interfaces
5	Prof. Thomas Brueckel	JCNS, Germany	Addressing the climate crisis: How can magnetismcontribute?
6	Prof. Tanusri Saha Dasgupta	IACS, India	Designing 2D Ferromagnetism
7	Prof. Kalobaran Maiti	TIFR Mumbai, India	Antiferromagnetism in a topological Kondo system,SmBi
8	Prof. Kalpataru Pradhan	SINP, Kolkata	Carrier-mediated inverted hysteresis and exchangebias in FM/FM heterostructures
9	Prof. E. V. Sampathkumaran	TIFR Mumbai, India	Unexpected Kondo-like anomalies and topological Hall effect features reported for heavy rare-earthsystems since 1990s
10	Prof. Andrzej Maziewski	TIFR Mumbai, India	Engineering of magnetic ordering and magneto-optical properties in ultrathinfilms
11	Prof. Stanislas Rohart	Univ. Paris-sud, France	Time response and maximum velocity of skyrmions in antiferromagnets
12	Dr. Sabine Puetter	JCNS, Germany	Thin film fabrication for users: Possibilities andperspectives
13	Prof. Antonio Azevedo	UFPE, Brazil	Interface-driven spintronic phenomena
14	Prof. Dipankar Das Sarma	IISc, India	Dynamically disordered magnetic state at sub-Kregime in a strongly interacting system
15	Prof. Pranaba K. Muduli	IIT Delhi, India	Ultrafast nucleation of single and multiple antiferromagnetic skyrmions
16	Prof. Takeshi Seki	IMR, Japan	Spin-Charge Conversion in Ferromagnetic Materials
17	Prof. Susana Cardoso	INESC MN, Portugal	To be updated soon
18	Prof. V. Chandrasekhar	TIFR Hyderabad, India	Homo- and heterometallic lanthanide complexes as aSingle-ion/Single-molecule Magnets
19	Prof. J. Arout Chelvane	DMRL, India	Processing and Characterization of Magnetostrictive Materials
20	Dr. Yixi Su	JCNS, Germany	Topology meets correlations: neutron scattering fromcorrelated topological materials
21	Prof. P.S. Anil Kumar	IISc, India	Enhancing the spin-orbit torque efficiency in Pt/CoFeB/Pt based perpendicularly magnetized system
22	Prof. Perumal Alagarsamy	IIT Guwahati, India	Ferromagnetic nanocomposites: the preparation using mechanochemical synthesis and the explorationtowards energy harvesting
23	Prof. Saibal Basu	BARC, India	Characterization of Interface Properties in Ultra-thinfilms: Pathway to Novel Magnetism
24	Prof. Ashwin Tulapurkar	IIT Bombay, India	Charge current generation from oscillating magnetization via the inverse of voltage-controlled magnetic anisotropy effect

Contributory Speakers

S. No.	Name	Address	Abstract title
1	Dr. Niru Chowdhury	IIT, Delhi	Formation of 360° domain walls in magnetic thin films with uniaxial and random anisotropy
2	Dr. Sagarika Nayak	NISER, Bhubaneswar	Role of spin-glass like frustration on exchange bias effect in $Fe/Ir_{20}Mn_{80}$ and $Ni_{50}Mn_{50}/Co_{40}Fe_{40}B_{20}$ bilayers
3	Ms. Mona M M Bhukta	Johannes Gutenberg University, Germany	Degenerate skyrmionic states in synthetic antiferromagnets
4	Mr. Gajanan Pradhan	INRIM, Italy	Effect of random anisotropy in stabilization of skyrmions and antiskyrmions
5	Dr. V. Thiruvengadam	NISER, Bhubaneswar	Effect of MoS_2 on magnetization reversal, magnetic domain structures and anisotropy of MoS_2/CoFeB heterostructures
6	Dr. Debajyoti De	Sukumar Sengupta Mahavidyalaya, West Bengal	Origin of exchange bias in nanocrystalline $CoCr_2O_4$
7	Ms. Adyashakti Dash	NISER, Bhubaneswar	Device geometry dependent deterministic skyrmion generation from a skyrmionium
8	Mr. Aditya Kumar	University of Mainz, Germany	Spin pumping with low spin orbit coupling material C_{60} in a $La_{0.67}Sr_{0.33}MnO_3/C_{60}$ system
9	Dr. Sougata Mallick	Université Paris-Saclay, France	Deterministic nucleation and efficient motion of skyrmions
10	Dr. Srijani Mallik	Université Paris-Saclay, France	Metal/$SrTiO_3$ and $KTaO_3$ two-dimensional electron gases for spin-to-charge conversion
11	Mr. Aroop K. Behera	Kansas State University, USA	Two-dimensional Heterostructure Field Effect Transistors with One-Dimensional electrical contacts leading to enhanced electrical performance and Ultra-Low Noise
12	Mr. Swapna Sindhu Mishra	Michigan State University, Michigan	Josephson junctions containing Ni/Ru/Ni synthetic antiferromagnets
13	Mr. Biswajit Sahoo	University of California, San Diego	Efficient charge to spin conversion in 5d transition metal oxide
14	Dr. Bandapelli Ravi Kumar	IISC, Bangalore	Effect of thermal annealing on the interfacial Dzyaloshinskii-Moriya interaction in perpendicularly magnetized Ta/Pt/CoFeB/Pt ultrathin films

Poster Session I

26.11.2021 (Friday): 5.00 – 6.00 PM (IST)

Poster ID	Author	Address	Abstract Title	FRAME room no. for poster presentation	Poster location
P01	Dr Shivesh Yadav	TIFR, Mumbai	Epitaxial growth, electrical, and magnetic properties of Mn_2PtPd thin films	01	A
P02	Mr S. Alaguraja	Thiagarajar College, Madurai	Structural, Optical And Electrical Properties Of Cadmium Sulfide Thinfilms For Photo Sensing Application	01	I
P03	Mr Sarathbavan Murugan	SRM Institute of Science and Technology, Chennai	Magnetic and piezoelectric properties of $NiFe_2O_4$ (NFO) and NFO/$Na_{0.5}Bi_{0.5}TiO_3$ (NBTO) Bi-layer films prepared by rf magnetron sputtering with different time duration at constant temperature with different substrates (Si (100) and Al_2O_3)	01	D
P04	Dr Rajkumar Modak	NIMS, Tsukuba	Combinatorial investigation of Sm-Co-based amorphous alloy films for zero-field transverse thermoelectric generation	01	L
P05	Mr Bibekananda Das	IIT, Madras	Asymmetric Spin-Transport at the Interfaces of Nanoscale Oxide Heterostructures	02	A
P06	Ms Sanjukta Jena	Central University of South Bihar, Gaya	Magnetic and electronic states of Mn and Co atoms at $Co_2Mn_{1.20}Ge_{0.38}$/MgO interfaces seen via soft x-ray magnetic circular dichroism	02	I
P07	Ms Tejaswini Chandrakant Gawade	CSIR-National Aerospace Laboratories, Bangalore	IrMn based Synthetic Antiferromagnetic Spin Valve with Thermal Stability	02	D
P08	Dr Haichour Amel	National Polytechnic School of Oran ENPO, Oran	Study of structural and optical properties of nickel oxide thin films	02	L
P09	Dr Harinath Aireddy	Alliance University Bangalore, Bangalore	Optical double cantilever beam magnetometer for electric field induced magnetization measurements	03	A
P10	Ms Aradhana Kumari	Central University of South Bihar, Gaya	Probing structural and electronic behaviour of pristine and Cr Doped VO_2 Thin Films	03	I
P11	Mr Mufeeduzzaman	Central University of South Bihar, Gaya	Effect of Cr doping on structural and magnetic properties of VO_2 thin films: Soft X-ray Magnetic Circular Dichroism Study	03	D
P12	Dr Ganesh Ji Omar	National University of Singapore, Singapore	Large Rashba Spin-Orbit Effect by Orbital Engineering at $SrTiO_3$–based Correlated Interfaces	03	L

P14	Mr Mainur Rahaman	University of Hyderabad, Hyderabad	Ferromagnetic resonance study of $Co_2Fe_{0.5}Ti_{0.5}Si$ thin films	04	I
P15	Mr Lanuakum A Longchar	University of Hyderabad, Hyderabad	Electrical- and magneto-transport in $Co_2FeAl_{0.5}Si_{0.5}$ thin films with varying degree of B2 crystallographic order	04	D
P16	Ms Dola Chakrabartty	NISER, Bhubaneswar	Room temperature skyrmion lattice in a hexagonal centrosymmetric kagome magnet	04	L
P17	Mr Brindaban Ojha	NISER, Bhubaneswar	Driving skyrmions with low threshold current density in Pt/CoFeB thin film	05	A
P18	Mr Azam Ali Khan	RRCAT, HBNI, Indore	Magnetoelectric properties of $NiFe_2O_4/SrRuO_3$/PMN-PT heterostructures	05	I
P19	Mr Bibhuti Bhusan Jena	NISER, Bhubaneswar	Magnetic coupling across CoO-NiO interface studied by LEED	05	D
P20	Mr Pushpendra Gupta	NISER, Bhubaneswar	Simultaneous observation of anti-damping and inverse spin Hall effect in $La_{0.67}Sr_{0.33}MnO_3$/Pt bilayers system	05	L
P21	Mr Koustuv Roy	NISER, Bhubaneswar	Spin pumping and inverse spin Hall effect study in CoFeB/ IrMn bilayers	06	A
P22	Ms Sonia Kaushik	UGC-DAE CSR, Indore	Interface selective study in Fe /^{57}Fe / C_{60} bilayer by placing ^{57}Fe marker at the interface; interface selectivity under x-ray standing wave condition	06	I
P23	Dr Anupama Swain	NISER, Bhubaneswar	Magnetization Reversal in Fe/$BaTiO_3$(110) Heterostructured Multiferroics	06	D
P24	Mr Shaktiranjan Mohanty	NISER, Bhubaneswar	Effect of Ir spacer layer on perpendicular synthetic antiferromagnetic coupling in Co/Pt multilayers	06	L
P25	Ms Esita Pandey	NISER, Bhubaneswar	Tailoring Dzyaloshinskii-Moriya interaction and domain wall dynamics in Pd/Co/C_{60}/Pd	07	A
P26	Mr Mohammed Azharudheen N	NISER, Bhubaneswar	Study of the phase stabilization and spin to charge conversion in $Co_{40}Fe_{40}B_{20}/MoTe_2$	07	I
P27	Ms Susree Sucharita Mohapatra	NISER, Bhubaneswar	Skyrmion Hall Effect in synthetic ferrimagnet	07	D
P28	Mr Abhisek Mishra	NISER, Bhubaneswar	Inverse spin Hall effect in sputter deposited MoS_2/CoFeB bilayers	07	L
P29	Ms Purbasha Sharangi	NISER, Bhubaneswar	Spinterface-Induced Modification in Magnetic Properties in $Co_{40}Fe_{40}B_{20}$/Fullerene Bilayers	08	A
P30	Mr Ujjawal Rathore	IIT, Delhi	Self-Modulation in nano-constriction based spin Hall nano-oscillators	08	I
P31	Mr Himanshu Bangar	IIT, Delhi	Large area growth of 2D-GeTe thin films using pulsed laser deposition for spintronics application	08	D
P32	Ms Swayang Priya Mahanta	NISER, Bhubaneswar	Tuning of magnetic properties by the formation of spinterface in CoFeB/Alq3 system	08	L

P33	Mr C Raghavendar	Pondicherry University, Puducherry	Effect of magnetostrictive strain upon the electronic transport in poly vinylidene fluoride thin films across Cu/PVDF/CoFe capacitor structures	09	A
P34	Mr Pankaj Pathak	IIT, Delhi	Voltage-controlled, deterministic domain wall rotation in asymmetric nanomagnetic ring structures for manipulating trapped magnetic nanoparticles in fluidic medium	09	I
P35	Dr. Ritwik Mondal	IOP the Czech Academy of Sciences, Prague	Spin pumping at terahertz nutation resonances	09	D
P36	Mr. K Sriram	IIT, Hyderabad	Effect of seed layer thickness on Ta crystalline phase and spin Hall angle	09	L
P37	Mr. Bibekananda Paikaray	IIT, Hyderabad	Skyrmion Dynamics in Nanodisk, Concentric and Eccentric Nano-Ring Structures	10	A
P38	Mr. Shekhar Tyagi	IIT Roorkee	Strain Driven Magnetic Properties in Epitaxial Layers of Site-Ordered Double Perovskite Pr_2NiMnO_6	10	I
P39	Mr. Manoj Talluri	IIT, Hyderabad	Giant Spin Pumping at Ferromagnet (Permalloy) - Organic Semiconductor (Perylene diimide) Interface	10	D

Poster Session II

27.11.2021 (Saturday): 5.00 – 6.00 PM (IST)

Poster ID	Author	Address	Abstract Title	FRAME room no. for poster presentation	Poster location
P40	Dr Venkatraj A	Dr. N.G.P. Institute of Technology, Coimbatore	Thermal stability and enhanced electrical properties of $Pb(Mg_{1/3}Nb_{2/3})O_3$ - $Pb(Yb_{1/2}Nb_{1/2})O_3$ - $PbTiO_3$ piezoelectric ceramic	11	A
P41	Mr V. Aravindan	Thiagarajar College, Madurai	Effect of Spin Orbit Coupling in Mn_2CoSb Inverse Heusler Alloy for Spintronics	11	I
P42	Mr Yaseen Ahmad	University of Jammu, Jammu	Synthesis and characterization of pure and doped spinel manganese ferrites	11	D
P43	Mrs Sonali Thakur	University of Jammu, Jammu	Studies on preparation, structural and magnetic properties of some barium strontium titanate - strontium nickel hexaferrite multiferroic composites	11	L
P44	Mr Soumalya Roy	IITRAM, Ahmedabad	Syntheses, Structures, and Magnetic Properties of Pentanuclear Spirocyclic Ni_4Ln Derivative: Field Induced Slow Magnetic Relaxation by Dysprosium and Erbium Analogue	12	A
P45	Mr Mohd Abushad	Aligarh Muslim University, Aligarh	Influence of Cr^{3+} ions on the physical properties of anatase TiO_2 nanostructures	12	I
P46	Dr Shyam Khobraji Gore	Dnyanopasak Shikshan Mandals ACS College, Jintur	Synthesis, Structural and Dielectric properties of Cobalt Bismuth Ferrite	12	D
P47	Ms K Pushpanjali Patra	IIT, Guwahati	Re-entrant Spin Glass Behavior in Frustrated Double Perovskite Ho_2CoMnO_6 Nanorod	12	L
P48	Ms Fouzia Khan	IGCAR, Kancheepuram	Synthesis, characterization and magnetic hyperthermia properties of fatty acid coated Fe_3O_4 magnetic nanoparticles	13	A
P49	Ms Manjari Shukla	IIT, BHU	Structural, magnetic and optical studies of Spin-Disordered $Ho_2Ge_xTi_{2-x}O_7$ system	13	I
P50	Ms Srujana Mahendravada	IGCAR, Kalpakkam	Comparison between energy minimization and curve fitting approaches for simulating isothermal DC magnetization curves for a Stoner-Wohlfarth particle	13	D
P51	Dr Manikandan Dhamodaran	IISC, Bangalore	Origin and Control of Room Temperature Ferromagnetism in Fe and Mn co-doped In_2O_3 Nanocubes	13	L
P52	Dr Tribedi Bora	NIT Meghalaya	Effect on magnetization reversal by substituting magnetic and non magnetic rare earth element in orthochromite	14	A

P53	Ms Riya Dawn	Central University of South Bihar,Gaya	Origin of Magnetization in Magnetic Beads Based on Fe_3O_4 Nanoparticles for Biomedical Applications via Soft X-Ray Circular Dichorism Study	14	I
P54	Mr Soham Chandra	Presidency University Kolkata	Magnetic Response of Ising Spin-1/2 Trilayered Ferrimagnet driven by Gaussian Random External Magnetic Field with Spatio-Temporal Variation	14	D
P55	Mr Ritupan Borah	IIT, Guwahati	Structural and Magnetic Characterization of Mn Doped Ni-Co Spinel Ferrite Nanoparticles with Surface Spin Disorder	14	L
P56	Mr Lalrinkima	Mizoram University, Aizawl	Electronic, structural and vibrational properties of inverse Fe_2IrSi: A DFT+U study	15	A
P57	Mr Suman Guchhait	IIT Kharagpur	The study of in-plane and out-of-plane magnetostrictive stress for $CoFe_2O_4$/Si composite	15	I
P58	Mr Rajnikant	IIT - BHU, Varanasi	Electronic structure calculation of $DyVO_4$	15	D
P60	Dr Mamatha D Daivajna	MIT Bengaluru	Study of Effect of Bi^{3+} Concentration and Particle Size Reduction on the Structural and Magnetic Properties of $Pr_{0.6}Sr_{0.4}MnO_3$	16	A
P61	Mr Naveen Kumar R	VIT, Vellore	Structural and thermal studies of Fe_2MnSn Heusler alloys	16	I
P62	Ms Rachana Sain	IIT - BHU, Varanasi	Effect of Polymorphous Transformation of Dy doped Sm_2O_3 Nanoparticles from Cubic to Monoclinic phase on the Optical Properties	16	D
P63	Ms Sikha Sarmah	NIT Meghalaya	A Comparative study on the inter-relation between Structural, Magnetic and Dielectric Properties of Cobalt Ferrites on a low and high concentration of Magnesium Substitution	16	L
P64	Ms Shalini Verma	IIT, Guwahati	Tuning of Electrical and Magnetic properties of Samarium iron garnet by Holmium substitution	17	A
P65	Mrs Tania Chatterjee	CSIR- CGCRI, Kolkata	Nonmonotonic magneto electric coupling in reduced-graphene-oxide-$BiFeO_3$ nano composite	17	I
P66	Dr Kapil Yeshwant Salkar	Dhempe College of Arts and Science, Goa	Electrical properties of $In_{(2-x)}Nd_xO_3$ dilute magnetic semiconductor nanoparticles	17	D
P67	Dr Rajeswari Roy Chowdhury	IISER Bhopal	Unconventional Hall effect and its modification in 2D van der Waals ferromagnet Fe_3GeTe_2	17	L
P68	Dr Pavan Venu Prakash Madduri	IIITDM Kurnool	Intrinsic and field-induced magnetic ordering in Ni_5Al_3/NiO nanoparticle compacts	18	A
P69	Mr Bimalesh Giri	NISER, Bhubaneswar	Evolution of antiskyrmion phase in tetragonal ferrimagnetic Heusler Mn-Pt(Pd)-Sn-In system	18	I
P70	Mr Charanpreet Singh	NISER, Bhubaneswar	Dual magnetic order and corresponding large anomalous Hall response in a Kagome magnet	18	D
P71	Ms Suchandra Goswami	The Neotia University, West Bengal	Ni grafted RGO - a nanocomposite with tunable magnetic properties	18	L

P72	Ms Smrutirekha Hota	SOA University, Bhubaneswar	Electronic structure and magnetic properties of iron selenide KFe_2Se_2: A first principle study	19	A
P73	Dr Manoj Kumar Singh	University of Allahabad, Prayagraj	Structural, Magneto-dielectric properties of $0.9BiFeO_3$-0.1 $CaTiO_3$ nanocomposite	19	I
P74	Mr SK Jamaluddin	NISER, Bhubaneswar	Tuning the anomalous Hall effect in MnPt(Ir)Sn Heusler system	19	D
P75	Mrs Bushra Khan	University of Allahabad, Prayagraj	Structural, Multiferroic and Magneto-Impedance Characteristic of $KBiFe_2O_5$	19	L
P76	Ms Preeti Yadav	University of Allahabad, Prayagraj	Structural and optical properties of $Bi_{1-x}Ca_xFeO_3$ nanoparticles synthesized by sol-gel method	20	A
P77	Ms Arushi Pandey	University of Allahabad, Prayagraj	Structural properties of the hydrothermally synthesized multifunctional CZTS nanoparticles	20	I
P78	Mr Aminur Rahaman	Yogoda Satsanga Palpara Mahavidyalaya, Palpara	**Tetramer orbital-ordering induced lattice-chirality in ferrimagnetic, polar $MnTi_2O_4$**	**20**	D
P79	Mr Mukesh Suthar	IIT - BHU, Varanasi	Structural and magnetic properties of aluminium doped Y-type barium hexaferrites	20	L
P80	Mr Sebin Joseph Sebastian	IISER Thiruvananthapuram	Quasi-one-dimensional magnetism in the spin-1/2 antiferromagnet $BaNa_2Cu(VO_4)_2$	21	A
P81	Mr Prashant Kumar	CSIR-National Physical Laboratory, New Delhi	Enhanced static and spin dynamic magnetic properties of annealed $CoFe_2O_4$ nanoparticles	21	I
P82	Mr Ajay Kumar	IIT Delhi	A correlation between the structural and magnetic properties of $Sr_{2-x}La_xCoNbO_6$	21	D
P83	Mr Malaya Kumar Sahoo	NISER, Bhubaneswar	Synthesis, Crystal Structure and Magnetic Properties of a new series of Cobalt-Iron Bimetallic Hybrid-Framework	21	L
P84	Dr. Mohmad Asif Khan	Govt Degree College for Women, Anantnag	Comparative Study of magnetic Properties of Ni doped Nd Orthoferrites	22	A
P85	Mr. Gaurav Kumar Shukla	IIT, BHU	Anomalous Hall effect from gapped nodal line in the Co_2FeGe Heusler compound	22	I
P86	Naushad Ahmed	IIT, Hyderabad	Experimental and Theoretical Insights into the Magnetic Exchange, Geometry and Electronic Structure Affecting the Slow-Magnetic Relaxation Behaviours of 3d, 4f and 3d-4f Based Molecular Magnets	22	D

FRAME LINK

Room links for virtual Interaction with speakers

Room 1: https://framevr.io/sms-virtual-room-01

Room 2: https://framevr.io/sms-virtual-room-02

Room 3: https://framevr.io/sms-virtual-room-03

Room links for posters

Room No.	Link
01	https://framevr.io/sms-room-01
02	https://framevr.io/sms-room-02
03	https://framevr.io/sms-room-03
04	https://framevr.io/sms-room-04
05	https://framevr.io/sms-room-05
06	https://framevr.io/sms-room-06
07	https://framevr.io/sms-room-07
08	https://framevr.io/sms-room-08
09	https://framevr.io/sms-room-09
10	https://framevr.io/sms-room-10
11	https://framevr.io/sms-room-11
12	https://framevr.io/sms-room-12
13	https://framevr.io/sms-room-13
14	https://framevr.io/sms-room-14
15	https://framevr.io/sms-room-15
16	https://framevr.io/sms-room-16
17	https://framevr.io/sms-room-17
18	https://framevr.io/sms-room-18
19	https://framevr.io/sms-room-19
20	https://framevr.io/sms-room-20
21	https://framevr.io/sms-room-21
22	https://framevr.io/sms-room-22

Zoom meeting Details

Day 1
Join Zoom Meeting
https://us06web.zoom.us/j/97197251120?pwd=a3Axbk81a2RLNWI2M0NMZFkwaEdEZz09
Meeting ID: 971 9725 1120
Passcode: xqTX7w
Youtube link: https://youtu.be/1C0WPj05cCM

Day 2
Join Zoom Meeting
https://us06web.zoom.us/j/81540010882?pwd=VGRNTG03cnA3MVVuWHBPcEJtN2l0Zz09
Meeting ID: 815 4001 0882
Passcode: 826610
Youtube link: https://youtu.be/5Zeb6wYRAv8

Day 3
Join Zoom Meeting
https://us06web.zoom.us/j/88411349624?pwd=S3lnNjJBWGk4ZWR5cVc2UTFZMWRkZz09
Meeting ID: 884 1134 9624
Passcode: 162419
Youtube link: https://youtu.be/zCdErZeabs8

For any kind of assistant during poster session and virtual interaction feel free to reach out to the following volunteers:
1. Swayang- +919861396365
2. Kshitij - +918946880021

For any kind of assistant during the seminars please feel free to contact in following numbers:
1. Dr. Subhankar Bedanta - +919438057896
2. Abhisek - +917008331149
3. Shaktiranjan - +917978635925

IT01

Universal domain wall dynamics in disordered ferroic materials

Wolfgang Kleemann
Angewandte Physik, Universität Duisburg-Essen, Germany
wolfgang.kleemann@uni-due.de

Abstract: The occurrence of universal dynamic modes of domain walls in disordered ferroic materials is reviewed on ferromagnetic (multi)layers [$(CoFe/Al_2O_3)_{10}$, Pt/Co/Pt] and ferroelectric crystals [$KTiOPO_4$, $Sr_{0.61}Ba_{0.39}Nb_2O_6$:$Ce^{3+}$]. Based on the model of rough domain walls in a random medium [1] three dynamic phase transitions, *viz.* relaxation ↔ creep ↔ slide ↔ switch, are observed at different field amplitudes with increasing order, $h_0 = h_\omega$, h_{t1} and h_{t2} [2], using *ac* susceptibility data.

The *ac* susceptibility of a **superferromagnetic** multilayer **$[Co_{80}Fe_{20}$(1.4 nm)/Al_2O_3(3 nm)$]_{10}$** is measured as a function of temperature, frequency, and field amplitude and compared to static and dynamic hysteresis loops [3]. Its properties are successfully mapped onto the predicted [1] dynamical phase transitions, which link the relaxation (R), creep (C), sliding (SL) and switching regimes (SW) of pinned domain walls (DW) (Fig. 1).

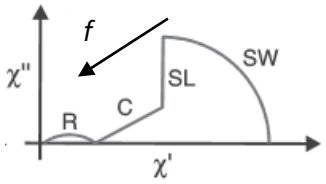

Fig. 1. Schematic Cole-Cole plot of susceptibility components, χ'' *vs.* χ', of randomly pinned DW under *ac* driving fields over a large frequency (f) range [4].

Magnetization reversal in a periodic magnetic field is studied on an ultrathin, ultrasoft **ferromagnetic Pt/Co(0.5nm)/Pt** trilayer exhibiting weak random DW pinning [4]. The DW motion is imaged by polar magneto-optic Kerr effect microscopy and monitored by superconductig quantum interference device spectroscopy (Fig. 2). In close agreement with model predictions, the complex linear *ac* susceptibility corroborates the dynamic DW modes segmental relaxation, creep, slide, and switching.

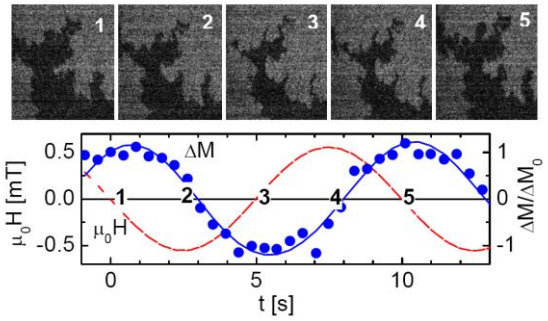

Fig. 2. *P*-MOKE micrographs (0.2 x 0.15 mm^2, upper panel) of a Pt/Co(0.5 nm)/Pt trilayer taken equidistantly with Δt = 2.5 s during one period of an f = 0.1 Hz *ac* field with amplitude $\mu_0 H_0$ = 0.45 mT (lower panel) [4].

Creep and relaxation of domain walls under *ac* electric fields are observed in an ideal model system, **periodically poled $KTiOPO_4$**, to occur in different regimes, which are separated by dynamic phase transitions at frequencies $f_m(T) = f_{m0} \exp(-\Delta E/k_B T)$, with f_{m0} = 3 x 10^9 Hz and ΔE = 0.6 eV [5]. Power law dispersion of the creep susceptibility, $\chi \propto 1 + (i\omega\tau)^{-\beta}$, with $\beta \approx 0.4$, and large non-linearity encountered at $f < f_m$, is contrasted with Cole-Cole-type relaxational dispersion, $\chi \propto (1 + [i\omega\tau]^{1-\alpha})^{-1}$ with $\alpha \approx 0.3$, at $f > f_m$.

The charge-disordered three-dimensional **uniaxial relaxor ferroelectric $Sr_{0.61}Ba_{0.39}Nb_2O_6$** splits up into metastable polar nanoregions (PNR) and paraelectric interfaces above T_c = 337 K [6]. The frozen PNR are verified by piezoresponse force microscopy, respond domain-like to dynamic light scattering and dielectric excitation, reveal nonergodicity at $T > T_c$ via global aging, and coalesce into domains below T_c (Fig.3). Unexpectedly, the percolating system of unperturbed interfaces becomes ferroelectric with two-dimensional Ising-model-like critical exponents α = 0, β = 1/8, and γ = 7/4 as corroborated by calorimetry, second harmonic generation, and susceptometry, respectively [6].

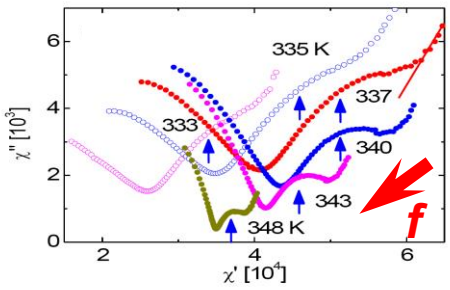

Fig. 3. Relaxation anomalies of both DW and PNR are observed in $Sr_{0.61}Ba_{0.39}Nb_2O_6$:$Ce^{3+}$ as marked by arrows [6]. The straight line at T_c = 337 K denotes a creep-like proportionality $\chi'' \propto \chi' - \chi_\infty$.

REFERENCES

[1] T. Nattermann *et al.*, PRL **87** (2001) 107005.
[2] W. Kleemann, Ann.Rev.Mat.Res. **37(**2007)415.
[3] X. Chen *et al.*, PRL **87** (2001) 137205.
[4] W. Kleemann *et al.*, PRL **99** (2007) 097203.
[5] Th. Braun *et al.*, PRL **94** (2005) 117601.
[6] W. Kleemann *et al.*, PRL **97** (2006) 065702

IT02

Emergent Phenomena in Nanoscale Magnonics

Anjan Barman

Department of Condensed Matter Physics and Material Sciences, S. N. Bose National Centre for Basic Sciences, Salt Lake, Kolkata 700106, India

E-mail address and URL: abarman@bose.res.in, a_barman@yahoo.com; https://ufnml.weebly.com

Magnonics is a rapidly emerging research field which investigates the excitation, propagation, control and detection of spin waves through engineered magnetic media consisting of either passively or actively controlled modulation of magnetic properties. The salient features of magnonics include low energy consumption, easy integrability and compatibility with CMOS structure, reprogrammability, shorter wavelength, smaller device features, anisotropic properties, negative group velocity, non-reciprocity and efficient tunability by various external stimuli. Recently, classical magnonics is merging with quantum effects, *e.g.* spin-orbit coupling, the spin Hall and spin pumping effect, Dzyaloshinskii-Moriya interaction (DMI), superconductivity, nonlinearity, topology, etc. to give rise to exciting new properties and novel functionalities in devices [1,2].

Here, we introduce some of these emerging hybrid phenomena in magnonics. We show strong coupling between acoustic waves (phonons) and magnons in two-phase multiferroic nanomagnets leading towards hybrid magneto-elastic modes, which are starkly different from the spin-wave modes of the system [3]. We further demonstrate resonant amplification of existing spin-wave mode and generation of new magneto-elastic modes in the GHz frequency range by surface acoustic waves [4] in nanomagnet arrays. We, then discuss dynamic dipolar coupling driven strong magnon-magnon coupling in ferromagnetic nanocross elements [5,6]. The coupling strength and cooperativity showed a significant variation with the applied microwave power stimulating the dipolar coupling. Finally, we discuss the development of on-demand magnonic nanochannels in a CoFeB/MgO heterostructure showing voltage controlled magnetic anisotropy (VCMA). By applying desired voltage in patterned nanoscale electrodes on the CoFeB/MgO system, the nanochannels can be switched ‘on’ and ‘off’ at will. The magnon dispersion shows a tunable band gap generating due to magnon-magnon coupling of spin waves propagating through adjacent nanochannels, giving rise to both reprogrammability and reconfigurability in this device [7].

The author gratefully acknowledges funding from Department of Science and Technology, Department of Information Technology and S. N. Bose National Centre for Basic Sciences.

[1] A. Barman et al., Magnetization Dynamics in Nanoscale Magnetic Materials : A Perspective, *J. Appl. Phys.* **128**, 170901 (2020).
[2] A. Barman et al., The 2021 Magnonics Roadmap, *J. Phys. : Cond. Matt.* **33**, 413001 (2021).
[3] S. Mondal et al., *ACS Appl. Mater. Interfaces* **10**, 43970 (2018)
[4] A. De et al., *Nanoscale* **13**, 10016 (2021).
[5] K. Adhikari et al., *Phys. Rev. B* **101**, 054406 (2020).
[6] K. Adhikari et al., *Nanotechnology* **32**, 395706 (2021).
[7] S. Choudhury et al., *Science Advances* **6**, eaba5457 (2020).

IT03

Ferromagnetic/non-magnetic multi-layered systems: Understanding damping, spin transport and the role of proximity induced magnetism

Del Atkinson
Durham University, Department of Physics, Durham, DH1 3LE, UK
Email: del.atkinson@durham.ac.uk

Abstract: Various physical mechanisms in nanomagnetism take place across the interface between magnetic (FM) and non-magnetic heavy metal (HM) thin-film layers. These interactions mediate phenomena that are significant for spintronics applications, such as interfacial anisotropy, Dzyaloshinskii-Moriya interactions (iDMI) and the proximity-induced-magnetization (PIM) of heavy metals. The linkage between interfacial phenomena has been the subject of debate, such as the relationship between DMI and proximity induced magnetisation and the role of PIM in spin transport across FM/HM interfaces.

Understanding interfacial spin transport is key to developing magnetoelectonic devices, however, the details of the model parameters involved are not always clear. Debate has surrounded the determination of values for the spin-diffusion length from spin-pumping analysis and spin-pumping through insulating layers. The focus here is on the relationships between interfacial phenomena and spin-transport across the interface.

In this talk the key parameters are discussed in the context of detailed ferromagnetic resonance-based spin-transport analysis of a variety of structures of both ferromagnetic and heavy metal layers to quantify the spin-transport parameters. This is coupled with structural analysis to understand the details at the interface. Results show enhanced spin-mixing conductance is observed for more closely matched ferromagnet and heavy metal crystal structures, and, significantly, the inclusion of a thickness-dependent spin-diffusion length is needed for better agreement with other methods [3]. The question of tunnelling of spin pumped current through an insulating oxide layer is also discussed and it is shown that the film structure must be understood [4].

Finally, the relationship between proximity-induced magnetism (PIM) at the heavy metal/ferromagnet interface and spin-transport across such interfaces has generated significant debate and is addressed here. Proximity induced magnetism in Pt is introduced with examples from recent work on Pt layered with ferro and ferri-magnetic metallic alloys [1, 2]. Any potential link between Pt PIM and damping/spin-transport was investigated using element specific XMCD and FMR measurements made on the same CoFe/Au/Pt and NiFe/Au/Pt thin film samples with a varying thickness Au spacer layer. A direct relationship was found between the magnitude of Pt PIM and magnitude of damping enhancement in both FM systems [5]. The results demonstrate that electronic hybridization of the heavy metal and ferromagnet is required for a full understanding of damping enhancement and that detais of the interface are critical to understand spin-transport in spintronic devices.

ACKNOWLEDGEMENT

Funding is acknowledged for the UK EPSRC studentships to R. Rowan-Robinson and C. Swindells and a Royal Society Industry Fellowship for DA. We acknowledge beam time and support at the EPSRC XMaS beamline at the ESRF and beamline 4-ID-D at APS.

REFERENCES

[1] Rowan-Robinson R., Stashkevich A.A., Roussigne Y., Belmeguenai M., Cherif S-M, Thiaville A., Hase T.P.A., Hindmarch A.T. & Atkinson D. **nature.com/scientific reports** 7: 16835 (2017)
[2] Swindells C., Nicholson B., Inyang O., Choi Y., Hase T.P.A. & D. Atkinson **Phys. Rev. Res.** 2, 033280 (2020)
[3] Swindells C. ,Hindmarch A.T., Gallant A.J. & Atkinson D. **Phys. Rev. B** 99, 064406 (2019)
[4] Swindells C., Hindmarch A.T., Gallant A.J. &Atkinson D. **Appl. Phys. Letts.** 116, 042403 (2020)
[5] C. Swindells C., Głowi´nski H., Choi Y., Haskel D., Michałowski P., Hase T., ,Ku´swik P. & Atkinson, **Appl. Phys. Letts.** 119, 152401 (2021)

IT04

Evidence of the inverse Rashba-Edelstein effect in heavy metal/Cu interfaces

Rui Yu[1,†], Bingfeng Miao[1, 2,†], Qi Liu[1], Kang He[1], Weishan Xue[3], Liang Sun[1, 2], Mingzhong Wu[4], Yizheng Wu[2,5], Zhe Yuan[3], Haifeng Ding[1, 2,*]

[1]National Laboratory of Solid State Microstructures and Department of Physics, Nanjing University, Nanjing, 210093, P.R. China

[2]Collaborative Innovation Center of Advanced Microstructures, Nanjing, 210093, P.R. China

[3]Center for Advanced Quantum Studies and Department of Physics, Beijing Normal University, Beijing 100875, P.R. China

[4]Department of Physics, Colorado State University, Fort Collins, CO 80523, USA

[5]Department of Physics, Fudan University, 220 Handan Road, Shanghai 200433, P. R. China

[†]These authors contribute equally to this work.

Email: (hfding@nju.edu.cn)

Abstract: Spin charge conversion is the key ingredient of the new generation of spintronics. Spin Hall effect (SHE), Rashba-Edelstein effect (REE) and their inverse effects are the essential mechanisms for the spin-charge conversion. In contrast to the well-studied SHE-related spin-charge conversion, REE-induced spin-charge conversion remains in debate especially in metallic systems [1-3]. In this talk, we will present the observation of the direct evidence of the inverse-REE in heavy metal/Cu interfaces with two independent measurement techniques. The spin-charge conversion of heavy metal/Cu reverses its sign upon flipping their stacking order at ultra-thin heavy metal thickness but have the same sign at higher thickness. The experimental findings are supported by first principle calculations which show Rashba-band splitting near the Fermi level. We further develop a method to estimate the amplitude of the inverse-REE effect [4].

ACKNOWLEDGEMENT

This work was supported by the National Key R&D Program of China (Grant No. 2017YFA0303202 and 2018YFA0306004), the National Natural Science Foundation of China (Grants No. 11734006, No. 11974165, No. 51971110, No. 11727808, and No. 61774018), and the Natural Science Foundation of Jiangsu Province (Grant No. BK20190057). Work at CSU was supported by the U.S. National Science Foundation under Grants No. EFMA-1641989 and No. ECCS-1915849.

REFERENCES

[1]. R. Sanchez, et al., **Nature Communications,** 4, 2944 (2013)

[2]. D. Yue et al., **Phys. Rev. Lett**, 121, 037201 (2018)

[3] J. Shen et al., **Phys. Rev. Lett**, 126, 197201 (2021)

[4] R. Yu, et al., **Phys. Rev. B,** 102, 144415, (2020)

IT05

Addressing the climate crisis: How can magnetism contribute?

Thomas Brückel
Forschungszentrum Jülich GmbH, Jülich Centre for Neutron Science (JCNS-2) and Peter Grünberg Institut (PGI-4), JARA-FIT, 52425 Jülich, Germany
Email: t.brueckel@fz-juelich.de

The climate crisis is one of the greatest environmental catastrophes the world has ever faced. This huge challenge for mankind is being addressed by an energy revolution moving away from fossil fuels to renewable energy sources, accompanied by the development of energy saving technologies. Magnetism contributes at various levels, for example with potential energy saving for cooling applications based on the magnetocaloric effect (MCE).

We have performed extensive studies of structure, magnetism, magnetocaloric effect and spin dynamics in the $Mn_{5-x}Fe_xSi_3$ series of compounds [1-6]. While the magnetocaloric effect is moderate for these compounds, they are composed of abundant and non-toxic elements and can be grown as large single crystals. This allows us to perform inelastic neutron scattering studies of the spin and lattice dynamics thus giving insight into the microscopic mechanism of the MCE. For the compound $MnFe_4Si_3$ a strong response of the critical fluctuations has been detected and identified as an important feature connected to the MCE effect [4]. The compound Mn_5Si_3 exhibits an inverse magnetocaloric effect. Inelastic neutron scattering reveals that contrary to the intuitively expected behavior, the application of a magnetic field can induce additional spin fluctuations giving rise to an increase of the magnetic entropy. This mechanism provides a microscopic explanation of the inverse magnetocaloric effect [5]. The microscopic insight into the mechanism of the magnetocaloric effect can serve as a guideline in the quest for novel MCE materials.

ACKNOWLEDGEMENT

Many scientists have contributed to the results reported, in particular: O. Gourdon, N. Biniskos, K. Schmalzl, S. Raymond, J. Voigt, K. Friese, J. Persson, N. Maraytta.

REFERENCES

[1] M. Gottschlich et al.; Journal of Materials Chemistry 22 (2012), 15275
[2] O. Gourdon et al.; Journal of Solid State Chemistry 216 (2014), 56
[3] P. Hering et al.; Chemistry of Materials 27 (2015), 7128
[4] N. Biniskos et al.; Physical Review B 96 (2017), 104407
[5] N. Biniskos et al.; Physical Review Letters 120 (2018), 257205
[6] N. Maraytta et al.; Journal of Alloys and Compounds 805 (2019), 1161

IT06

Designing 2D Ferromagnetism

Tanusri Saha-Dasgupta
S.N.Bose National Centre for Basic Sciences, Kolkata, INDIA.
Email: tanusri@bose.res.in

Abstract: With a goal to expand on the candidate materials exhibiting two-dimensional (2D) magnetism, we explore the possible stabilization of 2D ferromagnetism in two different systems, a) Boronated holey graphene [1] and b) Layered inorganic-organic hybrid perovskites.[2,3]. In the first problem,[1] motivated by the existence of nitrogenated monolayer holey graphene (C_2 N), we consider the boronated counter part (C_2B), and show through first-principles simulation while C_2N is nonmagnetic and semiconducting, C_2B is ferromagnetic and metallic. We provide microscopic understanding of this contrasting behavior. In the second problem, considering the Cu based layered inorganic-organic hybrid perovskites, we derive their 2D counterparts which are found to be stable, the corresponding cleavage energies being a factor of 2-2.5 smaller than that to derive graphene from graphite. The antiferrodistortive arrangement of Cu2+ ions in the inorganic layer of the 2D structure promotes ferromagnetism, which together with single ion anisotropy is found to give rise to finite-temperature long-range ordering of Cu spins, as established through solution of a generalized spin Hamiltonian. [2] We further propose a yet-unexplored class of 2D ferromagnets derived out of Cr-based organic-inorganic layered compounds. [3]

REFERENCES

[1] Dhani Nafday, Hong Fang, Puru Jena, Tanusri Saha-Dasgupta, Phys. Chem. Chem Phys. 21, 21128 (2019).

[2] Dhani Nafday, Dipayan Sen, Nitin Kaushal, Anamitra Mukherjee, Tanusri Saha-Dasgupta, Phys. Rev. Res (Rapid Commun), 1, 032034 (R) (2019).

[3] Dipayan Sen, Gour Jana, Nitin Kaushal, Anamitra Mukherjee, and Tanusri Saha-Dasgupta, Phys. Rev. B 102, 054411 (2020).

IT07

Antiferromagnetism in a topological Kondo system, SmBi

Kalobaran Maiti
Department of Condensed Matter Physics and Materials Science, Tata Institute of Fundamental Research, Homi Bhabha Road, Colaba, Mumbai 400005, India
Email: kbmaiti@tifr.res.in

Abstract: We studied the electronic properties of an antiferromagnetic Kondo lattice system, SmBi employing various bulk physical properties measurements and high-resolution angle-resolve photoemission spectroscopy (ARPES). Magnetization measurements show signature to two antiferromagnetic transitions. ARPES data show signature of Dirac cone in the surface electronic structure and interesting evolution of the surface states across the magnetic transition. Thus, SmBi appears to be an interesting topological semimetal which can be a good platform to realize exotic fundamental science and advance technology.

1. INTRODUCTION

Rare-earth based materials are studied extensively as 4f-conduction states hybridization gives rise to varied exotic properties such as valence fluctuation, heavy fermionic behavior, Kondo physics, unconventional superconductivity, etc. Recently, it is envisaged that the Kondo insulators could host topologically protected surface states which is outstanding as one can tune the topological properties by tuning temperature. Keeping this in view, we studied the electronic properties of a Kondo lattice semimetal, SmBi which forms in rock salt structure. Materials in this (RBi) class are studied extensively reporting interesting electronic properties. For example, LaBi exhibit multiple Dirac cones. (Pr,Sm)Sb and (Pr,Sm)Bi show extreme magneto-resistance. Here, we review our results obtained for SmBi via magnetic and ARPES measurements [1,2].

2. EXPERIMENTAL

High quality single crystals of SmBi were grown using flux method and characterized by XRD and EDX. The orientation and single crystallinity were determined by Laue diffraction. The dc magnetic susceptibility study was done using a SQUID magnetometer. The ARPES measurements were performed at 6 K and 15 K using high-resolution *m*-laser ARPES setup at the Hiroshima Synchrotron Radiation Center (HiSOR) ($h\nu$ = 6.3 eV) with energy resolution of 260 μeV and angle resolution of 0.05°.

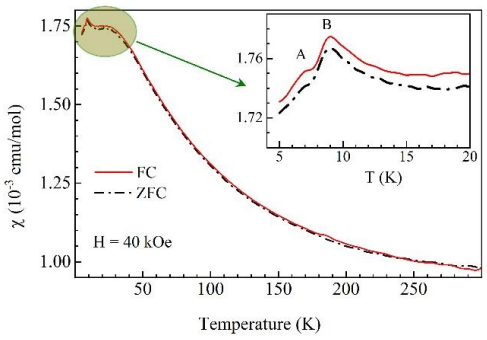

Fig. 1. Magnetic Susceptibility with temperature. Inset shows the shaded region in an expanded scale.at Γ along two cuts. (f) MDC at ε_F along cut1.

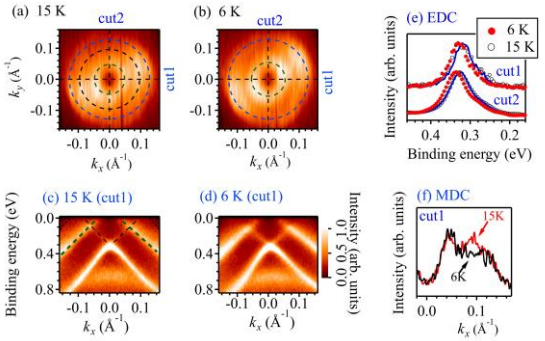

Fig. 2. Fermi surface at (a) 15 K and (b) 6 K. The band dispersions along cut1 at (c) 15 K and (d) 6 K. (e) EDC at Γ along two cuts. Lines are the 6K data shifted by 11 meV. (f) MDC at ε_F along cut1.

3. RESULTS AND DISCUSSIONS

In Fig. 1, we show the magnetic susceptibility data as a function of temperature. The experimental results show a typical paramagnetic temperature dependence down to about 50 K. At low temperatures, we observe two antiferromagnetic transitions at 7K and 9K denoted by A and B, respectively.

In Fig. 2, we show the high resolution ARPES data exhibiting three Fermi surfaces at 15 K [Fig 2(a)]. One of them vanishes at 6 K [Fig. 2(b)]. This is also evident in the MDC plots in Fig. 2(f). A Dirac cone at Γ is observed in the surface electronic structure [Fig. 2(c) and (d)]. The Dirac states appear to remain similar; an energy shift of 11 meV away from ε_F is observed at 6 K as shown in Fig. 2(e).

4. CONCLUSIONS

In summary, we studied the electronic properties of SmBi using magnetic and ARPES measurements. Experimental results show antiferromagnetic transitions at 7K and 9 K. Destruction of surface Fermi surface due to the magnetic order. Topological order appears to survive within the magnetically ordered state.

REFERENCES

[1]. A. P. Sakhya *et al*. Phys. Rev. Mater. 5 (2021) 054201.
[2]. A.P. Sakhya *et al*. (unpublished)

IT07

Carrier-mediated inverted hysteresis and exchange bias in FM/FM heterostructures

Kalpataru Pradhan*

Saha Institute of Nuclear Physics, Kolkata

*kalpataru.pradhan@saha.ac.in

We study interface-driven magnetization reversal mechanism in FM/FM heterostructures using a classical Kondo lattice model including superexchange interactions and anisotropy interactions in an external magnetic field. Here we focus on heterostructures of two ferromagnets with very different coercive field. Our model Hamiltonian mimics the experimental setup of $SrRuO_3$ (SRO) and $La_{0.7}Sr_{0.3}MnO_3$ (LSMO) heterostructures. Using spin-fermion Monte Carlo calculations we show that there is a strong exchange bias between LSMO and SRO layers similar as in the experiments. As a result we observe the inverted hysteresis at low temperatures similar to that of experiments. At high temperatures (just below the ferromagnetic transition temperature of SRO) SRO layers switches first followed by unconventional switching of LSMO and SRO layers on reducing the magnetic field. In this talk I will review some of the experimental results and present our model Hamiltonian calculations to understand the inverted hysteresis and unconventional switching in LSMO and SRO heterostructures.

IT09

Unexpected Kondo-like anomalies and topological Hall effect features reported for heavy rare-earth systems since 1990s

E.V. Sampathkumaran[1,2]

[1]UGC-DAE-Consortium for Scientific Research, Mumbai Centre, BARC Campus, Trombay, Mumbai 400085

[2]Homi Bhabha Centre for Science Education, Tata Institute of Fundamental Research, V. N. Purav Marg, Mankhurd, Mumbai, 400088

(E-mail: sampathev@gmail.com)

Abstract: We have reported some unexpected electrical transport and Hall anomalies (now called "topological Hall Effect) in heavy rare-earth alloys containing strictly localized 4f orbitals three decades ago. These results, now attracting theoretical and experimental attraction, will be briefly brought out.

1. INTRODUCTION

It has been widely recognized that the systems containing well-localized 4f electrons, like Gd, are not as interesting as those exhibiting 4f localization-delocalization phenomenon, like those containing Ce. Here, we bring out certain transport anomalies we have been observing in many heavy rare-earth anomalies for the past three decades ago, which are now attracting in the current literature.

2. PARAMAGNETIC STATE ANOMALY

A minimum in the temperature dependence of electrical resistivity (ρ) is a characteristic feature of the Kondo effect. In the case of f-electron metallic systems, one observes the same for those rare-earth ions for which 4f level is situated close to Fermi level, like Ce. However, in the case of localized-4f systems like heavy rare-earths (called "normal" systems), no such minimum is expected, and the spin disorder contribution has been believed to be a constant in the paramagnetic state. In violation of this fundamental belief in solid state physics, in late 1990s, we reported Kondo-like anomalies in ρ (Fig. 1, left) (and also in heat-capacity) in a Gd-based system, Gd_2PdSi_3, which has been a bearing on the interpretations of low-temperature resistivity upturns in many other materials (e.g., the so-called 'non-Fermi liquids) in the literature [1]. Subsequently, we reported such Kondo-like features in many other in "normal" rare-earth intermetallics (see Ref. 2 for a review). No convincing explanation could be offered for the past 3 decades, and a theory has emerged recently explaining in terms magnetic frustration and RKKY interaction due to itinerant electrons [3].

3. HALL ANOMALY IN THE MAGNETICALLY ORDERED STATE

Subsequent detailed work by us in late 1990s on Gd_2PdSi_3 is of great significance in the context of 'topological Hall Effect (THE)' discovered about a decade later in 2000s [in MnSi and $Fe_{0.5}Co_{0.5}Si$] A hallmark of such THE systems is that there is an additional contribution to Hall resistivity in the magnetic field and temperature range in which a novel magnetic texture (called "magnetic skyrmions") forms. We like to bring out [see also Ref. 4] that this Hall anomaly (that was not explainable at that time) was reported as early as 1999 in Gd_2PdSi_3 [1], particularly in an intermediate field range (following metamagnetic transitions), as shown in Fig. 1 (right). This work served as the key result to search for 'magnetic skyrmions' by resonant x-ray scattering in this compound successfully by Kurumaji et al [5] recently. While summarizing this aspect, we propose possible new materials for topological Hall Effect and magnetic skyrmions.

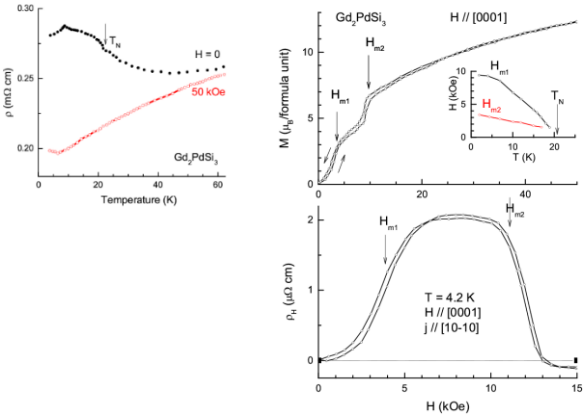

Fig. 1: (Left) Electrical resistivity as a function of temperature and (Right) isothermal magnetization and Hall resistivity for Gd_2PdSi_3 (taken from Ref. 1).

REFERENCES

1. R. Mallik et al, Europhys Lett. 41 (1998) 315; S.R. Saha et al., Phys. Rev. B60 (1999) 12162.
2. Ram Kumar and E.V. Sampathkumaran, J. Magn. Magn. Mater. 538 (2021) 168285.
3. C.D. Batista et al, Rep. Prog. Phys. 79 (2016) (2016) 084504; Z. Wang et al Phys. Rev. Lett. 117 (2016) 206601.
4. E.V. Sampathkumaran, arXiv:1910.09194.
5. T. Kurumaji et al., Science 365 (2019) 914

IT10

Engineering of magnetic ordering and magneto-optical properties in ultrathinfilms

A.Maziewski
Faculty of Physics, University of Bialystok, Ciolkowskiego 1L, 15-425 Bialystok, Poland
Email: magnet@uwb.edu.pl

Transitions between in-plane and out-of-plane magnetization states called as spin reorientation transition (**SRT**) are discussed considering both non-reversible (sample deposition, light or ion irradiations) and reversible (in-plane applied field, small temperature annealing) processes. The magnetic properties were characterterized using magneto-optical magnetometry and domain imaging as well as magnetic force microscopy (**MFM**). Magnetic ordering was also studied by micromagnetic simulations considering the quality factor **Q** (the ratio of the magnetic uniaxial anisotropy and demagnetization energy) and strength D of Dzyaloshinskii–Moriya interaction (**DMI**). Some results of Q and D engineering in ultrathin Co are presented.

Substantial influence of interfaces in ultrathin films gives wide possibilities to tune magnetic anisotropy and create DMI, responsible for existence of interesting magnetic arrangements such as skyrmions or spin spirals. Experimental results were obtained for ultrathin Co layers with different surrounding: Pt, Au, W, Mo and NiO.

Fig.1 shows an example of femtosecond-laser-light (40fs pulse duration, 800nm wavelength) induced nonreversible modification of initially in-plane magnetized Co film. Two white "rings", with out-of-plane magnetization, can be distinguished (Fig.1a) in the image registered with use of Polar Magneto-Optical Kerr Effect (**PMOKE**). Submicrometer domain structure (Fig.1b) was imaged by MFM from the area marked by the red rectangle in (a). Four SRTs connected with light intensity induced Q modifications are clearly visible. The reduction of magnetic domains size down to submicrometer size while approaching to SRT is expected [2].

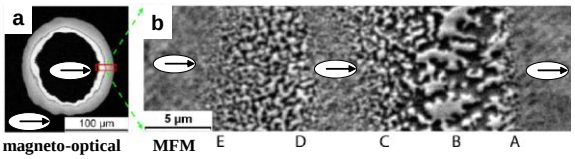

Fig.1. Remnant images from fs light irradiated spot of Pt/Co/Pt stack, registered by PMOKE (a) and MFM (b) [1].

A set of X/Co/Y (where X, Y = Au, Pt) trilayers (grown by the molecular beam epitaxy) with in-plane magnetization alignment in as-deposited state was irradiated with Ga^+ ions in the wide range of ion fluence and energies [3, 4]. Non-reversible changes of magnetic anisotropy (similar to the reported for light irradiation [1]) and modifications of magneto-optical spectra were observed. Maximal increase of magnetooptical parameters was observed for Pt/Co/Pt trilayer. The reduction of DMI interaction in Pt/Co/Au samples after Ga^+ irradiation was measured using Brillouin light scattering spectroscopy [5].

It was found that small temperature annealing allowed creation of reversible SRT in Co/NiO system [6]. After sample demagnetization using such annealing the submicrometer domains were observed in remnant state at room temperature.

Micromagnetic simulations [7] were performed to determine the magnetic states (domains with narrow walls, spin spirals, conical spin spirals, and in-plane magnetization configuration) in ultrathin film adjusting two material parameters: perpendicular magnetic anisotropy characterized by the quality factor Q, and DMI constant D.

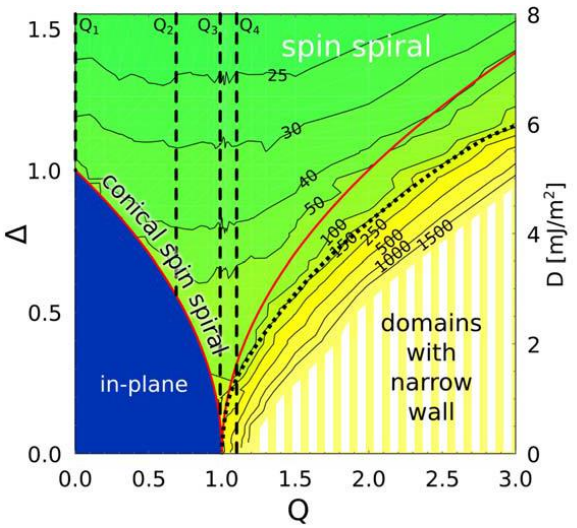

Fig.2. (Q, D) diagram of magnetization states, density plot presents the domain structure period (marked in nm near contour lines) versus Q and D [7].

A partial financial suppport from the National Science Centre of Poland is acknowledged (projects no. 2016/23/G/ST3/04196, 2020/37/B/ST5/02299.).

[1] M. M.Kisielewski et al., IEEE Trans. Magn. 53, 2301204 (2017).
[2] A.Maziewski et al, Phys. Status Solidi A 211, 1005 (2014) (and references therein).
[3] P. Mazalski et al., New J. Phys. 23, 023015 (2021).
[4] M.Jakubowski et al., J. Phys. Cond. Mat. 31, 185801 (2019).
[5] R.Gieniusz et al., J. Magn. Magn. Mat. 537, 168160 (2021).
[6] P. Mazalski et al., J. Magn. Magn. Mat. 508, 166871 (2020).
[7] J. Kisielewski et al., New J. Phys. 21 (2019) 093022.

IT11

Time response and maximum velocity of skyrmions in antiferromagnets

S. Rohart, S. Panigrahy, S. Mallick and J. Sampaio
Laboratoire de Physique des Solides, CNRS, Université Paris-Saclay, Orsay, France
Email: stanislas.rohart@universite-paris-saclay.fr

Abstract: We build an effective Thiele equation to describe the skyrmion dynamics in antiferromagnetic situation. With a minimal number of parameters, this model describes the suppression of gyrotropic deflection, energy dissipation and introduces inertia, inversely proportional to the antiferromagnetic coupling.

1. INTRODUCTION

Antiferromagnetic materials are often listed as a direction to improve the efficiency of spintronic phenomena [1]. For skyrmion motion, it enables enhanced velocities and a suppression of the gyrotropic deflection [2-4], two crucial aspects toward applications. In this talk, we discuss a theoretical framework to describe the dynamics in such a situation. Based on two coupled Thiele equations, one for each sub-lattice, it enable to describe the dynamics and to catch the physical origin specificity of such an antiferromagnetic situation. The model describes real antiferromagnets, where the two lattices correspond to the two magnetic orientations as well as ferrimagnets and synthetic antiferromagnets, where the key difference between these materials is the antiferro-magnetic coupling strenght.

2. MODEL AND RESULTS

Each sublattices are described by their magnetization M_S, angular momentum L_S, damping parameter α, and current induced force $\boldsymbol{F}$. The interlattice antiferromagnetic coupling J_{AF} also induces two coupling forces, one for each lattice, that are opposite in sign. Combining the two Thiele equations provides an effective equation for the velocity skyrmion pair $\boldsymbol{v}$

$$\boldsymbol{G_{eff}} \times \boldsymbol{v} - (\alpha D)_{eff}\boldsymbol{v} + \boldsymbol{F} = M\dot{\boldsymbol{v}} \quad (1)$$

where $\boldsymbol{G}_{eff}$ corresponds to the difference of the two lattice gyrotropic vectors (proportional to the angular momentum difference), $(\alpha D)_{eff}$ is the sum of the two lattice dissipation factors (proportional to the sum of αL_S in each lattice) and M is a mass. Contrarily to ferromagnetic situations where both gyrotropic and dissipation forces are proportional to the angular momentum, here these forces are decoupled. The effective gyrotropic force is proportional to the total angular momentum and vanishes in perfectly compensated situations, hence a gyrotropic deflection suppression. The effective dissipation on the contrary always remain finite and positive with a dissipation power

$$P \propto -(\alpha D)_{eff}\boldsymbol{v}^2 \quad (2)$$

Due to the finite coupling, a new term appears, proportional to the skyrmion pair acceleration $\dot{\boldsymbol{v}}$, and involves a mass $M \propto J_{AF}$, induced by the opposite gyrotropic vectors in each lattice. This term induces a transient regime, from the equilibrium with perfectly aligned skyrmions to a steady state regime with slightly separated skyrmions, in the direction perpendicular to the velocity, with a time response $\tau = M/(\alpha D)_{eff} \propto 1/J_{AF}$. In synthetic antiferro-magnets, where the coupling is moderate, this time is of the order of 0.1-1 ns whereas in ferrimagnets or antiferromagnets, this time is of few ps. The larger the driving force, the larger the skyrmion separation. Beyond a maximum force, the coupling force reaches a maximum, which defines the maximum velocity achievable in the system, before a total skyrmion decoupling

$$v_{max} \propto \frac{J_{AF}}{\Sigma L_S} \min\left(R, \frac{2\Delta}{\pi}\right) \quad (3)$$

where ΣL_S is the sum of the angular momentum of each lattice, R is the skyrmion size and Δ is the micromagnetic domain wall width parameter. This velocity is independent on the damping parameter.

3. DISCUSSION

This model describes the skyrmion dynamics in antiferromagnets, with a minimal number of parameters. It explains the suppression of the gyrotropic deflection and enlighten on the energy dissipation. It introduces inertia to the skyrmion pair, that limits the time response, when the antiferromagnetic coupling is moderate, and sets a maximum skyrmion velocity.

ACKNOWLEDGEMENT

This work has been supported by the French agency for research (ANR) [ANR-17-CE24-0025], Labex NanoSaclay [ANR-10-LABX-0035] and CEFIPRA [IFC/5808-1/2017].

REFERENCES

[1] A. Manchon *et al.* Rev. Mod. Phys. 91, 035004 (2019).
[2] F. Büttner, et al, Sci. Rep. 8, 4464 (2015);
[3] J. Barker and O. A. Tretiakov, Phys. Rev. Lett. 116, 147203 (2016);
[4] X. Zhang, et al., Nat. Com. 7, 10293 (2016).

Thin film fabrication for users: Possibilities and perspectives

S. Pütter
Forschungszentrum Jülich GmbH, Jülich Centre for Neutron Science (JCNS) at Heinz Maier-Leibnitz Zentrum (MLZ), Garching, Germany

s.puetter@fz-juelich.de

The Jülich Center for Neutron Science develops and uses scattering methods for research into structural and magnetic order of functional materials. For users, access to neutron measurements is provided at the Heinz Mayer-Leibnitz Zentrum in Garching, Germany. On top, a special service is offered for several years, i.e. the users may also apply for thin film sample fabrication utilizing Molecular Beam Epitaxy (MBE).

The JCNS thin film laboratory runs an oxide MBE system for the growth of various types of samples, for example "classical" magnetic thin films, transition metal oxide heterostructures or thin metal films for soft matter studies, acting as defined surfaces. In this presentation, we will give an overview for high quality thin film samples all fabricated in the JCNS thin film laboratory, like $SrCoO_x$, Fe_4N or [Pt/Co/Ta] multilayers and their magnetic properties. The focus lies on stoichiometry, morphology and thickness precision and detailed information about the possibilities and constraints in sample fabrication for users will be given.

The MBE setup is equipped with effusion cells, electron guns for electron beam evaporation and a plasma source for use with oxygen or nitrogen. A large variety of deposition materials are offered. Compounds may be produced either by codeposition or by shutter modulated growth of individual layers. For in-situ surface structure analysis reflection high and low energy electron diffraction is utilized while Auger electron spectroscopy is applied for in-situ chemical surface analysis.

For quasi in-situ neutron reflectometry of thin films, which are sensitive to ambient air, a small versatile transfer chamber is may be used for sample transfer from the MBE laboratory to the neutron reflectometer MARIA and measurement under UHV conditions.

Recently the MBE setup has been moved into a larger laboratory and a new feature, i.e. the determination of the in situ flux rate of atoms using the principle of atomic absorption spectroscopy is about to be established. This method will enhance the precision in stoichiometry drastically.

You may apply for neutron experiments and thin film sample fabrication at mlz-garching.de For financial support see NFFA (Nanoscience Foundries and Fine Analysis) Europe (NFFA.eu).

IT13

Interface-driven spintronic phenomena

J. Mendes[1], R. L. Rodriguez-Suárez[2], S. Rezende[3], A. Azevedo[3]
[1]Departamento de Física, UFV, 36570-900 Viçosa, MG, Brazil
[2]Facultad de Física, PUC, Av. Vicuña Mackenna 4860, Casilla 306, Santiago, Chile
[3]Departamento de Física, UFPE, 50670-901 Recife, PE Brazil

Email: antonio.azevedo@ufpe.br

Abstract: The investigation of spin-related properties of electrons, which flow in potentials with translational inversion asymmetry, has led to the discovery of significant spintronics phenomena mainly driven by the spin orbit interaction (SOI). This interaction in inversion asymmetric potentials gave birth to the Bychkov-Rashba effect in surface states that locks spin to moment and stands out for the mutual conversion between charge and spin. The state of the art of interface-driven spintronic phenomena will be reviewed, as well as recent results in which the interaction between the spin current and the charge current is investigated in two-dimensional systems and interfaces.

1. INTRODUCTION

The intrinsic lack of translational symmetry in surfaces and interfaces opened new perspectives to investigate spintronics phenomena mainly driven by the SOI. Among these phenomena, we highlight spin moment locking, spin to charge interconversion, spin-transfer torque, Dzyaloshinskii-Moriya interaction, nontrivial spin textures, etc.

In this talk, it will be presented results of spin to charge interconversion in ferromagnetic/2D-materials, where the ferromagnetic is the insulating garnet $Y_3Fe_5O_{12}$ (YIG) grown by liquid phase epitaxy. We used spin pumping and spin Seebeck techniques to inject a spin current into the non-magnetic material and due to the Rashba-Edelstein effect it is converted in a perpendicular charge current. Among the 2D materials, we investigated single layer of graphene, dichalcogenide layers of MoS_2 and the topological insulator $(Bi_{0.22}Sb_{0.78})_2Te_3$. We also will present results of spin to charge interconversion by means of Ag nanoparticles embedded in Pt/YIG bilayers. Other preliminary results involving YIG/Bi and Pr-YIG/Pt will be presented discussed.

2. SPIN PUMPING INVESTIGATION

In bulk materials, the conversion between spin current and charge current is obtained by means of the inverse spin Hall effect (ISHE), which is described by,

$$\boldsymbol{j}_C = (2e/\hbar)\theta_{SH}(\boldsymbol{j}_S \times \boldsymbol{\sigma}). \qquad (1)$$

Here, $\boldsymbol{j}_S$ ($\boldsymbol{j}_C$) is the spin (charge) current densities, $\boldsymbol{\sigma}$ is the spin index and θ_{SH} is the spin Hall angle that measure the spin charge interconversion efficiency. Any voltage signal that does not adhere to the equation (1) cannot be interpreted as due to spin-charge interconversion. On the other hand, when a 3D spin current is injected through an interface with strong SOI, it generates a 2D charge current by means of the inverse Rashba-Edelstein effect (IREE) and the ratio $j_C/j_S = (2e/\hbar)\lambda_{IREE}$, where λ_{IREE} measures the conversion efficiency.

3. RESULTS

Over the last few years, we have investigated the spin to charge conversion in many FM/NM interfaces, where FM = YIG. As YIG is an insulator, we get rid of parasitic effect that greatly complicates the analysis. For example, Fig. 1 shows the schematic of the spin pumping process in YIG/graphene as well as the ISHE voltage measured for three different in-plane directions [1]. We have shown that the spin-to-charge current conversion, at the graphene layer, is explained by the extrinsic spin-orbit interaction induced by the proximity effect with the ferromagnetic layer.

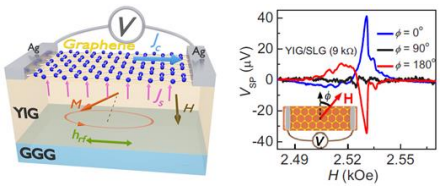

Fig. 1. Schematic of the YIG/graphene used to measure the ISHE voltage shown at right.

We also investigated the spin-to-charge conversion in YIG/MoS_2, Permalloy/$(Bi_{0.22}Sb_{0.78})_2Te_3$, YIG/Bi and Pr-YIG/Pt, among other systems. We also discovered that when nanoparticles of Ag are embedded into Pt layers, the spin-to-charge current conversion efficiency increases by a factor of 5 in comparison with pure Pt [2-4].

I also intend to discuss very new results of spin to charge current conversion in YIG/Bi and Pr-YIG/Pt. In spite of being the heaviest metal, Bi does not convert spin-to-charge current. In addition, the Pr-YIG films exhibit easy plane anisotropy that favor the appearance spin textures compatible with topological Hall effect.

ACKNOWLEDGEMENT

If the authors wish to acknowledge UFPE, CNPq, FINEP and FACEPE, for financial support.

REFERENCES

[1]. Mendes et al, Phys. Rev. B **99** (2019) 214446.
[2]. Mendes et al, Appl. Phys. Lett. **112**, (2018) 242407.
[3]. Mendes et al, Phys. Rev. B **96**, 180415(R) (2017).
[4]. Alves-Santos et al, Phys. Rev. B **96**, 060408(R) (2017).

IT14

Dynamically disordered magnetic state at sub-K regime in a strongly interacting system

D. D. Sarma
Solid State and Structural Chemistry Unit, Indian Institute of Science, Bengaluru 560012
Email: sarma@iisc.ac.in

Abstract: Despite high-temperature magnetic susceptibility of Y_2CuTiO_6 exhibiting a large Curie Weiss scale of ~134 K, AC magnetic susceptibility, μSR, and specific heat data show that magnetic ordering and spin freezing are absent down to 50 mK. Heat capacity and magnetization as a function of the applied magnetic field and the temperature exhibit scaling collapses that are reminiscent of the random singlet physics. The suppression of any ordering or freezing scale, if at all present, by more than three orders of magnitude compared to the Curie-Weiss scale, in conjunction with the scaling behaviors, indicates exciting possibilities such as disorder-stabilized long range quantum entangled ground states. [1]

ACKNOWLEDGEMENT

This work as well as its several extensions have been carried out in collaboration with M. Baenitz, P. J. Baker, S. Bhattacharjee, S. Chattopadhyay, K. Damle, D. Das, R. Das, H. Fabian, T. Herrmannsdoerfer, A. Hossain, L. Hubertus, D. C. Joshi, P. Keerthi S, S. Kundu, P. Mahadevan, A. V. Mahajan, R. Mathieu, J.-C. Orain, S. Pujari, and K. M. Ranjith.

REFERENCES

[1]. S. Kundu, Akmal Hossain, Pranava Keerthi, Ranjan Das, M. Baenitz, Peter J. Baker, Jean-Christophe Orain, D. C. Joshi, Roland Mathieu, Priya Mahadevan, Sumiran Pujari, Subhro Bhattacharjee, A. V. Mahajan, and D. D. Sarma, Signatures of a spin-1/2 cooperative paramagnet in the diluted triangular lattice of Y_2CuTiO_6, Phys. Rev. Lett. **125**, 117206 (2020)

IT15

Ultrafast nucleation of single and multiple antiferromagnetic skyrmions

Kacho Imtiyaz Ali Khan1 , Naveen Sisodia1 , P.K. Muduli1*
Department of Physics, IIT Delhi, Hauz Khas, New Delhi, India
*Email: muduli@physics.iitd.ac.in

Abstract: In this work, we numerically investigate the ultrafast nucleation of antiferromagnetic (AFM) skyrmion using in-plane spin-polarized current and present its key advantages over conventionally used out-of-plane spinpolarized current. We show that the threshold current density (J^o) required for the creation of AFM skyrmion is almost an order of magnitude lower for the in-plane spin-polarized current. For the in-plane cases, the nucleation time (τ_n) for the AFM skyrmion is found to be 12−7 ps for the corresponding current density of $1-3\times10^{13}$ A/m^2, which is much lower compared to out-of-plane. We also demonstrate ultrafast nucleation of multiple AFM skyrmions that is possible only with in-plane spin polarized current and discuss how the current pulse width can be used to control the number of AFM skyrmions. The results show more than one order of magnitude improvement in energy consumption for ultrafast nucleation of AFM skyrmions using in-plane spin-polarized current, which is promising for applications such as logic gates, racetrack memory and neuromorphic computing.

1. INTRODUCTION

Antiferromagnetic (AFM) skyrmions could be a better alternative to FM skyrmions for racetrack memory devices due to their trivial topology (zero topological charge) which completely suppresses the skyrmion Hall effect [1,2]. Fractional AFM skyrmion lattice has been recently observed experimentally in spinel MnSc2S4 consisting of three antiferromagnetically coupled sub-lattices [3]. The predicted velocity of AFM skyrmions is much higher compared to that of the FM skyrmion [4]. Several methods have been proposed to nucleate AFM skyrmion such as by spin polarized current [5] and by use of ultrashort laser pulse [6]. So far, the studies on nucleation of AFM skyrmions using spin polarized current have focused on out-of-plane spin polarized current, which needs an out-of-plane magnetized spin polarizing layer for operation.

2. METHOD

In this work, we solve LLG equation using the micromagnetic simulation package Mumax3. Material parameters are taken for Refs. [7,8], we use the exchange stiffness A_{ex} = −10 pJ/m, Gilbert damping coefficient α = 0.3, the saturation magnetization Ms = 580 × 10^3 A/m, the DMI constant D = 3.5 × 10−3 J/m^2 , and the PMA constant K = 0.8 × 106 J/m^3 . Here, Keff is the effective anisotropy strength after overcoming the magnetostatic interactions ($K_{eff} = K - \mu 0 Ms^2/2$). The polarization efficiency of the spin-polarized current is |P| = 0.56. The field-like torque is assumed to be zero (ξ = 0). Since we utilize CPP (current perpendicular to plane) geometry the spin current is always flowing in the z-direction along the thickness of the film (J = J^0). As shown in Fig1(a,b), our findings show that the threshold current density required for the nucleation of AFM skyrmion using in-plane polarized spin current (J^0xy) is almost one order less compared to the commonly utilized out-of-plane polarized spin current (J^0zz). We attribute this difference to the characteristic trajectories of the oscillation eigenmodes excited in the two cases due to the phenomenon of spin transfer torque (STT).

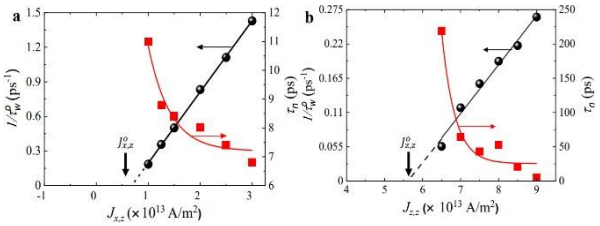

Fig.1. Dependence of inverse of threshold pulse width τ^0_w (black circles) and nucleation time τ_n (red squares) on the current density for (a) in-plane, and (b) out-ofplane spin polarized cases.

ACKNOWLEDGEMENT

K.I.A.K gratefully acknowledges UGC-CSIR and Department of Science and Technology (DST), Government of India for financial support. The authors thank IIT Delhi HPC facility for computational resources.

REFERENCES

[1] J. Barker, & O. A. Tretiakov, Phys. Rev Lett. 116 147203 (2016).
[2] B. Göbel, I. Mertig, & O. A. Tretiakov, Phys. Rev. 895 1 (2021).
[3] S. Gao, et al., Nature 586 37 (2020).
[4] T. Dohi et al, Nat. Commun. 10 5153 (2019).
[5] X. Zhao et al., Appl. Phys. Lett. 112 252402 (2018).
[6] R. Khoshlahni et al., Phys. Rev. B 99 054423 (2019).
[7] X. Zhang et al., Sci. Rep. 6 24795 (2016).
[8] R. M. Menezes et al., Phys. Rev. B 99 104409 (2019).

IT16

Spin-Charge Conversion in Ferromagnetic Materials

Takeshi SEKI
Institute for Materials Research, Tohoku University, Sendai 980-8577, Japan
Center for Spintronics Research Network, Tohoku University, Sendai 980-8577, Japan

National Institute for Materials Science, Tsukuba 305-0047, Japan
Email: takeshi.seki@tohoku.ac.jp

Abstract: We introduce our research activities about the spin-charge conversion phenomena in ferromagnetic materials. First, the spin anomalous Hall effect (SAHE) in a ferromagnet is explained, which can be used as a source of spin current. The large SAHE in $L1_0$-FePt allowed us to switch the magnetization of free layer in a giant magnetoresistance stack. Next, we share our recent study on self-induced spin-orbit torque (SOT) in a Ni-Fe single ferromagnetic layer. By comparing the results between the very thin Ni-Fe layers with and without structural inversion symmetry, the mechanism of self-induced SOT is discussed.

1. INTRODUCTION

The control of spin current (J_s), which is the flow of spin angular momentum, is the basis for the development of spintronics. In particular, highlyefficient conversion from charge current (J_c) to J_s and vice versa is the key for spintronic devices to improve their performance and to provide them with multi-functionalities. A promising way for conversion is to exploit large spin Hall effect (SHE) in nonmagnets (NMs). However, the spin-polarization vector of J_s is geometrically determined and is not controllable for the SHE in NM, which are drawbacks for practical applications.

As in the case of SHE in NMs, one can expect the spin-charge conversion in ferromagnets (FMs). In 2015, we reported the conversion from J_s to J_c in the ferromagnetic $L1_0$-FePt [Ref. 1], which was one of the pioneering studies on the spin-charge conversion in FMs. At the same time, the concept of spin anomalous Hall effect (SAHE) was proposed [Ref. 2], theoretically predicting that AHE also generates J_s in FM. An important feature of SAHE is that the spin-polarization vector of J_s can be controlled by the magnetization (M)of FM. This suggests that large SAHE may enable us to realize the field-free magnetization switching of a perpendicularly magnetized free layer.

In addition to J_s flowing from one FM to another FM,it has recently been revealed that the J_s generated in theFM can affect the magnetization of FM itself, which iscalled the self-induced spin orbit torque (SOT). This fact opened a new avenue for SOT-based device applications although the mechanism of self-induced SOT is still under debate. Thus, the spin-charge conversion in FMs becomes a recent intriguingresearch topic.

In this talk, we introduce two research topics related to the spin-charge conversion in FMs. One is the large SAHE in $L1_0$-FePt [Ref. 3], and the other is the self-induced SOT in a Ni-Fe single ferromagnetic layer [Ref. 4].

2. LARGE SPIN ANOMALOUS HALL EFFECT

By employing the giant magnetoresistance device consisting of $L1_0$-FePt / Cu / Ni-Fe, the spin anomalous Hall angle (α_{SAH}) for the $L1_0$-FePt was evaluated to be 0.25 ± 0.03 from the linewidth modulation of ferromagnetic resonance spectra by dc current application. The investigation of α_{SAH} at different configurations between J_c and M allows us to discuss the symmetry of SAHE and gives the unambiguous evidence that SAHE provides a source of J_s. Thanks to the large α_{SAH}, we also have successfully demonstrated SAHE-induced magnetization switching of Ni-Fe layerin the $L1_0$-FePt / Cu / Ni-Fe trilayer.

3. SELF-INDUCED SPIN ORBIT TORQUE

The self-induced SOT was evaluated for the very thin Ni-Fe layers with and without structural inversion symmetry: “asymmetric” and “symmetric” Ni-Felayers. The asymmetric Ni-Fe samples (Asym-Py)have the film stack of Si-O Subs. // Ni-Fe(t) / Al-O(5) (in nanometer) while the symmetric Py samples (Sym-Py) are composed of Si-O Subs. // Al-O(5) / Ni-Fe(t) / Al-O(5). Spin-torque ferromagnetic resonance was measured for the two kinds of devices. For both structures, the field-like component coming from Oersted field clearly appeared. On the other hand, the damping-like component was observed only for the asymmetric Ni-Fe with the thickness less than 3 nm. This damping-like torque is attributable to the significant spatial change in the properties of Ni-Fe. We also propose a toy model to analyze the self-induced SOT.

REFERENCES

[1] T. Seki *et al.*, Appl. Phys. Lett. **107**, 092401 (2015).
[2] T. Taniguchi *et al.*, Phys. Rev. Applied **3**, 044001 (2015).
[3] T. Seki *et al.*, Phys. Rev. B **100**, 144427 (2019).
[4] T. Seki *et al.*, Phys. Rev. B **104**, 094430 (2021).

IT18

Homo- and heterometallic lanthanide complexes as a Single-ion/Single-molecule Magnets

V. Chandrasekhar

Department of Chemistry, Indian Institute of Technology Kanpur, Kanpur-208 016, India and

Tata Institute of Fundamental Research Hyderabad, Hyderabad-500 046, India

vc@iitk.ac.in; vc@tifrh.res.in

Single molecule magnets (SMMs) are metal complexes that contain one or more paramagnetic metal ions. These can be magnetized below certain temperatures and can retain the magnetization below these temperatures for an indefinite period. This talk will give a brief introduction about the design strategies of SMMs emphasizing the role of magnetic anisotropy in the design and assembly of such complexes. The talk would focus on heterometallic complexes as well as mono- and dinuclear lanthanide complexes (Figure).[1-2] The SMM magnetic properties of these complexes would be presented.

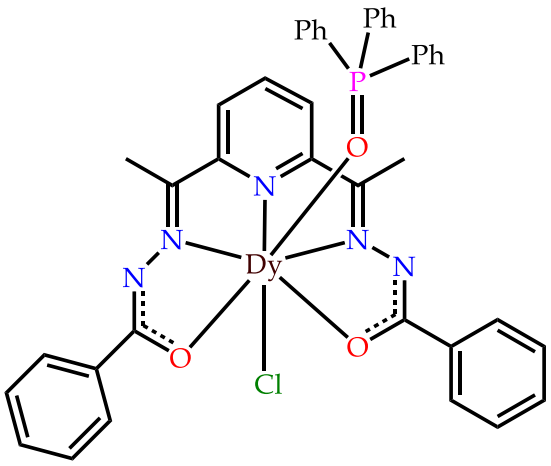

Figure: A pentagonal bipyramidal Dy(III) complex that shows slow relaxation of magnetization[1]

References

1. Kalita, P.; Ahmed, N.; Bar, A. K.; Dey, S.; Jana, A.; Rajaraman, G.; Sutter, J-P.; Chandrasekhar, V.
Inorg. Chem. 2020, 59, 6603-6612.

2. Acharya, J.; Ahmed, N.; Flores Gonzalez, J.; Kumar, P.; Cador, O.; Singh, S. K.; Pointillart, F.; Chandrasekhar, V.
Dalton Trans. **2020**, *49*, 13110-13122.

IT19

Processing and Characterization of Magnetostrictive Materials

J. Arout Chelvane
Defence Metallurgical Research Laboratory, Kanchanbagh, Hyderabad – 500 058
Email: jac@dmrl.drdo.in

Abstract: In this talk, it is intended to provide an overview of the R&D pursued at DMRL on magnetostrictive materials with emphasis of microstructural correlations with property development, both in bulk and thin films of alloys of R-Fe.

1. INTRODUCTION

Magnetostrictive materials belong to an important class of smart magnetic materials by virtue of exhibiting a very strong coupling between magnetic and mechanical energies. This coupling effectively paves way for utilizing these materials in potential applications such as ultrasonic transducers, sensors, actuators, delay lines, energy harvesting devices etc. Although magnetostrictive property is exhibited by almost all ferro and ferrimagnetic materials, the rare earth (R) – iron (Fe) intermetallic compounds of type RFe_2 display maximum magneto-mechanical characteristics owing to large magnetostriction exhibited by them at RT. Among several R-Fe type compounds, maximum magnetostriction, either positive or negative, is derived from Tb-Fe (positive) and Sm-Fe (negative) at room temperature. There are technological challenges involved in tailoring the properties for maximising the performance ability. Some of the key issues are (i) reducing the magnetocrystalline anisotropy by mixing appropriate rare earths (ii) imparting a sharp grain orientation along the easy magnetization axis and (iii) minimising the volume fraction of the deleterious phases formed in association with the main magnetostrictive phase, RFe_2. The research work undertaken at DMRL was directed towards achieving these characteristics in the material by means of directional solidification. A presentation will be made in this talk highlighting the evolution of microstructure, development of grain orientation and a plausible correlation of these two with magnetostriction. Envisaging the importance of these materials in thin film form, an R&D programme was launched in recent time at DMRL. Infrastructure needed to produce and characterize device quality magnetostrictive thin films were created. The preliminary work led to establish a process-structure-property correlation in developing the films. In this talk, it is intended to provide an overview of the R&D pursued at DMRL on magnetostrictive materials with emphasis of microstructural correlations with property development, both in bulk and thin films of alloys of R-Fe.

II. METHODOLOGY

Bulk magnetostrictive materials are processed by vacuum induction melting and casting followed by directional solidification employing zoning and modified Bridgman techniques. Electron beam evaporation and sputtering techniques have been adopted for growing rare earth and iron based magnetostrictive thin films. Detailed structural, microstructural and magnetic characterization employing grazing incidence X-ray diffraction, transmission electron microscopy, Kerr microscopy and magnetization measurements were carried out.

III. RESULTS AND DISCUSSIONS

Zoning and modified Bridgman techniques were found to be effective in improving the magnetostriction of RFe_2 alloys. Upon directional solidification, magnetostriction as high as 1600 ppm has been realized owing to the formation of strong texture close to the easy magnetization direction and microstructure devoid of secondary phases. Acoustic transducer fabricated using these magnetostrictive rods showed high sound pressure level at low frequencies in par with the conventional piezo ceramic materials.

Tb-Fe and Tb-Fe-Co based thin films grown by electron beam evaporation exhibited different magnetic anisotropies based on the film thickness and composition. Anisotropy tuning carried out using rapid thermal processing and ion irradiation showed spin reorientation transition from out-of-plane to in-plane direction. Detailed magnetic microscopy studies carried out magnetic force microscopy complemented the magnetization results. The reason behind the spin re-orientation transition was unraveled using detailed transmission electron microscopy studies. Magnetostriction as high as 400 ppm has been achieved in sputtered Tb-Fe-Co thin films.

ACKNOWLEDGEMENTS

Director, DMRL is acknowledged for constant support and encouragements.

IT20

Topology meets correlations: neutron scattering from correlated topological materials

Yixi Su[1], Fengfeng Zhu[1], Xiao Wang[1], Lichuan Zhang[2], Yuriy Mokrousov[2], Stefan Blügel[2], Thomas Brueckel[3]

[1]Jülich Centre for Neutron Science (JCNS) at Heinz Maier-Leibnitz Zentrum (MLZ), Forschungszentrum Jülich, D-85747 Garching, Germany

[2]Peter Grünberg Institute (PGI-1), Forschungszentrum Jülich, D-52425 Jülich, Germany

[3]Jülich Centre for Neutron Science (JCNS-2) and Peter Grünberg Institute (PGI-4), Forschungszentrum Jülich, D-52425 Jülich, Germany

Email: (y.su@fz-juelich.de)

Abstract: Recent theoretical predictions and experimental realizations of exotic fermions and topologically protected phases in condensed matter have led to tremendous research interests in topological quantum materials. Especially, correlated topological materials, such as magnetic Dirac and Weyl semimetals, and intrinsic magnetic topological insulators etc., in which both non-trivial topology of single-electron band structures and electronic correlation effects are essential for the underlying physics, have emerged as an exciting platform to explore novel electronic and magnetic phenomena. In this talk, I will present a couple of the selected examples of our recent neutron scattering studies of correlated topological materials, including magnetic Dirac semimetal $EuMnBi_2$ [1] and topological magnon insulators in two-dimensional van der Waals ferromagnets $CrSiTe_3$ and $CrGeTe_3$ [2].

ACKNOWLEDGEMENT

We would like to thank the contributions from our co-workers and collaborators: Junda Song (JCNS-MLZ), Thomas Mueller (JCNS-MLZ), Karin Schmalzl (JCNS-ILL), Wolfgang Schmidt (JCNS-ILL), Martin Meven (RWTH Aachen & JCNS-MLZ), Alexandre Ivanov (ILL), Jitae Park (MLZ), Jianhui Xu (HZB & MLZ)

REFERENCES

[1] Fengfeng Zhu, *et al*., Phys. Rev. Research **2**, 043100 (2020).

[2] Fengfeng Zhu, *et al*., Sci. Adv. **7**, eabi7532 (2021).

IT21

Enhancing the spin-orbit torque efficiency in Pt/CoFeB/Pt based perpendicularly magnetized system

Soubhik Kayal, Saikat Maji, Ankan Mukhopadhyay and P. S. Anil Kumar*

Department of Physics, Indian Institute of Science, Bangalore 560012, India

Investigations on the current-induced magnetization reversal (CIMR) in the heterostructures of heavy metal (HM) and ferromagnet (FM) have intensified in the past decade from the fundamental and technological point of view. This HM/FM-based heterostructure possesses vertical structural asymmetry and can create spin-orbit torque (SOT) with the influence of current. While the magnetic easy-axis of this heterostructure stays along perpendicular to the surface (PMA), the CIMR can be performed with the assistance of an external in-plane (IP) bias magnetic field. To achieve the CIMR in an HM/FM/HM PMA heterostructure, the mirror symmetry must be broken along the lateral direction by applying an external IP bias field. Here the dissipative damping-like SOT is responsible for the deterministic switching. In contrast, the conservative field-like SOT has no active role in the magnetization switching process. Later, it has demonstrated that the in-plane bias field can be eliminated by incorporating the lateral space inversion asymmetry to a heterostructure consisting of HM/FM/HM, which can introduce a new field like torque. Another way of providing the in-plane field is by introducing an IP stray field by putting another ferromagnetic layer with an in-plane magnetic anisotropy (IMA) on the top HM layer. In this study on Ta/Pt/CoFeB/Pt/Ta/CoFeB/Pt heterostructure having PMA properties with broken lateral symmetry and consists of an IMA ferromagnetic layer on the top HM layer, both field-like, and the damping-like torque has been used to achieve the magnetic field-free current-induced magnetization switching with a lower critical current density of $8.65 \times 10^{10} A/m^2$. The CIMR was achieved for the above system at a lower critical current density of $3.35 \times 10^{10} A/m^2$ with the assistance of a 60mT IP bias field.

*anil@iisc.ac.in

IT22

Ferromagnetic nanocomposites: the preparation using mechanochemical synthesis and theexploration towards energy harvesting

Aneeta Manjari Padhan[1], Sugato Hajra[2], M. Sahu[2], Hoe Joon Kim[2], Perumal Alagarsamy[1]
[1]Department of Physics, Indian Institute of Technology Guwahati, Guwahati – 781 039, Assam, India.

[2]Department of Robotics Engineering, DGIST, Daegu 42988, Republic of Korea.

E-mail: perumal@iitg.ac.in; alagarsamy.perumal@gmail.com

Abstract: Recently, integrating transition metal (TM) and metal oxide (MO) based composites with tailored properties has opened up many opportunities to obtain multifunctional nanoengineered candidates for device concepts and applications. In this work, the ferromagnetic TM and MO nanocomposites are prepared using one of the industrially viable and cost-effective techniques, i.e., the high-energy planetary ball mill process, by taking NiO and Al, Ti, and Mg elements. The mechanical alloying produced ferromagnetic nanocomposites of NiO-Ni-(Al_2O_3, TiO_2, MgO) depending on the Al, Ti, and Mg elements through thermodynamically preferred solid-state reduction reaction, depending on the composition towards stoichiometric. Interestingly, the utilization of such nanocomposites in the triboelectric nanogenerators facilitates harvesting biomechanical energy and makes it suitable for several energy harvesting device applications in daily life.

1. INTRODUCTION

The development of transition metal (TM) – metal oxide (MO) composites with tunable properties has received tremendous research attention due to its applications. Interestingly, these nanocompositesexhibit amalgamated properties caused by their physical properties, which can be tempted/modulated by interactions between their constituents. In particular, the establishment of TM and MO based nanocomposites, composed of antiferromagnetic (AFM) and ferromagnetic (FM) constituents, is of exceptional interest due to their excellent thermal/chemical stability, large tunability, extreme sensitivity to change in composition and structure, easy mode of fabrication, multifunctional behaviors, culminating in potential technological applications. Mainly, the NiO-based nanocomposite depicts interesting magnetic phenomena, such as tunable blocking temperature, exchange bias, Curie temperature, *etc.* [1] Hence, we have attempted preparing nanocomposites of NiO-Ni-(Al_2O_3, TiO_2, MgO) through thermodynamically preferred solid- state reduction reaction using NiO-(Al, Ti, Mg) in a high-energy planetary ball mill. The developed nanocomposites are explored to harvest energy from biomechanical activities in real-life applications.

2. EXPERIMENTAL SECTION

The NiO-Ni-(Al_2O_3, TiO_2, MgO) nanocomposites were prepared by solid-solid mechanochemical (MC) reactions between NiO and Al, Ti, Mg elements. MC reactions were carried out in a high-energy planetary ball mill under dry mill conditions. The milling was carried out in a controlled argon (Ar) environment at 500 rpm milling speed for different milling periods. Further, the milling process with a constant ball to powder ratio of 10:1 was programmed to run for 15 min after pausing for 15 min to prevent possible temperature rise. All the milling conditions were optimized carefully by analyzing the overall variationsin structural evolution and magnetic properties of the resultant nanocomposite using various sophisticatedtechniques.

3. RESULTS AND DISCUSSION

While as-mixed powders exhibit sharp Bragg reflections corresponding to NiO-(Al,Ti,Mg)elements, the milled powders depict the peaks corresponding to NiO, Ni, Al_2O_3, TiO_2, MgO phases and confirm the MC reduction of NiO by Al, Ti, and Mg. The magnetic properties of the milled powders are strongly dependent on the content of the Al, Ti, and Mg added to NiO, which change the type of the MC reduction reaction from a gradual one to a self- propagated combustion type. The microstructuralstudies reveal the formation of FM Ni in AFM NiO and non-magnetic Al_2O_3, TiO_2, MgO matrix.Furthermore, a strong correlation between structural, microstructural, vibrational, and magnetic properties is obtained, depending on the Ni and NiO phases.Hence, the coexisting FM and AFM phases were crucial in determining the magnetic anisotropy- induced ferromagnetism. The high-temperature thermomagnetization studies confirmed the induced ferromagnetism caused by the higher Ni contents due to the MC reduction.

The nanocomposites were finally employed in fabricating the nanogenerator device for energy harvesting to power up low-power electronics such as a wristwatch and LEDs. The detailed and systematic approaches of fabricating ferromagnetic nanocomposites, the structural, microstructural, vibrational, and magnetic properties, and their implementation in nanogenerator devices will be presented.

ACKNOWLEDGEMENT

The authors would like to acknowledge CSIR, New Delhi, for the research grant [03(1166)/ 10/ EMR-II]. Also, DST, New Delhi [SR/S2/CMP-19/2006; SR/FST/PII-020/2009; SR/FST/PSII-037/2016] and CIF, IIT Guwahati are acknowledged.

REFERENCES

[1]. A.M. Padhan, Ph.D. Thesis (2019), IIT Guwahati.
[2]. A.M. Padhan et al., Nano Energy 91 (2022) 106662.

IT23

Characterization of Interface Properties in Ultra-thin films: Pathway to Novel Magnetism

Saibal Basu

Homi Bhabha National Institute, Anushaktinagar, Mumbai 400094, India

At present the research in thin film is heavily focused towards tailoring and characterizing magnetism at the interfaces of ultra-thin (few nanometers to hundreds of nanometers) thin film heterostructures with layers of multiple components. It is an established fact that the magnetism at the interfaces of two dissimilar ultra-thin layers e.g. a ferromagnet and an antiferromagnet or a ferromagnet and a non-magnetic material have shown various novel magnetic structure. Exchange bias is an example of such a phenomenon due to coupling between a ferromagnet and an antiferromagnet. The future of spintronics depends on successful spin transfer across an interface between two materials. The physical and magnetic properties at the interface dictates magnetic coupling and magnetic structure of the entire heterostructure. It also controls spin or charge transfer. In this regard a detailed microscopic characterization of structure and magnetism at the interfaces is necessary in thin film multilayers. We have observed several novel magnetic structure in ultra-thin film multilayers. Some of the examples are magnetic structures in thin film multilayers that are not seen in bulk. We found helical magnetic structure in Co-Gd multilayers, that is specific to thin films and is not seen in bulk. Coupling between ferromagnetic oxide material with oxide superconductors like YBCO have shown that in proximity geometry, there are interesting magnetic dead-layers at the interfaces. Several such examples will be highlighted in the talk. We used Polarized Neutron Reflectometry as the primary tool along with other complementary techniques and bulk measurements.

IT24

Charge current generation from oscillating magnetization via the inverse of voltage-controlled magnetic anisotropy effect

Ambika Shanker Shukla[1], Akanksha Chouhan[1], Rachit Pandey[1], M. Raghupathi[1], Tatsuya Yamamoto[2], Hitoshi Kubota[2], Akio Fukushima[2], Shinji Yuasa[2], Takayuki Nozaki[2], Ashwin A. Tulapurkar[1]*

1 Solid State Devices Group, Department of Electrical Engineering, Indian Institute of Technology Bombay, Mumbai 400076, India.
2Spintronics Research Center, National Institute of Advanced Industrial Science and Technology, Tsukuba, Ibaraki 305-8568, Japan.

Control of magnetization direction of is a central topic in spintronics. Spin-transfer torque effect has been successfully used to switch magnetization of a nano-magnet. Control of magnetization by voltage is being extensively explored as a possible candidate for writing in magnetic random access memories. This is based on the control of magnetic anisotropy by voltage i.e. VCMA effect. The various effects used in spintronics also have inverse effects, which could find potential applications as well. Spin pumping is the reciprocal of the spin transfer torque effect, and creates spin current via oscillating magnetization. In this talk, I will describe our experimental findings of reciprocal of the VCMA effect [1]. By this effect, we can generate charge current from oscillating magnetization, which can be used for probing magnetization dynamics.

To demonstrate this effect, we fabricated stack consisting of bottom layer/FM/MgO/top layer. Pillars of 80 um X 3 um with top and bottom contacts were formed (port 1). A co-planar waveguide (CPW) insulated from the pillar was formed on the top (port 2). The scattering parameters (S parameters) of this two-port device were measured for different orientations of the external magnetic field. The VCMA effect gives rise to transmission from port 1 to port 2, whereas the transmission from port 2 to 1 arises from the inverse VCMA effect. The role of VCMA and its inverse were confirmed by the angular dependence of the S-parameters. A circuit model will be discussed to explain the observed results. Further ways of measuring the inverse effect would also be discussed.

[1] Sci. Adv. 6, eabc2618 (2020)

CT01

Formation of 360° domain walls in magnetic thin films with uniaxial and random anisotropy

N. Chowdhury[*1], W. Kleemann[2], O. Petracic[3], F. Kronast[4], A. Doran[5], A. Scholl[5], S. Cardoso[6] and P. Freitas[6], S. Bedanta[1]

[1]LNMM, School of Physical Sciences, NISER, Jatni-752050, India.

[2] Physics Department, Universität Duisburg-Essen, 47048 Duisburg, Germany.

[3]Jülich Centre for Neutron Science and Peter Grünberg Institut, JARA-FIT Forschungszentrum Jülich GmbH, 52425 Jülich, Germany.

[4]Helmholtz-Zentrum Berlin für Materialien und Energie, Albert-Einstein-Strasse 15, 12489 Berlin, Germany.

[5]Advanced Light Source, Lawrence Berkeley National Laboratory, 1 Cyclotron Road, Berkeley, California 94720, USA.

[6]INESC-Microsystems and Nanotechnologies and Instituto Superior Tecnico, Universidade de Lisboa, Lisbon 1000, Portugal.

Email: niruchowdhury@gmail.com

Abstract: In this work, we discuss the possible origin of 360° domain walls (DWs) observed in metal-insulator multilayer system observed via X-ray photoemission electron microscopy (XPEEM) and magneto-optic Kerr effect (MOKE) microscopy along easy (EA) and hard axis (HA), respectively. We attribute the formation of this non-trivial 360° DWs to the presence of an orientational dispersion of anisotropy axes in the film grains that is comparable to an overall uniaxial anisotropy term. Our results are confirmed numerically using micromagnetic simulations.

1. INTRODUCTION

Ferromagnetic thin films have been investigated for last few decades for the advancement of the fundamental research and data storage technology [1]. Hence, it is necessary to understand the magnetic properties like domain structure and magnetization reversal of these magnetic thin films. Formation of domains depends on energy minimization of exchange energy, magnetostatic energy and anisotropy energy. Among various types of domain walls (DWs), the observation of 360° DWs is rare and interesting because they separate regions (domains) with the same magnetization state. These DWs are formed due to the pinning centres in the magnetic thin film or by combination of two 180° Néel walls [2].

2. EXPERIMENTAL DETAILS

Metal-insulator multilayers (MIMs) of $[Co_{80}Fe_{20}(t$ = 1.8 nm)/Al_2O_3(3 nm)]$_9$ was prepared by ion beam sputtering. A small in-plane magnetic field of $\mu_0 H$ = 10 mT was applied during the deposition of the layers. Magnetic domain imaging was performed by XPEEM using x-ray magnetic circular dichroism [3] and longitudinal magneto-optic Kerr effect (LMOKE) based microscopy. Micromagnetic simulations were performed using the object-oriented micromagnetic framework (OOMMF) for better understanding of the observed results. Random anisotropy (K_r) in addition to uniaxial anisotropy (K_u) was incorporated in these simulations to mimic the granularity of the films.

3. RESULTS AND DISCUSSION

Figure 1(a) shows the domain image observed using XPEEM along EA at field close to coercive field which shows the 360° DWs (black threadlike structure) separating the similar magnetized (white coloured) region on its either side. Figure 1(b) shows the LMOKE microscopy images of 360° DWs (black loop like feature) formed along HA. Our OOMMF simulations that indicate that 360° DWs were formed when either $K_r \sim K_u$ or $K_r > K_u$ for both EA and HA [4]. Along EA, two 180° DWs of opposite chirality merges to form the stable 360° DWs (Fig 1(c)). However, along HA the random anisotropy of the grains cannot outweigh the exchange energy. Therefore, spins do not follow coherent rotation with magnetic field. This results in opposite sense of rotation of the spins leading to the formation of 360° DWs.

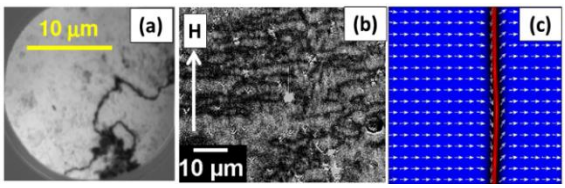

Fig.1: Observation of 360° DWs via (a) XPEEM along EA, (b) MOKE microscopy along HA, (c) OOMMF simulation.

ACKNOWLEDGEMENT

The authors would like to acknowledge DAE and DST of government of India for the financial support, HZB for synchrotron radiation beamtime. This research used resources of the Advanced Light Source, a U.S. DOE Office of Science User Facility under contract no. DE-AC02-05CH11231.

REFERENCES

[1]. C. Chagpert *et al.*, J. Magn. Magn. Mater. **148** 165-166 (1995).

[2]. L. J. Heyderman *et al.*, J. Magn. Magn. Mater. **96** 125 (1991).

[3]. J. Stöhr *et al.*, Surf. Rev. Lett. **5**, 1297 (1998).

[4]. N. Chowdhury, et al., Phys. Rev. B 98, 134440 (2018).

CT02

Role of spin-glass like frustration on exchange bias effect in $Fe/Ir_{20}Mn_{80}$ and $Ni_{50}Mn_{50}/Co_{40}Fe_{40}B_{20}$ bilayers

Sagarika Nayak*[1], Palash Kumar Manna[1], Vijayabaskaran Thiruvengadam[1], Braj Bhusan Singh[1], J. Arout Chelvane[2] and Subhankar Bedanta*[1]

[1]Laboratory for Nanomagnetism and Magnetic Materials (LNMM), National Institute of Science Education and Research (NISER), HBNI, Jatni-752050, Odisha, India,

[2]Advanced Magnetics Group, Defence Metallurgical Research Laboratory (DMRL), Kanchanbagh,

Email: (sagarika@niser.ac.in)

Abstract: We have studied the ferromagnetic (Fe,CoFeB)/ antiferromagnetic (IrMn, NiMn) exchange bias systems to investigate the role of the interface on magnetic properties. We have observed the presence of spin-glass-like interface in these systems from different magnetic measurements. The fitting of the training effect data with different models indicates the relaxation of frozen and rotatable spins present at the interface. Including various static magnetic measurements, ac susceptibility measurement is performed in CoFeB/NiMn exchange bias systems to find the presence of spin glass phase.

1. INTRODUCTION

Modern spintronic based devices such as magnetic random-access memory (MRAM) and magnetic read head sensor have been designed on the principles of exchange bias effect [1]. A unidirectional interfacial exchange coupling between a ferromagnet (FM) and an antiferromagnet (AFM) is the primary reason for the shift of the magnetic hysteresis loop [2]. However, 'bulk' spins of the AFM can also have a strong impact in tuning the exchange bias properties [3]. Spin-glass-like frustration plays a significant role on exchange bias. The interface of the FM/AFM system can also be spin-glass-like which also tunes the magnetic properties [4]. FM/spin glass (SG) is the model system to study the role of frustration on exchange bias effects.

2. RESULTS AND DISCUSSSION

In both the systems, we found the decrease of exchange bias field (H_{EB}) with cooling field (H_{FC}). Also, the exponential decay of H_{EB} and coercive field (H_C) with temperature is found in both the systems. These studies indicate the presence of spin-glass-like frustration in the Fe/IrMn and NiMn/CoFeB exchange bias systems. Further, we performed the training effect measurements and fitted the data using various models. It is found that interfacial rotatable spins relax 8 times faster than interfacial frozen spins in Fe/IrMn systems [4] whereas the relaxation ratio of rotatable and frozen spins is 21 in NiMn/CoFeB systems [5] which increases with increase in thickness of NiMn indicating the contribution of 'bulk' NiMn spins in training relaxation.

2.1. Equations

The above figure shows the fitting of the training effect data of NiMn/CoFeB samples using spin configurational relaxation model (eq. 1) and frozen and rotatable spin relaxation model (eq. 2), respectively.

$$H_E(n+1) - H_E(n) = -\gamma_H [H_E(n) - H_{E\infty}]^3 \qquad (1)$$

$$H_{EB}(n) = H_{EB\infty} + A_f \exp(-n/P_f) + A_i \exp(-n/P_i) \qquad (2)$$

3. FIGURE

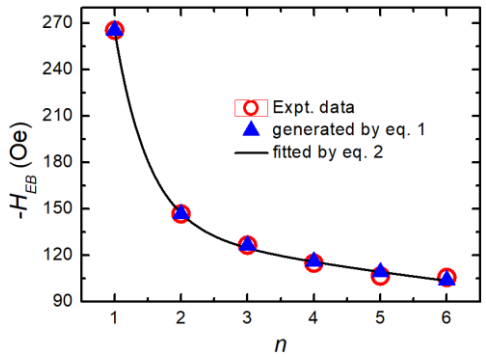

Figure 1: show the plot of H_{EB} vs loop number (n) of the sample NiMn(5 nm)/CoFeB(5 nm). The open red circles are the experimental data points, blue triangular data points are generated from eq. 1 and black solid line is the fitted data using eq. 2.

ACKNOWLEDGEMENT

The authors thank the Department of Atomic Energy (DAE) for providing the financial support.

REFERENCES

[1]. K. O'Grady et al, J. Magn. Magn. Mater., **322** (2010) 883.

[2]. K. D. Usadel and U. Nowak, Phys. Rev. B, **80** (2009) 014418.

[3] S. Nayak et al.,J. Magn. Magn. Mater., **499** (2020) 166267.

[4] S. Nayak et al., Phys. Chem. Chem. Phys., **23** (2021) 6481.

CT03

Degenerate skyrmionic states in synthetic antiferromagnets

Mona Bhukta[1,3], Braj Bhusan Singh[1], Sougata Mallick[2], Stanislas Rohart[2], and Subhankar Bedanta[1,*]

[1]Laboratory for Nanomagnetism and Magnetic Materials, School of Physical Sciences, National Institute of Science Education and Research (NISER), HBNI, Jatni 752050, India

[2]Laboratoire de Physique des Solides, Universite Paris-Saclay, CNRS UMR 8502, F-91405 Orsay Cedex, France.

[3]Institute of Physics, Johannes Gutenberg University, Staudingerweg 7, 55128 Mainz, Germany

Email: sbedanta@niser.ac.in

Abstract: Magnetic skyrmions correspond to localized whirling spin configurations, which are characterized by a topological charger (Q = ±1).There are various skyrmionics states have been evolved in recent time in different magnetic systems. Higher order skyrmions (Q >2) and coexistence of skyrmion and antiskyrmion in frustrated ferromagnets has been predicted using J1-J2-J3 classical Heisenberg model which indicate that skyrmion and antiskyrmion have more promising properties and degree of freedom in frustrated system. In this work, We have successfully modelled a SAF thin film system in which equivocation in DMI interaction between two antiferromagnetically coupled layers leads to spin frustration in both the FM layers.

1. INTRODUCTION

Skyrmion has drawn significance research interest in future magnetic logic and memory devices due to their small size and the ability to set them into motion with significantly smaller critical current densities. It is shown using micromagnetic simulation that in frustrated ferromagnets (FM) both antiskyrmion and skyrmion can exist at the same time [1]. In 2017 X. Zhang *et. al* showed that other higher order (Q>1) skyrmions could exist as a metastable state in the frustrated ferromagnets [2]. These results indicate that there are more promising properties and states of skyrmions and antiskyrmions in frustrated magnetic system.

In this work, we propose another approach of using a synthetic antiferromagnetic (SAF) system where a frustrated interaction arises due to the coupling between the magnetic textures in the FM layers, which enables the stabilization and coexistence of 6 novel elliptical topological textures.

2. THEORETICAL MODEL AND SIMULATION

Schematic of our model system of SAF where two FM layers are separated by a metallic spacer layers shown in the figure 1. Magnetic moments of the top FM layer point towards downward direction whereas magnetic moments of the bottom FM layer point towards upward direction

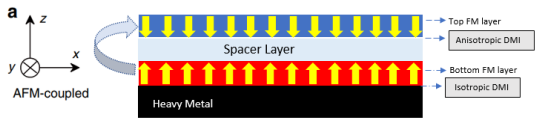

. Fig.1. Schematic of our model system

We have simulated our system using a set of extensible solvers (OXS) using the micromagnetic solver of the Object Oriented MicroMangetic Framework (OOMMF). It predicts the magnetization dynamics using the Landau-Lifshitz-Gilbert (LLG) equation. The Hamiltonian of our system is

$$E_T = \int\int \{A\sum_i[\left(\frac{d\boldsymbol{m}_i}{dx}\right)^2 + \left(\frac{d\boldsymbol{m}_i}{dy}\right)^2] + D_{iso}\left(L^x{}_{1,xz} + L^y{}_{1,yz}\right) + D_{aniso}\left(L^x{}_{2,xz} - L^y{}_{2,yz}\right) + K\sum_i\left(m_{i,z}^2\right) - J_{RKKY}\,\boldsymbol{m}_1.\boldsymbol{m}_2\}dxdy$$

CT01

Where m_i represent the normalized spin at site i. J_{ex}, D K and J_{RKKY} are the strength of exchange coupling, DMI interaction Perpendicular Magnetic Interaction and RKKY interaction respectively.

3. RESULTS AND DISCUSSION

When the top and bottom layers containing their natural textures (i.e. antiskyrmion and skyrmion, respectively) are antiferromagnetically coupled, the interlayer coupling cannot completely be in energetically favourable condition in all directions. Hence, there will be an energy frustration in the system. We have simulated the pro-posed model to explore the effect of the strength of the RKKY coupling on the textures by relaxing 9 different initial textures combining W= 1, 0 and -1 in both the layers. At intermediate coupling limit of J_{RKKY} , we obtained textures with energy frustration as well as found the existence of Q = 0 skyrmion and able to stabilize the skyrmion and antiskyrmion in a single film as shown in below figure 2.

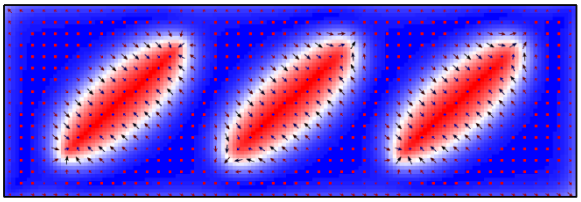

Fig.2. Existence of three different kinds of topological charges (Q= 1, -1 and 0) in the top FM layer at intermediate coupling limit.

ACKNOWLEDGEMENT

The authors thank DAE, Govt. of India and the Indo-French collaborative project supported by CEFIPRA for providing the research funding. BBS acknowledges DST for INSPIRE Faculty fellowship.

REFERENCES

[1]. A. Leonov *et al*, Nature communications, **6,** 8275 (2015).

[2]. X. Zhang *et al*, Nature. Communications **8,** 1717 (2017).

CT04

Effect of random anisotropy in stabilization of skyrmions and antiskyrmions

Gajanan Pradhan[1], Brindaban Ojha[1], Subhankar Bedanta[1]

[1]Laboratory for Nanomagnetism and Magnetic Materials (LNMM), School of Physical Sciences, National Institute of Science Education and Research (NISER), HBNI, P.O.- Bhimpur Padanpur, Via Jatni, 752050, India

Email: g.pradhan@inrim.it

Abstract: Ever increasing demand of skyrmion manipulation in nanodevices has brought up interesting research to understand the stabilization of these topologically protected chiral structures. To understand the actual shape and size of skyrmions and antiskyrmions observed experimentally, we have performed micromagnetic simulations to investigate their stabilization in presence of random anisotropy in magnetic thin film system. We show via simulations that the shape of a skyrmion and an antiskyrmion can get distorted due to the presence of different local anisotropy energy. The skyrmion or antiskyrmion shape gets distorted with the presence of random anisotropy energy in the system.

1. INTRODUCTION

Magnetic skyrmions are non-trivial particle-like configuration of spins having topological protection. The understanding of nucleation and propagation of an individual skyrmion in a nanotrack of magnetic thin film is important for future skyrmion based applications [1, 2]. Formation of skyrmions in thin films is prominently due to the presence of Dzyaloshinskii-Moriya interaction (DMI) in the system. Another special type of skyrmion known as the antiskyrmion was first predicted to exist in systems having bulk DMI and has recently been observed in Heusler compounds with D_{2d} symmetry at room temperature. It has also been predicted that magnetic thin films having anisotropic iDMI with C_{2v} symmetry like Au/Co/W films can also host potential antiskyrmions[3]. In our simulations, the net anisotropy at each local site is the vector addition of uniaxial anisotropy and the random anisotropy parameters. The net anisotropy thus has different magnitude and direction for each site. The value of uniaxial anisotropy constant (K_u) and random anisotropy constant (K_r) are varied for which the shape and size of stable spin configurations of skyrmion and antiskyrmion are observed in detail.

2. EXPERIMANTAL METHODS

The three-dimensional micromagnetic simulations are performed OOMMF. The simulations are performed for a 1 nm thick square nanoelement over an area of 200 nm × 200 nm. The values of α and γ are 0.3 and -2.211× 105 m $A^{-1}s^{-1}$, respectively. We have considered the Ms, the exchange stiffness (A) and the DMI constant to be 580 kA m^{-1}, 15 pJm^{-1} and 3.8 mJm^{-2}, respectively.

3. RESULTS AND DISCUSSION

We have varied the value of uniaxial anisotropy constant (K_u) and random anisotropy constant (K_r) to understand the change in shape and size of skyrmions and antiskyrmions. Fig. 1 shows the formation and stabilization of a Neel skyrmion in a square nanoelement. The effective anisotropy for each local sites is the vector addition of uniaxial and random anisotropy. The skyrmion or antiskyrmion size is affected due to this spacial variation of net anisotropy over the simulation area. Fig. 1(a)–(c) show the evolution of anti-skyrmionic state. The antiskyrmion size increases and reaches a squared antiskyrmionic state. The squareness of the antiskyrmion can be attributed to high M_s value. The increase in size of the antiskyrmion in case II is not large as compared to I since K_r is significantly less than the Ku. However, the shape of the final stable antiskyrmionic state is distorted as shown in Fig. 1(f). This change in shape of the antiskyrmion is due to the inclusion of local random anisotropy energy in the system. Similar studies have been performed in skyrmions. The effective size of the stable state of skyrmion (Sk) and antiskyrmion (ASk) was measured for different random anisotropy, uniaxial anisotropy and DMI energies.

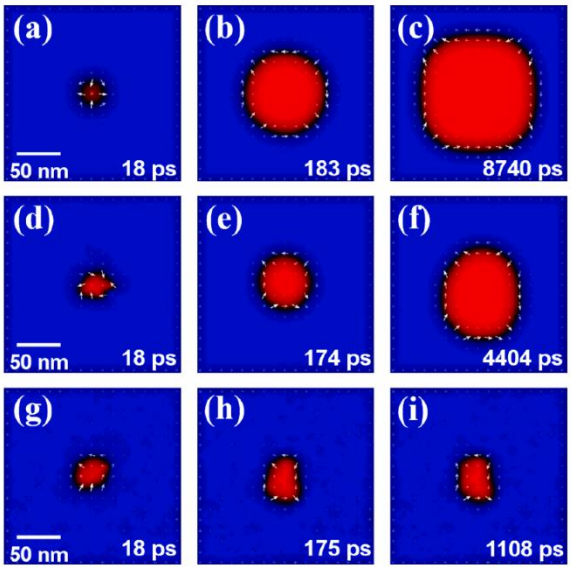

Fig.1. Formation and evolution of an antiskyrmion from initial ferromagnetic state for three different cases. In case I (a)–(c), K_u = 0.8 MJm^{-3} and K_r = 0 MJm^{-3}. In case II (d)–(f), K_u = 0.8 $MJm^{-3}$and K_r = 0.1 MJm^{-3} ($K_r \ll K_u$). In case III (g)–(i), K_u = 0.8 MJm^{-3} and K_r = 0.8 MJm^{-3} ($K_r = K_u$).

ACKNOWLEDGEMENT

We would like thank DAE, Govt. of India and CEFIPRA for research funding.

REFERENCES

1. W. Jiang, et al. Science 349.6245 (2015): 283-286.
2. A. Hrabec, et al. Nat comm 8.1 (2017): 1-6.
3. A.K. Nayak, et al. Nature 548.7669 (2017): 561-566.

CT05

Effect of thermal annealing on the interfacial Dzyaloshinskii-Moriya interaction in perpendicularly magnetized Ta/Pt/CoFeB/Pt ultrathin films

B. Ravi Kumar, Sreekar Guddeti, and P. S. Anil Kumar*
Department of Physics, Indian Institute of Science, Bangalore-560012, Karnataka, India

Magnetic field driven domain-wall motion in the creep regime is investigated with Kerr microscopy in out-ofplane magnetized as-deposited and annealed Ta/Pt/CoFeB/Pt multilayers. In addition to the effect of thermal annealing on the quasi-static magnetic properties of Ta (3 nm)/Pt (3 nm)/CoFeB (t_{CoFeB} nm)/Pt (2 nm) film stacks where $t_{CoFeB} = \{0.72, 0.93\}$, the study focuses on the modified interfacial Dzyaloshinskii-Moriya interaction (iDMI) that governs the dynamics of chiral domain walls. The strength of the iDMI decreases with increase in both t_{CoFeB} at a fixed annealing temperature, and annealing temperature for a fixed t_{CoFeB}. While the former behaviour arises due to the interfacial nature of iDMI, the latter correlates with the annealing induced suppression of magnetization and enhancement of interface roughness that could be respectively ascribed to B-segregation and Co-Fe-Pt intermixing.

CT06

Effect of MoS_2 on magnetization reversal, magnetic domain structures and anisotropy of MoS_2/CoFeB heterostructures

V. Thiruvengadam, Abhisek Mishra, Shaktiranjan Mohanty and Subhankar Bedanta
Laboratory for Nanomagnetism and Magnetic Materials (LNMM), School of Physical Sciences, National Institute of Science Education and Research (NISER), HBNI, P.O. - Bhimpur, Padanpur, Via-Jatni, 752050, India
Email: thiru.baskar@gmail.com

1. INTRODUCTION

Heterostructures of transition metal dichalcogenide(TMD)/ferromagnet(FM) have been studied for various spin based phenomena such as Anomalous Hall effect, Rashba spin-orbit coupling, quantum spin Hall effect, spin-valley locking, perpendicular magnetic anisotropy, spin injection and spin orbit torque [1-4]. All these spin based phenomena in TMD/FM heterostructures are due to the combined effect of high spin –orbit coupling in TMD and spin polarization behaviour of FM materials. However, the effect of TMD on magnetic properties such as magnetization and domain reversal of FM has not been studied so far. Therefore the focus of this work is to study the effect of MoS_2 and its thickness on magnetization reversal, magnetic domain structures and anisotropy of CoFeB in MoS_2/CoFeB heterostructures. In this context I will present my research work divided into two parts (i) fabrication of MoS_2 thin film; (ii) Magnetic studies on MoS_2/CoFeB heterostructures.

2. EXPERIMENTAL TECHNIQUES

Crystalline MoS_2 films were fabricated by two steps; (a) RF magnetron sputtering of MoS_2 films followed by (b) sulfurization of as deposited films. Resulting thin films were characterized using Raman spectroscopy and scanning electron microscopy. MoS_2(x nm)/CoFeB heterostructures with x = 6 & 28 nm were fabricated using sputtering technique. Magnetic studies of these heterostructures were performed using magneto optic Kerr effect (MOKE) based microscopy, ferromagnetic resonance spectroscopy (FMR).

3. FABRICATION OF MOS_2 THIN FILM

In the first part of my presentation, I will discuss about the effect of sulphurization temperature on sputtered MoS_2 thin film characterized using Raman spectroscopy [5]. This study confirms that as sputtered

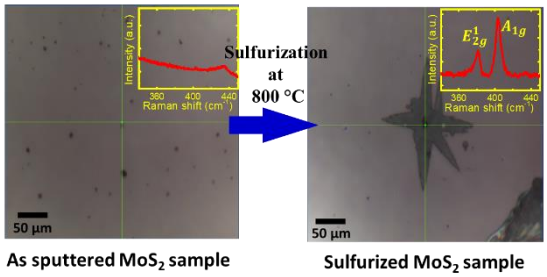

MoS_2 films are discontinuous, amorphous in nature and it crystalizes into a layered structure during sulphurization at temperature ≥ 750 °C (fig. 1).

Fig. 1. Crystallization of as deposited amorphous MoS_2 by sulfurization reaction at 800 °C

4. MAGNETIC STUDIES ON MoS_2/CoFeB HETEROSTRUCTURES

In the second part, I will discuss the effect of MoS_2 on the magnetization reversal, magnetic domain structure and anisotropy of the adjacent CoFeB thin film in MoS_2/CoFeB heterostructures (fig. 2a) [6]. Magnetic studies on the MoS_2/CoFeB heterostructures exhibit an angle dependent change in magnetic domain structure and coercivity of magnetic hysteresis loops (fig. 2b). This clearly indicates that the MoS_2 induces an uniaxial anisotropy on CoFeB in MoS_2/CoFeB heterostructures.

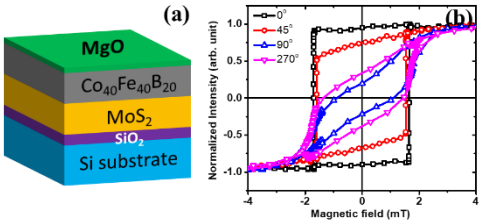

Fig. 2. (a) Schematic of MoS_2/CoFeB heterostructure, (b) angle dependent magnetic hysteresis loops of the heterostructure

5. SUMMARY

Ultra-thin crystalline MoS_2 films were successfully fabricated by sputtering technique followed by sulfurization process. The MoS_2 layer in the MoS_2/CoFeB heterostructures induces an uniaxial anisotropy on CoFeB. The induced anisotropy found to increases with increase in thickness of MoS_2.

ACKNOWLEDGEMENT

We acknowledge the financial support by the DAE, the DST-SERB of government of India, the DST-Nanomission [project sanction No. SR/NM/NS- 180 1018/2016(G)]

REFERENCES

[1]. S. M. Ng et al, ACS nano **6** (2020) 7077
[2]. Y. Liu et al, Nano-Micro Letters **12** (2020) 1-26
[3]. T. Garandel et al, Physical Review B **7** (2017) 075402
[4]. J. Hidding et al, Frontiers in Materials **7** (2020) 383
[5]. V. Thiruvengadam et al, Advanced Materials Letters, **12** (2021) 21021603
[6]. V. Thiruvengadam et al, https://arxiv.org/abs/2108.05130

CT07

Origin of exchange bias in nanocrystalline $CoCr_2O_4$

S. Goswami[a], P. Gupta[b], S. Bedanta[b,c*], M. Chakraborty[a†], D. De[a,d‡]
[a]Material Science Research Lab, The Neotia University, 24 Pgs (South), West Bengal 743368, India.
[b]Laboratory for Nanomagnetism and Magnetic Materials, School of Physical Sciences, National Institute of Science Education and Research, HBNI, Bhubaneswar, Odisha 752050, India.
[c]Center for Interdisciplinary Sciences, National Institute of Science Education and Research, HBNI, Bhubaneswar, Odisha 752050, India.
[d]Sukumar Sengupta Mahavidyalaya, Keshpur, Paschim Medinipur 721150, West Bengal, India.
Email: ([*]sbedanta@niser.ac.in, [†]manashi.chakraborty@tnu.in, [‡]debajyoti.de@tnu.in)

Abstract: This article reports exchange bias (EB) and memory effect in nanocrystalline $CoCr_2O_4$ with a detailed understanding of the origin of the observed effects. Despite orthodox core-shell interaction or 'surface' domination, conventional EB effect is observed where the EB field (H_E) sharply decreases with temperature and vanishes over the spiral ordering temperature (T_S) of the samples. Results indicate that the exchange bias is due to inherent magnetic inhomogeneity: interaction between spiral spin order and collinear ferrimagnetic order below T_S. A sample with particle size 7 nm reveals the characteristics of superspin-glass (SSG), confirmed by magnetic memory effects both in time (t) and temperature (T) dependent magnetization protocols.

1. INTRODUCTION

Here we report, a comparative study of three samples of $CoCr_2O_4$ with different particle sizes and interparticle interactions focusing on EB and magnetic memory effect. Two of them are nanocrystalline with average particle sizes 12 nm and 7 nm, where the later is embedded in silica (SiO_2) matrix. The third one is a bulk (particle size >150 nm) sample of $CoCr_2O_4$, prepared via the same synthesis route. We have given an explanation on the origin of EB and highlighted distinct magnetic properties of nanocrystalline $CoCr_2O_4$ than their bulk counterpart [1,2].

2. RESULT AND DISCUSSION

Nanocrystalline $CoCr_2O_4$ samples of different particle sizes are prepared using conventional sol-gel route. For the preparation of the bulk sample (with average particle size >150 nm) of $CoCr_2O_4$, the procedure as followed for nanocrystalline sample is repeated with final calcination at 1000 °C for 24 h. For better readability the three samples of $CoCr_2O_4$ with average particle sizes 12, 7 and 150 nm have been named as CCO–12, CCO–7@SiO_2 and CCO–B, respectively. Characterizations of the samples are performed by Transmission Electron Microscopy (TEM), powder X-ray diffractometer (PXRD). Time and temperature dependent dc and ac magnetization measurements are performed via commercial SQUID magnetometer in zero field cooled (ZFC) and field cooled (FC) modes.

Temperature dependent magnetization ($M(T)$), measured at H = 10 mT in ZFC and FC modes are recorded for CCO–12, CCO–7@SiO_2 and CCO–B, where transition from ferrimagnetic to non-collinear spiral, and finally a lock-in transition is visible. For the analysis of EB effect, magnetic hysteresis (M-H) loops are recorded at 5 K between ± 9 T (for CCO–12) / ± 7 T (for CCO–7@SiO_2 and CCO–B) after cooling the samples from the paramagnetic region in FC (H_{cool} = 0.05, 0.5, 1, 2.5, 5 T) and ZFC modes. EB effect is also studied for wide range of temperatures. Carefully noticing the EB effect for all the three samples one may find that, H_E possess maximum value at lowest temperature (5 K), then decreases sharply with increase in T and experiences a sudden loss soon after crossing the spin-spiral ordering temperature (T_S).

Memory effect in T variation of FC and ZFC magnetizations, isothermal relaxation and memory in isothermal remnant magnetization (IRM) are recorded for CCO–7@SiO_2.

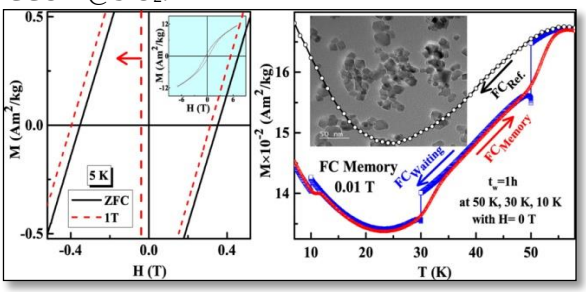

Fig 1: EB and memory effect (in thermal variation of FC magnetization) for CCO–7@SiO_2.

3. CONCLUSION

In this article, the magnetic properties of $CoCr_2O_4$ in nano and bulk forms are studied focusing on the exchange bias effect. Detailed study is performed for three samples of the same composition where (i) surface spins dominate (CCO–12), (ii) where interparticle interaction plays an important role (CCO–7@SiO_2) and (iii) where surface spins are less active (CCO–B). Dependence of EB with T_S indicates origin of exchange interaction arising from competition between collinear FiM spins and conical spiral spins below the spin-spiral transition (T_S).

REFERENCES

[1] S. Goswami, P.K. Manna, S. Bedanta, S.K. Dey, M. Chakraborty, D. De *Journal of Physics D: Applied Physics* **53** (2020), 305303.
[2] S. Goswami, P. Gupta, S. Bedanta, M. Chakraborty, D. De *Journal of Alloys and Compounds* **890** (2022), 161916.

CT08

Device geometry dependent deterministic skyrmion generation from a skyrmionium

Adyashakti Dash, Brindaban Ojha, Shaktiranjan Mohanty, AshishK Moharana, Subhankar Bedanta∗
Laboratory for Nanomagnetism and Magnetic Materials, School of Physical Sciences,
National Institute of Science Education and Research (NISER), HBNI, Jatni 752050, India
Email: adyadash15@gmail.com, sbedanta@niser.ac.in

Abstract: A magnetic skyrmionium can be perceived as an association of two magnetic skyrmions with opposite topological charges. In this work, we have investigated the transformation of skyrmionium into multi-skyrmionic states via domain wall (DW) pairs in three different devices with variable geometric configurations. The same device geometries were considered for single ferromagnetic layer as well as synthetic antiferromagnetic (SAF) system. It is observed that by tuning the current density, deterministic generation of skyrmions is possible via the spin transfer torque (STT). The proposed device is efficiently adjustable to change the number of skyrmions. The results may lead to development of skyrmion-based devices for neuromorphic and unconventional computing.

1. INTRODUCTION

Magnetic skyrmions are topologically protected, localized non-collinear textures which have antiparallel magnetization core with respect to the periphery.[1] They have been flagged as promising candidate for efficient storage and information processing for their longer stability, compact size, non-volatility and gyrodynamics.[1]–[3] Various concepts and prototypes for skyrmion-based devices have been proposed to study dynamics of isolated as well as train of skyrmions.[4] The influence of edge geometries and defects on phase transitions and evolution of spin textures have already been studied earlier but still needs further investigations.[5]–[7] However, the deterministic generation of multi skyrmionic states has not been studied extensively. In this work, we perform a systematic study demonstrating the conversion of a skyrmionium into various skyrmionic states using three different geometric designs. We have also studied the effect of current density to achieve different states of skyrmion in a single FM layer as well as in a SAF. The demonstrated transformation process could lead to development in skyrmion-basedspintronics. The obtained results are interesting for interdisciplinary research on skyrmion-based neuromorphic and unconventional computing.

3. METHODOLOGY

Micromagnetic simulation using Object Oriented MicroMagnetic Framework (OOMMF) with the Dzyaloshinskii-Moriya interaction (DMI) extension is performed using sample of 800 nm × 300 nm × 0.6 nm. Time-dependent spin dynamics for CIP geometry is used for translation as shown in fig. 1.

ACKNOWLEDGEMENT

The authors thank DAE, Govt. of India and the Indo-French collaborative project supported by CEFIPRA for providing the research funding.

REFERENCES

1] T. H. R. Skyrme,Proc. Roy. Soc. Lond. A, vol. 260, pp. 127–138, 1961.
[2] N. Kiselevet al.,Journal of Physics D: Applied Physics, vol. 44, no. 39, p. 392001, 2011.
[3] A. Fertet al.,Nature Reviews Materials, vol. 2, no. 7, pp. 1–15, 2017.
[4] K. Everschor-Sitteet al.,Journal of Applied Physics, vol. 124, no. 24, p. 240901, 2018.
[5] W. Jianget al.,Science, vol. 349, no. 6245, pp. 283–286, 2015.
[6] X. Zhanget al.,Phys. Rev. B, vol. 94, p. 094420, Sep 2016.
[7] X. Chenet al.,Applied Physics Letters, vol. 111, p. 202406, 11 2017.

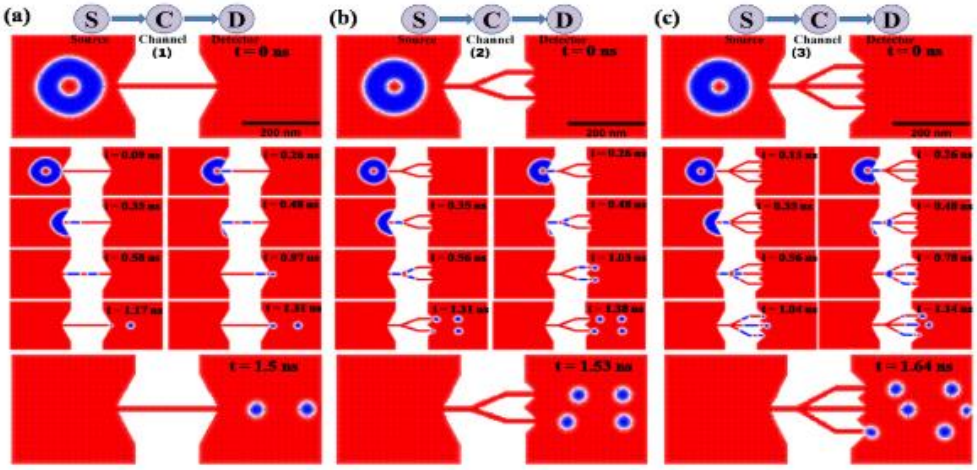

Fig.1. The conversion of skyrmionium into various states of skyrmions in (a) 1-1 channel design: Dvc-1 (b) 1-2 channel design: Dvc-2 (c) 1-3 channel design: Dvc-3 for single FM layer.

CT09

Spin pumping with low spin orbit coupling material C_{60} in a$La_{0.67}Sr_{0.33}MnO_3/C_{60}$ system

Aditya Kumar[a,b], Pushpendra Gupta[a], Purbasha Sarangi[a], Isita Pandey[a], Abhisek Mishra[a], Subhankar Bedanta[a]

[a]*Laboratory of Nanomagnetism and Magnetic Materials (LNMM),*

School of Physical Sciences, National Institute of Science Education and Research (NISER),

HBNI, P.O.- Bhimpur Padanpur, Via -Jatni, 752050, India

[b]*Corresponding author: aditya.kumar@niser.ac.in*

Keywords: Spin-pumping, ISHE, Anti-damping, Fullerene

Transmission and detection of spin current are crucial for the implementation of spintron- ics. Many heavy metals and oxides have been popularly studied as spin current detectors dueto their high spin orbit coupling. This method of spin current generation and detection hasalso been studied in structures with fullerene (C_{60}) as a spacer layer between $La_{0.67}Sr_{0.33}MnO_3$ (LSMO) and Pt. However, LSMO/C_{60} structure has not been studied separately. Recent works have shown that C_{60} shows curvature enhanced SOC. LSMO on the other hand is anFM with high spin polarization and has been studied 'to show high spin pumping voltage in FM/HM structure. With this background, we studied magnetization dynamics in LSMO/C_{60} bilayer structure. We performed CPW based FMR to analyse the effect of C_{60} layer on the magnet damping. We found that the bilayer samples showed a lower value of the Gilbert damping constant compared to the monolayer sample. We also performed ISHE measure- ments of the samples to confirm and quantify spin pumping in the system. We measuredspin pumping voltage (V_{SP}) in bilayer samples to be close to $2\mu V$. These results show the presence of anti-damping in the LSMO/C_{60} system and detection of spin current in a low spin orbit coupling material.

CT10

Deterministic nucleation and efficient motion of skyrmions

Sougata Mallick[1,2], Sujit Panigrahy[1], Brindaban Ojha[3], Héloïse Damas[4], Michel Hehn[4], Gajanan Pradhan[1], André Thiaville[1], Nicholas Reyren[2], Karim Bouzehouane[2], Juan-Carlos Rojas-Sanchez[4], Subhankar Bedanta[3], Vincent Cros[2], Albert Fert[2], and Stanislas Rohart[1]

[1]Laboratoire de Physique des Solides, Université Paris-Sud, Université Paris-Saclay, Orsay Cedex, France
[2]Unité Mixte de Physique, CNRS, Thales, Université Paris-Saclay, Palaiseau, France
[3]LNMM, SPS, National Institute of Science Education and Research, Bhubaneswar, HBNI, Jatni, India
[4]Université de Lorraine, CNRS, Institute Jean Lamour, F-54000 Nancy, France

Email: sougata.physics@gmail.com; sougata.mallick@cnrs-thales.fr

Abstract: Magnetic skyrmions are quasiparticle-like chiral textures that appear in materials with broken inversion symmetry. Implementation of skyrmions in data storage technologies requires the ability of stabilizing them at room temperature and efficiently driving the textures under spin-orbit torque (SOT). Few of the challenges to implement skyrmions in data storage devices are stabilizing them in the absence of external magnetic field, requirement of low threshold current density to drive the skyrmions, achieving high skyrmion mobility, moving them in straight line with reduced skyrmion Hall effect (SkHE), etc. In this presentation, I will discuss some of our results in the aforementioned context and outline a future perspective to improve the existing results.

1. INTRODUCTION

Requirement of device miniaturization and low power consumption has shifted the research towards low dimensional magnetic solitons viz. magnetic vortices, chiral domain walls (DWs), skyrmions, etc. A collective effort has been focussed on addressing the key aspects of skyrmions owing to their exotic potential applications in next generation racetrack memory, stochastic, neuromorphic computing, etc. [1]. In the following, we address some of the important features of realizing skyrmion based spintronic devices:

2. DISCUSSION

(i) Stabilizing '0' field skyrmion: Information process in skyrmionic devices is based on controlled nucleation and motion of individual textures. This compels most experimental designs to accommodate external field so that isolated low density skyrmions can be stabilized and manipulated individually. However, requirement of external magnetic field leads to additional cost of power and area overhead in the devices. Applying a field becomes further complicated due to the vanishing magnetization of new promising systems such as synthetic antiferromagnets or ferrimagnets. In this context, we present a new methodology of stabilizing skyrmions in the absence of any magnetic field by precise control of the thickness (anisotropy) of the ferromagnetic layer (here bilayer of Co thin film). We increase the characteristic length [2] of the films till the limit where the system gathers enough energy to retain the skyrmionic textures at remanence. We further demonstrate that the skyrmions can be nucleated and moved under current pulses without altering the stability in the absence of field.

(ii) Moving skyrmions with low threshold current: A crucial criterion for real life applications of skyrmionic devices is requirement of a low power to drive them. This makes the materials with low pinning energy landscape indispensable. It has been reported that CoFeB, which is essentially an amorphous soft magnetic material, crystallizes to bcc structure after annealing leading to perpendicular anisotropy in the system. Presence of an amorphous phase (which subsequently crystallizes to bcc phase) leads to low density structural defects in comparison to the 3d ferromagnetic materials [3]. In this context, we use thin films of $Pt/Co_{40}Fe_{40}B_{20}/MgO$ thin films to host the skyrmions. We show that the skyrmions start moving at a current density of $\sim 0.8\times10^{11}$ A/m^2, which is significantly lower than the existing literature.

(iii) Efficient mobility using ferromagnetic materials: One fundamental problem that hinders implementation of skyrmions in racetrack memory devices is not being able to move them in straight path due to SkHE. Further, conventional ferromagnets labour under some basic limitations viz. stray field restriction of smallest bit size, precessional dynamics limiting the operating speeds, etc. However, antiferromagnets (AFM) lack stray fields and exhibit faster dynamics than ferromagnets. Interestingly, in ferrimagnets the sublattices with opposing spin orientations can completely compensate each other to achieve behaviour similar to that of an AFM, with additional flexibility of tuning the properties with temperature, being individually detectable, etc. In this context, we use amorphous rare earth transition metal (RE-TM) based ferrimagnets (GdFeCo, TbCo) to host skyrmions and drive them efficiently with reduced SkHE under the strong intrinsic SOTs [4] and gradient-driven DMI [5]. We have stabilized skyrmions in the ferrimagnetic heterostructures and the experiments regarding the current induced skyrmion motion is ongoing.

ACKNOWLEDGEMENT

SM acknowledge CEFIPRA (IFC/5808-1/2017), ANR Topsky (17-CE24-0025), and DARPA TEE (MIPR#HR0011831554) for the financial support.

REFERENCES

[1] A. Fert *et al.*, *Nat. Rev. Mat.* **2**, 17031 (2017)
[2] O. Boulle *et al.*, *Nat. Nano.* **11**, 449 (2016)
[3] C. Burrowes *et al.*, *APL* **103**, 182401 (2013)
[4] D C-Berrocal *et al.*, *Adv. Mat.* **33**, 2007047 (2021)
[5] Z. Zheng *et al.*, *Nat. Comm.* **12**, 4555 (2021)

CT11

Metal/$SrTiO_3$ and $KTaO_3$ two-dimensional electron gases for spin-to-charge conversion

Srijani Mallik[1], Luis M. Vicente-Arche[1], Maxen Cosset-Cheneau[2], Sara Varatto[1], Julien Brehin[1], Paul Noël[2], Diogo Vaz[1], Felix Trier[1], Tanay A. Gosavi[3], Chia-Ching Lin[3], Dmitri E. Nikonov[3], Ian A. Young[3], Anke Sander[1], Agnès Barthélémy[1], Jean-Philippe Attané[2], Laurent Vila[2] and Manuel Bibes[1]

[1]Unité Mixte de Physique, CNRS, Thales, Université Paris-Saclay, 91767 Palaiseau, France
[2]Université Grenoble Alpes, CEA, CNRS, INP, IRIG-Spintec, Grenoble, France
[3]Components Research, Intel Corporation, Hillsboro, Oregon 97124, USA

Email: srijani.mallik@cnrs-thales.fr

Abstract: Since their discovery in 2004 [1], two-dimensional electron gases (2DEGs) based on $SrTiO_3$ (STO) have been shown to possess a wide array of fascinating properties viz. superconductivity, Rashba spin-orbit coupling, gate voltage tunability, magnetism etc. While these discoveries challenge our understanding of quantum matter, they also trigger some interest for technological applications. Recently, Intel corporation has proposed a future spin-based logic device where the reading part relies on the spin-charge conversion making the oxide based 2DEGs a potential candidate. Here, we have discussed the formation of 2DEGs in STO and KTO by deposition of different reactive metals and compared their properties to achieve higher spin to charge conversion efficiencies.

1. INTRODUCTION

Recent studies on oxide spintronics relies exceedingly on the efficient spin-charge interconversion property of the 2DEGs which possesses a finite Rashba spin-orbit coupling. STO-based 2DEGs are usually generated by the deposition of epitaxial oxides like $LaAlO_3$ or of reactive metals such as Al [1, 2]. Along with STO, $KTaO_3$ (KTO) is another promising oxide system to harbor the 2DEG by depositing reactive metals [3]. Such 2DEGs are highly promising for the interconversion between charge and spin currents through the direct and inverse Edelstein and spin Hall effects. It is expected that KTO may possess a larger spin–orbit coupling in comparison to STO as Ta is a 5d element and heavier than Ti. In this work, we compare the formation and magnetotransport as well as spin-charge conversion properties of 2DEGs generated in STO and KTO by the growth of Al, Ta and Y metals.

2. EXPERIMENTAL DETAILS

Ultrathin films of Al, Ta and Y were grown on single crystalline STO and KTO substrates at room temperature using magnetron sputtering technique. The valence states of Ti and Ta for STO and KTO, respectively were measured both in-situ and ex-situ by X-ray photoelectron spectroscopy (XPS). Further, the transport properties were measured using physical properties measurement system (PPMS). Finally, the spin to charge conversion for all the samples were studied by varying the back gate voltage between $\pm$200 V in a cavity based ferromagnetic resonance system with 9.68 GHz frequency.

3. RESULTS AND DISCUSSION

Both in-situ and ex-situ XPS study on STO and KTO based samples revealed the quantification of reduced Ti or Ta states associated with 2DEG formation, their reoxidation by exposure to the air, and the transformation of the metal into its binary oxides. The carrier densities and mobilities of all the samples are extracted from the magnetoresistance and Hall curves measured during the magnetotransport measurements [3, 4]. The reduction of Ti and Ta states upon deposition of the reactive metals as well as the carrier densities of the 2DEGs strictly depend on the work function and the oxide formation enthalpy of the metals [4]. Finally, we investigate the spin-charge conversion as a function of gate voltage by performing spin-pumping ferromagnetic resonance experiments on similar metal/STO and KTO samples with a capping of an extra NiFe layer. Here the NiFe layer acts as the ferromagnetic layer to inject a spin-polarized current in the adjacent 2DEG. The trends for spin to charge conversion efficiency for different metal/STO systems provide a systematic study as a function of the carrier density and the transparency of the metal oxide tunnel barrier [4]. Further a comparison between the figure of merit of the spin-charge conversion has been performed [3]. Our results strongly influence the path to choose the correct metal/STO and KTO interface to achieve higher spin to charge conversion for future spin-based information readout e.g., Magneto Electric Spin Orbit (MESO) logics proposed by Intel corporation [5].

ACKNOWLEDGEMENT

The authors acknowledge support from the ERC Advanced Grant No. 833973 “FRESCO,” and Intel’s Science and Technology Center – Feinman.

REFERENCES

[1] A. Ohtomo and H. Y. Hwang, Nature (London) 427, (2004) 423.
[2] T. C. Rödel *et al*., Adv. Mater. 28, (2016) 1976.
[3] L. M. Vicente-Arche et al., Adv. Mater. (2021)
[4] L. M. Vicente-Arche, S. Mallik *et al.*, Phys. Rev. Mater. 5, (2021) 064005.
[5] S. Manipatruni *et al*., Nature (London) 565, (2019) 35.

CT12

Two-dimensional Heterostructure Field Effect Transistors with One-Dimensional electrical contacts leading to enhanced electrical performance and Ultra-Low Noise

Aroop K. Behera[1], Charles Thomas Harris[2,3], Douglas V. Pete[2,3], Collin J. Delker[3], Per Erik Vullum[4], Marta B. Muniz[5,6], Ozhan Koybasi[7], Takashi Taniguchi[8], Kenji Watanabe[9], Branson D. Belle[5], and Suprem R. Das[*,1,10]

[1] Industrial and Manufacturing Systems Engineering, Kansas State University, Manhattan, Kansas 66506, USA
[2] Center for Integrated Nanotechnologies, Sandia National Laboratories, Albuquerque, New Mexico 87123, USA
[3] Sandia National Laboratories, Albuquerque. New Mexico 87185, USA
[4] Department of Materials and Nanotechnology, SINTEF, Høgskolringen 5, Trondheim, NO-7034, Norway
[5] Department of Sustainable Energy Technology, SINTEF, Forskningsveien 1, 0373, Norway
[6] Institut de Physique de la Matière Complexe, Ecole Polytechnique Fèdèrale de Lausanne (EPFL) 1015 Lausanne, Switzerland
[7] Department of Microsystems and Nanotechnology, SINTEF DIGITAL, Oslo, Norway
[8] Research Center for Fundamental Materials, National Institute for Materials Science. 1-1 Namiki, Tsukuba, 305-044, Japan
[9] International Center for Materials nanoarchtectonics, National Institute for Materials Science, 1-1 Namiki, Tsukuba, 305-044, Japan
[10] Electrical and Computer Engineering, Kansas State University, Manhattan, Kansas 66506, USA
*Contact Author: srdas@ksu.edu

Abstract:
Two-dimensional heterostructure field effect transistors (2D-HFETs) with one-dimensional edge contacts have shown impressive electrical transport properties with ultra-high mobility values. A lot of work concerning the *1/f* low frequency noise (LFN) has already been done on graphene FETs fabricated on SiO_2 with surface contacts, however such studies on heterostructure FETs with 1-D contacts are extremely limited. In this talk we present a systematic temperature dependent electrical transport and low-frequency noise study on our edge contacted single layer atomically thin graphene channel encapsulated by hexagonal boron nitride to show ultra low Hooge's noise parameter of 10^{-5}. We model the measured electrical transport characteristics on the basis of underlying scattering mechanisms caused by the interactions of charge carriers and relevant phonons to correlate the high electrical performance to the observed noise behavior. Our study provides a pathway to fabricate low-noise 2D graphene-based FETs for future use in digital electronics.

CT13

Josephson junctions containing Ni/Ru/Ni synthetic antiferromagnets

Swapna Sindhu Mishra, Reza Loloee, Norman Birge
Department of Physics and Astronomy, Michigan State University, East Lansing, MI 48824, USA
Email: mishras7@msu.edu

Abstract: Josephson junctions containing ferromagnetic layers have applications in cryogenic memory. Phase control has been successfully demonstrated with spin-valve devices containing a Ni fixed layer and a NiFe free layer [1,2]. However, the magnetic switching reliability and critical current magnitude of these junctions need to be further improved. One idea to improve the switching reliability is to replace the thin Ni fixed layer with a thicker unbalanced Ni/Ru/Ni synthetic antiferromagnet (SAF). In this work, we take the initial step of characterizing the magnetic properties and measuring the supercurrent transmission through balanced Ni/Ru/Ni SAFs [3]. We observe that the supercurrent decays slowly with Ni thickness.

1. INTRODUCTION

There is rich physics at the superconductor-ferromagnet interface. The ground state phase difference in Josephson junctions containing thin ferromagnets can be toggled between "0" and "π" states, making them good candidates for use in a cryogenic memory. A prototype of this Josephson Magnetic Random Access Memory has been developed by Northrop Grumman with Ni as a fixed layer and NiFe as a free layer in a spin-valve configuration [2]. However, thin Ni has multidomain switching and can affect the magnetic reliability of the device. One idea is to replace the thin Ni with a thicker unbalanced Ni/Ru/Ni SAF. In this work, we study the magnetic and transport properties of balanced Ni/Ru/Ni SAFs to gauge their viability.

2. THIN FILMS

For Ni(2.0)/Ru(d_{Ru})/Ni(2.0) thin films, we found the 1st antiferromagnetic peak at 0.9 nm and the 2nd peak at 2.3 nm (Fig. 1) [3].

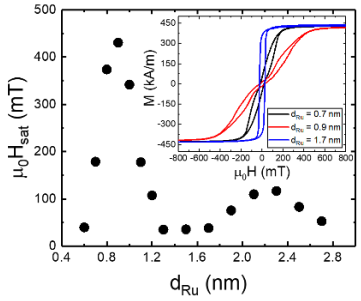

Fig.1. Saturation field vs Ru thickness in Ni(2.0)/Ru(d_{Ru})/Ni(2.0) thin films. **Inset**: M vs H curves of selected samples [3].

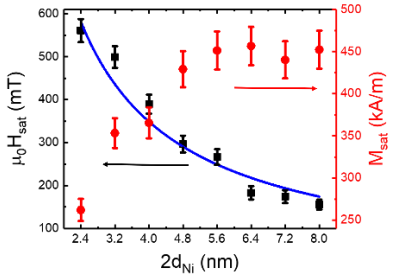

Fig.2. Saturation field and moment vs total Ni thickness in Ni(d_{Ni})/Ru(0.9)/Ni(d_{Ni}) thin films [3].

For Ni(d_{Ni})/Ru(0.9)/Ni(d_{Ni}) samples, we found that H_{sat} behaves as expected and M_{sat} increases with $2d_{Ni}$ and eventually plateaus around 450 kA/m indicating some dead layers at the Ni/Ru interface for thin Ni samples (Fig. 2) [3].

2. JOSEPHSON JUNCTIONS

In Ni(d_{Ni})/Ru(0.9)/Ni(d_{Ni}) Josephson junctions, I_cR_N (critical current x normal state resistance) decays exponentially without oscillations as supported by theory (Fig. 3). We found the decay constant to be 7.5±0.8 nm (excluding first point). This is longer compared to plain Ni because of phase cancellation from opposing ferromagnetic layers [3].

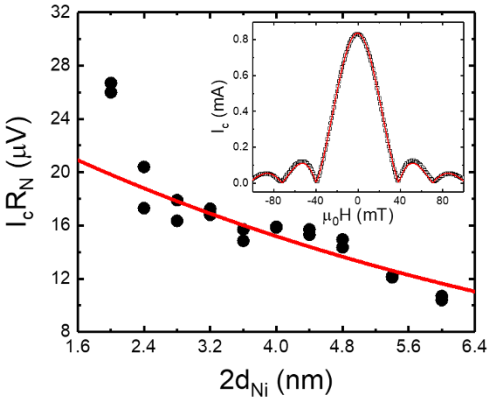

Fig. 3. I_cR_N vs total Ni thickness ($2d_{Ni}$) in Ni(d_{Ni})/Ru(0.9)/Ni(d_{Ni}) Josephson junctions. **Inset**: Typical Fraunhofer pattern (I_c vs H) in these SAF junctions [3].

ACKNOWLEDGEMENT

This research was supported by Northrop Grumman Corporation.

REFERENCES

[1] E. C. Gingrich, B. M. Niedzielski, J. A. Glick, Y. Wang, D. L. Miller, R. Loloee, W. P. Pratt, and N. O. Birge, Nat. Phys. 12, 564 (2016).

[2] I. Dayton, T. Sage, E. Gingrich, M. Loving, T. Ambrose, N. Siwak, S. Keebaugh, C. Kirby, D. Miller, A. Herr, Q. Herr, and O. Naaman, IEEE Magn. Lett. 9, 3301905 (2018).

[3] S.S. Mishra, R. Loloee, and N.O. Birge Appl. Phys. Lett. 119, 172603 (2021).

CT14

Efficient charge to spin conversion in 5d transition metal oxide.

Biswajit Sahoo and Eric Fullerton

Abstract: Recent focus has been on developing materials with a large spin Hall angle (SHA), the ratio of the charge to spin current density, for use in efficient spintronic devices. Transition metal oxides (TMOs) such as iridium oxide IrO_2 are attractive candidates that have large conductivity and high spin orbit coupling (SOC). In this work, we have fabricated bilayers of $IrO_2/Co_{40}Fe_{40}B_{20}$ samples to investigate the SHA in IrO_2 with different thicknesses and crystal structures.

Introduction:

With charge based electronics reaching their limitations, more attention is being focused on developing systems utilising pure-spin current. SHNOs are robust devices generally consisting of a bilayer thin film structure with a non-magnetic (NM) metal and a ferromagnetic (FM) material. This device utilises high density pure spin currents to drive local regions of magnetic nanostructures into auto-oscillating precession. Spin current in these devices is realized by converting a charge current via the spin Hall effect (SHE) and concentrating by the characteristic bow-tie shaped constriction. To efficiently drive auto-oscillation a high charge to spin conversion efficiency, i.e. the spin Hall angle (SHA), is imperative. Non-magnetic heavy metals with high spin-orbit coupling (SOC) metals such as Pt, Ta, W, Pd etc are commonly used for this purpose. However, transition metal oxides (TMOs) such as iridium oxide IrO_2 have large conductivity and high SOC comparable to heavy metals, making them attractive candidates to explore as generators of spin current in SHNOs. IrO_2 is a Dirac semimetal and possesses Dirac nodal lines (DNL's) in its band structure which is gapped by its strong SOC. This can lead to very high spin Hall conductivity and correspondingly produce a large SHA in this material. Researchers have shown the values of SHA ranging from 6% in amorphous [1], 25% in polycrystalline [2], and 75% in crystalline (001)[3] IrO_2 thin films, thus making it a prospective material to be explored in SHNOs.

An advantage of SHNO is that one need not have a large current flow through the magnetic layer. Thus one can use a relatively resistive FM with low damping such as CoFeB. In this work, we fabricate bilayers of amorphous/poly-crystalline IrO_2 as the NM and $Co_{40}Fe_{40}B_{20}$ as the FM to create SHNO devices to generate single mode auto-oscillations. X-ray reflectivity (XRR), X-ray diffraction (XRD) and atomic force microscopy (AFM) are used to verify the smoothness and crystallinity of IrO_2 . We perform ST-FMR measurements on this system for different thicknesses of IrO_2 yielding SHA to be 31% in IrO_2 which is comparable to Pt. The resistivity of IrO_2 thin film is found to be 142 μΩ-cm, putting it in the metallic regime and close to that of CoFeB (120 μΩ-cm). Large SHA and high conductivity makes IrO_2 a robust candidate for further applications such as spin Hall nano-oscillators and magnetization switching.

ACKNOWLEDGEMENTS:

This work was supported as part of Quantum Materials for Energy Efficient Neuromorphic Computing (Q-MEEN-C), an Energy Frontier Research Center funded by the U.S. Department of Energy (DOE), Office of Science, Basic Energy Sciences (BES), under Award # DE-SC0019273.

REFERENCES:

[1] Fujiwara et al., Nat. Commun. 4, 2893 (2013).

[2] Sahoo et al. Adv. Quantum Technol. 4, 2000146 (2021)

[3] Bose et al, ACS Appl. Mater. Interfaces, 12, 55411 (202

P01

Epitaxial growth, electrical, and magnetic properties of Mn_2PtPd thin films

Shivesh Yadav, Vijay Khopkar, Shikhar Gupta, Debjyoti Paul, Devendra Buddhikot, Nilesh Kulkarni, Shouvik Chatterjee

Department of Condensed Matter Physics and Material Science, Tata Institute of Fundamental Physics, Mumbai-400005

Email: shivesh.yadav@tifr.res.in, shouvik.chatterjee@tifr.res.in

Abstract: Mn_2PtPd has been predicted to crystallize in the form of a tetragonally distorted Heusler structure with I4/mmm ($TiAl_3$-type) crystal symmetry. Furthermore, it is expected to have an antiferromagnetic ground state with very high Neel temperature. Depending on the ordering of the constituent elements in the crystal lattice and the relative concentration of Pt and Pd, this compound can show different long-range magnetic order, which makes the compound's magnetic properties highly tunable. Here, we report first synthesis of epitaxial, single crystalline Mn_2PtPd thin films with (001) out-of-plane orientation on MgO substrates using RF magnetron sputtering. Our films have tetragonal crystal structure with P4/mmm symmetry, indicative of atomic disorder between Pt and Pd sites, which is consistent with previous reports on bulk polycrystalline samples. However, in contrast to the bulk samples, our thin films show hysteresis in field dependent magnetization curves, anomalous Hall effect, and butterfly shaped negative magnetoresistance, all of which persist even at room temperature. We will discuss the roles of dimensional confinement and interfacial effect in modifying the magnetic structure in Mn_2PtPd in thin film geometries.

P02

STRUCTURAL,OPTICAL AND ELECTRICAL PROPERTIES OF CADMIUM SULFIDE THINFILMS FOR PHOTO SENSING APPLICATION

Alaguraja.S[1*]
Assistant Professsor

Department of Physics

Thiagarajar College, Madurai – 625 009

[*]Corresponding Author Email Id – alagurajaps@gmail.com

Abstract

Cadmium Sulfide (CdS) is one of the highly photo sensitive and good semiconductor material of II-VI group elements. Cadmium Sulfide (CdS) have different applications in optoelectronic devices like solar cells, photo detectors etc. In the present CdS thin films were deposited using the brush plating technique on conducting glass substrates. The films were polycrystalline possessing single-phase hexagonal structure . Optical band gap of 2.39 eV was obtained. Electrical Properties of the Cadmium Sulfide (CdS) thin films were studied with I-V measurement system . Photovoltage, photocurrent and corresponding output power were measured in order to determine the output power.

K**eywords:** CdS, thin films, UV-Visible, PVcell,etc.,

P03

Magnetic and piezoelectric properties of $NiFe_2O_4$ (NFO) and NFO/$Na_{0.5}Bi_{0.5}TiO_3$ (NBTO) Bi-layer films prepared by rf magnetron sputtering with different time duration at constant temperature with different substrates (Si (100) and Al_2O_3)

M. Sarathbavan[1] and K. Kamala Bharathi[1,2]

[1]*Department of Physics and Nanotechnology, SRM Institute of Science and Technology, Kattankulathur, Chennai-603203*

[2]*Nanotechnology Research Center (NRC), SRM Institute of Science and Technology, Kattankulathur, Chennai-603203*

Email id; sarathbavanphysics@gmail.com

Abstract

In the present study high quality rf magnetron sputtering was used to Bi-layer films of $NiFe_2O_4$ (NFO) and $NiFe_2O_4$(NFO) /$Na_{0.5}Bi_{0.5}TiO_3$(NBTO) piezoelectric and magnetic films several techniques, such as rf or dc sputtering, ion plating, cluster and chemical vapor deposition (CVD), as well as the planar-magnetron sputtering which is the main concern in this paper, have been developed in recent years to deposit highly oriented films of $NiFe_2O_4$ - $Na_{0.5}Bi_{0.5}TiO_3$ piezoelectric and Magnetic deposition on si and Al_2O_3 substrates. The sputtering equipment (Advance process technology, pune) was used to prepare Bi-layer films of $NiFe_2O_4$ (NFO) and $NiFe_2O_4$ (NFO) /$Na_{0.5}Bi_{0.5}TiO_3$ (NBTO) piezoelectric and magnetic films.

Substrate temperature: 500 °C rf power: 80 W, sputtering time: 5 min- 4 hr, gas pressure: 5.0 X 10^{-2} Torr. The substrate temperature is measured with a thermocouple and depends both on the applied rf power and on the substrate-heater current. A substrate temperature rise of about 500 °C is observed during sputtering with an rf input power of 80 W. Sputtering is performed mass flow controller (MFC) in argon (80%)/ oxygen (20%) premixed gas. The pressure in the sputtering chamber is 3.0 X 10^{-2} to 5.0 X 10^{-2} Torr during sputtering and is continuously pumped. The NBTO and NFO targets used in our experiment are prepared by sintering a pressed NBTO and NFO powder cake. The diameter of the NBTO and NFO target is 5 cm. These targets are placed on Cu-plate. In the recent years, complex oxide materials exhibiting magnetic, dielectric, semiconducting properties and have attracted the interest of several researcher groups. The preparation of pure and composite nickel ferrite thin films will be fabricated by RF magnetron sputtering technique. The bi-layer thin films of $NiFe_2O_4$ (NFO) and $NiFe_2O_4$ (NFO) /$Na_{0.5}Bi_{0.}5TiO_3$ (NBT) fabricated and studied. X-ray diffraction, X-ray photoelectron spectroscopy (XPS), Raman spectroscopy analysis, Field

Emission Scanning Electron Microscopic (FESEM), Energydispersive X-ray (EDX) analysis, Magnetic Force microscopy (MFM) analysis will be employed for structural and morphological characterization. DC and AC susceptibility measurements at various temperatures and magnetoelectric coupling properties of these films will be explored employing SQUID magnetometer and vibrating sample magnetometer (VSM). Temperature variation fieled cooled (FC) and zero field cooled (ZFC) magnetization

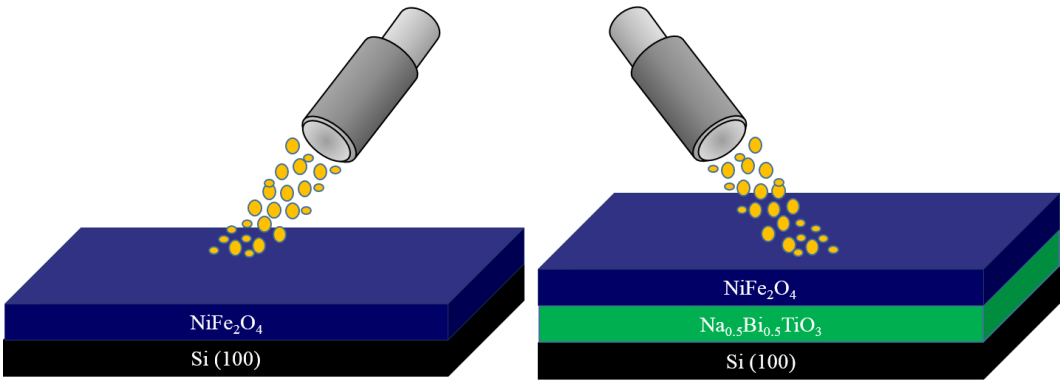

P04

Combinatorial investigation of Sm-Co-based amorphous alloy films for zero-field transverse thermoelectric generation

Rajkumar Modak[1], Yuya Sakuraba[1,2], Takamasa Hirai[1], Takashi Yagi[3], Hossein Sepehri-Amin[1], Hiroto Masuda[4], Takeshi Seki[1,4,5], Koki Takanashi[4,5,6], Weinan Zhou[1], Tadakatsu Ohukubo[1], Ken-ichi Uchida[1,4,5]

[1] National Institute for Materials Science, Tsukuba, 305-0047, Japan

[2]PRESTO, Japan Science and Technology Agency, Saitama 332-0012, Japan

[3]National Institute of Advanced Industrial Science and Technology, Tsukuba 305-8560, Japan

[4]Institute for Materials Research, Tohoku University, Sendai 980-8577, Japan

[5]Center for Spintronics Research Network, Tohoku University, Sendai 980-8577, Japan

[6]Center for Science and Innovation in Spintronics, Tohoku University, Sendai 980-8577, Japan

Email: MODAK.Rajkumar@nims.go.jp

Abstract: Using combinatorial material science and lock-in thermography we have systematically investigated the transverse thermoelectric performance of Sm-Co based alloys using composition spread films. This high throughput material investigation revealed some of the best Sm-Co based alloys with large anomalous Ettingshausen effect (AEE)/anomalous Nernst effect (ANE). Apart from large AEE/ANE we also discovered some of the unique material properties in these alloys, for example - amorphous in nature, low thermal conductivity, finite coercivity, finite remanence magnetization, in-plane easy-axis of magnetization with strong out-of-plane anisotropy field; which are desirable parameters to develop external magnetic field-free thermoelectric devices.

1. INTRODUCTION

In recent years, the research on spin caloritronics is showing a new direction with the demonstration of many magneto-thermoelectric effects by advanced heat measurement techniques.[1-3] The magneto-thermoelectric effects that output heat currents in magnetic materials exhibit unique heat control functionalities, which potentially enable active thermal management of electronic and spintronic devices. However, the practical application requires systematic device engineering and introduction of new materials as most of the conventional materials have very low thermoelectric conversion efficiency. As an effort to find good spin-caloritronic materials, Miura *et al*.[4] found that $SmCo_5$-type magnets exhibit a large AEE, which is a transverse magneto-thermoelectric effect that generates a heat current in the direction perpendicular to the applied charge current and magnetization. In this study, we report systematic investigations on AEE in Sm-Co-based amorphous films, while polycrystalline bulk magnets were used in the previous study.[4]

2. RESULT AND DISCUSSION

In this work, we have investigated the composition dependence of AEE for the Sm_xCo_{100-x} composition-spread film with x varying from 0 to 100 at%, fabricated on a single-crystalline MgO substrate by the combinatorial sputtering technique,[5,6] and confirmed that $Sm_{20}Co_{80}$ exhibits the largest AEE signal. For the optimized composition, Co is systematically replaced with Fe by fabricating $Sm_{20}(Co_{100-y}Fe_y)_{80}$ composition spread films with y varying from 0 to 100 at%. Significant enhancement in the AEE-induced temperature modulation was observed in the film with 23% Fe substitution. For further confirmation and understanding the results in detail, we have fabricated a uniform $Sm_{20}Co_{80}$ and $Sm_{20}(Co_{77}Fe_{23})_{80}$ films and evaluated various magneto-transport properties along with the direct measurement of ANE, the Onsager reciprocal of AEE. A relatively large ANE coefficient of 1.1 ± 0.2 μVK^{-1} and 1.5 ± 0.2 μVK^{-1} were observed for $Sm_{20}Co_{80}$ and $Sm_{20}(Co_{77}Fe_{23})_{80}$ films, respectively, which is consistent with the estimation from the composition-spread film. We have further demonstrated the performance of a prototype ANE-based heat-flux sensing device[7] fabricated on 50-μm-thick flexible polyethylene naphthalate substrate.

3. CONCLUSION

Here, we developed Sm-Co-based amorphous thin films for potential application in magnetic field free thermoelectric devices. The presence of high in-plane remanent magnetization and coercive force in our films makes it advantageous over conventional materials for applications including heat flux sensors, as these materials can generate thermoelectric output without an external magnetic field. Importantly, these amorphous films can be fabricated on any surfaces. Thus, these films are suitable to realize flexible thermoelectric devices. Also, exploring the possibility of thermopile structures and hybrid films consisting of these films and other magnetic materials will be useful to construct ANE/AEE devices that operate at zero magnetic field.

REFERENCES

[1]. K. Uchida et al., Nature **558** (2018) 95.
[2]. T. Seki et al., Appl. Phys. Lett. **112** (2018) 152403.
[3]. K. Uchida, Proc. Jpn. Acad., Ser. B **97** (2021) 69.
[4]. A. Miura et al., Appl. Phys. Lett. **115** (2019) 222403.
[5]. H. Masuda et al., Commun. Mater. **1** (2020) 75.
[6]. R. Modak et al., APL Mater. **9** (2021) 031105.
[7]. W. Zhou et al., Appl. Phys. Express **13** (2020) 043001.

P05

Asymmetric Spin-Transport at the Interfaces of Nanoscale Oxide Heterostructures

Bibekananda Das and Prahallad Padhan
Department of Physics, Indian Institute of Technology Madras, Chennai-600036, India
Email: bibekanandadas404@gmail.com

Abstract: A series of $La_{0.7}Sr_{0.3}MnO_3$(LSMO)/ZnO heterostructures with different ZnO thickness were grown on (001) oriented Si using RF magnetron sputtering at 700 ℃. First principle density functional theory study indicates that the charge transfer at the Si-LSMO interface reduced the charge state of Mn ions causes interfacial anti-ferromagnetic coupling, however, there is a very small charge transfer occurs at the LSMO-ZnO interface. The charge transfer induced interfacial antiferromagnetic coupling at Si-LSMO interface and spin-orbit coupling are responsible for the positive magnetoresistance (MR) in LSMO thin film. However, the spin-dependent scattering at the LSMO-ZnO interface suppresses the positive MR and the out-of-plane negative MR increases with ZnO thickness. The study of this heterostructures may provide useful information for development of spintronic devices.

INTRODUCTION

The parent compound $LaMnO_3$ is an antiferromagnetic insulator at low temperature. But 30% Sr doped $LaMnO_3$ is a ferromagnetic metal undergoes a metal to insulator phase transition near the Curie temperature (T_C ~369 K) [1]. Zinc oxide (ZnO) possess wurtzite crystal structure and is a wide direct band gap semiconductor of the II-VI family. It has direct band gap of ~3.37 eV at room temperature and free exciton energy of ~60 meV [2]. LSMO/ZnO heterostructure shows rectifying behavior, photo-carrier injection effect and ultra-violet photo-voltaic effect [3,4].

EXPERIMANTAL METHODS

The LSMO/ZnO heterostructures were grown on (001) oriented Si using RF magnetron sputtering in a pulsed plasma deposition manner. The heterostructures were grown at 700 ℃. A series of heterostructures were synthesized by varying the thickness of top ZnO layer with the same bottom LSMO layer thickness. The deposition pressure was 9.0×10^{-3} mbar with Ar and O_2.

RESULTS AND DISCUSSION

The X-ray diffraction study confirms the oriented growth of LSMO and ZnO layers. From low angle X-ray reflectivity measurement, the LSMO thickness was found to be 120 Å and ZnO layers thickness was found to be 372 Å-930 Å. The magnetic moment measurement performed using SQUID-VSM shows a decrease in the T_C of LSMO thin film (T_C ~326 K) in the LSMO/ZnO heterostructures (T_C ~295 K) and independent of ZnO thickness. The LSMO thin film and LSMO/ZnO show spin-glass transition, which indicates the presence of non-collinear Mn ions spins. The density of state calculations show the occurrence of charge transfer at the Si-LSMO interface, which causes the interfacial antiferromagnetic coupling, but at the LSMO-ZnO interface, the charge transfer is very small. Fig. 1(a) shows the field dependence of in-plane MR $\left(MR = \frac{R(H)-R(0)}{R(0)}\right)$, where the in-plane current makes 45° with magnetic field.

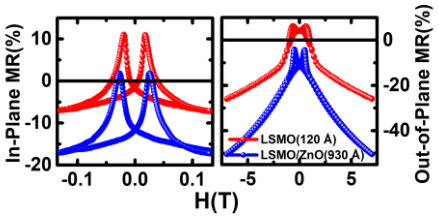

Fig.1. In-plane (a) and out-of-plane (b) MR of LSMO thin film and LSMO/ZnO heterostructure

Maximum positive (~11%) and negative (~7%) in-plane MR obtained for LSMO thin film, however, the positive MR is suppressed in the LSMO/ZnO heterostructures (Fig. 1(a)). Similarly, LSMO thin film shows a maximum positive and negative out-of-plane MR of ~6 % and ~26%, respectively (Fig. 1(b)). The maximum negative out-of-plane MR (~50%) was obtained in the LSMO (120 Å)/ZnO (930 Å) heterostructure at 10 K and 7 T (Fig. 1(b)). In LSMO/ZnO heterostructures, the positive out-of-plane MR becomes zero, and the negative out-of-plane MR increases from 45% to 50% as the ZnO thickness increases from 372 Å to 930 Å. The charge transfer induced interfacial antiferromagnetic coupling at the Si-LSMO interface and spin-orbit coupling due to non-collinear Mn ion spins favor positive MR in LSMO, but spin dependent scattering at the LSMO-ZnO interface suppressed the positive MR and increased the negative MR.

CONCLUSION

The growth of the ZnO layer on LSMO suppressed the positive MR and T_C, however, it enhanced the negative MR. The dual sign MR behavior of LSMO and enhancement of negative MR by the ZnO layer can be used in the spintronics applications.

REFERENCES

[1]. A. Urushibara et al, Phys. Rev. B **51** (1995) 14103.
[2]. A. Janotti and C. G. Van de Walle, Rep. Prog. Phys. **72** (2009) 126501.
[3]. K. Lord et al, Appl. Phys. Lett. **89** (2006) 052116.
[4]. K. X. Jin et al, J. Phys. D **42** (2009) 015001.

P06

Magnetic and electronic states of Mn and Co atoms at $Co_2Mn_{1.20}Ge_{0.38}$/MgO interfaces seen via soft x-ray magnetic circular dichroism

S. Jena[1] and V. R. Singh[1,2*]

[1]*Department of Physics, Central University of South Bihar, Gaya-824236 (Bihar) India*
[2]*Department of Physics, University of Tokyo, Bunkyo-ku, Tokyo 113-0033, Japan*

***Corresponding author: vijayraj@cusb.ac.in**

Abstract: The half-metallic ferromagnetic materials have widely studied as magnetic storage devices and magnetic sensors because a high efficiency is expected for spintronic device applications, including tunnel magnetoresistance (TMR) devices and giant magnetoresistance devices [1-3]. In these materials have a nonzero density of states (DOS) at the Fermi level and the majority spin states have a metallic character, while there is band gap at Fermi level in minority spin states, resulting in 100% spin polarization at the Fermi level (E_F) [3]. Literature suggests that a higher TMR ratio is obtained for Mn compositions $\beta > 1.0$ in Ge-deficient $Co_2Mn_\beta Ge_\delta$ electrodes (where $\delta < 1$).

In this work, the magnetic states of Mn and Co atoms in Mn-rich and Ge-deficient $Co_2Mn_{1.20}Ge_{0.38}$ (CMG) (*t*)/MgO (*t*=2, 4 and 53 ML) Heusler alloy thin films facing an MgO barrier were studied by means of x-ray absorption spectroscopy (XAS) and soft x-ray magnetic circular dichroism (XMCD). In particular, the CMG film-thickness dependence of the Mn and Co magnetic moments was investigated. A Co^{2+}-like multiplet structure was not observed in all the Co $L_{2,3}$-edge XAS and XMCD, indicating that, even in the ultrathin samples, the Co atoms were not oxidized, and were more strongly spin polarized than those in the thicker samples. With a decrease in the CMG film thickness to 2 ML, the spin magnetic moment of Mn increased and the Mn $L_{2,3}$-edge XAS do not show a Mn^{2+}-like multiplet structure films is in contrast to the Co-rich CMG thin films as studied by Asakura *et al.*[4], where the Mn atoms are strongly oxidized. The results show that Mn-rich CMG films are beneficial for device fabrications in spintronics when the film thickness has to be reduced to a few monolayers.

References:

1. S. Kammerer, A. Thomas, A. Hutten, and G. Reiss, Appl. Phys. Lett. **85**, 79 (2004).

2. Y. Sakuraba, T. Miyazaki, and H. Kubota, Appl. Phys. Lett. **88**, 192508 (2006).

3. T. Ishikawa, T. Uemura, M. Arita, and M. Yamamoto, Appl. Phys. Lett. **89**, 192505 (2006).

4. D. Asakura, A. Fujimori, T. Taira, and M. Yamamoto, Phys. Rev. B **82**, 184419 (2010).

P07

IrMn based Synthetic Antiferromagnetic Spin Valve with Thermal Stability

Tejaswini C. Gawade[1,2] , P. Chowdhury[1,2]
[1]Nanomaterials Research Laboratory, Surface Engineering Division, CSIR - National Aerospace Laboratories, Bangalore 560 017, India
[2] Academy of Scientific and Innovative Research (AcSIR), Ghaziabad - 201 002, India
Email: pchowdhury@nal.res.in

Abstract: Spin valve synthetic antiferromagnetic (SAF) structure was optimized for different pinned layer thicknesses and magnetoresistance properties were studied. Long term thermal annealing at 150°C in air confirms the stability of the spin valve stack.

1. INTRODUCTION

The magnetic strength of the pinned layer can be enhanced intensely by replacing the pinned layer by an antiferromagnetically coupled FM1/Ru/FM2 tri-layer, where Ru is a very thin non-magnetic interlayer that gives rise to strong antiferromagnetic interlayer exchange coupling called as synthetic antiferromagnetic (SAF) layer [1]. In this trilayer structure, the thicknesses of individual layer are very critical to enhance the exchange bias field (EB) and the thermal stability in the spin valve (SV) stack. In this report, we varied the layer thicknesses to have a SV stack which is stable at 150 °C in air for 10 days.

2. EXPERIMENTAL

Bottom SAF-SV structures, SiO_2/NiFeCr (4)/NiFe (1)/IrMn (6)/CoFe (t_{PL1}) /Ru (0.9)/CoFe (t_{PL2})/Cu (2.3)/CoFe(3)/Ta 5 (in nm), were prepared on Si/SiO_2 substrates using an ultra-high vacuum DC magnetron sputtering system with a base pressure of 1.0 x 10^{-8} mbar and an Ar gas pressure of 3.5 x 10^{-3} mbar. Samples were annealed at 220° C for 1 hour in 1,300 Gauss field in vacuum, and then it was field cooled at room temperature to introduce exchange biasing. The magnetoresistance measurements were carried out by using four probe at room temperature. Both t_{PL1} and t_{PL2} were varied in the range of 1 to 3 nm to developed the stack with the condition as follows: $0<\Delta t = t_{PL2} - t_{PL1} \geq 0$.

2.1. Result and discussion

Depending on the thickness difference, Δt, between the two pinned layers, PL2 and PL1, they are aligned in antiparallel condition. When $\Delta t \leq 0$ (see Fig. 1 (a)), the pinning direction (PL1) is set parallel to the annealing field direction. Subsequently, the pinned direction of PL2 reverses its direction because PL1 and PL2 are set into an antiparallel configuration by a strong interlayer exchange interaction (1 erg/cm2) [2]. Meanwhile, when $\Delta t > 0$ (see Fig. 1(b)), though both PL1 and PL2 are in antiparallel configuration at zero field, due to weak coupling between them, PL2 rotates along the field direction because the net moment of P2 is higher than P1. As a consequence, negative and positive Δt result in inverse and normal MR transfer curves, respectively. The fig. 1 shows, the pinning layer thickness difference is highly affecting the spin valve structure curve. Keeping Δt=+/-ve(1nm) and varying the free layer thickness, the maximum MR% was achieved at 4 nm free layer.

.

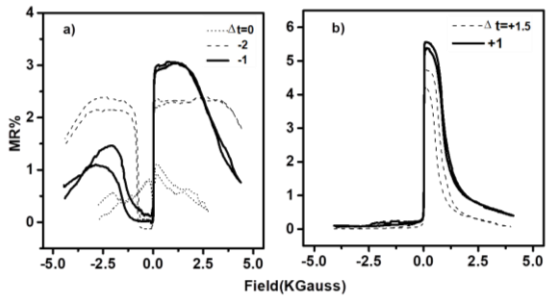

Fig 1. The MR curve for SAF structure a)with $\Delta t \leq 0$ and b)$\Delta t > 0$

2.2 Thermal stability

The thermal stability of the SV-SAF stack was studied while exposed at 150 °C in air for a period of 10 days. Fig. 2 shows the MR properties of an IrMn spin-valve at 150°C over a period on 240 hours. ΔR/R and ΔR are observed to remain constant at this temperature. These results suggest that sputtered SAF-SV structure is suitable for device applications.

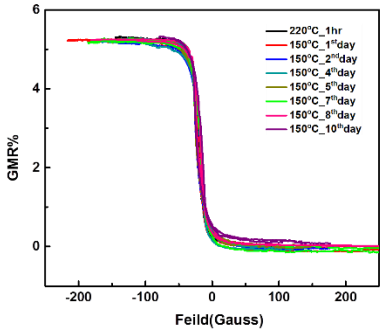

Fig 2: Long term thermal treatment in atmospheric condition at 150°C.

ACKNOWLEDGEMENT

Authors would like to thank the Director, NAL for supporting this activity.

REFERENCES

[1]. K. M. H. Lenssen, A.E.T.Kuiper, and F. Roozeboom,, J. Appl. Phys., vol. 85, p. 5531, 1999.

[2]. S. S. P. Parkin, J. Appl. Phy

P08

Study of structural and optical properties of nickel oxide thin films

Amel HAICHOUR* & Nasr-Eddine HAMDADOU

Laboratory of Micro and Nanophysics (LaMiN), National Polytechnic School of Oran, ENP Oran- Maurice AUDIN, BP1523 El-Mnaouer, Oran 31000, Oran, Algeria.

* ***haichouramel75@gmail.com***

Abstract: The aim of this work is to study structural and optical properties of nickel oxide (NiO) thin films deposited on chemically and ultrasonically cleaned glass substrate, heated at 350°C by spray pyrolysis technique. Using 0.1M aqueous solution of nickel chloride $NiCl_2.6H_2O$ annealed at 400°C for 2 hours in air.

The thickness measurements, structural and optical properties of the films were characterized using stylus profilometer, grazing incidence X-ray diffraction and UV-Vis spectrophotometer in the spectral rang 190 - 1100 nm, respectively. Profilometer analysis revealed that the thin films thickness is about 610 nm.The X-ray diffraction (GXRD) analysis indicates that the films have cubic polycrystalline structure with preferred orientation along (200) corresponding to 2θ = 43.30° and lattice parameter a = 4.18 Å. Various microstructural properties have been calculated such as average particle size, dislocation density, texture coefficient and strain. Optical and dielectric parameters have been determined, from UV-Vis spectrophotometer data.

Keywords: Thin films, nickel oxide, spray pyrolysis, GXRD, optical parameters.

P09

Optical double cantilever beam magnetometer for electric field induced magnetization measurements

H. Aireddy[1,2], S. Guchhait[1] and A. K. Das[1]

[1]Department of Physics, Indian Institute of Technology, Kharagpur, India-721302

[2]Alliance University, Bangalore, India-562106

Email: harinathaireddy364@gmail.com

Abstract: Optical double cantilever beam magnetometer (ODCBM) was designed, fabricated and demonstrated its ability to measure magnetic properties of ferromagnetic thin films as a function of magnetic field. Notably, for the first time, here we demonstrate the well-established and simple cantilever beam technique for electric field modification of magnetization and magnetostriction measurements of ferromagnetic/ferroelectric heterostructures by considering the induced strains in ferromagnetic thin films through the converse piezoelectric effect in piezoelectric films. This magnetometer is simple in construction, inexpensive to manufacture, easy to operate along with noise subtraction provision and having sensitivity nearly 8 nm in the determination of cantilever beam deflection.

1. INTRODUCTION

Various measurement techniques such as vibrating sample magnetometer (VSM)[1], superconducting quantum interference device (SQUID)[2,3], and magneto-optic Kerr effect (MOKE)[4-6] have been employed to probe the electric field control of magnetization property of multiferroic materials. The use of cantilever beam magnetometer (CBM) first demonstrated by Koch and his co-workers, with the deflection of the cantilever substrate measured by the differential capacitance technique, for the quantitative measurement of the magnetization, magnetocrystalline anisotropy (MCA), and magnetostriction of the thin films under an ultrahigh vacuum (UHV) condition [7]. Sander et al. [8] demonstrated a modified CBM in which the cantilever beam bending was measured using laser reflection from the cantilever substrate. These systems are suitable for in-situ characterizations of the thin films, under ultrahigh vacuum conditions only. Here, we present an optical double cantilever beam magnetometer which allows electric field induced magnetization and magnetostriction ex-situ measurements of the FE/FM heterostructures at room temperature.

2. FIGURES AND IMAGES

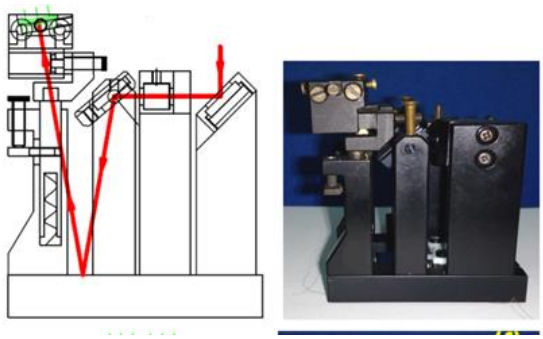

Fig. 1: A schematic diagram as well as the photographs of the fabricated optical double cantilever beam setup (front view).

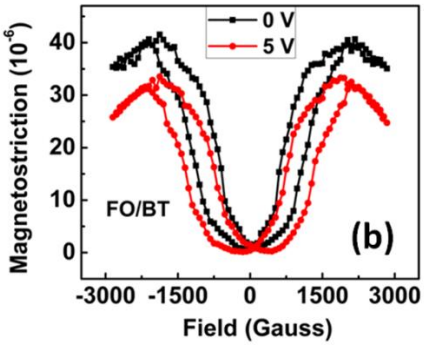

Fig.2: Magnetostriction (λ) versus magnetic field (H) characteristics of Fe_3O_4/ $BaTiO_3$/Si heterostructure at room temperature for the ON (5 V – red circle symbol plus line) and OFF (0 V - black square symbol plus line) condition of applied bias voltage.

ACKNOWLEDGEMENT

We acknowledge the CSIR, India (project No. 03 (1339/15/EMR-II) for financial support.

REFERENCES

[1]. M. Liu, S. Li, O. Obi, J. Lou, and S. Rand, Appl. Phys. Lett. **98**, 222509 (2011).

[2]. C. Thiele, K. Dörr, O. Bilani, J. Rödel, and L. Schultz, Phys. Rev. B **75**, 054408 (2007).

[3]. S. M. Wu, Shane A. Cybart, P. Yu, M. D. Rossell, J. X. Zhang, R. Ramesh, and R. C. Dynes, Nature Materials **9**, 756 (2010).

[4]. M. Weisheit , S. Fahler , A. Marty , Y. Souche , C. Poinsignon , D. Givord , Science 315, 349 (2007).

[5]. T. Maruyama , Y. Shiota , T. Nozaki , K. Ohta , N. Toda , M. Mizuguchi , A. A. Tulapurkar , T. Shinjo , M. Shiraishi , S. Mizukami , Y. Ando , Y. Suzuki , Nat. Nanotechnol. 4, 158 (2009).

[6]. H. J. A. Molegraaf , J. Hoffman , C. A. F. Vaz , S. Gariglio , D. Van Der Marel , C. H. Ahn , J. M. Triscone , Adv. Mater. 21, 3470 (2009).

[7]. M. Weber, R. Koch, and K. H. Rieder, Phys. Rev. Lett. **73**, 1166 (1994).

[8]. D. Sander, A. Enders, and J. Kirschner, Rev. Sci. Instrum, **66**, 4734 (1995).

.

P10

Probing structural and electronic behaviour of pristine and Cr Doped VO_2 Thin Films:

Aradhana Kumari[$1], Ashutosh Kumar[$1,2], Riya Dawn[1], Joseph B. Franklin[3], Raviteja Vinjamuri[4], Santosh Kr. Sahoo[4], Uttam Kr. Goutam[5], Virendra Kr. Verma[6], Ramcharan Meena[7], Asokan Kandasami[7,8], Somnath Mahapatra[9], Kundan Kumar[10], Akhilananda Kumar[1,2], Vijay Raj Singh*[1]

[1]*SpinTec Laboratory, Department of Physics, Central University of South Bihar, Gaya, 824236, Bihar, India*

[2]*Department of Physics, Central University of South Bihar, Gaya, 824236, Bihar, India*

[3]*Department of Energy Storage and Distribution Resources, Lawrence Berkeley National Laboratory, Berkeley, CA, 94720, USA*

[4]*Department of Metallurgical and Materials Engineering, National Institute of Technology, Rourkela, 769008, India*

[5]*Technical Physics Division, Bhabha Atomic Research Centre, Trombay, Mumbai, 400085, India*

[6]*Department of Physics, Madanapalle Institute of Technology & Science, Angallu, Madanapalle, 517325, India*

[7]*Materials Science Division, Inter-University Accelerator Centre, Aruna Asaf Ali Marg, New Delhi, 110067, India*

[8]*Department of Physics & Centre for Interdisciplinary Research, University of Petroleum and Energy Studies (UPES), Dehradun, Uttarakhand, 248007, India*

[9]*Department of Physics and Astronomy, National Institute of Technology, Rourkela, 769008, India*

[10]*Department of Physics, Ranchi University, Ranchi, 834008, India*

***Corresponding author: vijayraj@cusb.ac.in**

[$]Equally contributed to this work.

Abstract: In a rapidly evolving scientific discipline of spintronics, there is currently much interest to hunt for dilute magnetic semiconductors (DMSs) with high Curie temperature (*Tc*), with an emphasis on the investigation of various semiconductor host. Here, we used the host semiconductor VO_2 and the transition metal Cr which is magnetic ion doped in VO_2 to investigate the electronic environment of Cr ions in VO_2 and to note down the changes in the electronic structure of VO_2, which are important for understanding its electrical, optical, and magnetic characteristics.

The Cr doped VO_2 [i.e., $V_{1-x}Cr_xO_2$ (VCO), x = 0, 0.05 and 0.10] thin films were deposited on r-sapphire substrate by means of pulse laser deposition technique. X-ray diffraction (XRD), Raman, Vibrating sample magnetometer (VSM) and various high energy spectroscopic techniques were used for the characterization of VCO films which clearly revealed that the films are preferentially grown along the a-axis and possess a single phase of monoclinic (M1) in VO_2 and triclinic (T) in $V_{0.95}Cr_{0.05}O_2$ and $V_{0.9}Cr_{0.1}O_2$ samples. The absence of impure phase in VCO films were confirmed using XRD and Raman spectroscopic study; which verified the single M1 and T-phase of VO_2 and $V_{0.95}Cr_{0.05}O_2$ thin films [1-2]. AFM measurements revealed that the films are atomically smooth, homogeneous and possess the Root mean square roughness (RMS) ~3 and ~4Å for VO_2 and $V_{0.95}Cr_{0.05}O_2$ respectively.

Photo-electron spectroscopic techniques were used for figuring out the electronic states of Cr ion in the VO_2 matrix and to study the nature of interaction between Cr and the cations and therefore, ruling out the possibilities of the Cr metal clusters in VCO films. The XPS study revealed that valency of Cr ions doped in VCO films were examined to be +3. whereas, the vanadium was in the mixed state of 4+ and +5 which was found to be consistent XAS spectroscopic measurements in total electron yield mode [3-4]. The magnetic hysteresis measurements were carried out at room-temperature using VSM, which clearly manifested the presence of ferromagnetic behaviour in the VCO films.

REFERENCES:

[1]. R. Basu, V. Srihari, M. Sardar, S.K. Srivastava, S. Bera, S. Dhara, Probing phase transition in VO_2 with the novel observation of low-frequency collective spin excitation, Scient. Reports **10** (2020) 1977.

[2]. S.S. Majid, D.K. Shukla, F. Rahman, S. Khan, K. Gautam, A. Ahad, S. Francoual, R.J. Choudhary, V.G. Sathe, J. Stempfer, Insulator-metal transitions in the T phase Cr-doped and M1 phase undoped VO_2 thin films, Phys. Rev. B. **98** (2018) 075152.

[3]. M.W. Haverkort, Z. Hu, A. Tanaka, W. Reichelt, S.V. Streltsov, M.A. Korotin, V.I. Anisimov, H.H. Hsieh, H.-J. Lin, C.T. Chen, D.I. Khomskii, L.H. Tjeng, Orbital-Assisted Metal-Insulator Transition in VO_2 Phys. Rev. Lett. **95** (2005) 196404.

[4]. T. Schmitt, L.-C. Duda, M. Matsubara, M. Mattesini, M. Klemm, A. Augustsson, J.-H. Guo, T. Uozumi, S. Horn, R. Ahuja, A. Kotani, J. Nordgren, Electronic structure studies of V_6O_{13} by soft x-ray emission spectroscopy: Band-like and excitonic vanadium states, Phys. Rev. B **69** (2004) 125103.

P11

Effect of Cr doping on structural and magnetic properties of VO_2 thin films: Soft X-ray Magnetic Circular Dichroism Study.

M. Zzaman[1,2], V. K. Verma[3], R. Shahid[2], V. R. Singh[1*]

[1]Department of Physics, Central University of South Bihar, Gaya 824236, India.
[2]Department of Physics, Jamia Millia Islamia University (Central University) New Delhi 110025, India.
[3]Department of Physics, Madanapalle Institute of Technology & Science Angallu, Madanapalle -517325, India.
***Corresponding author: vijayraj@cusb.ac.in**

Abstract : The metal to insulator transition (MIT) in the strongly correlated oxide materials such as vanadium dioxide (VO_2) is one of the most fascinating phenomena due to its potential applications in sensors, actuators, thermochromic devices, thermometers and many other multifunctional electronic devices [1]. The MIT temperature of VO_2 is around 340 K, close to room temperature (RT) and a first-order MIT from insulating monoclinic (RT) M1 phase (space group -- $P2_1/c$) to metallic rutile (high-temperature) R phase (space group -- $P4_2/mnm$) makes VO_2 a very suitable and promising material to develop the ultrafast switching and sensing in advance technology devices [2]. The V atoms in the rutile R phase are uniformly spaced along the rutile *c*-axis while in the insulating monoclinic phase, a zig-zag pattern formation occurs due to the simultaneous pairing and as well as tilting among V atoms [3].The VO_2 and CrO_2 are well-known examples of the anti-ferromagnetic insulator and ferromagnetic metal, respectively [2]. However, experimentally and theoretically, it has been found that for Cr substitution (10-20%) in the rutile phase, VO_2 has initiated to behave as a ferromagnetic insulator. X-ray absorption spectroscopy (XAS), which is not only atom-specific but also being sensitive to the valence state reveals the presence of Cr^{3+}-V^{5+} pairs and is responsible for an unusual ferromagnetic insulating state [4].
In this work, we focused on $V_{1-x}Cr_xO_2$ ($0 \leq x \leq 0.3$) (VCO) thin films and studied the effect of Cr-substitution on its structural, electronic and magnetic properties. The VCO films were deposited on R-sapphire substrates using a pulse laser deposition method. Soft X-ray absorption spectroscopy (XAS) and soft X-ray magnetic circular dichroism (XMCD) studies of VCO thin films were performed to reveal and understand the origin of magnetization and their enhancement with Cr-substitution. The XAS spectra suggest that the V and Cr ions are in V^{4+} and V^{5+}, and Cr^{3+} states respectively. The XMCD spectra indicate that the V and Cr ions are ferromagnetic in nature at room temperature. These results also indicate that the VCO films are in the ferromagnetic insulating state and charge-ordered at the V and Cr sites. These results are consistent with the first principle density functional theory calculations.

References:

[1] K. G. West, J. Lu, L. He, D. Kirkwood, W. Chen, T. P. Adl, M. S. Osofsky, S. B. Qadri, R. Hull, S. A. Wolf, J. Supercond. Novel Magn. 21 (2008) 87.

[2] F. J. Morin, , Phys. Rev. Lett. 3 (1959) 34.

[3] D. B. McWhan, M. Marezio, J. P. Remeika, P. D. Dernier, Phys. Rev. B 10 (1974) 490.
[4] L. F. J. Piper, A. DeMasi, S. W. Cho, A. R. H. Preston, J. Laverock, K. E. Smith, K. G. West, J. W. Lu, S. A. Wolf, Phys. Rev. B 82 (2010) 235103.

P12

Large Rashba Spin-Orbit Effect by Orbital Engineering at $SrTiO_3$–based Correlated Interfaces

Ganesh Ji Omar, A. Ariando
Department of Physics, National University of Singapore
Email: ganesh_ji@u.nus.edu; ariando@nus.edu.sg

Abstract: Large spin-orbit effect is an essential element for efficient spin-orbitronics that utilizes the interplay between charge and spin degree of freedom. This spin-orbit effect is generally small in heavy-metal [1-7]-based or requires large external applied voltages in complex-oxide-based heterostructures [8].
Here, I will firstly discuss t_{2g} electron gas theory and this approach to discuss lattice and orbital polarization induced at the $SrTiO_3$-based interfaces. Then, I will present our experimental data to show how Ti-O lattice polarization can be tuned via atomic control of orbital hybridization. This unique approach can present a large Rashba spin orbit effect at zero applied voltages by interfacial atomic control of orbital hybridization that introduces Ti-O lattice polarization at the $SrTiO_3$-based interfaces. The observed spin orbit effect (~ 3.5×10^{-12} eV-m) is four-fold larger than that observed in conventional $SrTiO_3$-based interfaces at zero bias voltage. I will conclude our work by showing the orbital hybridization and Ti-O lattice polarization are verified through *ab initio* electronic structure calculations and high-resolution atomic microscopy. Our results present a unique approach to achieve Ti-O lattice polarization at $SrTiO_3$ interfaces and open hitherto unexplored avenues of generating and controlling Rashba spin orbit effect via orbital engineering to design next-generation spin-orbitronics.

ACKNOWLEDGEMENT

This research is supported by the Agency for Science, Technology and Research (A*STAR) under its Advanced Manufacturing and Engineering (AME) Individual Research Grant (IRG) (A2083c0054). We thank W. Kong, H. Jani, M. S. Li, J. Zhou, Z. S. Lim, S. Prakash, S. W. Zeng, S. Hooda, T. Venkatesan, Y. P. Feng, S. J. Pennycook, L. Shen for their contribution to this work.

REFERENCES

[1] Rojas-Sánchez, J. C. *et al.*, Phys. Rev. Lett. **116**, 096602, (2016).
[2] Deorani, P. *et al.*, Phys. Rev. B **90**, 094403, (2014).
[3] Cheng, C. *et al.*, **8**, 17854-17860, (2016).
[4] Sánchez, J. C. R. *et al.*, Nat. Commun. **4**, 2944, (2013).
[5] Koga, T., *et al.*, Phys. Rev. Lett. **89**, 046801 (2002).
[6] Studer, M., *et al.*, Phys. Rev. Lett. **103**, 027201, (2009).
[7] Schultz, M. *et al.* Semicond. Sci. Technol. **11**, 1168-1172, (1996).
[8] Caviglia, A. D. *et al.* Phys. Rev. Lett. **104**, 126803, (2010).

P14

Ferromagnetic resonance study of $Co_2Fe_{0.5}Ti_{0.5}Si$ thin films

Mainur Rahaman[1], Somesh Kumar Sahoo[2], Arabinda Haldar[2], M. Manivel Raja[3], S. N. Kaul[1,*], and S. Srinath[1,]**

[1] School of Physics, University of Hyderabad, Hyderabad-500046, Telangana, India

[2] Department of Physics, Indian Institute of Technology Hyderabad, Kandi 502285, Telangana, India

[3] Defence Metallurgical Research Laboratory, Hyderabad-500058, Telangana, India

E-mail: [*] sn.kaul@uohyd.ac.in and [**] srinath@uohyd.ac.in

Abstract: 100 nm $Co_2Fe_{0.5}Ti_{0.5}Si$ (CFTS) thin films were grown on Si (100) by ultra-high vacuum dc magnetron sputtering at different substrate temperatures (TS) 200°C, 300°C, 450°C, 500°C and 550°C. Co-planar waveguide-based ferromagnetic resonance (CPW-FMR) measurements were carried out on these CFTS films. The film deposited at 500°C has $L2_1$ crystal structure, a minimum value of 2.02 for Landé splitting factor g, maximum saturation magnetization (M_s = 780 G), and minimum Gilbert damping constant (α = 0.0055).

1. INTRODUCTION

Gilbert damping constant (α) is a very important parameter in deciding whether a given magnetic system is an appropriate choice for spintronic devices or not. A low value of α is very crucial for MTJ and STT based storage devices [1,2]. Co-based Heusler compounds are potential systems among various ferromagnetic compounds to have low damping constant [3,4]. In this work, using frequency dependence FMR analysis the effect of disorder on magnetization, magnetic anisotropy, Landé splitting factor, and Gilbert damping constant (α) in $Co_2Fe_{0.5}Ti_{0.5}Si$ Heusler alloy thin films is carried out. Resonance field and linewidth are measured by varying the microwave-field frequency (4 GHz to 17 GHz) at a fixed arbitrary dc magnetic field azimuthal angle (∥ configuration).

2. EXPERIMENTAL DETAILS & RESULTS

100 nm thin $Co_2Fe_{0.5}Ti_{0.5}Si$ (CFTS) films were grown on Si (100) substrate by co-sputtering the stoichiometric Co_2FeSi and Co_2TiSi alloy targets at substrate temperatures (TS) ranging from 200 °C to 550 °C by ultra-high vacuum magnetron sputtering. Post-deposition, the films were annealed in-situ at TS for 30 min. Based on the deposition temperature, these films are labeled as TS200, TS350, TS450, TS500, and TS550. Energy-dispersive X-ray absorption spectroscopy yielded the actual alloy composition as $Co_{2.01}Fe_{0.51}Ti_{0.24}Si_{1.24}$. X-ray diffraction (XRD) patterns reveal broad fundamental peak (220) for TS200 and TS350 film, and three sharp peaks (111), (220), and (422) for the remaining films. Thus, the crystalline structure gradually evolves from amorphous to ordered $L2_1$ structure as the TS increases; the TS500 film has the highest $L2_1$ order.

Fig.1(a) shows that the frequency (f) vs. H_{res} plots, measured using the broad-band (3–17 GHz) FMR setup, are well described by the Kittel resonance condition [5] (the fits through the data points):

$$f = \frac{\gamma}{2\pi}\sqrt{(H_{res} + H_k) \times (H_{res} + H_k + 4\pi M_s)} \quad (1)$$

where $\gamma = \frac{g\mu_B}{\hbar}$ is the gyromagnetic ratio, M_s, saturation magnetization where H_k and g are the in-plane (IP) anisotropy field, Lande g-factor respectively. The IP anisotropy is found to be very weak, and g has the minimum value of 2.02 for the TS500 film with the highest $L2_1$ order. α is determined from the linear fits (straight lines) to the frequency-dependent `peak-to-peak' FMR linewidth (ΔH) data (solid circle), shown in Fig.1(b), based on the equation 2 [6].

$$\Delta H = \Delta H_{inh} + \frac{2}{\sqrt{3}}\frac{2\pi\alpha f}{\gamma} \quad (2)$$

Where, ΔH_{inh} is the inhomogeneous contribution to the linewidth. The lowest value of α is found to be 0.0055 for the TS500 film. The different parameters obtained from the analysis are tabulated in table 1.

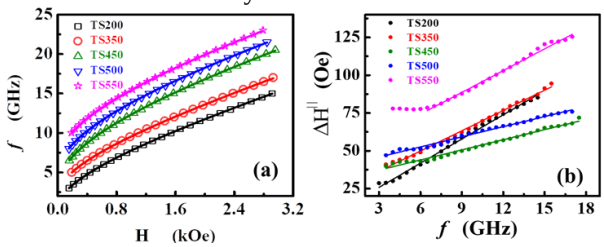

Fig.1. (a) Frequency (f) dependence of the resonance field (H_{res}) in the ∥ configuration. TS350, TS450, TS500 and TS550 data are shifted by 1.5, 3, 4.5 and 6 GHz respectively w.r.t. TS200 data (b) Linear variation of the FMR linewidth ($\Delta H^{\parallel}$) with f.

Table 1. The various fitting parameters evaluated from eq. (1) and (2)

Film ID	M_s (G)	H_k (Oe)	g	α
TS200	442(2)	21(1)	2.14(1)	0.0138(2)
TS350	479 (8)	29 (2)	2.14(1)	0.0116(2)
TS450	754 (1)	10 (1)	2.05(1)	0.0056(1)
TS500	779 (13)	5 (1)	2.02(1)	0.0055(1)
TS550	752 (10)	16(1)	2.06(1)	0.0120(2)

ACKNOWLEDGEMENT

The author, Mainur Rahaman, would like to acknowledge DST-INSPIRE fellowship, India, for financial support.

REFERENCES

[1]. J. C. Slonczewski, J. Magn. Magn. Mater. **159** (1996) L1

[2]. B. S. Lee et. al IEEE.**104** (2016) 2024

[3]. S. Mizukami et. al, J. Appl. Phys. **105** (2009) 07D306

[4]. B. K. Hazra et. al, J. Phys. D: Appl. Phys. **52** (2019) 325002

[5]. C. Kittel, Phys. Rev.**73** (1948) 155

[6]. C. E. Patton, J. Appl. Phys. **39** (1968) 3060

P15

Electrical- and magneto-transport in $Co_2FeAl_{0.5}Si_{0.5}$ thin films with varying degree of B2 crystallographic order

Lanuakum A. Longchar 1, Binoy Krishna Hazra 1, M. Manivel Raja 2, R. Rawat 3, S. Srinath 1,* and S. N. Kaul 1,**

1School of Physics, University of Hyderabad, Hyderabad-500046, Telangana, India

2 Defence Metallurgical Research Laboratory, Hyderabad-500058, Telangana , India

3 UGC-DAE Consortium for Scientific Research, Indore-452001, Madhya Pradesh, India

Email: *srinath@uohyd.ac.in and **sn.kaul@uohyd.ac.in

Abstract: Detailed analysis of *zero-field* resistivity, ρ(T, H = 0), and *in-field* resistivity, ρ(T, H = 80 kOe),data on 50 nm $Co_2FeAl_{0.5}Si_{0.5}$ (CFAS) thin films, grown on Si(100) substrate at different temperatures, reveals the following. The film grown at 500˚C has the highest B2 crystallographic order, lowest residual resistivity and lowest temperature (T_{min}) at which ρ(T, H = 0) and ρ(T, H = 80 kOe),go through a minimum. While the disorder-induced electron-diffuson scattering and weal localization effects dominate at $T < T_{min}$, the electron-magnon scattering and electron-phonon scattering give dominant contributions at $T > T_{min}$.

1. INTRODUCTION

Band structure calculations on CFAS predict increased stability of half-metallicity due to the fact that the Fermi energy level (E_F) lies in the gap between spin-up and spin-down sub-bands [1]. Thus, by adjusting the concentration ratio of Al and Si, E_F can be tuned to achieve a stable half-metallic compound.$Co_2FeAl_{0.5}Si_{0.5}$is known to have high T_c~1150K, high spin polarization: 70% and 81% for B2 and $L2_1$ structures at room temperature, and large magnetic moment of 5.5 μ_B/f.u [2]. The change in E_F caused by disorder is expected to have a strong effect on the electric- and magneto-transport properties [1]

2. DATA AND ANALYSIS

Effect of site-disorder on the half-metallic behaviour has been studied in 50 nm $Co_2FeAl_{0.5}Si_{0.5}$ (CFAS) thin films, grown on Si(100) substrates at different substrate temperatures (T_S): room temperature = 27˚C, 350˚C, 450˚C, 500˚C and 550˚C, by ultrahigh vacuum dc magnetron sputtering, and labelled as RT, TS350, TS450, TS500 and TS550. The grazing incidence x-ray diffraction patterns reveal that *B2 structural order* grows with increasing T_S and peaks at T_S= 500˚C.

Zero-field resistivity, ρ(T, H = 0), (Fig. 1) and *in-field* resistivity, ρ(T, H = 80 kOe), (inset Fig. 1) have been analyzed in terms of the relation [3,4].

$$\rho_{(T,H)} = \rho_0 - \delta_{dif}\, lnT - \xi_{wl} T^{3/2} + \beta_{e-m} T^2 + \alpha_{e-p}\left(\frac{T}{\theta_D}\right)^5 \int_0^{\theta_D/T} x^5 \frac{e^x}{(e^x-1)^2}\, dx \qquad (1)$$

Where ρ_0 is the residual resistivity, other terms denote contributions to ρ from the electron-diffuson (*e – dif*) scattering, weak localization (wl), electron-magnon (*e – m*) and electron-phonon (*e – p*) scattering. ρ_{5K} decreases with increasing B2 order (T_S) and goes through a minimum for the TS500 CFAS film with maximum B2 order. Diffuson and wl, responsible for *negative* TCR for $T < T_{min}$, compete with the *positive* TCR *e – m* and *e - p* contributions to produce the resistivity minimum. H has no influence on the diffuson (and *e – p*) contribution but suppresses *wl* and *e – m* scattering. Consequently, the minimum shifts to lower temperatures and results in negative magnetoresistance.

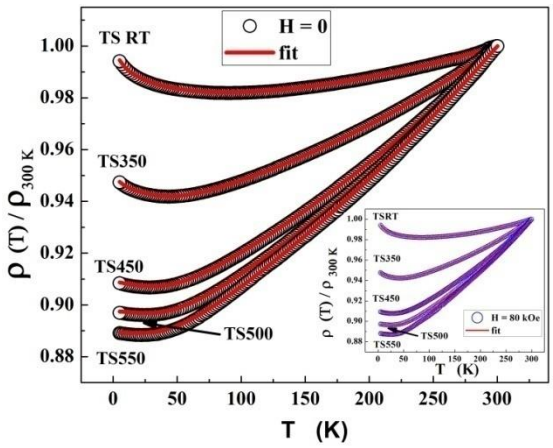

Fig.1. ρ(T,H=0) (open circles) and ρ(T,H = 80 KOe) (inset) (blue open circles) with theoretical fits (continuous curves) in the temperature range 5K - 300K based on eqn.(1)

ACKNOWLEDGEMENT

Lanuakum A. Longchar acknowledges the financial assistance received from the UGC-DAE CSR and UGC-SRF.

REFERENCES

[1]. G. H. Fecher and C. Felser, J. Phys. D **40**, (2007) 1582.

[2]. M. Vahidi et al., Appl. Phys. Lett. Mat. **2**, (2014)046108

[3].B. K. Hazra et al., Phys. Rev. B **96**, (2017)184434.

[4]. S. N. Kaul et al., Phys.

P16

Room temperature skyrmion lattice in a hexagonal centrosymmetric kagome magnet

Dola Chakrabartty, Sk Jamaluddin, Suvendu Kumar Manna, Ajaya K. Nayak
School of physical sciences, National Institute of Science Education and Research, HBNI, Jatni-752050
Email: dola.chakrabartty@niser.ac.in

Abstract: Magnetic skyrmions are proposed as potential candidates for the next generation spintronic applications owing to their topologically stable magnetic texture. Here, we report the finding of a tunable room temperature skyrmion lattice in a new centrosymmetric kagome ferromagnetic material. We have also demonstrated the controlled switching between topological skyrmion and non-topological bubbles with application of non-zero in-plane magnetic fields.

1. INTRODUCTION

Magnetic skyrmion is a topologically nontrivial chiral spin texture, whose topological protection helps it to avoid defects and move at lower cut off current density. These properties of the skyrmions make it a potential candidate for highly density and low power consuming racetrack memory devices. Although the magnetic skyrmions are mostly observed experimentally in the noncentrosymmetric systems [1], recently skyrmion like spin textures have also been found in centrosymmetric magnets with uniaxial magnetocrystalline anisotropy (UMA) [2-4]. Competing dipolar interaction and UMA is the fundamental mechanism for stabilization of skyrmions in these materials. The topological number of skyrmions (+1, 0, -1) in these systems can be easily tuned with several external stimulis like, thickness and magnetic fields, etc. Therefore, finding of new room temperature (RT) skyrmion hosting centrosymmetric materials is one of the most interesting current research topics in spintronics.

2. EXPERIMENTAL DETAILS

The c-oriented TEM lamella of about 100 nm thickness are prepared from polycrystalline sample using Ga based focused ion beam (FIB) technique. Lorentz transmission electron microscopy (LTEM) measurements are performed using a JEOL-F200 microscope.

3. RESULT AND DISSCUSSION

We have explored room temperature hexagonal skyrmion lattice in a new centrosymmetric kagome ferromagnet Mn_4Ga_2Sn using LTEM. The sample exhibits a Curie temperature (Tc) of 320 K and a spin reorientation transition (T_{SR}) from high temperature easy axis to low temperature easy plane anisotropy around 85 K. The stripe domain magnetic ground state is transformed into skyrmion lattice with increasing magnetic field applied along the c- axis. The hexagonal skyrmion lattice at 250 K is shown in Fig. 1(a). Existence of skyrmions with opposite helicities are observed due to degenerate energy state of both the skyrmions in the centrosymmetric magnets. A switching mechanism of chiral skyrmion (topological number ± 1) to non-chiral type II bubble (topological number 0) is also demonstrated by applying a nonzero in plane magnetic field excitation as shown in Fig. 1(b). Micromagnetic simulations are also carried out using object oriented micromagnetic framework (OOMMF) code to further verify the experimentally observed spin textures. The results illustrate exclusive control on the topological magnetic domains with varying magnetic field in the sample and makes it useful for future spintronic application.

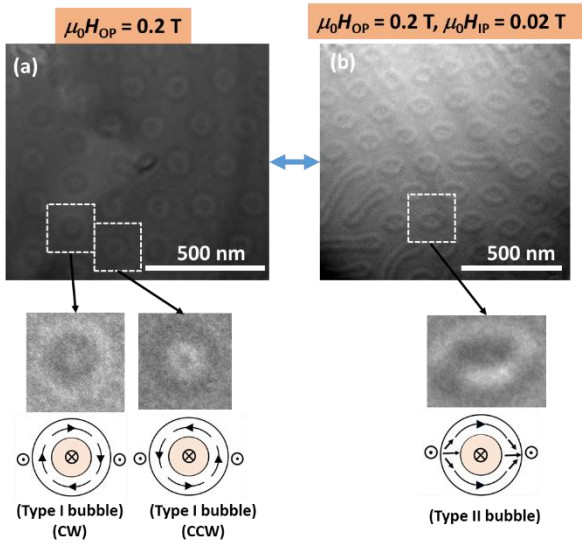

Fig.1. Skyrmion and type two bubble lattice at 250 K. (a) Hexagonal skyrmion lattice, (b) type II bubble lattice with additional in-plane magnetic field of 0.02 T.

REFERENCES

[1]. S. Mühlbauer *et al.*, *Science.* **323** (2009) 915-919.
[2]. W. Wang *et al.*, *Adv. Mater.* **28** (2016) 6887-6893.
[3]. Z. Hou *et al.*, *Adv. Mater.* **29** (2017) 1701144.
[4]. X. Yu *et al.*, *Adv. Mater*. **29** (2017) 1603958.

P17

Driving skyrmions with low threshold current density in Pt/CoFeB thin film

Brindaban Ojha,[1] Sougata Mallick,[2] Minaxi Sharma,[1] Andr´e Thiaville,[2] Stanislas Rohart,[2] and Subhankar Bedanta[1]

[1]Laboratory for Nanomagnetism and Magnetic Materials (LNMM), School of Physical Sciences, National Institute of Science Education and Research (NISER), HBNI, Jatni-752050, Odisha, India

[2]Laboratoire de Physique des Solides, Universit´e Paris-Saclay, CNRS UMR 8502, F-91405 Orsay Cedex, France

Email: sbedanta@niser.ac.in

Abstract: We have studied Pt/CoFeB/MgO heterostructures in which skyrmions have been stabilized at room temperature (RT). It has been observed that the shape of the skyrmions are perturbed even by the small stray field arising from low moment magnetic tips while performing the magnetic force microscopy (MFM), indicating presence of low pinning landscape in the samples. This hypothesis is indeed confirmed by the low threshold current density to drive the skyrmions in our sample, at velocities of few 10 m/s.

1. INTRODUCTION

Skyrmions are nano-scale sized, topologically protected spin configurations [1]. Further, the solitonic nature of the skyrmions allows them to behave like particles under the influence of electrical excitations. These properties make them promising candidates for logic and storage technology [2, 3]. Competition between Heisenberg exchange interaction, Dzyaloshinskii-Moriya interaction (DMI) and perpendicular magnetic anisotropic energy can lead to stabilization of non-collinear spin textures viz. skyrmions [2, 3]. The most widely used combination for such a system is a heterostructure of heavy metal (HM)/ferromagnet (FM)/oxide (O). In this context, we chose the combination of $Pt/Co_{40}Fe_{40}B_{20}/MgO$ to investigate the current-driven dynamics of the skyrmions under the influence of SOT. We show that the threshold current density to drive the skyrmions is significantly lower than the existing literature.

2. EXPERIMENTAL DETAILS

We have prepared Ta (5 nm)/Pt (6 nm)/ $Co_{40}Fe_{40}B_{20}$ (t_{CoFeB})/MgO (2 nm)/Ta (3 nm) heterostructure on thermally oxidized Si/SiO_2(100 nm) substrates. The samples are named as S1, S2, S3, S4, S5, S6 and S7 for t_{CoFeB} = 1.1, 1.2, 1.5, 1.6, 1.7, 1.75 and 1.9 nm, respectively. Ta, Pt, and CoFeB layers were deposited using DC magnetron sputtering while e-beam evaporation technique was employed to prepare MgO. Magneto optic Kerr effect-based microscope (MOKE) and superconducting quantum interference device (SQUID) are performed for the magnetization measurements. Magnetic force microscopy (MFM) and electron beam lithography (EBL) is performed for skyrmions imaging and dynamics study, respectively.

3. RESULTS AND DISCUSSION

The MOKE measurements confirm that the samples S1, S2, S3 and S4 are out-of-plane (OOP) magnetized while samples S5, S6 and S7 are in-plane (IP) magnetized. We have deduced the effective anisotropy (K_{eff}) constant using the relation $K_{eff} = -\frac{1}{2}(H_s M_s)$ (negative sign indicates the IP anisotropy), where H_s and M_s are saturation field, and spontaneous magnetization, respectively and spin reorientation transition happens at t_{CoFeB}=1.65 nm. As, t_{CoFeB} of sample S3 and S4 are near SRT, we have performed MFM measurements to confirm the existence of skyrmions. We should note that the shape of the skyrmions is significantly perturbed even by the stray field of the lowest moment magnetic tips. This indicates the presence of low pinning landscape in the CoFeB thin film. Sample S3 is selected for the study of current-induced dynamics due to its potentially low pinning energy landscape and better control under applied magnetic field. We have prepared a nanotracks (3 parallel tracks with width ~1.2 mm separated by ~2.8 mm from each other) with Ti/Au contact pads using EBL. The skyrmion velocity as a function of applied current density is measured by calculating the average displacement of all the skyrmions present in the track. Fig. 1(a) and (b) show the skyrmion displacements marked by different colours before and after the application of one current pulse. Beyond a threshold current density of ~ 0.8×10^{11} A/m^2, the skyrmions start moving in the track (see Fig. 1(c)). The threshold current density is lower than the previous report.

5. ACKOWLEDGEMENTS

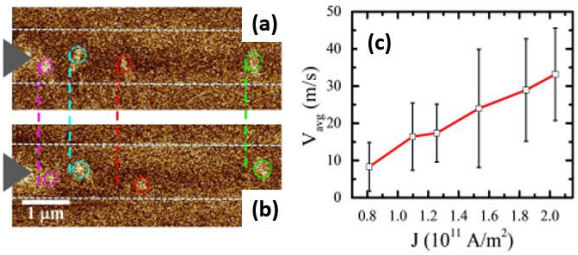

Fig.1 (a) and (b) represents the position of skyrmions before and after applied pulsed current respectively. (c) Av. velocity as a function of current density.

The authors thank DAE, Govt. of India and the IndoFrench collaborative project supported by CEFIPRA (IFC/5808-1/2017), and the French National Research Agency (ANR) (Topsky, ANR-17-CE24-0025) for providing the research funding. We would like to thank Dr. Braj Bhusan Singh for valuable discussion. We thank Raphael Weil for his help in microfabrication.

6. REFERENCES

[1]. A. Fert et al., Nature Nanotech, **8**, 152–156 (2013).

[2]. N. Nagaosa et al., Nature Nanotech, **8**, 899 (2013).

[3]. A. Fert et al., Nature Rev. Mater., **2**, 17031 (2017).

P18

Magnetoelectric properties of $NiFe_2O_4/SrRuO_3$/PMN-PT heterostructures

Azam Ali Khan[1*], Anju Ahlawat[2], S. Satapathy[1]
[1]LBAD, Raja Ramanna Centre for Advanced Technology, Indore 452013, India
[2]UGC DAE, Consortium for Scientific research, Indore 452001, India
***Email: azamrrcat@gmail.com**

Abstract: Strong magneto-electric (ME) coupling for nonvolatile memory applications might be realised via electric-field controlled magnetism. Here we present the electric field driven nonvolatile modulated magnetization in the thin film heterostructures of $NiFe_2O_4/SrRuO_3/Pb(Mg1/3Nb_{2/3})_{0.7}Ti_{0.3}O_3$ (PMN-PT). The combined impact of charge and strain altered the magnetization of the NiFe2O4 layer in $NiFe_2O4$/ $SrRuO_3$/PMN-PT heterostructures substantially. The cation (Fe^{3+}/Ni^{2+}) redistribution in the electric field poled $NiFe_2O_4$ films occurs on tetrahedral and octahedral sites, supporting the link between magnetism and ferroelectric characteristics, according to XMCD data.

INTRODUCTION

Multiferroic materials are expected to play a vital role in developing next-generation technology [1–3]. Materials, which exhibit two or more ferroic orders (ferroelectric, ferromagnetic ferroelastic, and ferrotorodic) simultaneously, are called multiferroics materials [4,5]. These materials possess magneto-electrical multifunctional properties owing to more than one ferroic order. On top of this, the cross-coupling among these ferroic orders can envisage novel physical phenomena and provide an extra edge in device engineering. A range of promising multiferroics materials applications includes energy harvesting, signal generation and ultrafast processing, high density and fast information storage, and so on. A major important aspect of multiferroics materials is controlling the magnetisation (**M**) direction by applying an electrical pulse (**E**). Conventionally, the direction of **M** is controlled by changing the direction of electrical current in semiconductors and metals. However, the flow of current leads to energy dissipation and delay in response. Therefore, multiferroics material can be used to fabricate faster and more energy-efficient memory devices. In these memory devices, M's direction can be controlled by **E** for writing and reading the memory bits. A particularly promising direction is to search the material in which ferroelectricity is induced by magnetic order. In this scenario, cross-coupling in ferroic orders would be high. Consequently, switching E can switch the state of M and vice versa.

1. Results and Duscussion

In this work we have studied non-volatile modification in the magnetism of $NiFe_2O_4$ films by induced strain and charge effect at the interfaces in the electric field poled $NiFe_2O_4/SrRuO_3/Pb(Mg_{1/3}Nb_{2/3})_{0.7}Ti_{0.3}O_3$ (PMN-PT) heterostructures. XMCD studies reveal rearrangement of Fe/Ni ions at the tetrahedral and octahedral site in the electric poled NFO films, which infers that the magnetic structure of NFO is modified after electric field poling. These observations establish room temperature magneto electric coupling in NFO/SRO/PMN-PT heterostructures. The magnetoelectric coupling is further quantified in terms of ME coupling coefficient α, which can be repeatedly switched by applied positive and negative electric pulses. The switching results demonstrate that two stable states of α can be used for binary information storage providing an easy and efficient way of data writing/reading process in memory devices. The study shows that the states of α can be well controlled between positive and negative by applying selective electric fields. Consequently, two-level, four-level, and eight-level nonvolatile memory devices can be demonstrated at room temperature. The concept of using α for memory storage is new and it may offer numerous benefits such as low power consumption,

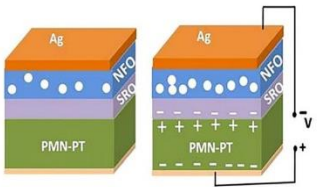

Fig. 1.(a) schematic of NFO/SRO/PMNPT thin films before poling; **(b)** after electric field poling.

avoid destructive reading process, and easy writing/reading process.

2. Conclusions

In conclusion, the nonvolatile modification in the magnetism of NFO films is observed by induced strain and charge effect at the interfaces in the electric field poled $NiFe_2O_4/SrRuO_3/Pb(Mg_{1/3}Nb_{2/3})_{0.7}Ti_{0.3}O_3$ (PMN-PT) heterostructures.

References

[1] Saha, A. Sundaresan, C.N.R. Rao Mater. Horizons. (2013)
[2] W. Eerenstein, N.D. Mathur, J.F. Scott, Nature. 442 (2006) 759–765
[3] J. Hu, L. Chen, Y. Wu, L. Yu, X. Zhao, S. Cao, J. Zhang, W. Ren, Chinese Sci. Bull. 59 (2014) 5170–5179.
[4] M. Fiebig, J. Phys. D. Appl. Phys. 38 (2005) 123–152
[5] C.-W. Nan, M.I. Bichurin, S. Dong, D. Viehland, G. Srinivasan, J. Phys. D. Appl. Phys. 38 (2005) 123–152

P19

Magnetic coupling across CoO-NiO interface studied by LEED

Bibhuti Bhusan Jena[1,2], Arunava Kar[2], Sukanta Barman[3], Suman Mandal[4], Krishnakumar S. R. Menon[2]
[1]Laboratory for Nanomagnetism and Magnetic Materials (LNMM), School of Physical Sciences, National Institute of Science Education and Research (NISER), HBNI, Jatni-752050, India
[2]Surface Physics and Material Science Division, Saha Institute of Nuclear Physics, HBNI, 1/AF Bidhannagar, Kolkata-700064, India
[3]Department of Physics, Raja Peary Mohan College, 1 Acharya Dhruba Pal Road, Uttarpara, Hooghly712258, West Bengal, India
[4]Physics and Electronics Department, CHRIST (Deemed to be University), Bangalore 560029, India
Email: (bibhuti.jena4@gmail.com)

Abstract: The surface antiferromagnetic (AFM) ordering of CoO-NiO bilayer have been probed by using Low-energy Electron Diffraction (LEED) technique. We observe coherent exchange scattered half-order spot in LEED which is only visible at low electron beam energy (<40 eV) and arises below a certain temperature with a periodicity of the magnetic unit cell of CoO(001) and NiO(001) surface, confirming its magnetic origin. Our results show that the surface Néel temperature (T_N) of CoO layers is enhanced significantly from its bulk T_N value and approaching the T_N of the NiO layers, as the thickness of the CoO layers is reduced to the monolayer limit. The observed magnetic proximity effect is attributed to a combination of a short-range and a weaker long-range magnetic coupling, explaining the long antiferromagnetic order propagation length in AFM–AFM superlattices and bilayers.

1. INTRODUCTION

Magnetic materials with different magnetic order when in contact with each other, often gives rise to interesting physical phenomena due to the interfacial magnetic coupling, such as giant magnetoresistance effect, interfacial magnetism, exchange bias effect, interfacial superconductivity [1-2], etc. The interest in AFM materials has been on the rise ever since they are shown to have great potential in the next generation spintronic devices [3]. However, the vanishing magnetization caused by their compensated magnetic structure renders them a difficult class of materials to study and manipulate.

For the investigation of AFM–AFM coupling across the interface, we have employed low energy electron diffraction (LEED) method. In the present study, we explore the evolution of the surface Néel temperature of the CoO layers as a function of the CoO and NiO film thicknesses. Our studies show that the magnetic behaviour of CoO layers in proximity to NiO layers is very different; thinner layers of CoO show higher Néel temperature compared to the thicker layers. Moreover, the magnetism of CoO layers is also found to be dictated by the underlying NiO layers, enabling to tune the CoO Néel temperature at will.

2. EXPERIMENTAL DETAILS

CoO/NiO films on Ag(001) substrate were prepared in a standard UHV setup having base pressure better than 1×10^{-10} mbar. The CoO and NiO layers were prepared by reactive deposition of Co and Ni at an oxygen pressure of 1.0×10^{-6} mbar at 473 K [4-5]. LEED measurements were performed using a four-grid LEED apparatus to determine the crystalline quality of the deposited oxide films as well.

3. RESULTS

By measuring the half-order spot intensity *vs.* sample temperature, the surface Néel temperature of the CoO films has been obtained, which was used to study the interfacial effect of an AFM in contact with another AFM material. The surface T_N of the CoO-NiO system as a function of the CoO/NiO film thicknesses were measured, confirming the enhancement of the T_N of CoO layers proximity to NiO layers.

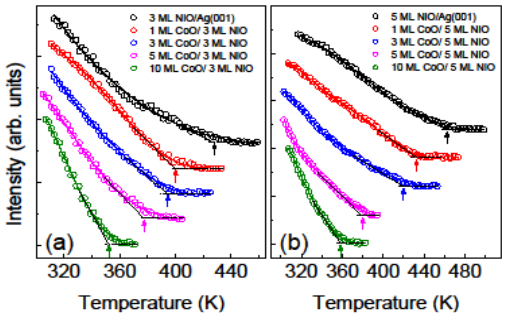

Fig.1. Temperature-dependent variation of the (1/2, 0) LEED spot intensity for different CoO coverages for (a) 3 ML NiO/Ag(001), (b) 5 ML NiO/Ag(001) systems after the Debye–Waller correction. The estimated value of the surface T_N for each case is shown by arrows.

ACKNOWLEDGEMENT

We acknowledge the Micro-Nano initiative program of the Department of Atomic Energy (DAE), Government of India, for generous funding and support.

REFERENCES

[1]. Baibich M N, *et al.* 1988 *Phys. Rev. Lett.* **61** 2472
[2]. B. B Jena et al 2021 J. Phys. D: App 54 325001
[3]. Fina I *et al* 2014 *Nat. Commun.* 51
[4]. Das J *et al* 2015 *J. Spectrosc. Relat. Phenom*
[5]. Barman S *et al* 2018 *J. Cryst. Growth 487 28*

P20

Simultaneous observation of anti-damping and inverse spin Hall effect in $La_{0.67}Sr_{0.33}MnO_3$/Pt bilayers system

Pushpendra Gupta[1*], Braj Bhusan Singh[1], Koustuv Roy[1], Anirban Sarkar[2], Markus Waschk[2], Thomas Brueckel[2], and Subhankar Bedanta[1,3]

[1]Laboratory for Nanomagnetism and Magnetic Materials (LNMM), School of Physical Sciences, National Institute of Science Education and Research (NISER), HBNI, P.O.- Bhimpur Padanpur, Via Jatni, 752050, India

[2]Forschungszentrum Jülich GmbH, Jülich Centre for Neutron Science (JCNS-2) and Peter Grünberg Institut (PGI-4), JARA-FIT, 52425 Jülich, Germany

[3] Center for Interdisciplinary Sciences (CIS), National Institute of Science Education and Research (NISER), HBNI, Jatni-752050, India

Email: pushpendra.gupta@niser.ac.in

Abstract: Manganites have shown potential in spintronics due to their low damping and insulating characteristics. Here, we studied the damping properties of $La_{0.67}Sr_{0.33}MnO_3$/Pt bilayer samples which are prepared using oxide molecular beam epitaxy. We have observed decrease in damping coefficient (α) with increase in Pt thickness. Further, we investigated inverse spin Hall effect (ISHE) and observed that ISHE signal gets enhanced with Pt thickness. ISHE voltage was higher when α was low. We observed maximum spin pumping voltage of 20.05 μV for the sample with Pt thickness of 3 nm. We have evaluated spin Hall angle for these samples.

1. INTRODUCTION

Pure spin current based devices are potential for faster and low power consumption [1]. Generation of pure spin current has been demonstrated by ferromagnetic resonance (FMR) through spin pumping mechanism [2]. This pure spin current can loss their spin angular momentum in the presence of high spin orbit coupling (SOC) material e.g. Pt, W, Ta. The loss of spin angular momentum can develop voltage by asymmetric scattering of spins, which is known as inverse spin Hall effect (ISHE) [3]. So far studies have been concentrated mostly on Pt and FM metals. However, magnetic oxides are less explored. La0.67Sr0.33MnO3 (LSMO) is well known FM oxide for exhibiting high Curie temperature (TC=350 K) and nearly 100% spin polarization (in bulk) [4]. In this work, in order to get high spin Hall angle, high resistive Pt film is grown on LSMO thin film.

2. EXPERIMENTAL DETAILS

LSMO (20 nm)/Pt (tPt = 0, 3 and 10 nm) bilayer samples have been prepared on SrTiO3(001) substrate using an oxygen plasma assisted molecular beam epitaxy system [5]. ISHE measurements are performed using home modified coplanar wave-guide (CPW) based ferromagnetic resonance (FMR) spectroscopy.

3. RESULTS

We have studied the static and dynamic properties of the LSMO/Pt systems. A decrease in α has been observed with increase in Pt thickness. We performed angle dependent ISHE at frequency of 7 GHz. From angle dependent ISHE measurement spin Hall angle were calculated 0.033 and 0.014 for samples with 3 and 10 nm of Pt, respectively.

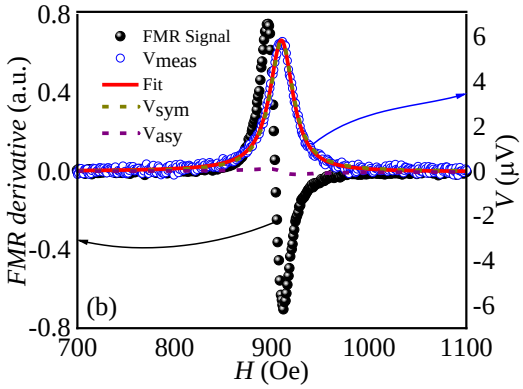

Fig.1. Fig. (1) ISHE signal corresponding to FMR signal for S3.

ACKNOWLEDGEMENT

The authors acknowledge DAE and DST, Govt. of India, for the financial support for the experimental facilities. Mr. Pushpendra Gupta acknowledge UGC for JRF fellowship grant. Dr. B. B. Singh thanks DST for INSPIRE faculty fellowship. Mr. Koustuv Roy thanks CSIR for JRF fellowship. Dr. S. Bedanta acknowledges German Academic Exchange Services (DAAD) for the fellowship to visit Forschungszentrum Jülich for this collaborative work

REFERENCES

[1]. C. Chappert, A. Fert, and F. N. Van Dau, Nature Materials 6, 813 (2007).
[2]. O. Mosendz, J. Pearson, F. Fradin, Phys. Rev. Lett. 104, 046601 (2010).
[3]. J. Hirsch, Phys. Rev. Lett. 83, 1834 (1999).
[4]. J.-H. Park, E. Vescovo, H.-J. Kim, Nature 392, 794, (1998).
[5]. P. Gupta, B. B. Singh, K. Roy *et al.*, Nanoscale, 13, 2714, (2021)

P21

Spin pumping and inverse spin Hall effect study in CoFeB/ IrMn bilayers

Koustuv Roy[1], Abhisek Mishra[1], Pushpendra Gupta[1], Shaktiranjan Mohanty[1], Braj Bhusan Singh[1], Subhankar Bedanta[1,2,*]

[1]Laboratory for Nanomagnetism and Magnetic Materials (LNMM), School of Physical Sciences, National Institute of Science Education and Research (NISER), HBNI, Jatni-752050, Odisha, India

[2]Center for Interdisciplinary Sciences (CIS), National Institute of Science Education and Research (NISER), HBNI, Jatni 752050, India

Email: *koustuv.roy@niser.ac.in*

Abstract: Spin current propagation efficiency through the ferromagnet (FM)/ Heavy metal (HM) interface is one of current interest in modern research. Generation of spin current and its dissipation through a HM efficiently depends on the low damping FM layer and high spin orbit coupling (SOC) of HM layer. Recently. antiferromagnetic materials (AFM) has been shown potentials to replace HM due to high resistivity, and high SOC. AFM may work as an efficient spin source also. Here, we report spin pumping via measuring inverse spin Hall effect on CoFeB/ IrMn (AFM) bilayers.

1. INTRODUCTION

Efficient generation of spin current and its manipulation e in different materials is one of the emergent research topics in modern days due to applications in the development of power efficient and faster spintronics devices. Spin pumping [2] and inverse spin Hall effect (ISHE) [3] are the tools to study the spin current efficiency in the materials. In last one decade, ISHE and spin pumping are heavily investigated in ferromagnet (FM)/ heavy metal (HM) heterostructures. Recently the antiferromagnetic (AFM) materials are found to be a good replacement of heavy metals (HM) due to presence of high spin orbit coupling [4]. Understanding the role of different AFM layers in ISHE or spin pumping study is still limited. In this context, we have performed the ISHE in CoFeB/ IrMn bilayers, where IrMn is an AFM layer.

2. EXPERIMENTAL DETAILS

A series of samples of the structure CoFeB(20 nm)/ Cu(3 nm)/ IrMn(*t* nm)/ AlOx(3 nm) have been prepared on top of Si(100) substrate using dc magnetron sputtering where the '*t*' value varies from 0 to 20 nm. The deposition is performed at the base pressure of 1×10^{-9} mbar. All the samples are prepared using 20 rpm rotation to avoid the growth induced uniaxial anisotropy and better uniformity. The sample layers are prepared with the Ar flow of 10 sccm. The Cu layer is used to improve the growth of IrMn as a buffer layer and also avoid any induced magnetism in IrMn layer. AlOx layer is prepared to protect the sample from environmental contamination. The ISHE measurements are performed on home modified broadband FMR based set-up [5].

3. RESULTS AND DISCUSSION

The FMR measurement is carried out at +15 dBm rf excitation power. Fig. 1 shows the measured ISHE voltage for the sample with IrMn(10 nm) at φ value of 30°. The angle φ denotes the angle between contacts to measure voltage and direction of applied dc magnetic field (*H*). Angle dependent ISHE study is carried out in order to disentangle the different spin rectification effect components.

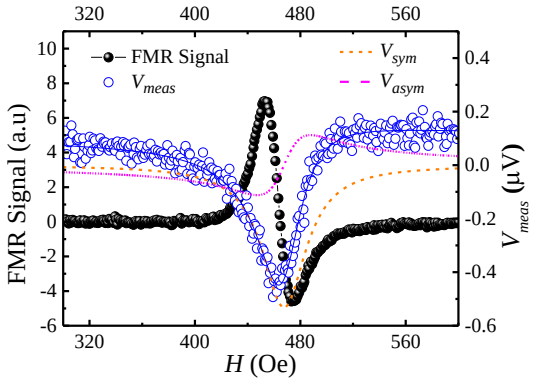

Fig.1. Voltage (V_{meas}) measured across the sample with applied magnetic field along with FMR signal for sample with IrMn(10 nm) at the φ value of 30°.

The angle dependent ISHE study reveals the spin pumping component in the measured voltage in the sample with IrMn(10) is -1.08 μV, which found to be higher than other rectification effects. The systematic damping and ISHE measurement analysis are carried out for all the samples to understand the spin current efficiency on the bilayers [6].

ACKNOWLEDGEMENT

The authors acknowledge DAE and DST, Govt. of India, for the financial support for the experimental facilities. KR and PG thanks CSIR and UGC for SRF fellowship respectively. BBS acknowledges DST for INSPIRE Faculty fellowship.

REFERENCES

1. S.D. Bader *et al.*, Annual Review of Condensed Matter Physics **1**, 71-88 (2010).
2. Y. Tserkovnyak *et al.*, Rev. Mod. Phys. 77, 1375 (2005).
3. E. Saitoh *et al.*, Appl. Phys. Lett. **88**, 182509 (2006).
4. Wei Zhang *et al.*, Phys. Rev. B **92**, 144405 (2014).
5. Singh *et al.*, Physica Status Solidi (RRL) **13**, 1800492 (2019).
6. Roy *et. al.*, J. Phys. D: Appl. Phys. **54**, 425001 (6pp) (2021).

P22

Interface selective study in Fe /^{57}Fe / C_{60} bilayer by placing ^{57}Fe marker at the interface; interface selectivity under x-ray standing wave condition

Sonia Kaushik[1], Avinash G. Khanderao[1], Md. Shahid Jamal[1], Ilya Sergeev[2], H.C. Wille[2], V. Raghavendra Reddy[1] and Dileep Kumar[1,*]

[1]UGC-DAE Consortium for Scientific Research, University Campus, Khandwa Road, Indore -452001, India

[2]Deutsches Elektronen-Synchroton DESY, Notkestraße 85, 22607 Hamburg, Germany

*Email (corresponding author): dkumar@csr.res.in

Abstract : Organic spintronics is one of the most advancing research fields for the last few decades. The interface of ferromagnetic metals and organic semiconductors plays a significant role in fabricating spin-valve devices. The magnetic properties of these interfaces play a vital role in the spin injection and extraction processes in organic spintronic devices [1-2]. In the present work, a thin film of Fe is deposited onto a C_{60} layer, and the magnetic property of the film is observed using magneto-optic Kerr effect measurements. This is understood precisely through interface resolved grazing incident nuclear resonance scattering (GINRS) measurements under X-ray standing wave (XSW). Since GI-NRS is an isotope sensitive technique, an ultra-thin marker layer of ^{57}Fe is deposited at the Fe/C_{60} interface. To generate XSW, Fe/C_{60} bilayer is deposited between high dense Molybdenum layers to make a waveguide structure. The position of the antinode is varied by changing incident angles to select interfaces. Present work provides an understanding of interfacial magnetism at metal-organic interfaces using GI-NRS technique. GI-NRS technique is made depth resolved to probe magnetism in the interface region, for which lab-based techniques seems to be inefficient. Reduced hyperfine fields has been obtained in the diffused layers of ^{57}Fe at the interface due to the formation of superparamagnetic clusters [3].

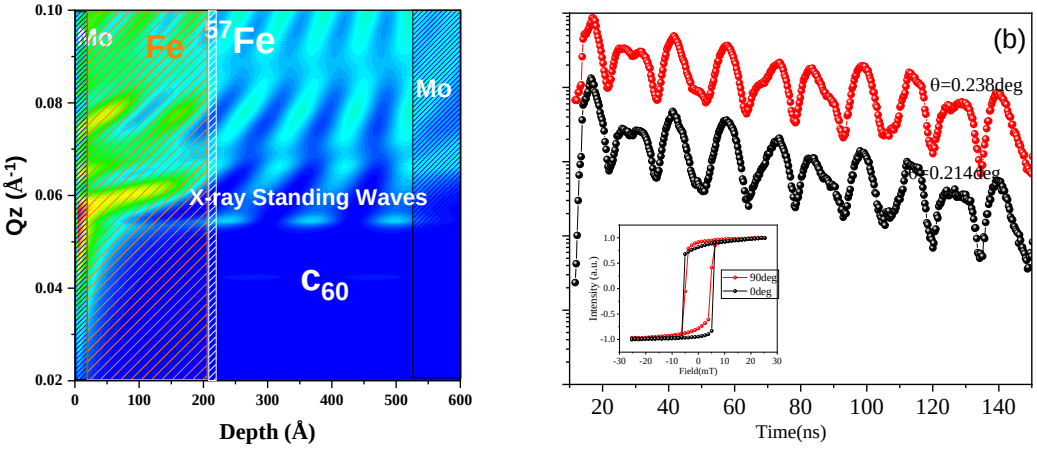

Fig. 1(a) Schematic of waveguide structure gives rearrangement of x-ray field intensity (EFI) as a function of the scattering vector q,: here Fe/C_{60} bilayer is sandwiched between two Mo layers, (b) GI-NRS time spectra of the ^{57}Fe in sample structure Si/Mo/C_{60}/^{57}Fe(1nm)/Fe/Mo.

REFERENCES

1. Mallik, S. *et al.* Tuning spinterface properties in iron/fullerene thin films. *Nanotechnology* **30**, 435705 (2019).

2. Khanderao, A. G., Sergueev, I., Wille, H. C. & Kumar, D. Interface resolved magnetism at metal–organic (Fe/Alq3) interfaces under x-ray standing wave condition. *Appl. Phys. Lett.* **116**, 101603 (2020).

3. Kaushik, S. *et al.* Study of obliquely deposited 57Fe layer on organic semiconductor (Alq3); interface resolved magnetism under x-ray standing wave. *Hyperfine Interact* **242**, 24 (2021).

P23

Magnetization Reversal in Fe/$BaTiO_3$(110) Heterostructured Multiferroics

Anupama Swain[1,4], Katsuyoshi Komatsu[2], Mitsuru Itoh[2], Tomoyasu Taniyama[2,3], and Venkataiah Gorige[4]

[1]School of Physical Sciences, NISER, Jatni 752050, India

[2]Laboratory for Materials and Structures, Tokyo Institute of Technology, Midori-ku, Yokohama, Japan

[3]Department of Physics, Nagoya University, Furo-cho, Chikusa-ku, Nagoya 464-8602, Japan

[4]School of Physics, University of Hyderabad, Hyderabad 500046, India

Email: swainanupama@niser.ac.in

Abstract: Magnetization reversal has been demonstrated in an Fe layer grown on $BaTiO_3$(110) single crystal substrate by utilizing the interface magnetic anisotropy induced by lattice strain and a small magnetic field bias. Cooling and heating cycles in the range of 150–325 K in an applied magnetic field of -35 Oe along [-111]pc enable to achieve the deterministic 180° magnetization reversal, where distinct magnetic anisotropies of Fe associated with different structural phases of $BaTiO_3$ will be the driving force. Electric field dependence of the magnetic coercivity shows hysteric behavior, which is attributed to the combined interfacial effect of magnetization rotation in Fe and ferroelectric polarization switching in $BaTiO_3$.

1. INTRODUCTION

In crystalline materials, magnetic moments, and electric dipoles are mutually exclusive due to symmetry constraints. Interestingly, the recent discovery of magnetoelectric (ME) multiferroics gives a ray of hope that leads to the coexistence of magnetic moments and electric dipoles in a single material with weak ME coupling at room temperature (RT) [1]. Alternatively, heterostructures of ferromagnetic (FM) and ferroelectric (FE) components are likely to be promising for device applications in the near future owing to their strong ME coupling at RT, flexibility in materials choice and design. Most importantly, FM/FEs provide a great opportunity for manipulating the magnetic properties by an electric field, which is an alternative approach beyond the traditional electric/spin current control of magnetism [2].

2. EXPERIMENTAL

Polycrystalline Fe films of 30 nm thickness with a 5-nm-thick Au cap were grown on a 500-μm-thick BTO(110) single crystal substrate at RT by using a molecular beam epitaxy. Ex-situ X-ray diffraction (XRD) measurements were carried out at RT in the θ–2θ scanning geometry. A vibrating sample magnetometer was used to measure the in-plane magnetization as a function of magnetic field orientation and temperature. Electric field (E) dependence of in-plane M–H loops using magneto-optical Kerr magnetometry. The ferroelectric hysteresis loops also were measured by using piezoresponse force microscopy.

3. RESULTS AND DISCUSSION

The XRD pattern of Fe/BTO measured at RT shows no prominent peaks corresponding to reflections from Fe, indicating that Fe films grown on BTO are polycrystalline with tiny crystallites since the growth of Fe films was carried out at RT. The in-plane M–H loops were measured with a view to understand the magnetic anisotropies of Fe/ BTO associated with the different ferroelectric phases of BTO at 293, 230, and 175 K that corresponds to the tetragonal (T), orthorhombic (O) and rhombohedral (R) phases of BTO, respectively. The polar plot of M_R/M_S in T phase shows isotropic behaviour, while in O and R phases it exhibits uniaxial magnetic anisotropy with the easy axis orientation along [-111]pc of BTO. The results indicate that the remanent magnetization in O and R phases should be almost aligned in the direction of easy axis irrespective of applied field direction and the alignment is much more prominent in R phase [3].

The in plane MT measurements at an applied field of -35 Oe depict that the strain-induced magnetic anisotropy associated with the different ferroelectric phases of BTO along with a small negative applied magnetic field makes it possible to achieve 180° magnetization reversal in Fe/BTO heterostructures. The in-plane M-H loops of Fe/BTO at different E shows that the applied $E \geq \pm 5$ kV cm^{-1} is large enough to bring the ferroelectric domains in the field directions, thereby causing a change in H_C. This indicates that the magnetization process is strongly coupled to the ferroelectric domain structures.

In summary, we have demonstrated strain mediated 180° magnetization reversal in Fe/BTO heterostructure via thermal and electric means. The magnetization reversal becomes possible with a unique set of magnetic anisotropies associated with the different ferroelectric phases of $BaTiO_3$ via interface elastic strain and small applied bias field.

ACKNOWLEDGEMENTS

The present work has been supported by collaborative research project (CRP-2015 & 2016) of Laboratory for Materials and Structures, Tokyo Institute of Technology. One of the authors (V. G.) would like to thank DST, UGC and CSIR of India for financial support.

REFERENCES

[1] H. Schmid, Ferroelectrics **162** (1994) 317.

[2] M. Opel et al, Phys. Status Solidi A **208** (2011) 232.

[3] V. Gorige et al, Phys. Status Solidi RRL 11 (2017) 1700294

P24

Effect of Ir spacer layer on perpendicular synthetic antiferromagnetic coupling in Co/Pt multilayers

Shaktiranjan Mohanty*, Minaxi Sharma, Brindaban Ojha,Ashish K moharana, Esita Pandey, Braj Bhusan Singh, Subhankar Bedanta

Laboratory for Nanomagnetism and Magnetic Materials (LNMM), School of Physical Sciences, National Institute of Science Education and Research (NISER), HBNI, Jatni-752050, Odisha, India
Email: *shaktiranjan.mohanty@niser.ac.in*

Abstract: Tunability, miniaturization and functionality of spintronics devices depend on the interface engineering of ferromagnetic (FM) and nonmagnetic (NM) ultrathin layers. In this context, synthetic antiferromagnets (SAFs), which consists of two or more FM layers separated by a spacer layer that may be metallic or a tunnel barrier, having antiparallel magnetization in the consecutive FM layers. Such kinds of SAFs gives extra degree of freedom over antiferromagnetic materials for the, measurements, manipulation of stray field, which helps to tune stability and sensitivity of the devices. Here we show the study of SAF nature in Co/Pt multilayers separated by Ir as a spacer. We have also studied the strain induced modification of the coupling strength of SAF structure.

Introduction

Development of next generation spintronics devices require the novel interface engineering of ferromagnetic (FM) layers to overcome the requirement of low current density to switch magnetization, high thermal stability, and fast speed of data writing reading etc. Magnetic tunnel junctions (MTJs) already established a jump in the enhancement of data storage capacity. [1]. Synthetic antiferromagnets (SAF) are the key part of these MTJs devices for better data retaining and thermal stability due to the absence of stray field. SAFs are basically with Ferromagnetic (FM) layers periodically interleaved with metallic or insulating spacers, where the magnetization of adjacent FM layers alternates owing to the antiferromagnetic (AF) interlayer exchange coupling (IEC). For metallic spacers, IEC is achieved via Ruderman-Kittel-Kasuya-Yosida (RKKY) type exchange interaction mediated by spin polarized charge carriers in the spacer [2]. By changing the thickness of non-magnetic material between two magnetic layers one can therefore tune the interaction from ferromagnetic preferring parallel alignment to antiferromagnetic, preferring antiparallel alignment, whereas for thick spacers the interlayer exchange coupling is suppressed . Using a SAF structure as either the free layer or the pinned layer, has the advantage of producing an adjustable net magnetic moment and reduced magnetostatic interaction between the layers and also provides a good field sensitivity [3].
Here fabricated SAF samples with Co as FM layer and Ir as a spacer layer and studied the magnetic properties. We then prepared the similar structure taking one FM layer both below and above the Ir spacer on a flexible polymide substrate. With the application of both compressive and tensile stress, we observed a substantial change in the interlayer exchange coupling of the SAF layers.

Experimental Details

All the samples were prepared using the multi deposition sputtering system manufactured by Mantis Deposition Ltd. For all the samples deposition, the chamber was maintained at a base pressure of ~ 2×10^{-7} mbar. During deposition, the substrate table was rotated at 15 rpm for all the layers. Domain imaging and hysteresis loop measurements have been performed by using magneto optic Kerr effect (MOKE) microscopy. Magnetization vs field was measured in a SQUID (Superconducting Quantum Interference Device) VSM. The sample structures are Si/Ta(3 nm)/ [Pt(3.5 nm)/Co(0.8 nm)]$_2$/Ir(t_{Ir} = 0.5, 1.0 1.5, 2 nm)/Co(0.8 nm)/ Pt(3.5 nm). Also one reference sample was prepared without the Ir spacer layer. The sample structure of the reference sample is Si/Ta(3 nm)/[Pt(3.5 nm)/Co(0.8nm)]$_2$/Ta(3 nm).

Result and Discussion

Among all the above mentioned structures, samples with Ir thickness 0.5 nm and 1.5 nm showAFM coupling between the Co layers. The samples with Ir thickness shows FMcoupling. Sample with 1. 5nm Ir thickness shows a strong AFM interlayer exchange coupling (Fig.1).

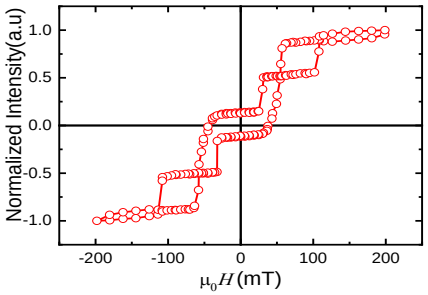

Fig. 1: Hysteresis loop obtained from the kerr Microscopy measurement for the SAF sample with Irthickness 1.5 nm

Acknowledgement

Authors would like to thank DAE & DST , Govt. of India for the financial support to carry out the experiments. BBS acknowledges DST for INSPIRE Faculty fellowship.

Reference

1. Chatterjee, J., Auffret, S., Sousa, R. *et al. Sci Rep* 8, 11724 (2018)
2. Kay Yakushiji *et al* 2015 *Appl. Phys. Express* 8 083003
3. Duine, R.A., Lee, K., Parkin, S.S.P. *et al., Nature Phys* 14, 217–219 (2018)

P25

Tailoring Dzyaloshinskii-Moriya interaction and domain wall dynamics in Pd/Co/C_{60}/Pd

Esita Pandey, Brindaban Ojha, Subhankar Bedanta
Laboratory for Nanomagnetism and Magnetic Materials, School of Physical Sciences, National Institute of Science Education and Research (NISER), HBNI, Jatni-752050, India
***Email: sbedanta@niser.ac.in**

Abstract: Spin dependent hybridization at the ferromagnet\organic semiconductor interface is very promising for fabricating highly efficient spintronic device. However, the ability of such spin polarized interface on tailoring domain wall dynamics and interfacial DM interaction is not understood well. In this context, we have studied the effect of inserting a low spin orbit coupling organic molecule (C_{60}) on the magnetic properties of PMA Pd/Co/Pd sample. The coercivity of the samples reduced systematically by increasing the thickness of the molecular layer. But a significant reduction of bubble domain size is found for a 0.5 nm thin layer of C_{60}. Magnetization relaxation mechanism became much faster in the Pd/Co/C_{60}/Pd samples due to the enhanced domain wall velocity measured by applying pulsed magnetic field. It reflects that the formation of a spin polarized interface (at Co/C_{60} interface), has reduced the magnetic anisotropy of the sample and enhanced the DW velocity in the creep region. The interfacial DM constant deduced by asymmetric DW expansion method shows an increase in DMI constant possibly due to the curvature enhanced spin orbit coupling in C_{60}.

1. INTRODUCTION

Interfacial Dzyaloshinskii-Moriya interaction (i-DMI) plays a crucial role for stabilizing chiral domain walls (DW) [1]. The strength of iDMI can be tuned by inserting different heavy metals (HM) in a symmetric PMA system [2]. As, organic molecules have recently shows an excellent tunability of PMA, hence in our work we have used an organic semiconductor (OSC) fullerene (C_{60}) to break the symmetry of an originally symmetric Pd/Co/Pd system [3]. As C_{60} exhibits a curvature enhanced spin orbit coupling [4], hence, the effect of introducing such OSC may significantly tailor effective iDMI constant and DW dynamics of the Pd/Co sample, which will be very promising from application viewpoint. A series of samples have been prepared by varying the thickness of C_{60} and their magnetic properties have been studied in detail.

2. EXPERIMENTAL DETAILS

We have prepared Pd/Co/C_{60}(t)/Pd samples, where only the thickness of C_{60} is varied in the series. Hysteresis loops and domain images have been recorded for all the samples using Kerr microscopy, whereas magnetic anisotropy is calculated using SQUID magnetometry. Magnetization relaxation measurements have been performed at sub-coercive field values by Kerr microscopy. DW velocity is measured at the creep region of the sample by symmetric domain expansion method whereas iDMI constants are evaluated by asymmetric domain expansion method.

3. RESULT AND DISCUSSIONS

A decrease in coercivity ($\mu_0 H_c$) of the samples have been observed with increasing thickness of C_{60}. After a certain thickness of C_{60} (~1.6nm) there are no further significant changes in $\mu_0 H_c$ has been observed, which gives an insight about the spinterface thickness of the sample. Bubble domain size is reduced significantly in the sample with 0.5 nm thickness of C_{60} from its reference sample. Such reduction might be attributed as a result of change in PMA and iDMI of the sample. Relaxation measurements revealed a faster relaxation phenomenon while insertion of C_{60} which indicates an effect of increased DW velocity. Thus, DW velocity is measured for all the samples and found that the velocity has increased by one order of magnitude in the sample with higher thickness of C_{60} than the reference sample, as shown in fig. 1. The experimental data are fitted by creep law written in following:

$$v = v_0 e^{\left[-\frac{T_d}{T}\left(\frac{H}{H_d}\right)^{-\frac{1}{4}}\right]} \quad \text{- (1)}$$

where, v_0 is a constant, T_d is the depinning temperature and H_d is the depinning field.

Such enhancement is further supported by a decrease in PMA and increase in iDMI strength in the samples with C_{60}. Thus, insertion of fullerene in Pd/Co/Pd helps to tune basic magnetic properties significantly due to interfacial hybridization at the Co/C_{60} interface.

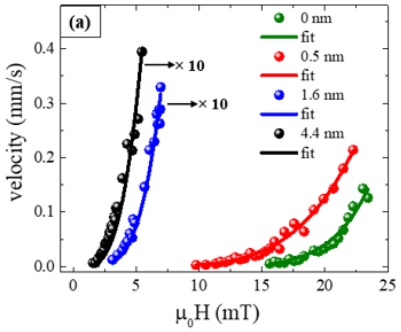

Figure 1. Velocity vs. $\mu_0 H$ plot for the Pd/Co/C_{60}(t)/Pd samples with varied t_{C60}.

4. REFERENCES

1. A. Thiaville et al., EPL **100**, 57002 (2012)
2. K. Shahbazi et al., Phys. Rev. B **99**, 094409 (2019)
3. K. Bairagi et al., Phys. Rev. Lett. **114**, 247203 (2015).
4. S. Liang et al., Sci. Rep. **6**, 19461 (2016)

P26

Study of the phase stabilization and spin to charge conversion in $Co_{40}Fe_{40}B_{20}/MoTe_2$

Mohammed Azharudheen*, Abhisek Mishra, Subhankar Bedanta

Laboratory for Nanomagnetism and Magnetic Materials (LNMM), School of Physical Sciences, National Institute of Science Education and Research (NISER), HBNI, Jatni-752050, India
Email: Email: *mohdazharudheen.n@niser.ac.in*

Abstract: Spin to charge conversion efficiency is one of the exciting topic in spintronics where Ferro magnet (FM)/Non magnet (NM) bilayers were largely explored. Recently, Transition metal dichalcogenides (TMD) are a emerged as possible candidate which can be serve as NM due to their high spin orbit coupling (SOC). Here we report the spin to charge conversion in $Co_{40}Fe_{40}B_{20}/MoTe_2$ bilayer.

1. INTRODUCTION

Search for the power efficient devices has openedd the way for spintronics where the spin degree of freedom is explored. One of the key property which couple the spin and charge degrees of freedom is SOC. Heavy metals (HM) like Pt,Ta are largely explored due to their large SOC. Since we have less number of HM and they are costly makes the limitation. In this context the TMD which have high SOC emerges as potential candidate. TMD have the general form of MX_2 where M is a transition metal and X is a halogen. Structurally van der wall interaction (vdW) mediates the inter layer coupling [1]. As a result one can thin down the material to monolayer by exploiting the week inter layer attraction. In the 2D regime TMD materials exhibit optical, electrical, and valleytronic proprieties. To fabricate TMD Mechanical exfoliation and chemical vapour deposition are the largely used but due the poor control over thickness, complicated chemical synthesis and limitation in the sample size end up in methods like sputtering.

Among various TMDs likeWTe_2, $MoTe_2$, MOS_2, $MOSe_2$ etc. MoTe2 is less explored due to challenges in stabilization of the phase [2]. $MoTe_2$ has high SOC and high mobility. Here we study the spin to charge conversion in $MoTe_2$ by Inverse spin hall effect (ISHE).

2. EXPERIMENTAL DETAILS

All the samples were prepared by DC magnetron sputtering with a base pressure ~$7x10^{-8}$ mbar on top Si(100) substrate.

Figure 1. Vsymmetric vs angle of R1 and S1

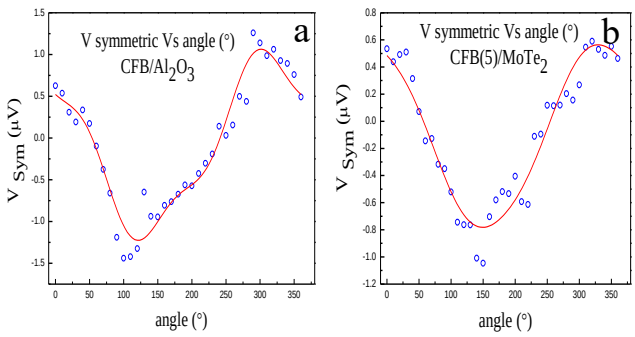

Both samples in the T**able 1** have been prepare with an argon floe of 20sccm. In order to reduce growth induced anisotropy substrate table rotated at 20 RPM. Thin layer of AlOx having thickness of 3 nm is used to protect the sample from the oxidation. The structural characterization were done by XRD and the surface morphology and the stoichiometry was performed with SEM.

The magnetization dynamics and ISHE studies were carried out with home modified FMR set up with a frequency range of (4-17) GHz [3].

3. RESULTS AND DISCUSSION

The presence of $MoTe_2$ in the 1 T semimetal phase was confirmed by Ramn peak at 159 cm^{-1} and XRD peak at 30º. Gilbert damping (α) of the samples are evaluated by FMR. The values of α for the samples R1, S2 are 0.0086,0.0092 respectively. It is clear that that α has increased when $MoTe_2$ deposited on top of CFB. It can be due to spin pumping, interface, proximity effect etc. in order to confirm the spin pumping we have performed the ISHE. Figure 1 shows the best fit of the Vsym Vs angle for the R1 and S1 Form the angle dependent ISHE study study it can be conclude that spin pumping voltage (Vsp) decreased in the sample with MoTe2 when compared to R1 [4]. It may be due to the rough interface between the CFB and the TMD.

Table 1. Fitted parameters of angle dependent ISHE

sample		Vsp(μV)	V_{AHE} (μV)
R1	CoFeb(12)/Al2O3(3)	2.169	1.608
S2	COFeb(12)/MoTe2((10)Al2 O3(3)	1.38	1.04

ACKNOWLEDGEMENT

The authors acknowledge DAE , Govt. of India, for the financial support for the experimental facilities.

REFERENCES

[1] S. Husain *et al*, Appl. Phys. Rev. **7**, 041312 (2020).
[2] J. Huang *et al*, Sci. Rep. **9,** 8810(2019).
[3] Singh *et al.*, Physica Status Solidi (RRL) **13**, 1800492 (2019).
[4] S.D. Bader *et al.*, Annual Review of Condensed Matter Physics **1**, 71-88 (2010).

P27

Skyrmion Hall Effect in synthetic ferrimagnet

Susree Sucharita Mohapatra, Shaktiranjan Mohanty, Brindaban Ojha, Subhankar Bedanta
Laboratory for Nanomagnetism and Magnetic Materials (LNMM), School of Physical Sciences, National Institute of Science Education and Research (NISER), HBNI, P.O. Bhimpur-Padanpur,Via –Jatni, Odisha-752050, India
***Email: sbedanta @niser.ac.in**

Abstract: In this work, we have studied skyrmion hall effect in synthetic ferrimagnet using micromagnetic simulations. We modelled a synthetic ferrimagnetic system where only the bottom NM/FM interface has isotropic/anisotropic DMI. We have applied spin polarised current to bottom layer to nucleate skyrmions/antiskyrmions and due to RKKY type interlayer exchange coupling and dipolar coupling, another skyrmions/antiskyrmion will be generated at top layer with different chirality. The interlayer exchange coupling J is varied to observe the effect of the coupling strength on skyrmion hall effect in both the layers. We have also varied the thickness of the non-magnetic spacer to examine the effect of dipolar coupling on the stabilization of skyrmions.

1. INTRODUCTION

The ever-increasing need for massive storage capabilities and processing speeds demands more energy consumption which hugely impacts our environment. Magnetic skyrmions are nanoscale sized, topologically-protected solitons and can be driven by very low current density.Room-temperature magnetic skyrmion has been also observed in heavy metal/ferromagnet heterostructures with broken inversion symmetry, owing to an interfacial Dzyaloshinskii-Moriya interaction (DMI) induced by strong spin-orbit interaction.[1]However skyrmion Hall effect is one of the problems for systems using skyrmions as information carriers.

The skyrmions in case of synthetic ferrimagnet move towards the edge diagonally with respect to the current flow because of topological magnus force producing a sizable skyrmion Hall effect. However, for SAF, the motion of skyrmions along the transverse direction is insignificant when the strength of interlayer exchange coupling is high.[2] For current-induced motion of skyrmion, skyrmion Hall angle is given by $\theta_{sk}=\tan^{-1}(l_y/l_x)$ where l_x and l_y are displacement in the x and y directions (x-direction is parallel to the direction of current).[1]

2. SIMULATION DETAILS

The 3D solver of the object oriented micromagnetic framework (OOMMF) i.e., Oxsii was used for the simulations. Isotropic DMI is used for the stabilization of skyrmions and anisotropic DMI is used for antiskyrmions. We have considered 3 systems where the ratios of saturation magnetization of top and bottom FM layers are 0.75, 1, and 1.25 respectively. The value of Ms for the bottom layer is fixed to be $700 \times 10^3 \frac{A}{m}$.The interlayer exchange coupling J is varied to observe the effect of coupling strength. We have also varied the thickness of the NM spacer from 1 to 10nm to check the effect of dipolar coupling on skyrmions stabilization in the top layer.

3.RESULTS AND DISCUSSION

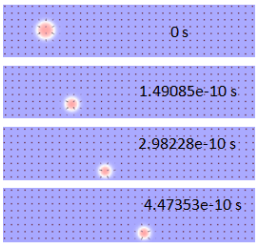

Fig.1: Skyrmion Hall Effect

Spin polarized current is applied to the bottom layer of the system to generate skyrmion/antiskyrmion and because of RKKY coupling,we can observe another skyrmion/antiskyrmion in the top layer.On increasing the thickness of the spacer,we observe that skyrmions cannot be stabilized in the top layer of the system. Skyrmion Hall angle is calculated for different J values for the 3 systems.For SAF, the skyrmions Hall angle is found to be negligible.

4. TABLE

Table 1. Calculation of Skyrmion Hall Angle

Ms_{top}/Ms_{bottom}	J J/m^2	θ_{sk} °
0.75	2×10^{-3}	36.86°
1.25	2×10^{-3}	4.57°

ACKNOWLEDGEMENT

We thank Department of Atomic Energy (DAE), Govt. of India for providing the funding to carry out the research work.

REFERENCES

[1]. Dohi, Takaaki, et al. "Formation and current-induced motion of synthetic antiferromagnetic skyrmion bubbles." *Nature communications* 10.1 (2019): 1-6.

[2]. Zhang, Xichao, Motohiko Ezawa, and Yan Zhou. "Thermally stable magnetic skyrmions in multilayer synthetic antiferromagnetic racetracks." *Physical Review B* 94.6 (2016): 064406.

P28

Inverse spin Hall effect in sputter deposited MoS_2/CoFeB bilayers

Abhisek Mishra*, V.Thiruvengadam, Pushpendra Gupta, Koustuv Roy, Braj Bhusan Singh, Subhankar Bedanta

Laboratory for Nanomagnetism and Magnetic Materials (LNMM), School of Physical Sciences, National Institute of Science Education and Research (NISER), HBNI, Jatni-752050, Odisha, India
Email:abhisek.mishra@niser.ac.in

Abstract: Two dimensional (2D) transition metal dichalcogenides are known to possess high spin orbit coupling that make them promising candidates for emerging spintronic devices. Here we report the measurement of spin to charge conversion in sputter deposited MoS_2 by inverse spin Hall effect (ISHE). Angle dependent measurements of ISHE are performed to identify various galvanometric rectification effects.

1. INTRODUCTION

Pure spin current is the key factor for development of next generation fast and power efficient spintronic devices [1]. Spin pumping is an established method to generate spin current via precessing magnetization from a ferromagnetic (FM) layer by microwave driven ferromagnetic resonance (FMR) in a ferromagnetic-nonmagnetic (FM/NM) system [2]. Heavy metals like Pt, Pd, Ta etc. having high spin orbit coupling (SOC), are crucial for the spin to charge conversion efficiently. However, for fabrications of power efficient and fast spintronic devices at commercial level, new material engineering is required. In this context, transition metal dichalcogenides (TMDC) have shown potentials for spin-charge conversion due to their high SOC at atomically thin layer. Their layered structure can lead to formation of atomically flat surfaces thereby facilitating the transport properties to be tuned easily [3]. However, fabrication of 2D materials in large area is still a challenge. Therefore, it requires a high throughput technique like sputtering.

Here we report the spin-charge conversion by observing ISHE in sputtered MoS_2 thin films through the spin pumping from amorphous CoFeB.

2. EXPERIMENTAL TECHNIQUE

Thermally oxidized Si (100) substrate was used to grow 28 nm thick MoS_2 thin film, which is deposited by radio frequency (rf) magnetron sputtering. On top of it, CoFeB (6 nm) was grown by dc magnetron sputtering. To avoid oxidation, MgO layer was grown as a capping layer by electron beam evaporation. The sample was kept in a flip chip manner on a coplanar wave guide for the measurement of ISHE in a home modified FMR setup [4].

3. RESULT AND DISCUSSION

Angle dependent measurements of ISHE were performed to measure the spin pumping voltage at +15 dBm power of radio frequency field transmitted in the coplanar waveguide. Fig.1 shows the measured voltage signal (V_{meas}) for the sample MoS_2(28nm)/CoFeB(6nm)/MgO(2nm) at an in-plane angle of φ= 36° with applied dc magnetic field (H). For this sample the spin pumping voltage was found to be 1.58 μV. Frequency dependent damping studies and power dependent studies were carried out to understand the origin of the voltage signals obtained.

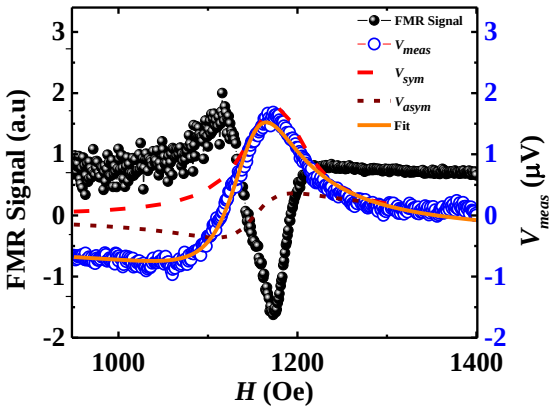

Fig.1. Voltage (V_{meas}) measured along with FMR signal for sample with MoS_2 (28 nm) at the φ value of 36°.

ACKNOWLEDGEMENT

The authors acknowledge the financial support by the Department of Atomic Energy (DAE) and Department of Science and Technology (DST-SERB) of Government of India for the DST-Nanomission [project sanction No. SR/NM/NS-1018/2016(G)]. PG and KR thank UGC and CSIR respectively for SRF fellowship. BBS acknowledges DST for INSPIRE Faculty fellowship.

REFERENCES

[1]. T.P.Pareek ,Phys. Rev. Lett. 92, 076601 (2004).
[2]. B. Heinrich *et al.*,Phys. Rev. Lett. 90, 187601 (2003).
[3]. Z.Hu *et al.*, Chem. Soc. Rev., 2018, 47, 3100
[4]. B.B.Sigh et *al.*, Phys. Status Solidi RRL 2019, 13, 1800492

P29

Spinterface-Induced Modification in Magnetic Properties in $Co_{40}Fe_{40}B_{20}$/Fullerene Bilayers

Purbasha Sharangi[1], Esita Pandey[1], Shaktiranjan Mohanty[1], Sagarika Nayak[1] and Subhankar Bedanta[1,2]

[1]Laboratory for Nanomagnetism and Magnetic Materials (LNMM), School of Physical Sciences, National Institute of Science Education and Research (NISER), HBNI, P.O.- Bhimpur Padanpur, Via Jatni, 752050, India

[2]Center for Interdisciplinary Sciences (CIS), National Institute of Science Education and Research (NISER), HBNI, Jatni, 752050 India

Email: purbasha@niser.ac.in

Abstract: Organic semiconductor/ferromagnetic bilayer thin films can exhibit novel properties due to the formation of spinterface at the interface. Buckminsterfullerene (C_{60}) has been shown to exhibit ferromagnetism at the interface when it is placed next to a ferromagnet (FM) such as Fe or Co. Formation of spinterface occurs due to the orbital hybridization and spin polarized charge transfer at the interface. In this work, we have demonstrated that one can enhance the magnetic anisotropy of the low Gilbert damping alloy CoFeB thin film by introducing a C_{60} layer. We have shown that anisotropy increases by increasing the thickness of C_{60} which might be a result of the formation of spinterface. However, the magnetic domain structure remains same in the bilayer samples as compared to the reference CoFeB film.

1. INTRODUCTION

In organic spintronics, organic semiconductors (OSCs) (e.g., C_{60}, Alq_3, Ruberene etc.) are used to transport or control spin polarized signals. The main advantages of OSCs are their low production cost, light weight, flexible and chemically interactive nature. There are several reports on organic spin valves, organic light emitting diodes (OLED) using C_{60} as a spacer layer. It has been shown that C_{60} (~2 nm) can be magnetized when it is placed next to a ferromagnetic (FM) layer.[1] d-p hybridization at the interface of FM/C_{60} modifies the density of states (DOS) and exhibits room temperature ferromagnetism. Such kind of interface is known as spinterface.[2] It has been found that ~ 2 nm of C_{60} exhibits magnetic moment ~ $3\mu_B$/cage at the epitaxial Fe/C_{60} interface.[1] There is a decrement in anisotropy in polycrystalline Fe/C_{60} system whereas for polycrystalline Co/C_{60} system anisotropy got enhanced.[3,4] However, to the best of our knowledge no such basic study has been performed on CoFeB system. For spintronic application a low damping material is always desired as it directly affects the speed of a device. The main advantage of taking CoFeB as a ferromagnet is that it exhibits low Gilbert damping parameter and it is amorphous in nature. In this regard, we have prepared CoFeB/C_{60} bilayer films and compared the magnetic properties to its reference CoFeB film.

2. EXPERIMANTAL MATHODS

CoFeB reference film with 5 nm thickness and bilayer (CoFeB/C_{60}) samples have been deposited on Si (100) substrate in a multi-deposition high vacuum chamber. The samples are named as S1, S2, S3, S4 and S5 for the thickness of C_{60} (tC60) taken as 0, 1.1, 2, 5, 15 nm, respectively. CoFeB, C_{60} and MgO layers have been deposited using DC sputtering, thermal evaporation and e-beam evaporation techniques, respectively.

3. RESULTS AND DISCUSSION

We have measured hysteresis loops along with domain images using MOKE based microscopy in longitudinal mode for all the samples. It has been observed that the change in domain structure is not significant between the single layer CoFeB and the bilayer CoFeB/C_{60} samples.

Further, to calculate the anisotropy of the system we have performed angle dependent ferromagnetic resonance (FMR) measurements. The measurement was performed at room temperature and a fixed frequency of 7 GHz. Figure 1 shows the H_{res} vs ϕ plots. The open circles represent the raw data and the solid lines are the best fits. The experimental data is fitted using Landau-Lifshitz-Gilbert (LLG) equation:[5]

$$f = \frac{\gamma}{2\pi}\left(\left(H + \frac{2K_2}{M_S}\,cos\ cos\ 2\phi\right)\left(H + 4\pi M_S + \frac{2K_2}{M_S}\phi\right)\right) \quad (1)$$

where, K_2 is the in-plane uniaxial anisotropy constant, ϕ is the in-plane angle between the easy axis w.r.t the applied magnetic field direction and M_S is the saturation magnetization.

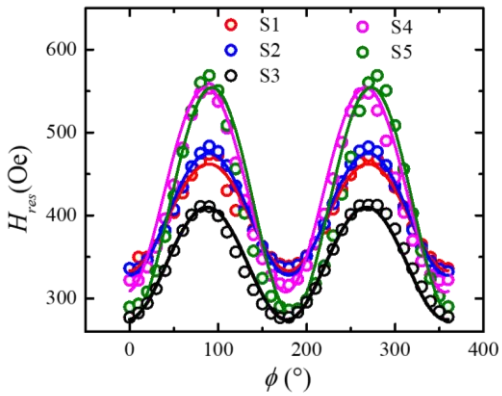

Fig.1. Angle dependent resonance field (Hres) plot for all the five samples to calculate the anisotropy constants of the system. Open circles represent the experimental data, while the solid lines are the best fits.

The extracted values of K_2 from the fitting of equation (1) for all the samples are shown in table1. It has been observed that the anisotropy of the system increases after inserting a C_{60} layer. The possible reason for this increment in the anisotropy might be due to the hybridization between *d* orbital of Co, Fe, and *p* orbital of C. Due to d-p hybridization at the interface, DOS of C_{60} is modified and forms a spinterface.

Table 1. The values of K_2 extracted from the fitting of LLG equation for all the samples.

Samples	K2 (erg/cc)
S1	2.56×10^4
S2	2.89×10^4
S3	3.12×10^4
S4	4.10×10^4
S5	4.31×10^4

ACKNOWLEDGEMENT

We would like thank DAE, DST-SERB, Govt. of India for funding.

REFERENCES

4. S. Mallik, et. al., Sci. Rep. **2018**, 8, 5515.
5. S. Sanvito, Nat. Phys **2010**, 6, 562-564.
6. S. Mallik, et. al., Nanotechnology, **2019**, 30, 435705.
7. S. Mallik, et. al, App. Phys. Lett., **2019**, 115, 242405.
8. S. Pan, et. al., Phys. Rev. Appl., **2017**, **7**, 064012

P30

Self-Modulation in nano-constriction based spin Hall nano-oscillators

Ujjawal Rathore1, Kacho Imtiyaz Ali Khan1, P.K. Muduli
1Department of Physics, Indian Institute of Technology, 110016
ujjawalrathore@gmail.com

Abstract: Spin Hall nano-oscillator (SHNO) is a nanoscale device that can generate microwave signal due to the spin-orbit torque. Here, we observe a phenomenon of self-modulation in SHNO using micromagnetic simulation. The self-modulation is characterized by the appearance of sidebands with a current-dependent modulation frequency in the range of 500 MHz to 1 GHz. At higher current, the self-modulation phenomena disappears, and only a single mode is observed. The mechanism of self-modulation will be explored using the mapping of spin-wave modes.

1. INTRODUCTION

SHNO is a nanoscale microwave signal generating device that can be used as a potential candidate for microwave communication and neuromorphic computing. It works on the basic phenomenon of spin Hall effect (SHE) in heavy metal (HM). When a charge current is applied to the HM layer a pure spin current is generated in the transverse direction with a spin polarization orthogonal to the direction of charge current. The spin current can consequently apply torque to the magnetization of the FM layer. When the current density is high enough to balance the damping of magnetization in FM, then auto-oscillation of magnetic moments occurs in the FM layer. Previoisly, the sideband is observed in NC-STNO due to magnetic droplet formation at the nano-contact [1]. Micromagnetically they shows that sideband is formed due to droplet oscillation.

2. RESULTS AND DISCUSSION

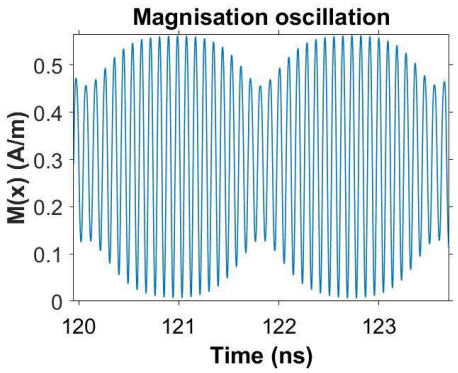

Fig.1. Auto-oscillation of X-component of magnetization at current 2.04 mA.

In this work, we show the evolution of sideband frequency for a particular current range in a nano-constriction (NC) based SHNO using micromagnetic simulation in mumax3.

Here, we have taken platinum (Pt) as HM layer, and permalloy (Py) as the FM layer with saturation magnetization of 0.6 MA/m, Gilbert damping of 0.04, exchange stiffness of 10 pJ/m, spin Hall angle is 0.04 [2]. The electrical current density is simulated using the COMSOL Multiphysics software [3], and exported data is imported in Mumax3 [4].

The auto-oscilltion of X-component if magnetization (Mx) is shown in Fig.1. The threshold current of auto-oscillation observed is 2.04mA. Just above the threshold, sidebands appear at frequency ±0.57 GHz from the main frequency 10.9 GHz (Fig.2). The modulation frequency is in the range of 500 MHz to 1GHz. The self-modulation phenomenon disappears at a higher current and only a single mode is observed.

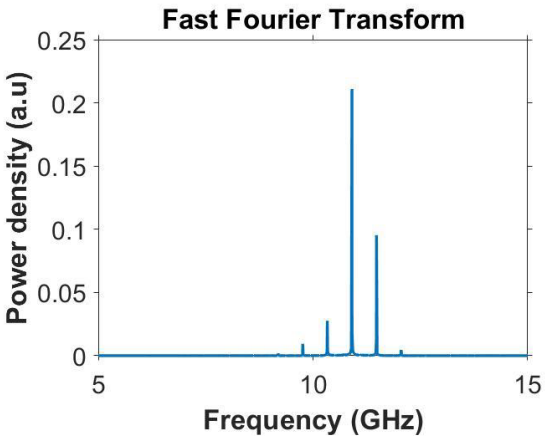

Fig.2. FFT of auto-oscillation at current 2.04 mA.

ACKNOWLEDGEMENT

The authors thank the IIT Delhi HPC facility for computational resources and support from Ministry of Human Resource Development (MHRD), India.

REFERENCES

[1] S. M. Mohseni *et. al.*, Science 339, 1295
[2] M. Dvornik *et. al., Phys. Rev. Appl.* 9, 014017 (2018)
[3] COMSOL, Inc., COMSOL MULTIPHYSICS software.
[4] A. Vansteenkiste *et. al., AIP Adv*. 4, 107133 (2014).

P31

Large area growth of 2D-GeTe thin films using pulsed laser deposition for spintronics application

Himanshu Bangar[1*], Sheetal Dewan[3], Richa Mudgal[1], Samaresh Das[2], and P.K. Muduli[1]

[1]Department of Physics, Indian Institute of Technology Delhi, Hauz Khas, New Delhi-110016, India
[2]Center for Applied Research in Electronics, Indian Institute of Technology Delhi, Hauz Khas, New Delhi-110016, India
[3]School of Interdisciplinary Research, Indian Institute of Technology Delhi, Hauz Khas, New Delhi-110016, India
***Email: bangarhimanshu9@gmail.com**

Abstract: In the proposed work, crystalline GeTe thin films have been obtained on Si (111) substrates using pulsed laser deposition technique. The GeTe thin films were characterized post-deposition, using XRD, Raman and AFM measurements which confirms the growth of uniform and epitaxial thin film of α-GeTe, The results are highly encouraging for the realization of α-GeTe thin films for spintronics applications.

1. INTRODUCTION

GeTe belongs to a unique class of materials called Ferroelectric Rashba SemiConductors (FERSCs), which are believed to show a great potential for application in spintronics due to a link between spin chirality in Rashba band and ferroelectric polarization [1]. This link could possibly help in electric control of spin transport via manipulation of ferroelectric polarization [2]. Through symmetry arguments, it is proposed that GeTe may exhibit unconventional spin-orbit torques (SOTs), which is very important for energy efficient switching of magnets with PMA [3].

To explore the potential applications of GeTe, large area and highly crystalline thin film growth of GeTe is a pre-requisite. Of all the growth techniques known, Pulsed Laser Deposition (PLD) technique is known to yield stoichiometric and crystalline thin films, with relatively lesser turn-around time.

2. MAJOR SECTIONS

High intensity KrF excimer laser (248 nm) was employed for ablating a ceramic target of GeTe at a laser power of 200 mJ in argon gas ambience. The thickness of the films was controlled using the number of laser shots. The GeTe thin films were grown at varying substrate temperature and argon gas pressure and characterized post-deposition, using XRD, Raman and AFM measurements.

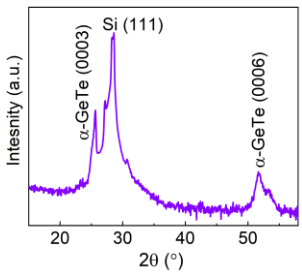

Fig.1 XRD measurement data showing α-GeTe and Si (111) peaks.

2.1. XRD measurements

The XRD measurements revealed the formation of crystalline GeTe thin films along (003) plane and showed variation in crystalline phases as a function of substrate temperature (Fig. 1).

2.2. Raman measurements

Raman measurements revealed distinct signature of E_{2g} and A_{1u} modes [4], which highlights the good quality of films obtained (Fig. 2).

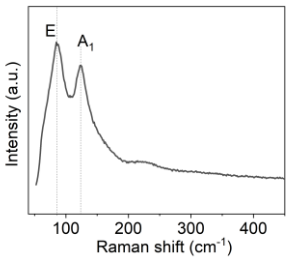

Fig. 2 Raman spectra acquired on GeTe thin film.

2.3. AFM measurements

The as-grown GeTe thin films were found to be homogenous and uniform across a large area of 1 cm x 1 cm, which highlights the efficacy of PLD technique for obtaining large area thin films. The average roughness of the films was estimated to be around 0.11 nm through AFM scans (Fig. 3).

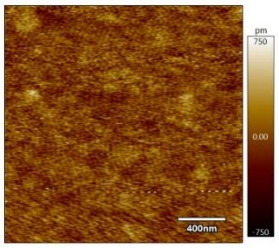

Fig. 3 AFM scan on GeTe thin film.

ACKNOWLEDGEMENT

We gratefully acknowledge the facilities provided by the Department of Physics and NRF at IIT Delhi. Himanshu also acknowledges CSIR for SRF.

REFERENCES

[1] R. Christian, et al., APL Mater. 3, 032501 (2016).
[2] D. Sante, et al., Adv. Mater. 25, 509 (2013).
[3] L. Yuting, et al., ACS Nano 14, 9389 (2020).
[4] R. Wang, et al., Sci. Rep. 6, 1 (2016).

P32

Tuning of magnetic properties by the formation of spinterface in CoFeB/Alq3 system

Swayang Priya Mahanta, Sagarika Nayak, Mohammed Azharudeen N, Subhankar Bedanta
Laboratory for Nanomagnetism and Magnetic Materials (LNMM), School of Physical Sciences, National Institute of Science Education and Research (NISER), HBNI, P.O. Bhimpur-Padanpur, Via –Jatni, Odisha-752050, India
***Email: sbedanta@niser.ac.in**

Abstract: The interface between the organic semiconductor (OSC)/ferromagnetic (FM) has attracted much attention recently. Charge/spin transfer may occur from the FM to OSC layer leading to the formation of "spinterface'' and can affects few magnetic properties like coercivity, domain structure, damping and anisotropy of the FM. Alq_3 is a promising organic molecule for spin transport over a long time. In this regard we have studied $Co_{20}Fe_{60}B_{20}$(CFB)/ Alq_3 bilayer system. Magnetic damping of CFB is in the order of 10^{-3}. We also have studied few magnetic properties like domains, hysteresis, anisotropy etc. of CFB/Alq_3 bilayer systems and observed significant modifications in various magnetic properties as compared to the reference CFB layer. The observed modifications can be attributed to the nature of spinterface.

1. INTRODUCTION

Spintronics is one of the emerging field for next generation devices to reduce their power consumption, to increase their memory and processing capabilities [1]. The technology manipulates spin degrees of freedom in addition to charge degree of freedom of current carriers. Spintronics has been widely explored in inorganic materials. Very recently, the use of organic molecules in spintronics devices has attracted much attention for future applications like magnetic sensors and memory devices [2]. Organic molecules are basically π-conjugated molecules which are composed of low atomic number elements like carbon (C), Hydrogen (H), Oxygen (O) and Nitrogen (N) etc. They are known for their low spin orbit coupling and less hyperfine interactions which makes them best candidates to transport spins over a long distance and long time. There are a number of OSCs like C_{60}, Alq_3, and Rubrene *etc.* Organic semiconductors could be utilised in novel spintronics devices in the future. As a result, further experimental and theoretical study is required to fully understand the mechanism of spin injection and spin transport.

2. EXPERIMENTAL DETAILS

For this study, we prepared three samples CFB (S1), CFB/Alq_3 (S2), Alq_3/CFB (S3) on Si (100) substrate. All the samples were capped with 3 nm of Cu layer. CFB and Cu layers were deposited using DC magnetron sputtering and Alq_3 layers were deposited using thermal evaporation technique in a multi deposition high vacuum chamber manufactured by EXCEL instruments, India.

Damping measurements were done using lock-in based FMR. The hysteresis loop and the domain images have been measured at room temperature using magneto-optic Kerr effect (MOKE) based microscopy manufactured by Evico magnetics GmbH, Germany. The hysteresis measurements have been performed within a field range of 5 mT by varying the angle φ in longitudinal modes. Here φ denotes the angle between the easy axis and applied field direction.

2.2. Results

We observed magnetic damping of 0.006 for CFB sample. Magnetic damping value increased significantly in S2 and S3 and the values are 0.11 and 0.01 respectively. Big stripes domains are present in CFB layers. Big domains are observed along easy axis for all the samples and domain size reduced while moving away from easy axis. Domain size and domain type changed when Alq3 layers were added above or below the CFB layers. The size got reduced in S2 and S3 as compared to S1 which is because of the nature of the FM/OSC interface in S2 and S3. We have also observed reduction in anisotropy and increment in coercivity as the effect of spinterface in S2 and S3.

3. FIGURES AND IMAGES

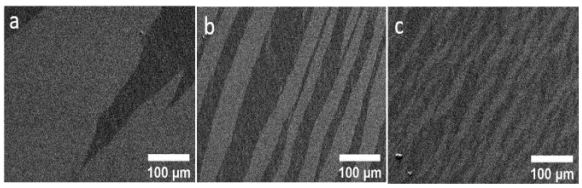

Fig.1. The image in the photograph shows the domains of sample S1, S2, S3 as a,b and c respectively at an angle of 45° away from easy axis.

ACKNOWLEDGEMENT

Authors would like to thank the Department of Atomic Energy (DAE) of Govt. of India for providing the funding to carry out the research.

REFERENCES

[1]. Atsufumi Hirohata, Keisuke Yamada, Yoshinobu Nakatani, Ioan-Lucian Pre-jbeanu, Bernard Diény, Philipp Pirro, and Burkard Hillebrands. Journal of Magnetism and Mag-netic Materials, 509:166711, 2020

[2]. Xiong, Z. H., Wu, D., Vardeny, Z. V. & Shi, J. Nature 427, 821–824 (2004).

P33

Effect of magnetostrictive strain upon the electronic transport in poly vinylidene fluoride thin films across Cu/PVDF/CoFe capacitor structures

C Raghavendar[a], Drishya A[a,b],Arul Chelvane[c], R. B. Gangineni[a]

[a]Department of Physics, School of Physical, Chemical and Applied Sciences, Pondicherry University. Kalapet, Puducherry 605014, India [b]department of Physics ,Amrita School of Arts & Sciences,Amrita Vishwa Vidyapeetham (Amritapuri Campus),Vallikavu, Kerala 690546,India.
[c]Defence Metallurgical Research Laboratory, Hyderabad 500 058, India .

Email:raghavachikkonda@gmail.com

Abstract: In this paper, the effect of magnetostrictive strain upon the electronic transport in poly vinylidene fluoride (PVDF) thin films across Cu/PVDF/CoFe capacitor structures is presented. The magnetoestrictive CoFe, PVDF and Cu thin films have been deposited using e-beam, spin coating and DC magnetron sputtering techniques. The non-linear electrical I-V characteristics reveal the different conduction processes across PVDF thin films at various voltage ranges. By applying the magnetic field, the strain is found to alter the electronic conduction across PVDF. Further, resistance versus magnetic field is correlated to the magnetization and its corresponding strain response with magnetic field.

. (Use Times New Roman 10 point).

1. INTRODUCTION

Organic ferroelectric polymers are found to be attractive for their functional properties such as ferroelectric, piezoelectric and pyroelectric natures and their significance in flexible electronic devices[1]. Magnetostrictive materials also show their significance in sonar applications due to their lattice dimensional change with magnetic field. The change in lattice dimensions is generally attributed to the strong L-S coupling and its relation to the magnetic domain variations [2]. Literature on bulk PVDF shows that it possess polymorphic structural phases such as α, β, γ and δ phases. Out of all the structural phases, β phase possess spontaneous polarization with theoretical P_S values of ~0.06Cm^{-2} [3].The polar-phase is commonly achieved by stretching or annealing at glass transition temperatures[4]. In thin film form, polar phase PVDF achieved by in-situ substrate annealing at 130°C[1]. In our recent findings, it is noted that interfacial contact at the electrodes determine the nature of electronic transport despite its polar structural phase. The interfacial contact leads to rectified I-V characteristics in (Hg, Ag)/PVDF/Au junctions[4]. In this paper, a systematic investigation is carried to evaluate the transport across Cu/PVDF/CoFe by straining the CoFe thin films by the application of magnetic field.

2. EXPERIMENTAL

The magnetostrictive CoFe stripes of 50 nm thickness and 1 mm wide films are deposited using e-beam evaporation technique at room temperature. The surface microstructure and the magnetic domain structure of the same is explored with AFM, MFM and LMOKE. The experimentally derived strain values corresponds to various thick CoFe films are presented elsewhere and for 50 nm CoFe thin film, ~ 150 μ strains is obtained [2]. The PVDF polymer has been coated using homemade spin coater at 2000,6000,10000 rpm with 4 wt% solution, which is made with DMSO

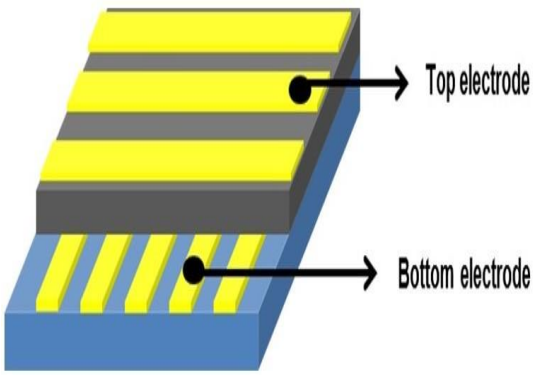

1. Schematic diagram of the Cu/PVDF/CoFe device structure along with the details of electrical contacts

solvent. Varied film thicknesses of 210 nm, 120 nm and 85 nm are prepared at 130°C and thickness is calibrated with Bruker MM8 AFM. The Cu top electrode with thickness of 200 nm is deposited using DC magnetron sputtering method with 1*10^{-2}mbar pressure at room temperature.

Further, keithley 238 is utilized to characterize the I-V characteristics under applied magnetic field. A 1T GMW magnet connected to bi-polar kepco power supply has been used to apply the magnetic field to the device structure. The schematic cross-point device structure along with the electrical contacts is presented in Fig.1.

3. RESULTS AND DISCUSSION

The surface microstructure of the PVDF thin films is shown in Fig.2 and reveals the increase in roughness with increase in thickness. Fig.3 a & 3 b shows the M vs. H of CoFe thin film and Resistance vs. H of Cu/PVDF/CoFe structure of different thick PVDF layer. A clear bi-stable magnetized squared hysteresis loop with coercive field of 175 Oe is noted. The maximum strain will be commonly noticed at the coercive fields due to the magnetic domain alignment in the direction of field [2]. Fig.3b shows the corresponding change in the resistance measured at 1 V with respect to applied magnetic fields and it shows clearly that the resistance follows the magnetic field and shows a maximum resistance at the coercive field which gets saturated above the coercive magnetic fields. Further, the I-V characteristics are measured up to voltages of ± 30 V with and without applied magnetic fields. Fig. 3a shows the coercive field of CoFe 50nm. Fig.3b represents the I-V characteristics with applied magnetic field close to the coercive magnetic field. A change in the electronic transport is noticed when the junctions are subjected to the magnetic fields.

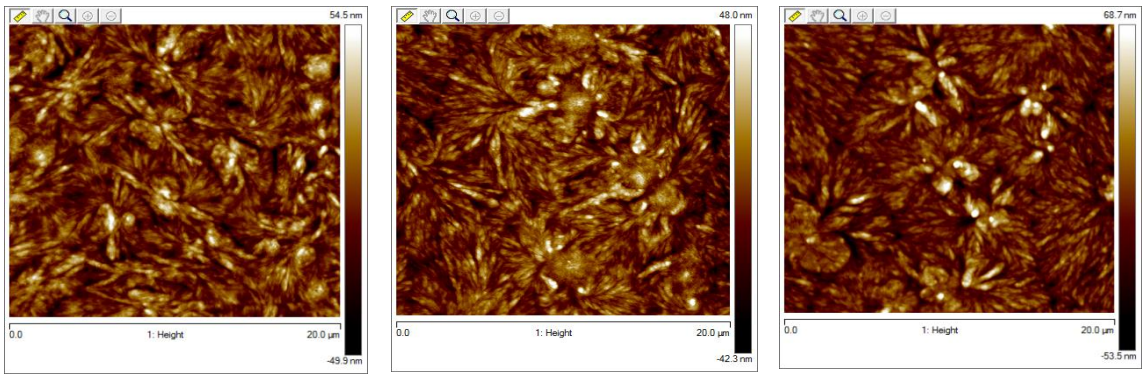

fig.2: AFM surface microstructural images of (a) PVDF(85nm)/CoFe ; (b)PVDF(120nm)/CoFe,; (c)PVDF (210nm)/CoFe

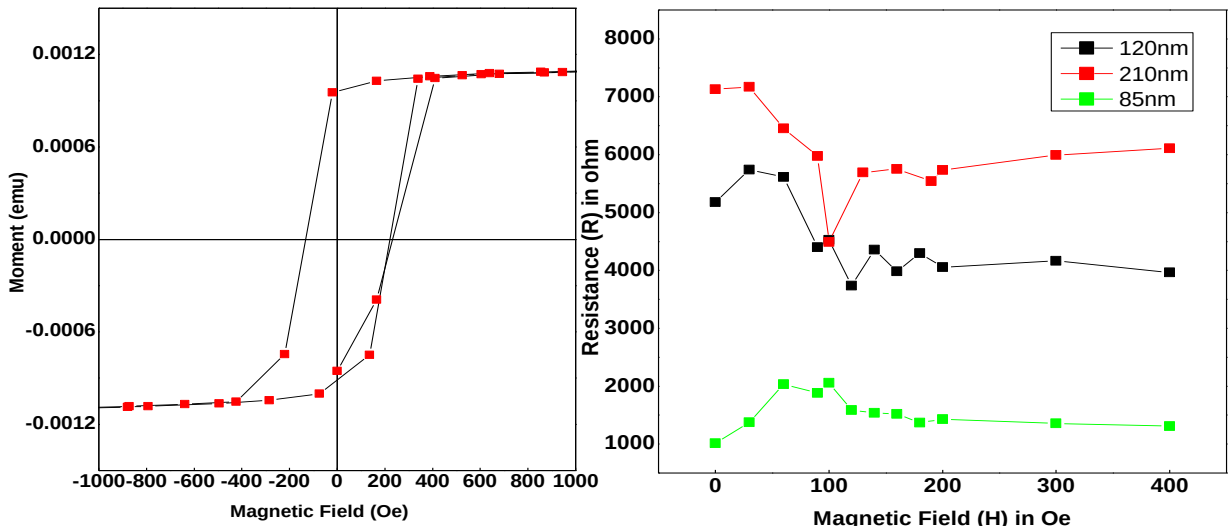

a). **b).**

figure.3: a) Magnetization versus magentic field of CoFe thin film and b) Resistance versus magnetic field of all PVDF layers are presented.

The electronic transport is further analyzed by representing as logI vs. logV and change in slope is attributed to the various conduction mechanisms, which are presented in Fig.4.

Figure.4

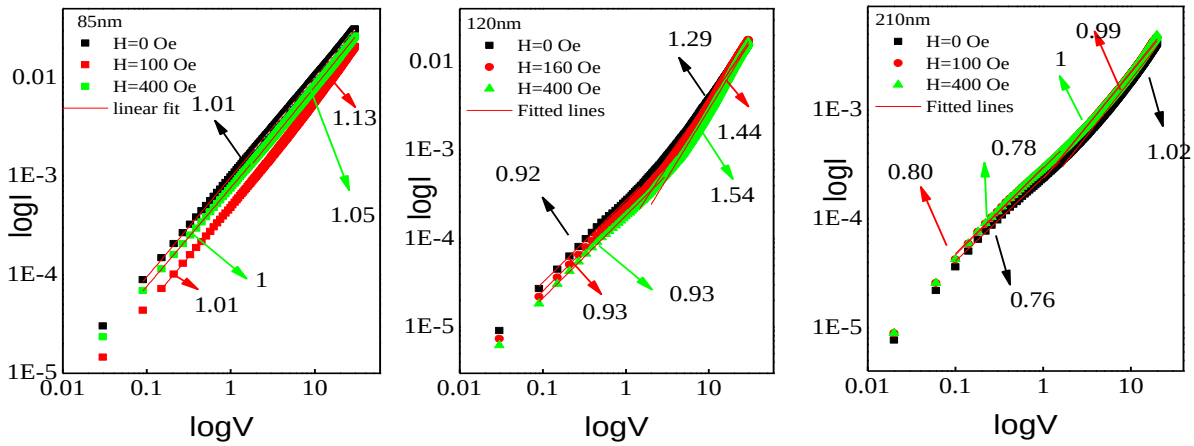

4. Summary and Conclusion

A systematic investigation of magnetostrictive strain influence is recorded in Cu/PVDF/CoFe junctions. It is noted that maximum change in resistance is observed at the coercive field and which is related to the maximum strain at the coercive field. In addition, strain transfer is found to be more efficient in 85 nm thick PVDF thin film based junctions. Furthermore, the electronic transport resulted in ohmic and space charge limited conduction processes. Our preliminary studies upon the strain influence upon the electronic transport may be useful for functional strain gauge applications.

5. Acknowledgements

R.B. Gangineni would like to acknowledge DMRL/O/CARS-19 dtd. 3l-05-201 7) project, DST-FASTRACK Project with Dy. No. SERB/F/0724/2013-2014, DAE-BRNS with sanction No: 2012/20/37P/09/BRNS, UGC-MRP/F.No-41-846/2012 (SR), UGC-SAP F.530/15/DRS/2009 and also Central Instrumentation Facility (CIF) at Pondicherry University**.**

6. References

[1] K. Pramod and R. B. Gangineni, “Influence of solvent evaporation rate on crystallization of poly(vinylidene fluoride) thin films,” *Bull. Mater. Sci.*, vol. 38, no. 4, pp. 1093–1098, 2015.

[2] K. Umadevi, J. Arout Chelvane, A. Talapatra, J. Mohanty, and V. Jayalakshmi, “Interplay of magnetic anisotropies on the magnetostrictive behavior of Fe–Co thin films,” *J. Mater. Sci. Mater. Electron.*, vol. 29, no. 20, pp. 17714–17721, 2018.

[3] H.S. Nalwa,*Ferroelectric Polymers:Chemistry:physics,and applications.CRC press,1995*

[4] K. Pramod and R. B. Gangineni, “Low voltage bipolar resistive switching in self-assembled PVDF nanodot network in capacitor like structures on Au/Cr/Si with Hg as a top electrode,” *Org. Electron. physics, Mater. Appl.*, vol. 42, pp. 47–51, 2017.

Voltage-controlled, Deterministic Domain Wall Rotation in Asymmetric Nanomagnetic Ring Structures for Manipulating Trapped Magnetic Nanoparticles in Fluidic Medium

Pankaj Pathak, Vinit Kumar Yadav, Dhiman Mallick
Department of Electrical Engineering, Indian Institute of Technology Delhi, India
Email: pankaj.pathak@ee.iitd.ac.in

In this work, elliptical rings of FeGaB on a single-crystal PMN-PT substrate are analyzed using Finite Difference Model (FDM). An external magnetic field along the minor axis of each magnetic ring is applied and subsequently removed after saturation. The DWs containing onion state is observed at a remanent state upto trackwidth where demagnetization energy to flip the magnetization 180° is higher. An external voltage across PMN- PT causes DWs to rotate at different angles depending on the ring dimension. Also, DW reversibility is analyzed after removing an external voltage. For lower trackwidth maximum in-plane 45° rotation and reversibility towards initial position are observed. On the other hand, for larger trackwidth complete in-plane 90° rotation is observed without DW reversibility Using an analytical model, the transport dynamics of MNPs is studied.

1. INTRODUCTION

Location-specific precise manipulation of magnetic nanoparticles (MNPs) in a fluidic environment is crucial for various biomedical applications. Although various techniques have been developed previously to manipulate MNPs, successful attempts in this direction are reported using controlling magnetic domain walls (DWs). In preceding studies, conventional methods such as external magnetic field and external current based methods have been investigated widely to control DWs. However, these methods are energy inefficient, spatially inaccurate and fall short to perceive the required manipulation. Lately, successful efforts towards this direction are reported using strain mediated magnetoelectrics (MEs) [1,2]. Although previous research suggests that the control and manipulation of the magnetic DWs using strain mediated MEs provides an ultra-low energy route for MNPs manipulation, still this manipulation ability in strain mediated MEs with magnetostrictive/piezoelectric heterostructure is restricted to magnetostrictive circular ring structures only where the obtained onion state is metastable, less thermally stable and can not be obtained easily. To overcome this, we have investigated elliptical rings of FeGaB on a single-crystal PMN-PT substrate to manipulate MNPs.

2. DOMAIN WALL ROTATION AND MNP MANIPULATION

In each magnetic ring, we observe DW transition from onion state having transverse (O-T) DWs to onion state having vortex (O-V) DWs when the external voltage is ramped up from 0volts. Two cases are observed. For lower trackwidth magnetic rings, stable O-V DWs are observed, which reorient towards the tensile strain direction. The upper value of this trackwidth is represented by t_{ol}. For each magnetic ring when trackwidth increases the reorientation angle towards tensile strain direction increases (fig 1). As the trackwidth is increased further, i.e. trackwidth > t_{ol} DWs again transforms from O-V to O-T. Generally, the additional rotation of the DWs beyond 45° requires strains in multiple angles which is achieved using a multielectrode system. Since in our model elliptical magnetic rings are analyzed it is observed that for trackwidth >t_{ol}, shape anisotropy energy is dominant contribution of total energy. This creates a favourable energy term along the easy axis of the magnetic ring and complete 90° rotation is observed. Based on the size-dependent DW rotation capabilities achieved for elliptical rings, the rotation of MNPs is predicted using an analytical model. It is observed that for thickness ≤ t_{ol}, MNPs can rotate maximum 45° and return to the initial position once an external voltage is removed. On the other hand, MNPs complete IP 90° rotation with no reversibility for thickness > t_{ol}.

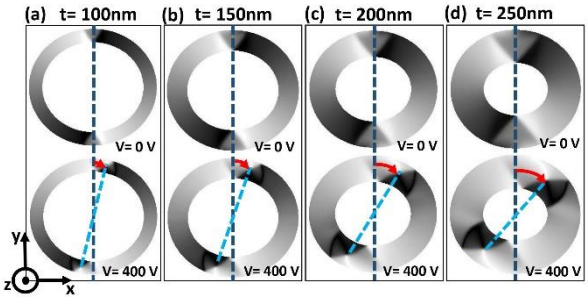

Fig1: Increase in the reorientation angle towards tensile strain direction with increase in trackwidth.

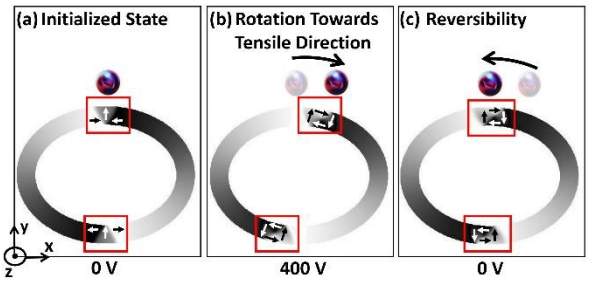

Fig2: (a) Trapping of MNP near initialized O-T DW at 0 volts (b) maximum rotation towards tensile strain direction at 400 volts and (c) MNP reversibility once the external voltage is removed.

REFERENCES

[1] P. Pathak and D. Mallick, IEEE Trans. Elect. Dev. 68, 4418 (2021).
[2] A. T. Chen and Y. G. Zhao, APL Mat.4, 032303 (2016)

Topic: Spin pumping and Spinorbitronics

P35

Spin pumping at terahertz nutation resonances

Ritwik Mondal[1,2]

[1]**Institute of Physics at the Czech Academy of Sciences, Prague, Czech Republic**
[2]**Uppsala University, Sweden**

Email: mondal@fzu.cz

Abstract: We investigate spin pumping current injected by the nutation resonances of a ferromagnet or an antiferromagnet into an adjacent metal. Comparing the dc spin pumping current between the normal precession and nutation resonances, we find that the ratio of spin pumping current at the nutation resonance to the precession resonance is more pronounced in antiferromagnets. We further show that the spin pumping current injected by the nutation resonance is opposite in sign as compared to the normal precession mode. This could offer a useful experimental signature for identifying such nutation resonances. Analysing the nature of the nutational eigenmodes, we show that the sign change in spin current is rooted in a reversal of the precession sense for the nutation mode(s). Furthermore, the nutational modes in antiferromagnets are found to be dominated by precession of one of the two sublattices only.

1. INTRODUCTION

The Landau-Lifshitz-Gilbert (LLG) equation has been used for last 50-60 years to understand the spin dynamics. Even we use LLG equation of motion in magnetic data storage devices. However, the LLG equation is fundamentally wrong at ultrafast timescales. The question is how can we use an equation that is wrong - well, it is wrong at the ultrafast timescales, while, it is correct at the shorter timescales. When the laser pulse hit a magnetic sample, initially the spin moment do not aling with the angular momentum. Such a situation gives rise to the fact that the spin moment starts rotating around the angular momentum causing spin nutation [1]. Such spin nutation additionally contributes to a second resonance peak in the ferromagnetic resonance spectrum — nutation resonance which has been observed in the experiments recently [2]. In this work, we investigate the Eigen modes of precession resonance and nutation resonance also investigate the injected spin current from ferromagnets and antiferromagnets to an adjacent metal.

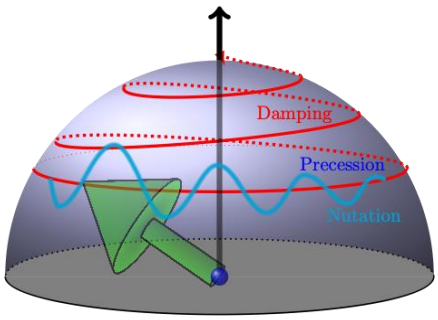

Fig.1. The schematics of ILLG dynamics. The color codes are similar as Eq. (1).

2. LINEAR RESPONSE THEORY

The inertial LLG (ILLG) equation can be written in the following form:

$$\frac{\partial \boldsymbol{M}}{\partial t} = -\gamma(\boldsymbol{M}\times\boldsymbol{H}) + \frac{\alpha}{M_0}\left(\boldsymbol{M}\times\frac{\partial \boldsymbol{M}}{\partial t}\right) + \frac{\eta}{M_0}\left(\boldsymbol{M}\times\frac{\partial^2 \boldsymbol{M}}{\partial t^2}\right) \quad .. \quad (1)$$

The first term here describes the spin precession around an effective field, the second term represents the phenomenological Gilbert damping, the third term denotes the spin nutation. Note that while the Gilbert damping α is dimensionless, η has a dimension of time. We calculate the magnetic susceptibility using the spin nutation term for a ferromagnet which has the following equation: $\chi_{\pm}(\omega) = \frac{\gamma M_0}{\Omega_0 - \omega - \eta\omega^2 \pm i\alpha\omega}$, where $\Omega_0 = \frac{\gamma}{M_0}(H_0 M_0 + 2K)$[3]. We calculate the dissipated power using the susceptibility expression showing that indeed there is an additional nutation resonance peak. We also investigate the Eigen modes of the precession and nutation resonances and find that while the precession mode rotates anticlockwise, the nutation mode rotates in the opposite sense. Further we compute the spin current injected from a ferromagnet and antiferromagnet to an adjacent layer that dictates the injection of spin current at the nutation resonance is more pronounced in antiferromagnets [4].

ACKNOWLEDGEMENT

We acknowledge the research funding from Alexander von Humboldt foundation and the Swedish Research Council via Grant No. VR 2019-06313.

REFERENCES

[1]. M.-C. Ciornei et al, Phys. Rev. B **83**, 020410 (2011).
[2]. Neeraj et al, Nat. Phys. **17**, 245 (2021)
[3]. Mondal et al, Phys. Rev. B **103**, 104404 (2021).
[4]. Mondal et al, arXiv:2110.05136 (2021)

P36

Effect of seed layer thickness on Ta crystalline phase and spin Hall angle

K. Sriram[1], Jay Pala[1], Bibekananda Paikaray[1], Arabinda Haldar[2], Chandrasekhar Murapaka[1,*]

[1]Department of Materials Science and Metallurgical Engineering, Indian Institute of Technology, Kandi, Sangareddy,502284, India.

[2]Department of Physics, Indian Institute of Technology, Kandi, Sangareddy, 502284, India

* E-mail Corresponding author: Electronic address: mchandrasekhar@msme.iith.ac.in

ABSTRACT

Spin-orbit coupling plays a key role in spin-to-charge interconversion and spin transport study in ferromagnet-heavy metal (FM-HM) bilayer structures is paramount important for spin based device[1]. Spin Hall angle quantifies the efficiency of spin-charge interconversion which is proportional to damping-like torque. The spin Hall angle strongly depends on the crystalline phase of the heavy metal[2]. It would be very interesting to investigate the effect of seed layer on crystalline phase of the heavy metal Ta and subsequently on the spin Hall angle. Here, we report that the crystalline phase of Ta strongly depends on the ferromagnetic seed layer and its thickness. We have observed a phase transition in Ta as the thickness of the seed layer increases which in turn affects the spin Hall angle of the Ta. We have found that Ta layers sputtered on Si substrate crystallizes in a single-phase α-cubic structure at relatively low deposition rates. However, when Ta is deposited on the permalloy (Py) seed layer at the same deposition rates it exhibits mixed-phase (α+β) which refers to the simultaneous presence of cubic and tetragonal structures. Crystalline phase of the Ta is found to depend strongly on the thickness of the seed permalloy layer and the strain at the Py/Ta interface. Ferromagnetic resonance(FMR) based spin pumping studies on the bilayer samples with two different phases of Ta reveal that the spin-mixing conductance and spin Hall angle in (α+β)-Ta are relatively higher as compared to α-Ta[3].

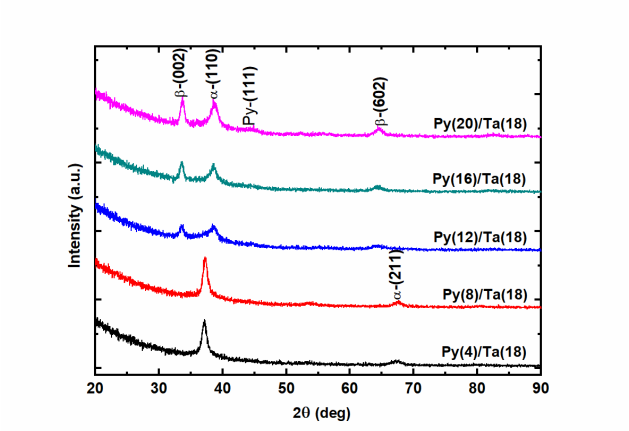

Figure: Py(t_{Py})/Ta(18) bilayer structure shows the Ta phase transition with a function of t_{Py}

P37

Skyrmion Dynamics in Nanodisk, Concentric and Eccentric Nano-Ring Structures

Bibekananda Paikaray[1], Mahathi Kuchibhotla[2], Chandrasekhar Murapaka[1, *], Arabinda Haldar[2, *]

[1] Department of Materials Science and Metallurgical Engineering, Indian Institute of Technology, Kandi, Sangareddy, Telangana, 502284

[2] Department of Physics, Indian Institute of Technology Hyderabad, Kandi, Sangareddy, Telangana, 502284

*** E-mail Corresponding authors: a) Electronic address: mchandrasekhar@msme.iith.ac.in, b) arabinda@phy.iith.ac.in**

Abstract: Skyrmions are found to be promising for next generation energy efficient spintronic applications. Moreover, ultrafast skyrmion dynamics in GHz-band offer an excellent opportunity to exploit such topologically protected nanostructures in high frequency applications. Here, we present a systematic investigation on the microwave properties of the skyrmions in nanodisk, concentric and eccentric ring structures using micromagnetic simulations. Two gyrotropic modes with clockwise and counter-clockwise gyration are observed in skyrmion when excited by an in-plane microwave field. The high frequency response is found to be enhanced by 4, 3.5 GHz by using a small bias field of 40 mT in nanodisk and concentric ring structure, respectively. The skyrmion dynamics are found to be extremely sensitive to the edge repulsions and a remarkably large frequency shift of 2 GHz of the skyrmion resonance modes is observed by simply varying the position of skyrmion in an eccentric ring structure. The results offer additional functionality of the skyrmionic structures for widely tunable microwave properties with ultra-energy efficient operation.

1. INTRODUCTION

Magnetic skyrmions are nanoscale swirling like magnetization textures with topological protection which can be stabilized in ferromagnetic systems with Dzyaloshinskii-Moriya interaction [1]. Skyrmions have attracted much attention recently in the field of spintronics, due to their nanoscale dimensions (10nm - 100 nm) and large stability due to topological protection. Currently, skyrmion are being explored for promising candidate for spintronic based memory and logic applications with low power consumption, fast processing and high density. Recent studies on skyrmion dynamics reveal that there are three types of skyrmion resonant modes: clockwise (CW), counter-clockwise (CCW) gyrotropic modes and breathing mode[2]. When subjected to an external microwave field perturbation, the guiding centre of an isolated skyrmion starts to gyrate CW and CCW which are associated with low and high frequency responses, respectively. Though several works are available on the microwave magnetization dynamics in nanostructures, investigation of the tunability of the skyrmion resonance modes is elusive.

2. SKYRMION DYNAMICS IN A NANODISK AND NANO-RING STRUCTURES

To study the skyrmion dynamics at remanence, the nanodisk is initialized with a Néel skyrmion having core oriented along –z direction using micromagnetic simulations MuMax3[3] as shown in Fig 1(a). The skyrmion resonance modes CW and CCW are excited by applying a sinc pulse field along an in-plane axis. Giant tunability (~ 4.2 GHz) for a small variation of the out-of-plane field which can be realized by using small DC current hoop in the nanodisk as shown in Fig 1(b). we have presented a systematic investigation of skyrmion dynamics and its tunability in concentric ring structures by varying OOP bias field as shown in Fig. 1(c). We have shown a huge frequency shift of 2 GHz by nucleating single skyrmion in narrower and wider regions of the inner circle as shown in Fig 1(d). This potential shift in frequency obtained from the eccentric ring can be attributed to the edge repulsions from the periphery of inner and outer circles. It offers a potential route for two (binary) distinct frequency states by simply driving the skyrmion in different positions of the eccentric ring. Such tunable skyrmion modes can be achieved by driving a skyrmion between different locations using an oscillating magnetic field or current (spin torque effect).

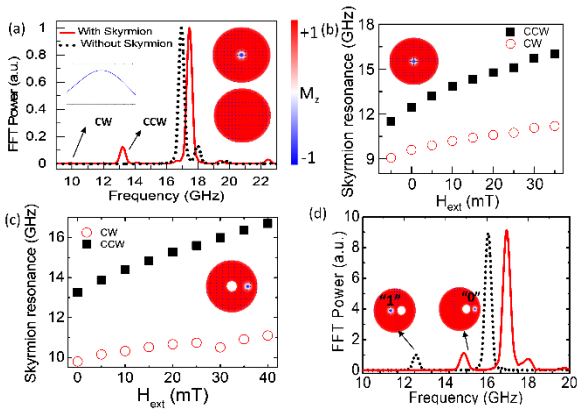

Fig.1. Dynamic responses of a disk (a) with a skyrmion (CW and CCW) and without a skyrmion. Variation of CW and CCW gyration modes of skyrmion with the bias field (b)Nanodisk (c)Nano-ring (d) Dynamic response of a single skyrmion stabilized at different locations of an eccentric ring.

ACKNOWLEDGEMENT

We would like to acknowledge funding from SERB Early Career Research Award (ECR/2018/002664), Ramanujan Fellowship(SB/S2/RJN-118/2016) and (DST/INSPIRE Fellowship/[IF180927]).

REFERENCES

[1] A. Fert et al, Nat. Rev. Mater. 2, 17031 (2017)
[2] K.Y.Guslienko et al, IEEE Magn. Lett. 8, 6 (2017)
[3] A. Vansteenkiste et al, AIP Adv. 4, 107133 (2014)

P38

Strain Driven Magnetic Properties in Epitaxial Layers of Site-Ordered Double Perovskite Pr_2NiMnO_6

Shekhar Tyagi [1], Rinku Kumar[2], Ramesh Chandra[2], Vivek K. Malik[1]
[1]Department of Physics, Indian Institute of Technology Roorkee, Roorkee-247667, Uttarakhand, India
[2]Nano Sacience Laboratory, Institute instrumentation center, Indian Institute of Technology Roorkee, Roorkee-247667, Uttarakhand, India
Email: vivek.malik@ph.iitr.ac.in

Abstract: We grow the epitaxial thin layers of varying thickness on different substrates, which were characterized in detail with high-resolution x-ray diffraction, vibrational spectroscopic and magnetic measurements. We observed absence of anti-ferromagnetic order, which in turn confirms the stabilization of the cationic site-ordered double perovskite structure in our thin films. To the best of our knowledge, this is our first report to date that sheds light on the strain engineering of magnetic properties in epitaxial layers of site-ordered double perovskite Pr_2NiMnO_6.

1. INTRODUCTION

Strain engineering is an effective tool to tailor the functional properties of materials in thin films, achieved through the lattice misfit between the substrate and the desired material. The nature of the strain can be compressive and tensile, directly depend on the appropriate substrate and the deposited material. Recently, the role of the strain in double perovskite films has been recognized in the discovery and development of new functional phases [1]. It plays a major role in deriving the physical properties of the materials such as structural, magnetic, electrical and vibrational, etc. It is often in practice that the structural change induced by substrate strain can strongly influence the transport and magnetic properties of the material in thin films. This study deals with the anti-site disordered double perovskite material Pr_2NiMnO_6, which has a monoclinic crystal structure (space group *P21/n*) with the lattice parameters a = 5.44Å, b = 5.47Å, and c = 7.69Å; which translates to a pseudo-cubic lattice with a_p = 3.86 Å [2,3]. The magnetic properties of this material are determined by the competition between ferromagnetism (ordered double perovskite) and anti-ferromagnetism (anti-site disordered double perovskite), which arise due to Ni^{2+}-O^{2-}-Mn^{4+} super-exchange interactions and exchange interactions of the Ni $^{2+}$-O $^{2-}$-Ni $^{2+}$ and Mn $^{4+}$-O $^{2-}$-Mn $^{4+}$, respectively.

2. EXPERIMENTAL METHODS

The polycrystalline Pr_2NiMnO_6 (PNMO) sample was prepared by standard solid state reaction method. The material was used to prepare a dense pellet of 20mm diameter as a target during deposition. Thin films of PNMO were grown on (001) oriented single crystal substrates of $LaAlO_3$ (LAO) and $(LaAlO_3)_{0.3}(Sr_2TaAlO_6)_{0.7}$ (LSAT) commercially procured from MTI-corp. USA, using pulsed laser deposition technique. A pulsed Excimer laser with 248nm wavelength (pulse width = 20 ns) providing an energy density of 3.6 J.cm^{-2} and repetition rate of 3Hz was used for the deposition. The substrate temperature was kept at 750°C during deposition in the presence of oxygen gas partial pressure of 0.630 mbar. After depositions, one-hour post annealing at the same temperature and 20°C per minute cooling rate resulted in best quality films. The phase purity of the films was confirmed by x-ray diffraction experiments. Reciprocal space mapping (RSM) measurements were carried out using Rigaku Smart Lab (9kW) high resolution X-ray diffractometer (HRXRD). Magnetic properties of the films were examined using Physical Property Measurement System (PPMS, Quantum Design Dyna Cool) in a temperature range of 5-350 K at 100 Oe magnetic field. Room temperature Raman spectroscopy measurements were performed using LABRAM HR-800 micro-Raman set-up equipped with 632.8 nm excitation laser source, an 1800 gr/mm grating and a peltier cooled CCD detector.

3. RESULTS AND DISCUSSION

. In this study, we grow the epitaxial thin films of Pr_2NiMnO_6 (PNMO) material with different thicknesses on (001) oriented single-crystal $LaAlO_3$ (LAO) and $(LaAlO_3)_{0.3}(Sr_2TaAlO_6)_{0.7}$ (LSAT) substrates using a pulsed laser deposition technique. The nomenclature S1, S2 and P1, P2 are used to denote {LAO / PNMO-50nm}, {LAO / PNMO-200nm} and {LSAT / PNMO-50nm}, {LSAT / PNMO-200nm} thin films, respectively.

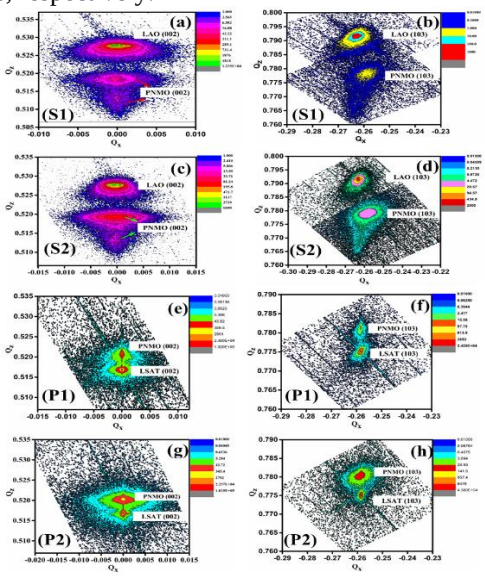

Fig.1. Reciprocal space mapping of S1, S2 and P1, P2 thin films.

The PNMO films were found to be highly oriented along the (001) direction, which was characterized by high-resolution X-ray diffraction technique. The in-plane and out-of-plane lattice parameters are derived from reciprocal space map measurements illustrated in fig. 1 which differ slightly (a = 3.86 Å and c = 3.83 Å), particularly in the case of LSAT films, demonstrating biaxial strain. Furthermore, in the case of LAO films with $a = c$ = 3.86 Å, we observed the presence of two-phase features, one of which is attributed to the stressed and the second to the relaxed. Interestingly, the relaxed phase shows a larger in-plane strain disorder (mosaic spread) than the stressed phase. The vibrational properties of the films at room temperature were examined by Raman spectroscopy, which showed the presence of two major Raman active modes at ~ 511 cm^{-1} and ~ 655 cm^{-1}, corresponding to the stretching mode of $(Ni/Mn)O_6$ octahedra. It is very important to note here that the Raman mode at ~ 511 cm^{-1} is part of the additional reflections that are generally activated due to the Brillouin zone and phonon branch folding, and the indication of cationic ordering at the Ni / Mn-site within the alternating layers of octahedra. These results validate the presence of a locally site-ordered double perovskite structure in our thin films. To investigate the effect of local structural adjustment in the magnetic properties, we performed the magnetization measurements as a function of temperature under the application of an applied magnetic field of 1000 Oe.

The magnetic data were recorded in the field-cooled (FC) and zero-field-cooled (ZFC) protocols for the films that showed two distinct transition temperatures associated with the stressed and relaxed phases in case of LAO films, and the presence of biaxial strain in case of LSAT films. Thus, the presence of the two-phase character and the biaxial strain control the magnetic properties by modulating the Ni^{2+}-O^{2-}-Mn^{4+} super-exchange interactions via a change in bond lengths/angles, resulting in two ferromagnetic orders.

ACKNOWLEDGEMENT

One of the author, Rinku Kumar would like to thank CSIR (Council of scientific and industrial research) (Grant No. 09/143 (0935)/2019-EMR-I) for financial support.

REFERENCES

[1]. M. P. Singh, K. D. Truong, S. Jandl, and P. Fournier, Phys. Rev. B 79, 224421, 2009.

[2]. P. Balasubramanian, S. R. Joshi, R. Yadav, F. M. F. Groot, A. K. Singh, A. Ray, M. Gupta, A. Singh, S. Maurya, S. Elizabeth, S. Varma, T. Maitra and V. Malik, J. Phys.: Condens. Matter 30 435603 (2018).

[3]. D. Topwal, D. D. Sarma, H. Kato, Y. Tokura, and M. Avignon, Phys. Rev. B 73, 094419 (2006).

P39

Giant Spin Pumping at Ferromagnet (Permalloy) - Organic Semiconductor (Perylene diimide) Interface

Talluri Manoj,[1] Srinu Kotha,[2] Bibekananda Paikaray,[1] Dasari Srideep,[2] Arabinda Haldar,[3] Kotagiri Venkata Rao*[2] and Chandrasekhar Murapaka*[1]

[1] *Department of Materials Science and Metallurgical Engineering, Indian Institute of Technology Hyderabad, Kandi-502285, Telangana, India*

[2] *Department of Chemistry, Indian Institute of Technology Hyderabad, Kandi-502285, Telangana, India*

[3] *Department of Physics, Indian Institute of Technology Hyderabad, Kandi-502285, Telangana, India*

* E-mail Corresponding Author: mchandrasekhar@msme.iith.ac.in

Abstract: Pure spin current based devices are attracting great interest in recent days. Spin current injection into non-magnetic materials is essential for the design and development of such pure spin current based devices. In this context, organic semiconductors (OSCs) can be potential non-magnetic materials over widely explored heavy metals. This is due to the relatively low spin-orbit coupling of OSCs, which is essential to host the spin current with a large spin diffusion length and long spin-relaxation time. This research work demonstrates the harvesting of spin currents at perylene diimide (PDI)/permalloy (Py) based OSC interface. The observed high linewidth broadening of 2.18 mT from ferromagnetic resonance spectra indicates the presence of giant spin pumping from Py to PDI. The resultant spin-mixing conductance, 1.54 x 10^{18} m^{-2} quantifies the amount of the spin current injected from Py to PDI, which is in the similar range of Ferromagnet/Heavy metals.

1. INTRODUCTION

Spintronic devices work based on the manipulation of spin property of electron along with its charge. Recent advances in the spintronics are on the generation, manipulation and detection of pure spin currents. The key advantage with pure spin current based devices is the absence of net flow of charge but a transfer of spin angular momentum. One of the prominent techniques developed for the generation of pure spin current is the spin pumping method where the spin current is injected from a ferromagnetic (FM) material to adjacent non-magnetic (NM) material. This process involves the excitation of magnetization precession in the FM under ferromagnetic resonance (FMR) conditions where the large precession of the magnetization leads to angular momentum transfer at the FM/NM interface. To date, several non-magnetic materials, mostly heavy metals such as Ta, Pt, etc. are vastly used as NM materials for spin-pumping studies. More recently, OSCs have received significant attention for spintronic device applications owing to their inherently small SOC strength as they are composed of low atomic number (Z) elements such as carbon and hydrogen, making them attractive for carrying the spin currents for longer distances. In this work, a soft magnetic material $Ni_{80}Fe_{20}$ (permalloy: Py) is chosen as FM acts as the spin source which enable efficient spin injection into the NM layers. We have chosen perylene diimide (PDI) based small molecular OSC NM material.

2. RESULTS

UV-Visible absorption spectroscopy and AFM images depicts J-aggregation of PDI molecules after spin coating. $Ni_{80}Fe_{20}$ (Py) was sputter-coated on top of PDI using a magnetron sputtering system. FMR spectra reveal the linewidth broadening of 2.18 mT for PDI/Py(16 nm) at 9 GHz which is more than one order of magnitude higher than OSCs reported so far.[1] The spin current injected from Py to PDI J-aggregates via spin mixing conductance is 1.54 x 10^{18} m^{-2} which was estimated from thickness dependence of α_{eff} which is in the range of widely explored FM/Heavy metal interfaces. The PDI which is deposited using spin coating has shown a disordered arrangement of J-aggregates and it has inherent higher charge carrier mobility as compared to DNTT, P_3MT and P_3HT4. We believe that the combination of both these factors that are mentioned above may be attributed to the enhancement of spin pumping into PDI from Py.[2]

3. FIGURES AND IMAGES

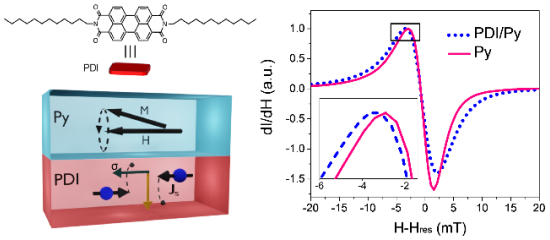

Fig: Schematic of PDI molecule and PDI/Py bilayer. FMR associated linewidth broadening in PDI/Py compared to Py

REFERENCES

[1]. A. Wittmann *et al., Phys. Rev. Lett.*, ***124***, *027204, 2020*

[2]. T. Manoj *et al., RSC Adv.*, ***11***, *35567–35574, 2021*

P40

Thermal stability and enhanced electrical properties of $Pb(Mg_{1/3}Nb_{2/3})O_3$ - $Pb(Yb_{1/2}Nb_{1/2})O_3$ - $PbTiO_3$ piezoelectric ceramic

Venkatraj Athikesavan

Dr.N.G.P. Institute of Technology, Coimbatore, Tamil Nadu, India - 641048

E-mail id – *venkatraj@drngpit.ac.in*

Abstract

PMN-PYN-PT (PMN = $PbMg_{1/3}Nb_{2/3}O_3$, PYN = $PbYb_{1/3}Nb_{2/3}O_3$, PT= $PbTiO_3$) were synthesized by conventional solid state reaction method and their thermal stability of piezoelectric properties was investigated. Results show that samples in the researched compositional range have high piezoelectric constant of d_{33}=473 pC/N. P-E hysteresis loops for the ceramic confirm good ferroelectric properties, exhibiting at (P_r ~ 17.5 μC cm-2 , E_c ~ 36.5 and P_m ~ 20.3) were obtained for PMN-PYN-PT. The thermal annealing behaviour at elevated temperature indicated that the ceramics exhibit good thermal stability, demonstrating that the ceramics are promising candidates for high temperature piezoelectric applications

P41

Effect of Spin Orbit Coupling in Mn_2CoSb Inverse Heusler Alloy for Spintronics

V. Aravindan[1], A. K. Rajarajan[2], V. Vijayanarayanan[1], M. Mahendran[1,*]

[1]Smart Materials Lab, Department of Physics, Thiagarajar College of Engineering, Madurai – 625 015, Tamil Nadu, India

[2] Solid State Physics Division, Bhabha Atomic Research Centre, Mumbai - 400 085, Maharashtra, India

*Email: manickam-mahendran@tce.edu

Abstract

We estimated the structural, mechanical, electronic, and magnetic properties of the Mn_2CoSb inverse Heusler alloy. The WIEN2k code was utilized in this study to do first-principles calculations using the Full-Potential Linearized Augmented Plane Wave (FP-LAPW) method. The Spin-orbit interaction in Mn_2CoSb can affect the electrical structure of the material because of the d-orbitals on the Mn and Co atoms. To determine the extent to which the spin-orbit interaction affects this material, we perform a first-principles study by implementing the spin-orbit coupling and examining how the band structure of Mn_2CoSb changes. This alloy exhibits half-metallic ferromagnetic behavior. The Mn_2CoSb alloy has an equilibrium lattice parameter of 5.98 Å and magnetic moments of 4 μ_B which is consistent with the well-known Slater-Pauling Rule: $M_t=Z_t-24$. The considered alloy exhibits 100% spin polarization at the Fermi level and a Curie temperature of 427 K, which makes it an ideal candidate for spintronic device applications such as spin injectors, Magnetic Tunnel Junctions (MTJ), spin valves, and Spin Torque Transfer-Random Access Memories (STT-RAM).

References

1. S.A. Wolf, D.D. Awschalom, R.A. Buhrman. 294 (2001) 1488–1495. https://doi.org/10.1126/science.1065389.
2. R.A. de Groot, F.M. Mueller, P.G. van Engen, and K.H.J. Buschow, Phys. Rev. Lett. (1983). https://doi.org/10.1103/physrevlett.50.2024.
3. V. Aravindan, A.K. Rajarajan, M. Mahendran, J. Electron. Mater. 50 (2021) 1786–1793. https://doi.org/10.1007/s11664-020-08688-5.
4. S.A. Khandy, I. Islam, D.C. Gupta, A. Laref, J. Solid State Chem. 270 (2019) 173–179. https://doi.org/10.1016/j.jssc.2018.11.011.
5. Y. Venkateswara, D. Rani, K.G. Suresh, A. Alam, J. Magn. Magn. Mater. 502 (2020) 166536. https://doi.org/10.1016/j.jmmm.2020.166536.

P42

Synthesis and characterization of pure and doped spinel manganese ferrites

Yaseen Ahmad, Bindu Raina, K.K. Bamzai*
Crystal Growth & Material Research (CGMR) Lab, Department of Physics,
University of Jammu, Jammu-180006 (India)
***Corresponding author e-mail: kkbamz@yahoo.com**

Abstract: Ferrites are interesting class of materials having unique physical, magnetic, optical and electric properties. They have lots of applications particularly in magnetic, biomedical, electromagnetic and microwave fields. In the present research work, magnesium and yttrium doped manganese ferrite based on the chemical formula $Mg_xMn_{1-x}Y_xFe_{2-x}O_4$ (x = 0.0, 0.05, 0.10, 0.15), in which yttrium is replacing iron and magnesium is replacing manganese, have been synthesized using chemical co – precipitation. The grown materials were then subjected to structural, morphological, optical and magnetic studies using PXRD, SEM, UV – Vis and VSM characterizations respectively. The crystal structure of all the samples is cubic spinel. Magnetic studies reveal the soft magnetic nature of the samples. The detailed results will be presented and discussed.

P43

Studies on preparation, structural and magnetic properties of some barium strontium titanate - strontium nickel hexaferrite multiferroic composites

Sonali Thakur, Bindu Raina and K. K. Bamzai*

Crystal Growth & Material Research Lab, Department of Physics,
University of Jammu, Jammu-180006 (India)
*Corresponding author, email: kkbamz@yahoo.com

Abstract: Polycrystalline multiferroic composites with composition (x) $Ba_{0.5}Sr_{0.5}TiO_3$ – (1-x) $SrNi_{0.25}Fe_{11.75}O_{19}$, where x = 0 to 1 materials have been synthesized using the solid-state reaction technique and have been characterized for structural, morphological, optical and magnetic properties using Powder X – ray diffraction (XRD), high resolution scanning electron microscopy (HRSEM), ultraviolet – visible (UV – Vis) spectroscopy and Vibrating sample magnetometer (VSM). XRD and HRSEM analysis confirm the co – existence of two phases in the composites. The optical band gap decreases from 3.5 to 1.65 eV with increasing the ferrite content in the composites. Magnetic analysis shows the increasing nature of magnetization (M_s) with increasing the amount of ferrite component in the composite. The detailed results will be presented and discussed.

P44

Syntheses, Structures, and Magnetic Properties of Pentanuclear Spirocyclic Ni_4Ln Derivative: Field Induced Slow Magnetic Relaxation by Dysprosium and Erbium Analogue

Pooja Shukla[a] , **Soumalya Roy**[a] , Dependu Dolui[b] , Walter Cañón Mancisidor* [c-d] and Sourav Das*[a]
[a] Prof. Dr. Sourav Das, Pooja Shukla, Soumalya Roy, Department of Chemistry, Institute of Infrastructure Technology Research And Management, Near Khokhra Circle, Maninagar East, Ahmedabad-380026, Gujarat, India. Homepage: www.iitram.ac.in
[b] Dependu Dolui, Discipline of Chemistry, Indian Institute of Technology, Gandhinagar, Gujarat 382355, India.
[c] Dr. Walter Cañón Mancisidor, Facultad de Químicas y Biología, Departamento de Química de Materiales, Universidad de Santiago de Chile (USACH), Santiago, Chile.
[d] Dr. Walter Cañón Mancisidor, Center for the Development of Nanoscience and Nanotechnology (CEDENNA), Santiago, Chile.

- *Corresponding author: walter.canon@usach.cl; d.sourav245@gmail.com ,

Abstract

Five pentanuclear heterometallic isostructural complexes, $[Ni_4Ln(L)_2(LH)_2(CH_3CN)_3Cl]\cdot xH_2O\cdot yCH_3OH$ (Ln= Y^{III} (1), Gd^{III} (2), Tb^{III} (3), Dy^{III} (4) and Er^{III} (5)) [for 1 and 2, x = 2, y = 1; for 3, x = 6, y = 2; for 4, x = 5, y = 1; for 5, x = 2, y = 2)] were prepared by the reaction of (E)-2-(hydroxymethyl)-6-(((2-hydroxyphenyl) imino) methyl)-4-methylphenol (LH_3) with $LnCl_3\cdot 6H_2O$ and $Ni(OAc)_2\cdot 4H_2O$ in the presence of Tetrabutylammonium hydroxide (TBA-OH) base. The structural characterization reveals compounds 1-5 contains spirocyclic pentanuclear core $[Ni_4Ln(\mu_3\text{-}O)_4(\mu_2\text{-}O)_4]^{3+}$ where two triangular motifs $[Ni_2Ln(\mu_3\text{-}O)_2(\mu_2\text{-}O)_2]^{3+}$ that are fused together through a common vertex of Ln(III) ion. The central Ln(III) ion forms an eight-coordinated distorted triangular dodecahedron geometry while the Ni(II) ions forms a distorted octahedron geometry. Comprehensive dc magnetic studies reveal antiferromagnetic exchange interaction present between the Ni(II) centrs. The ac susceptibility measurement revels that dysprosium and erbium analogue shows field induced slow magnetic relaxation with an anisotropic barrier (U_{eff}) of 25.12 cm^{-1} and 22.13 cm^{-1} respectively.

Keywords: 3d–4f Heterometallic Complexes, Schiff based ligand, Spirocyclic complex, SMM

References

[1] D. Gatteschi, R. Sessoli, J. Villain, Molecular Nanomagnets, Oxford University Press, Oxford, 2006.

[2] R. Sessoli, L. Hui, A.R. Schake, S. Wang, J.B. Vincent, K. Folting, D. Gatteschi, G. Christou, D.N. Hendrickson, J. Am. Chem. Soc. 1993, 115, 1804-1816.

[3] L. Bogani, W. Wernsdorfer, Nat. Mater. 2008, 7, 179-186.

[4] M. N.Leuenberger, D. Loss, Nature 2001, 410, 789-793.

[5] M. Mannini, F. Pineider, C. Danieli, F. Totti, L. Sorace, P. Sainctavit, M. A. Arrio, E. Otero, L. Joly, J. C. Cezar, A. Cornia, R. Sessoli, Nature 2010, 468, 417-421.

[6] D. N. Woodruff, R.E. Winpenny, R. Layfield, Chem. Rev. 2013, 113, 5110- 5148.

[7] R. Sessoli, A. K. Powell, Coord. Chem. Rev. 2009, 253, 2328-2341.

[8] S. K. Langley, N. F. Chilton, B. Moubaraki, K. S. Murray, Inorg. Chem. Front. 2015, 2, 867-875.

[9] J. Tang, P. Zhang, Lanthanide Single Molecule Magnets, Springer-Verlag : Berlin Heidelberg, 2015. [10] L. Ungur, J.J. Le Roy, I. Korobkov, M. Murugesu, L.F. Chibotaru, Angew. Chem. Int. Ed. 2014, 53, 4413-4417.

[11] Y. Chen, J. Liu, L. Ungur, J. Liu, Q. Li, L. Wang, Z. Ni, L. F. Chibotaru, X. Chen, M. Tong, J. Am. Chem. Soc. 2016, 138, 2829-2837.

[12] J. Liu, Y. Chen, J. Liu, V. Vieru, L. Ungur, J. H. Jia, L. F. Chibotaru, Y. Lan, W. Wernsdorfer, S. Gao, X. Chen, M. A. Tong, J. Am. Chem. Soc. 2016, 138, 5441-5450.

[13] S. K. Gupta, T. Rajeshkumar, G. Rajaraman, R. Murugavel, Chem. Sci. 2016, 7, 5181.

[14] S. K. Langley, D. P. Wielechowski, V. Vieru, N. F. Chilton, B. Moubaraki, B. F. Abrahams, L. F. Chibotaru, K. S. Murray, Angew. Chem. Int. Ed. 2013, 52, 12014-12019.

[15] J. Liu, J. Wu,Y. Chen, V. Mereacre, A.K. Powell, L. Ungur, L.F. Chibotaru, X. Chen, M. Tong, Angew. Chem. Int. Ed. 2014, 53, 12966-12970.

[16] J. D. Rinehart, M. Fang, W. J. Evans, J. R. Long, J. Am. Chem. Soc. 2011, 133, 14236-14239.

[17] L. R. Piquer, E. C. Sanudo, Dalton. Trans. 2015, 44, 8771-8780.

[18] S. K. Langley, D. P. Wielechowski, B. Moubaraki, K.S. Murray, Chem. Commun. 2016, 52, 10976-10979.

[19] T. Kajiwara, M. Nakano, K. Takahashi, S. Takaishi, M. Yamashita, Chem. - Eur. J. 2011, 17, 196-205.

[20] A. Bencini, C. Benelli, A. Caneschi, R. L. Carlin, A. Dei, D. Gatteschi, J. Am. Chem. Soc. 1985, 107, 8128-8136.

P45

Influence of Cr^{3+} ions on the physical properties of anatase TiO_2 nanostructures

M. Abushad[1,*], Swaleha Naseem[2], M. Arshad[1], Azizurrahaman[3], Shahid Husain[1], Wasi Khan[1]
[1]Department of Physics, Aligarh Muslim University, Aligarh-202002, India
[2]Interdisciplinary Nanotechnology Centre, Aligarh Muslim University, Aligarh-202002, India
[3]Materials Science Programme, Indian Institute of Technology Kanpur, Kanpur-208016, India
Email: makhan907@gmail.com

Abstract:

In the present study, polycrystalline TiO_2 and Cr doped nanostructures with chemical formula $Ti_{1-x}Cr_xO_2$ ($0 \leq x \leq 0.20$) have been synthesized through a cost-effective acid-modified sol-gel method. The influence of Cr doping on the microstructure, thermal, magnetic and photocatalytic properties of TiO_2 were investigated in detail. The surface morphology of the samples was studied using *field emission scanning electron microscopy (FE-SEM)* that reveals non-uniform shapes and less agglomeration of the particles in the doped sample. Energy dispersive x-ray spectroscopy (EDS) confirms the elemental compositions with the appropriate stoichiometry of the elements. Raman spectra ensure the phase purity of the materials and also a blue shift with the incorporation of Cr ions in TiO_2. X-ray photoelectron spectroscopy (XPS) quantitatively measures the elemental compositions, chemical and electronic states of the elements, including their bond energy, appropriate stoichiometry, and oxidation states of the compositions. The availability of unpaired electrons and paramagnetic centres in Cr doped TiO_2 samples have been confirmed by electron paramagnetic resonance (EPR) analysis. The magnetic properties of all the synthesized samples were determined by the vibrating sample magnetometer that reveal weak ferromagnetic behavior for undoped sample. In case of Cr doped samples, a significant enhancement in the unsaturation magnetization was found. These results signify that the creation of oxygen vacancies and defects play a very crucial role to developed the ferromagnetic nature of oxide semiconductors. The Differential Thermal Analyser (DTA) analysis shows that the occurrence of structural phase transition at around 630 ^oC. The photocatalytic performance of the prepared samples was studied for the degradation of methylene blue (MB) dye under irradiation of visible light. The highest value photocatalytic efficiency was found for the 20% of Cr doped TiO_2. The improvement in the efficiency may be associated with the separation of electrons and holes by trapping sites created. These studied suggest that the appropriate incorporation of Cr ions makes TiO_2 very efficient for visible light-driven photocatalyst required for the applications in wastewater treatment.

Keywords: TiO_2 nanostructures; Raman scattering; Thermal properties; Magnetic properties; photocatalytic activity

P46

Synthesis, Structural and Dielectric properties of Cobalt Bismuth Ferrite

Tanay S. Gore[1], Santosh S. Jadhav[2], Umakant. B. Tumberphale[3], Ravi S. Kawale[2], V. B. Kawade[4], Shyam K. Gore[2*]

[1]Shri Shivaji College Parbhani,431401 Maharashtra, India,
[2]Dnyanopasak Shikshan Mandal's Arts, Commerce and Science College, Jintur-431509, India,
[3]Microwave Research Laboratory N. E. S. Science College Nanded-431606, India,
[4]Late. Laximibai Deshmukh Mahila Mahavidyalaya, Parli Vaijanath, Dist. Beed, India
Corresponding author: shyamkgore@gmail.com.

ABSTRACT

Bismuth doped cobalt ferrite $Co_{1-x}Bi_xFe_2O_4$ ($0 \leq x \leq 0.16$) nanostructures were synthesized by sol-gel combustion route. The samples were characterized by X-ray diffraction, transmission electron microscope (TEM) and dielectric properties. The XRD spectra revealed that all the ferrite samples have single phase cubic spinel structure. The crystallite size was calculated using Scherrer formula. The crystallite size of samples was found to be 23-35 nm. The lattice parameter and crystallite size were increased with Bi^{3+} substitution. The porosity increases and bulk density decreases with increasing lattice constant for all the samples. The TEM analysis confirms the cubic shape and nano sized dimensions of the particles for the synthesized ferrites. The SAED pattern confirms the lattice planes revealed by the XRD analysis. The cation distribution obtained from XRD analysis reveals the distribution of cations at tetrahedral and octahedral sites of the ferrites. The dielectric constant (ε'), dielectric loss (ε''), loss tangent ($\tan\delta$) and a. c. conductivity (σ_{AC}) for all samples have been studied as a function of frequency in range from 50Hz to 5MHz at room temperature.

Keywords: Lattice parameter; Cation distribution; Dielectric constant; Dielectric loss tangent; a. c. Conductivity

P47

Re-entrant Spin Glass Behavior in Frustrated Double Perovskite Ho_2CoMnO_6 Nanorod

K Pushpanjali Patra and S. Ravi
Department of Physics, Indian Institute of Technology Guwahati, Guwahati-781039, India
Email: sravi@iitg.ac.in

Abstract: A hydrothermal technique has been used to prepare single-phase nanorods of double perovskite Ho_2CoMnO_6 and studied its structural and magnetic properties. Room temperature XRD and Raman spectra reveals that the samples comes under monoclinic structure with $P2_1/n$ space group. The formation of nanorods with an average diameter of 79 nm is confirmed as per the microstructural images. Magnetization versus temperature (M-T) analysis shows three transitions, a ferromagnetic (FM) at 182 K, antiferromagnetic (AFM) at 97 K and a re-entrant spin glass (SG) at 31 K respectively. From the magnetization versus field (M-H) measurement at 5 K, a very low value of coercivity (H_c) and saturation magnetization (M_S) is observed. It is attributed to the presence of higher oxidation states of the ions as well as multiple interactions in the system.

1. INTRODUCTION

A variety of magnetic properties and potential applications, such as multiple memory elements, spin filter junctions, storage components and many more have sparked recent interest in complex perovskite oxides with the general chemical formula $R_2BB'O_6$ (R-rare-earth, B/B'-transition metals) [1]. The ordering of B/B' in double perovskites is crucial in establishing their structure, space group, and functional features. The magnetic ordering is determined by the Goodenough Kanamori rule [2], which governs the super exchange interactions between the B and B' ions. Despite this, the Co/Mn based double perovskite family (R_2CoMnO_6) has recently attracted a lot of scientific attention, due to its complex behavior in magnetism which leads to a variety of applications [3, 4]. Now authors are giving interest in Ho based double perovskite (Ho_2CoMnO_6 (HCMO)) as it leads to complex magnetic properties by interacting with the Co/Mn ions [3, 4].

2. RESULTS AND DISCUSSION

2.1. Structural Analysis

The Rietveld refinement of XRD data along with all the reflection peaks readily indexed are shown in Fig.1.(a). It reveals that the sample is formed in pure monoclinic phase ($P2_1/n$). The lattice parameters are found to be higher than those of the reported bulk sample [3]. FESEM and TEM microstructural recordings revealed a clear image of rods and the average width of rod is found to be 79 nm.

2.2. Magnetic Analysis

Thermomagnetic (M-T) measurements were carried out at H = 100 Oe, in both zero-field cooled (ZFC) and field cooled (FC) condition and they are shown in Fig.1.(b) with inset showing dM/dT versus T plot. The 182 K is the FM transition (T_C) which is attributed to the super exchange interaction of Co^{2+}-O^{2-}-Mn^{+4} networks. The transition at 97 K is AFM, due to possible interaction such as, (i) AFM coupling between Ho^{3+} and Co^{2+}/Mn^{4+} ions. (ii) AFM coupling between Co^{2+}- O – Co^{2+} and Mn^{4+}-O - Mn^{4+} networks, (iii) presence of Co^{3+} and Mn^{3+} ions leading to minor AFM in the system. However, the peak at 31 K is ascribed as the re-entrant spin-glass transition temperature (T_{sg}) which arises due to the competition between FM and AFM spins. A small hysteresis is observed at 5K without any saturation of magnetization even at ±9T, signifying large AFM contribution or uncompensated spin structures. We have obtained the saturation magnetization (M_S) value as 8.53 μ_B/f.u. which is quite small than the values obtained in bulk samples [3, 4]. The existence of higher oxidation states of ions, as well as the multiple interactions in the system, causes the M_S value to drop.

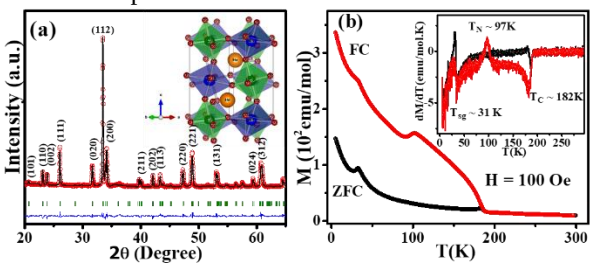

Fig.1.(a)RT XRD pattern along with its Rietveld refinement, inset shows its crystal structure and (b) M-T plot for both ZFC and FC condition at H = 100 Oe, inset shows dM/dT plot.

3. CONCLUSION

We have successfully prepared Single-phase Ho_2CoMnO_6 by hydrothermal route. Structural analysis reveals that it comes under monoclinic structure with $P2_1/n$ space group. From FESEM and FETEM we found the average width of the rod as 79 nm. Thermomagnetic study reveals three transitions such as FM at 182 K, AFM at 97 K and re-entrant spin glass at 31 K. The presence of multiple interactions in the compound leads to a lower value of saturation magnetization (M_S).

ACKNOWLEDGEMENT

We acknowledge Central Instrument Facility (CIF), IIT Guwahati for XRD, FESEM, FETEM facilities and DST-FIST for providing PPMS facility (SR/FST/PSII-037/2016).

REFERENCES

[1]. S. Vasala and M. Karppinen, Progress in Solid State Chemistry. 43, (2015) 1-36.

[2]. J. B. Goodenough, Phys. Rev. 100, (1955) 564−573.

[3]. D. Majumdar and I. Das, J. Appl. Phys. 129, (2021) 063901.

[4]. J. Blasco, J. L. Garcia-Munoz, J. Garcia, G. Subias, J. Stankiewicz, J. A. Rodriguez-Velamazán, and C. Ritter, Phys. Rev. B. 96, (2017) 024409.

P48

Synthesis, characterization and magnetic hyperthermia properties of fatty acid coated Fe_3O_4 magnetic nanoparticles

Fouzia Khan*, B.B. Lahiri, John Philip
SMARTS, CSTD, MMG, IGCAR, HBNI, Kalpakkam, Tamil Nadu, India, PIN 603102
Email: fouzia@igcar.gov.in

Abstract: Magnetic fluid hyperthermia properties were systematically probed for stearic and palmitic acid coated Fe_3O_4 nanoparticles, prepared using microwave assisted co-precipitation technique. Magneto-structural characterization studies confirm the presence of coating and superparamagnetic nature of the nanoparticles. Obtained results indicate significant field induced temperature rise in aqueous dispersions of the nanoparticles.

1. INTRODUCTION

Magnetic fluid hyperthermia (MFH) is one of the emerging technologies for cancer therapy, where Neel-Brown relaxation mediated magneto-thermal energy conversion of superparamagnetic nanoparticles (MNPs), under an exposure to a radio frequency alternating field (RFAMF), is exploited [1,2]. In the present study, Fe_3O_4 MNPs coated with two fatty acids, viz., stearic (SA) and palmitic (PA) acids were synthesized and MFH properties are probed systematically.

2. SYNTHESIS OF MAGNETIC PARTICLES

Required amounts of PA and SA were dissolved in acetone and added to the aqueous solution of sulphate salts of Fe^{2+} and Fe^{3+} (in stoichiometric ratio), followed by NaOH addition. Subsequently, the mixture was digested in a microwave synthesis reactor, for 15 minutes, at 60°C. The obtained coated MNPs were washed with water and dried at 80°C.

3. RESULTS & DISCUSSION

Room temperature powder X-ray diffraction studies indicated the formation of Fe_3O_4 MNPs with spinel ferrite structure ($Fd\bar{3}m$). The average crystallite sizes were estimated as ~ 11 ± 1 nm and ~ 10 ± 0.9 nm for the SA and PA coated MNPs, respectively. The corresponding hydrodynamic diameters were ~ 37 and 28 nm, respectively, indicating a slight agglomeration in the aqueous medium. The corresponding zeta potentials were ~ -34 mV and -20 mV, respectively. The presence of the SA and PA coating on the surface of the MNPs was confirmed using Fourier transform infrared spectroscopy. The inset of Fig. 1 shows the room temperature M-H curves for the SA and PA coated MNPs, where the saturation magnetizations were ~ 186 kA/m and ~ 207 kA/m, respectively. Further no hysteresis openings were observed, which indicated the superparamagnetic nature of the MNPs.

Hyperthermia studies were conducted on aqueous dispersions (~ 5 wt. %) of the MNPs at a fixed frequency of 126 kHz and under four different RFAMF amplitudes (H). Fig. 1 shows the typical temperature rise curves for the SA coated MNPs, where temperature increased beyond the hyperthermia limit (~ 42°C) in all the cases, which indicated the suitability of the MNPs for MFH. The heating efficiency was estimated in terms of a dosimetric quantity, known as specific absorption rate (SAR), which was determined from the initial rates of temperature rise, under non-adiabatic limit.

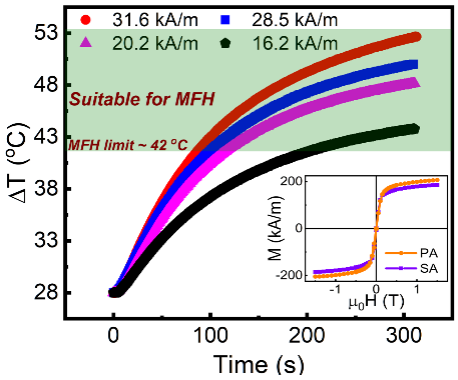

Fig.1. Temperature rise curves for the SA coated Fe_3O_4 MNPs. (Inset) Room temperature M-H curves for the SA and PA coated MNPs.

The highest SAR of ~ 26.8 ± 1.4 W/g_{Fe} was obtained for the SA coated MNPs at a RFAMF amplitude of 31.6 kA/m. The formation of a thicker layer for the SA coated MNPs, resulted in good colloidal stability (indicated by ~ 70% larger zeta potential) leading to a higher SAR, albeit with a slightly lower (~ 10%) saturation magnetization due to the contributions from the non-magnetic layer. Further, in agreement with the linear response model, the SAR values were found to increase linearly with H^2 [1]. The field dependent variation in SAR was also confirmed from dynamic hysteresis loop simulations.

4. CONCLUSIONS

Field induced heating efficiency was systematically probed for SA and PA coated Fe_3O_4 MNPs, synthesized using microwave assisted co-precipitation technique. Experimental findings indicated significant field induced temperature rise, which is useful for practical applications.

ACKNOWLEDGEMENT

The authors wish to acknowledge Dr. S. Raju and Dr. B. Venkatraman for their support and encouragement.

REFERENCES

[1]. R. E. Rosensweig, J. Magn. Magn. Mater. **252** (2002) 370.
[2]. S. Dutz et al., Nanomaterials **10** (2020) 1019.

P49

Structural, magnetic and optical studies of Spin-Disordered $Ho_2Ge_xTi_{2-x}O_7$ system

Manjari Shukla, Rajnikant Upadhyay and Chandan Upadhyay

School of Materials Science and Technology, Indian Institute of Technology (Banaras Hindu University), Varanasi, 221005

Email: ***manjaris.rs.mst15@iitbhu.ac.in***

Abstract: $Ho_2Ge_xTi_{2-x}O_7$ series had been synthesized through standard solid-state route. $Ho_2Ti_2O_7$ crystallizes in cubic $Fd\bar{3}m$ space group, and $Ho_2Ge_2O_7$ belongs to tetragonal $P4_12_12$ space group. The role of quantum fluctuations, along with the correlations within the ground states and low-temperature spin dynamics, had been discussed in details. The effects of chemical pressure upon the band gap tenability, from insulator ($Ho_2Ge_2O_7$) to high band semiconductor ($Ho_2Ti_2O_7$) has been elaborated.

1. INTRODUCTION

After the realization of implications of Anderson's resonating-valence-bond (RVB) theory to high-temperature superconductors, frustrated magnetism developed wide-spread recognition. $Ho_2Ge_2O_7$ and $Ho_2Ti_2O_7$ belongs to spin ice family having distorted pentagonal bipyramidal and pyrochlore structure respectively.

The Hamiltonian accounting the interaction between magnetic ions is based upon dipolar spin ice model (DSIM) and can be given as:

$$H = -J_{nn}\sum_{\langle ij\rangle}\vec{S_i}.\vec{S_j} + D_{nn}r_{nn}^3\sum_{\langle ij\rangle}\left[\frac{\vec{S_i}.\vec{S_j}}{|r_{ij}|^3} - \frac{3(\vec{S_i}.\vec{r}_{ij})(\vec{S_j}.\vec{r}_{ij})}{|r_{ij}|^5}\right]; \quad (1)$$

where J_{nn} and D_{nn} are the nearest neighbor exchange and dipolar coupling constants. [1-2]

Perturbation had been created in the interaction Hamiltonian through the application of chemical pressure in the parent matrix of holmium pyrotitanates and pyrogermanate for exploring the nature of spin fluctuations (classical/quantum) driving the spin dynamics at a lower temperature (T ~ 2 K and T ~ 15 K). Structural, magnetic, electronic, and optical properties of $Ho_2Ge_xTi_{2-x}O_7$ have been presented. Computational approach had been used for the density of state (DOS) and band structure calculation of $Ho_2Ge_xTi_{2-x}O_7$.

2. RESULT AND DISCUSSIONS

In $Ho_2Ge_2O_7$ matrix ac-susceptibility presents two spin relaxation, one at T ~ 2 K corresponding to ice-like spin freezing at second at T ~ 15 K due to single-ion anisotropy attributed to the thermal origin.

Fig 1. shows the real part of ac susceptibility of $Ho_2Ge_xTi_{2-x}O_7$ at H = 0.1, 0.5, 1, 5, 7.5, 10, 20 and 50 kOe at an applied ac-frequency of 500 Hz. The robust nature of the spin ice freezing (T ~ 2 K) for conventional cubic pyrochlore has been established in $Ho_2Ti_2O_7$. Low-temperature synchrotron x-ray diffraction pattern indicates an anomaly in lattice volume below 30 K, the curve of lattice volume vs. temperature when fitted using Debye-Grüneisen equation established crystal field-phonon coupling in $Ho_2Ti_2O_7$. Band gap of such systems puts them in an insulator class of materials and could be efficiently exploited for various applications where optical and magnetic properties are combined. The band gap of 5.20 eV drastically drops to 3.92 eV with immediate Ti^{4+} substitution in $Ho_2Ge_2O_7$. The absorption and emission (optical) spectral studies reflect a high probability of forbidden transition between the 4f states of Ho^{3+} ion that suitably places such systems in the category of materials for quantum information storage and biological imaging applications

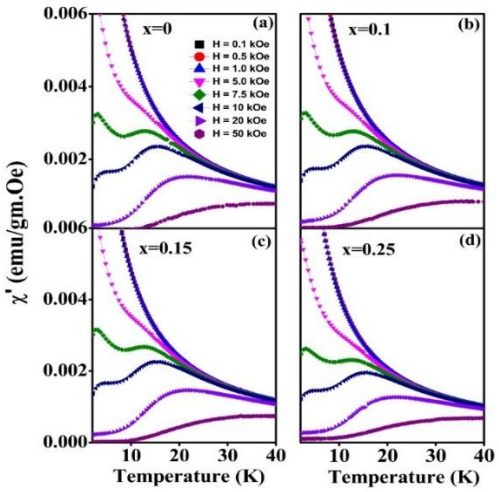

Fig. 1. Real part of ac susceptibility of $Ho_2Ge_xTi_{2-x}O_7$ for (a) x = 0 (b) x= 0.1 (c) x= 0.15 (d) x= 0.25 measured at H = 0.1, 0.5, 1, 5, 7.5, 10, 20 and 50 kOe at an applied ac-frequency of 500 Hz.

ACKNOWLEDGEMENT

A portion of this research was carried out at the light source PETRA III of DESY, a member of the Helmholtz Association (HGF). Financial support by the Department of Science & Technology (Government of India) provided within the framework of the India@DESY collaboration is gratefully acknowledged. We acknowledge the support from CIFC, IIT (BHU) for HRXRD measurements

REFERENCES

[1] L.D.C. Jaubert et al, J. Phys. Chem. Solids **23**, 1 (2011).

[2] B. Tomasello et al, Phys. Rev. B **92**, 1 (2015).

P50

Comparison between energy minimization and curve fitting approaches for simulating isothermal DC magnetization curves for a Stoner-Wohlfarth particle

Srujana M*, B. B. Lahiri, John Philip
Smart Materials Section, Corrosion Science and Technology Division, Metallurgy and Materials Group, Indira Gandhi Centre for Atomic Research, HBNI, Kalpakkam, Tamil Nadu, India, PIN 603102
Email: srujana27@igcar.gov.in

Abstract: Room temperature isothermal DC magnetization loops are simulated by numerically solving the classical Stoner-Wohlfarth model using Nelder-Mead algorithm and curve-fitting approaches. The obtained theoretical results are found to be in good agreement with the experimental data.

1. INTRODUCTION

Probing magnetization reversal in magnetic nanomaterials is important for fundamental studies as well as several technologically important applications, like transformers, motor-cores and various solid-state devices. Nnumerical modeling of hysteresis loops is being attempted for *a-priori* estimation of hysteresis properties and reducing experimental cost and time. Stoner-Wohlfarth (SW) model is the most widely used theoretical approach for single domain magnetic nanoparticles (MNPs). Here we report an energy minimization procedure to simulate the M-H loop, which is compared with the experimental data.

2. RESULTS AND DISCUSSIONS

The SW model considers coherent spin reversals in a single domain MNP with homogenous magnetization and uniaxial anisotropy energy density. Isothermal DC magnetization, at 300K, was measured for La, Sr-doped cobalt ferrite MNPs (size ~ 20 nm) and Fig. 1 shows the data. Further, M-H curves were theoretically simulated using energy minimization and curve fitting approaches.

2.1. Energy minimization

In the SW model, the free energy is expressed by the following equation [1].

$$E = K_{eff} V \sin^2(\theta - \varphi) - M_s(H - NM_s)\cos(\theta) \qquad (1)$$

Here, V, K_{eff}, M_s and N are the MNP volume, effective anisotropy energy density, saturation magnetization and demagnetization factor, respectively. The angles ϕ and θ are the orientations of the easy axis (anisotropy axis) and the magnetic moment with respect to the applied magnetic field. Stable states of magnetic moments were obtained from $dE/d\theta = 0$, $d^2E/d\theta^2>0$ and the magnetization reversal occurred for $d^2E/d\theta^2 = 0$. Here, the Nelder-Mead algorithm [2] was utilized for fast and efficient estimation of θ, corresponding to the energy minima, without the requirement of function gradients.The magnetization M was estimated as $M = M_s\cos(\theta)$ for each H and Fig. 1 shows the simulated M-H curve.

2.2. Parameterization and curve fitting

Alternatively, the SW hysteresis loop can be expressed by the following set of piece-wise continuous parametric equations, where $m' = M/M_s$, $h = H/H_a$, H_a being the anisotropy field, $m_o' = m(-0.5)$, A_n, and B_n are the regression parameters [3].

$$m_1'(2h \geq 2) = \frac{1 + \sum_{n=1}^{3} A_n (2h)^{-2n}}{1 + B_1 (2h)^{-2}}$$

$$m_2'(-1 \leq 2h \leq 2) = \frac{0.5 + \sum_{n=1}^{3} A_n (2h)^{n}}{1 + B_1(2h) + B_2(2h)^2} \qquad (2)$$

$$m_3'(-2 \leq 2h \leq -1) = m_o' - \left[\frac{\sum_{n=1}^{3} A_n (-2h-1)^n}{1 + \sum_{k=1}^{3} B_k (-2h-1)^k} \right]^{1/2}$$

The obtained M-H curve is shown in Fig. 1.It can be seen from Fig. 1 that the theoretically simulated M-H curves were in good agreement with the experimental data. The energy minimization procedure estimated a saturation magnetization of ~ 56.1 kA/m, against the experimental value of ~ 56.2 kA/m. In comparison to the curve fitting approach, the primary benefit of the energy minimization method is that the experimental M-H curve is not required *a-priori*.

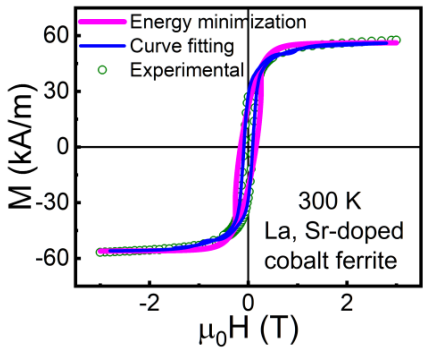

Fig.1. Comparison of experimental and theoretical (energy minimization and curve fitting) M-H curves.

3. CONCLUSIONS

The room temperature isothermal DC magnetization loops, simulated using free energy minimization and curve fitting approaches, were found to be in good agreement with the experimental data.

REFERENCES

[1]. E.C. Stoner, E. P. Wohlfarth, Philos. Trans. R. Soc. A **240** (1948) 599.
[2]. J. A. Nelder, R. Mead, Comput. J. **7** (1965) 308.
[3]. N.A. Zarkevich et al. J. Magn. Magn. Mater.**530** (2021) 167913.

P51

Origin and Control of Room Temperature Ferromagnetism in Fe and Mn co-doped In_2O_3 Nanocubes

Manikandan Dhamodaran[1*], Ramesh Karuppannan[1], Ramaswamy Murugan[2], Muthu Senthil Pandian[3], Ramasamy Perumalsamy[3]

[1]Department of Physics, Indian Institute of Science, Bangalore-560012, India.
[2]Department of Physics, Pondicherry University, Puducherry 605 014, India.
[3]SSN Research Centre, Sri Sivasubramaniya Nadar College of Engineering, Kalavakkam, Chennai, Tamil Nadu-603 110, India.
Email: (maniphysics.mani0@gmail.com)

Abstract: Single phase Fe and Mn co-doped In_2O_3 of different Fe/Mn doping concentration (Fe/Mn: 2% and 4%) were prepared by hydrothermal-annealing technique. HRTEM analysis demonstrated the regular nanocubes in shape and uniform size. Magnetic studies of the prepared samples exhibited RTFM with improved magnetic properties. Interestingly, $In_{1.94}Fe_{0.02}Mn_{0.04}O_3$ showed robust RTFM with the high coercivity and saturation magnetization of 145.48 Oe and 0.023 emu/g, respectively. The origin of observed RTFM was explained based on the bound magnetic polaron model.

1. INTRODUCTION

Diluted magnetic semiconductors (DMS) have drawn particular interest recently because of their potential spintronics and optoelectronics device applications [1-3]. In the present study, we have systematically investigated the influence of Fe and Mn co-doping on the structure, morphology and magnetic properties of nanoscale In_2O_3 through high-resolution transmission electron microscopy (HRTEM) and vibrating sample magnetometer (VSM) to divulge the origin and control of room temperature ferromagnetism (RTFM).

2. EXPERIMENTAL

$In_{2-x}Fe_{0.02}Mn_xO_2$ (x = 2 %, 4%, 6% and 8%) nanostructures were synthesized by hydrothermal-method. The appropriate stoichiometric amount of In, Fe and Mn precursors was dissolved in the 100 ml of both ethanol and distilled water mixed in the 1:1 ratio. The final transparent solution was transferred to the Teflon lined 150 ml autoclave and kept in an electric oven at 180 ℃ for 24 h. Finally, the obtained powder sample was further annealed at 350℃ for 2h in an electric furnace with air atmosphere.

3. RESULTS and DISCUSSION

3.1. HRTEM analysis

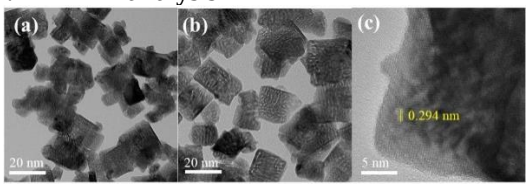

Fig. 1 (a, b) TEM and (c) HRTEM images of $In_{1.94}Fe_{0.02}Mn_{0.04}O_3$ and $In_{1.90}Fe_{0.02}Mn_{0.08}O_3$, respectively.

TEM and HRTEM images of $In_{1.94}Fe_{0.02}Mn_{0.04}O_3$ and $In_{1.90}Fe_{0.02}Mn_{0.08}O_3$ are shown in **Fig. 1**. TEM images (**Fig. 1a-b**) indicated the regular nanocubes in shape and uniform size. The average edge length of $In_{1.94}Fe_{0.02}Mn_{0.04}O_3$ and $In_{1.90}Fe_{0.02}Mn_{0.08}O_3$ nanocubes was 36.9 and 37.9 nm, respectively. The HRTEM analysis (**Fig. 1c**) showed the interplanar distance of 0.294 nm corresponded to (222) crystallographic plane of cubic In_2O_3.

3.2. Magnetic properties

Field dependent magnetization (M-H hysteresis loops) of the prepared $In_{1.94}Fe_{0.02}Mn_{0.04}O_3$, and $In_{1.90}Fe_{0.02}Mn_{0.08}O_3$ measured at 300 K is shown in **Fig.2**. The magnetic studies indicated the well-defined hysteresis loops with saturation at higher fields. More interestingly, the $In_{1.94}Fe_{0.02}Mn_{0.04}O_3$ exhibited robust RTFM with the high coercivity and saturation magnetization of 145.48 Oe and 0.023 emu/g, respectively. However, $In_{1.90}Fe_{0.02}Mn_{0.08}O_3$ indicated typical paramagnetic behaviour at higher field due to increase in the antiferromagnetic coupling between Mn and Fe dopants. The observed RTFM was related to the formation of bound magnetic polarons (BMP).

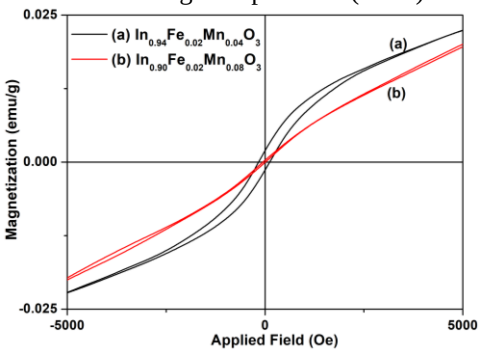

Fig. 2. M-H hysteresis loops of the prepared $In_{1.94}Fe_{0.02}Mn_{0.04}O_3$ and $In_{1.90}Fe_{0.02}Mn_{0.08}O_3$.

4. CONCLUSION

The influence of Fe and Mn co-doping on the morphology, electronic structure and magnetic properties of nanoscale In_2O_3 were investigated via complementary experimental techniques. We find that both Fe and Mn atoms substitute for In atoms within the bulk of the lattice, and attribute the ferromagnetic properties to oxygen vacancy mediated BMP within the host lattice. The comprehensive experimental investigations provide a link between observed RTFM and dopant-atom interactions within a host crystal.

REFERENCES

[1]. T. Dietl et al, Rev. Mod. Phys. **86** (2014)187.
[2]. T. Dietl et al, Science **287** (2000)1019.
[3]. L. Shen et al, Phys. Chem. Chem. Phys. **19** (2017) 29472.

P52

Effect on magnetization reversal by substituting magnetic and non magnetic rare earth element in orthochromite

Tribedi Bora[1], Seenipandian Ravi[2]
Department of Physics, National Institute of Technology Meghalaya, Shillong- 793003
Department of Physics, Indian Institute of Technology Guwahati, Assam-781039
Email: t.bora@nitm.ac.in

Abstract: Negative magnetization is observed in $NdCr_{0.85}Mn_{0.15}O_3$ and $LaCr_{0.85}Mn_{0.15}O_3$ compounds. The compensation temperature (T_{comp}) as well as the magnitude of negative magnetization values are found to be larger in $NdCr_{0.85}Mn_{0.15}O_3$ (A1 sample) compared to $LaCr_{0.85}Mn_{0.15}O_3$ (A2 sample). The observed negative magnetization is explained by considering the competition between weak ferromagnetic component of Cr^{3+} ions and the paramagnetic of Nd^{3+} and Mn^{3+} ions under the negative internal field.

1. INTRODUCTION

Orthochromites ($RCrO_3$, where R = rare earth element) have attracted the attention of researchers due to their interesting physical properties like magnetization reversal, exchange bias, *etc*. [1] and their potential applications like magnetic storage devices, thermo magnetic switches, *etc* [2]. In these compounds, the magnetic ordering is controlled by the magnetic interactions in Cr^{3+} -O^{2-} -Cr^{3+}, R^{3+} -O^{2-} -R^{3+} and R^{3+} - O^{2-} - Cr^{3+} networks .

2. EXPERIMENTAL DETAILS

Polycrystalline samples of $RCr_{0.85}Mn_{0.15}O_3$ where R = Nd and La were prepared by the standard sol gel route. The final sintering was carried out at 1100 ºC for 24 h. X-ray diffraction pattern of samples were recorded with the help of TTRAX III diffractometer. Magnetization (M) as a function of temperature (T) under Zero field cooled (ZFC) and Field cooled (FC) conditions at different applied fields were measured by using Vibrating Sample Magnetometer of model no. 7410.

3. RESULTS AND DISCUSSIONS

The XRD patterns of the prepared samples are found to be in single phase form. They were refined by Rietveld refinement using Pbnm space group. XRD patterns along with the Rietveld refinement for the samples are shown in Fig 1. The lattice parameters a and c and unit cell volume are found to be higher for A2 sample as compared to the A1 sample due to the higher ionic radii of La^{3+} (1.032 Å) as compared to Nd^{3+} (0.983 Å)ion.

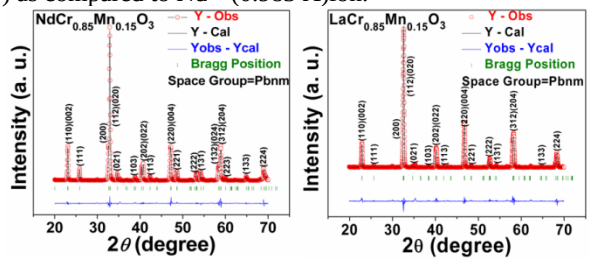

Fig 1: XRD patterns of A1 and A2 samples

M-T plots of these samples for the applied field H = 2000 Oe are shown in Fig 2. A2 sample under FC condition shows magnetization reversal (MR) with a compensation temperature T_{comp} = 80 K. A minimum magnetization value of, M_{min} = -14 emu/mol is observed at T_{min} = 58 K. At $T < T_{min}$, M rises sharply towards the positive value due to low temperature ordering. In A1 sample under FC condition, M increases with decrease in temperature followed by a plateau at $T < T_N$. The plateau persists down to around 150 K and beyond that a secondary rise in M is observed due to spin reorientation of Cr^{3+} ions. Beyond 150 K, FC M is found to fall below the ZFC M value. So it exhibits tendency towards MR.

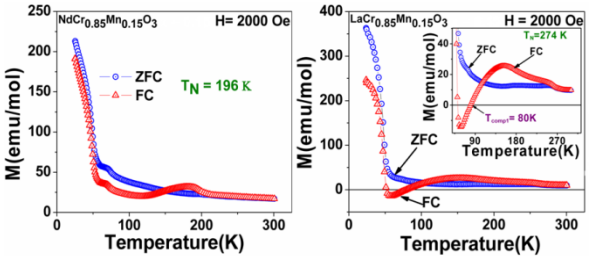

FIG 2: ZFC and FC M-T plots of A1 and A2 samples.

To understand the MR phenomenon, we have recorded *M-T* data at different applied fields ranging from 200 to 2000 Oe. Prominent negative magnetization is observed for these samples for low applied field. The magnitude of negative magnetization is found to decrease with increase in applied field and the corresponding T_{comp} value also decreases from 145 K at 200 Oe to 133 K at 500 Oe for A1 sample and from 95 K at 200 Oe to 80 K at 2000 Oe for A2 sample.

The observed negative magnetization can be explained by considering the competition between the weak canted FM component of Cr^{3+} ions (M_{Cr}) and the paramagnetic behavior of doped Mn^{3+} ions and Nd^{3+} ions under the influence of negative internal field (H_I) due to AFM ordered Cr^{3+} ions. According to this model, the measured FC M can be fitted to the following equation

$$M = M_{Cr} + \frac{C(H + H_I)}{(T - \theta_C)}$$

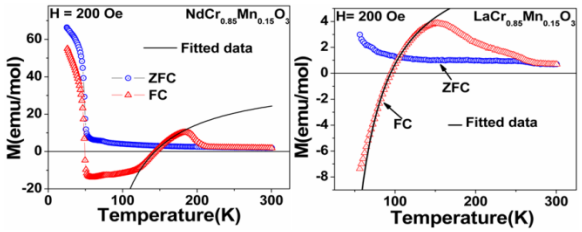

Fig 3. FC M-T curves for 200 Oe

The fitted data of A1 and A2 samples closely follow the experimental curves as shown in Fig 3. The negative magnetization and T_{comp} values are found to be larger for A1 sample as compared to the A2 sample due to the presence of the magnetic rare earth of Nd^{3+} ion in A1 sample and the presence of Nd^{3+} -O^{2-}- Cr^{3+} interaction.

REFERENCES

[1] Minh et al, J. Am. Ceram. Soc.**76** (1993) 563.
[2] Hughes et al, J. Magn. Magn. Mater. **235** (2001) 329

P53

Origin of Magnetization in Magnetic Beads Based on Fe_3O_4 Nanoparticles for Biomedical Applications via Soft X-Ray Circular Dichorism Study

Riya Dawn[1], Mufeeduzzaman[1,2], Ferry Faizal[3,4], Chandra Kiran[5], Aradhana Kumari[1], Raza Shahid[2], Camellia Panatarani[3,4], I Made Joni[3,4], Virendra Kumar Verma[6], Suresh Kumar Sahoo[7], Kenta Amemiya[8] and Vijay Raj Singh[1,*]

[1]Department of Physics, Central University of South Bihar, Gaya-824236, India

[2]Department of Physics, Jamia Millia Islamia (Central University), New Delhi 110025, India

[3]Department of physics, Universitas Padjadjaran, Jl. Raya Bandung-Sumedang Km 21, West Java, 45363, Indonesia

[4]Functional Nano Powder University Centre of Excellence (FiNder U CoE), Universitas Padjadjaran, Jl. Raya Bandung-Sumedang, Km 21, West Java, 45363, Indonesia

[5]Department of Animal Sciences, Central University of Kashmir, Ganderbal-191201, India

[6]Department of Physics, Madanapalle Institute of Technology & Science, Madanapalle-517325, India

[7]Department of Metallurgical and Materials Engineering, National Institute of Technology, Rourkela-769008, India

[8]Photon Factory, IMSS, High Energy Accelerator Research Organization, Tsukuba, Ibaraki 305-0801, Japan

Email: vijayraj@cusb.ac.in

Abstract: Magnetite (Fe_3O_4) nanoparticles (NPs) and SiO_2-coated Fe_3O_4 nanoparticles have successfully been synthesized using co-precipitation and modified Stöber methods, respectively. The samples were characterized using X-Ray Diffraction (XRD), Fourier Transform Infrared (FTIR) Spectroscopy, High-Resolution Transmission Electron Microscopy (HRTEM), Vibrating Sample Magnetometer (VSM) techniques, X-Ray Absorption Spectroscopy (XAS) and X-Ray Magnetic Circular Dichroism (XMCD). XRD and FTIR data confirmed the structural configuration of a single phase Fe_3O_4 and the successful formation of SiO_2 coated Fe_3O_4 NPs. XRD also confirmed that we have succeeded to synthesize the smallest NPs (sub-micron to nano-meter size) of Fe_3O_4 compared to the commercially available Fe_3O_4 (sub-micron to micron size) for the first time ever. This could enhance the performance for biological applications such as a better extraction of nucleic-acids in the case of Reverse Transcription Polymerase Chain Reaction (RT-PCR) method, which is one of the most viable procedures to detect CoVID-19 in recent days. HRTEM images showed the increasing thickness of SiO_2 coated Fe_3O_4 with the addition of the Tetraethyl Orthosilicate (TEOS). Room temperature VSM analysis showed the magnetic behaviour of Fe_3O_4 and its variations that occurred after SiO_2 coating. The saturation magnetization through VSM has been found for the S.0 and S.3 samples were 62.31 emu/gm and 21.86 emu/gm, respectively. The magnetic behaviour is further authenticated by XAS spectra analysis which cleared about the existence of SiO_2 shells that have transformed the crystal as well as the local structures of the magnetite NPs. We have performed XMCD measurements, which is a powerful element-specific technique to find out the origin of magnetization in SiO_2 coated Fe_3O_4 NPs. XMCD spectra have a positive peak at 708.0 eV, verifying Fe^{3+} is at tetrahedral (T_d) site and two negative peaks at 706.8 eV and 708.7 eV, verifying the octahedral (O_h) sites of Fe^{2+} and rest Fe^{3+}, respectively, which verifies a decrease in magnetization with increasing thickness of the SiO_2 coating.

P54

Magnetic Response of Ising Spin-1/2 Trilayered Ferrimagnet driven by Gaussian Random External Magnetic Field with Spatio-Temporal Variation

Soham Chandra
Department of Physics, Presidency University, 86/1 College Street, Kolkata 700 073, India
Email: soham.rs@presiuniv.ac.in

Abstract: In this work, a Metropolis Monte Carlo [1] study is performed on the magnetic response of a trilayered spin-1/2 ferrimagnetic system on square Bravais lattice, driven by Gaussian random external magnetic field with spatio-temporal variations. In the ABA type configuration, the surface layers are made up of A and the mid-layer is made up of B atoms [Fig. 1]. The magnetic coupling between the like atoms (A-A and B-B) is ferromagnetic while between the unlike atoms (A-B), it is antiferromagnetic. For the time dependent external Gaussian random field, the mean is always set to zero and the standard deviation is varied until spin-field energy is comparable to the dominant cooperative energy of the system. The findings show that the observed compensation and critical points shift depending upon the strength of external uniform random field. The compensation phenomenon even vanishes after crossing a finite threshold of standard deviation of the magnetic field for particular choices of the other controlling parameters. Thus, islands of ferrimagnetic phase without compensation appear within the phase area with compensation of field-free case, in the 2D Hamiltonian parameter space. So the standard deviation of the external random field acts as another controlling parameter in the dynamic Hamiltonian of the considered layered ferrimagnetic system.

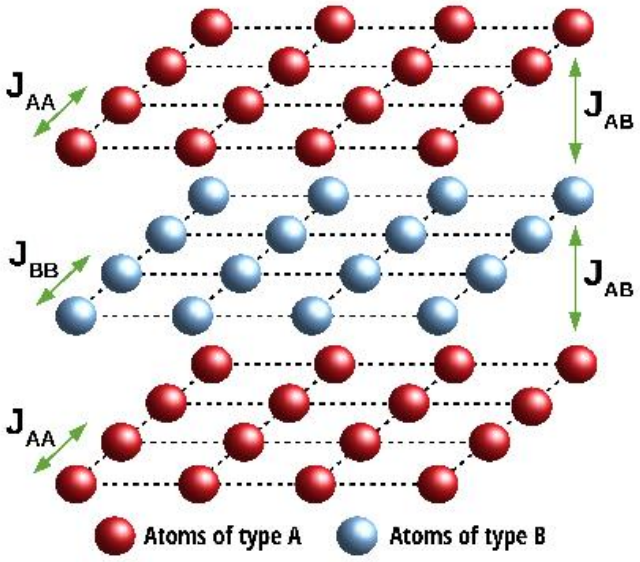

Fig.1. ABA square trilayered ferrimagnet with two types of theoretical atoms, A and B. [Courtesy [2]]

REFERENCES

[1]. Metropolis N., Rosenbluth A. W., Rosenbluth M. N., Teller A. H., and Teller E., J. Chem Phys. **21** (1953) 1087.
[2]. Chandra S., arXiv preprint, arXiv:2010.13643 (2020).

P55

Structural and Magnetic Characterization of Mn Doped Ni-Co Spinel Ferrite Nanoparticles with Surface Spin Disorder

Ritupan Borah[1] and S. Ravi[2]
Department of Physics, Indian Institute of Technology Guwahati, Guwahati - 781039
Email: ritupanborah@iitg.ac.in

Abstract: In the present work, single phase nanoparticles of $Ni_{0.5}(Co_{0.5-x}Mn_x)Fe_2O_4$ (x = 0 – 0.20) were synthesized by co-precipitation route. Effect of Mn substitution on structural, ferrimagnetic Curie temperature, saturation magnetization and exchange bias behavior has been investigated.

1. INTRODUCTION

Ferrites MFe_2O_4 (M= $Co^{2+,}$ Ni^{2+}), forms an inverse spinel structure $(Fe)[MFe]O_4$ with cubic crystallographic phase. Ni ferrite with a high value of resistivity, low magneto crystalline anisotropy and saturation magnetization is a suitable class of magnetic system for application purpose. However, substitution of Co and Mn may improve its multifunctional properties as both cations possess high value of magnetic moment. In this report we have prepared $Ni_{0.5}(Co_{0.5-x}Mn_x)Fe_2O_4$ (x = 0 – 0.20) nanoparticles by co-precipitation method and studied their structural and magnetic properties.

2. EXPERIMENTAL DETAILS

The nanoparticles were synthesised by the co-precipitation method as discussed in *ref. 1*. The final sintering of the samples was performed at 700^0C for 6 hours.

3. RESULTS AND DISCUSSIONS

The room temperature XRD patterns along with Rietveld refinements shown in Fig. 1 indicates that all the samples are crystallized in cubic crystal structure with space group $Fd\bar{3}m$. With Mn substitution, the lattice parameters are found to increase from 8.3021 Å for x = 0 to 8.3652 Å for x = 0.20 due to its larger ionic size as compared Co^{2+}.

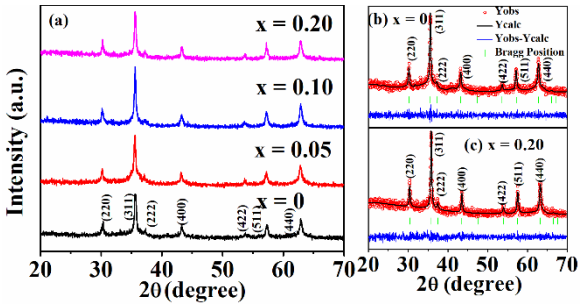

Fig. 2. (a) XRD patterns for x = 0 – 0.20 along with Rietveld refinement for (b) x = 0 & (c) x =0.20.

With Mn substitution the ferrimagnetic Curie temperature is found to decrease from T_C = 820 K for x = 0 to 780 K for x = 0.20 (Fig. 2 c). The reduction in Curie temperature can be attributed to the weakening of A – O – B superexchange interaction as a result of possible cation migration between sublattices and partial conversion of Fe^{3+} to Fe^{2+} ions upon Mn substitution.

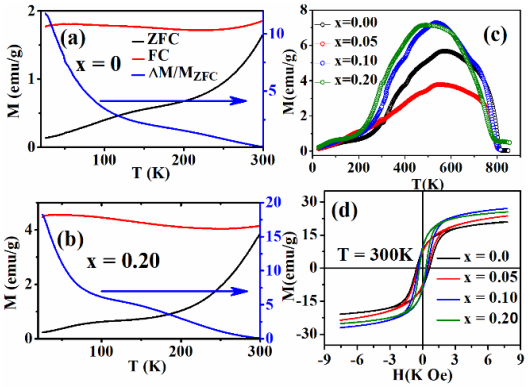

Fig. 2. ZFC and FC magnetization at low temperature (c) ZFC magnetization at high temperature and (d) M – H loops recorded at room temperature.

The saturation magnetization (M_S) values are found to increase with Mn substitution from 17 emu/g for x = 0 to 22 emu/g for x = 0.20 sample. On the other hand, coercivity is (H_C) found to decrease from 590 Oe for x = 0 to 304 Oe for x = 0.20 sample. In order to study the exchange anisotropy between the surface spins and core FIM interaction, exchange bias property has been explored at 5 K for x = 0.20 sample. The sample (x = 0.20) was first cooled down to T = 5 K under the application of a magnetic field of H = 1 T and M – H loop recorded with a maximum measuring field of 9 T.

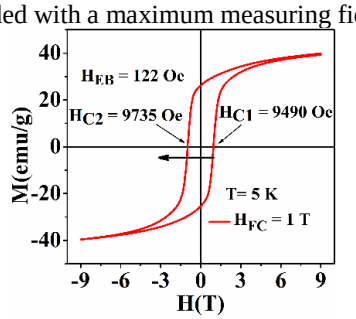

Fig. 3. MH loop recorded at T = 5 K after FC at 1 T.

The observed exchange bias behaviour (H_{EB} = 122 Oe) confirms the presence of surface spin disorder in the nanoparticles.

ACKNOWLEDGMENT

The authors acknowledge the DST for granting PPMS facility in the department of Physics, IIT Guwahati.

REFERENCES

1. Chaudhari, P. R., Gaikwad, V. M. & Acharya, Appl Nanosci 5, (2015), 711.

P56

Electronic, structural and vibrational properties of inverse Fe_2IrSi: A DFT+U study

Lalrinkima 1, D. P. Rai 2, C. E. Ekuma 3, T.C. Chibueze 4, L. A. Fomin 5, I. V. Malikov 5, L. Zadeng 1
[1]Department of Physics, Mizoram University Aizawl 796009, India
[2]Physical Sciences Research Center, Department of Physics,
Pachhunga University College Aizawl 796001, India
[3]Department of Physics, Lehigh University, Bethlehem, PA 18015
[4]Department of Physics & Astronomy, University of Nigeria, Nsukka, 410001, Nigeria
[5]Institute of Microelectronics Technology and High Purity Materials RAS, 142432 Chernogolovka, Russia
Email: rkasiakeng1@gmail.com

Abstract: We report the electronic, magnetic, structural, vibrational, and x-ray absorption spectroscopy of inverse full-Heusler Fe_2IrSi alloy. We employed state-of-the-art first-principle computational techniques. Our ab initio calculations revealed a semiconducting ferromagnetic half-metallicity with a magnetic moment of 5.01 μ_B, which follows the Slater Pauling rule. We show rich magnetic behavior due to spin-orbit coupling through the entanglement of the Fe-3d/Ir-5d. The large extension of the Ir-5d orbital and the itinerate Fe-3d states enhanced spin-orbit and electron-electron interactions, respectively. The analyses of our results reveal that electron-electron interactions are essential for the proper description of the electronic properties while spin-orbit coupling effects are vital to accurately characterize the x-ray absorption and x-ray magnetic circular dichroism spectra. We estimate the strength of the spin-orbit coupling by comparing the intensity of the white-line features at the L_3 and L_2 absorption edges. This led to a branching ratio that deviates strongly from the statistical ratio of 2, indicative of strong spin-orbit coupling effects in a novel, inverse full-Heusler Fe_2IrSi alloy.

FIGURES AND IMAGES

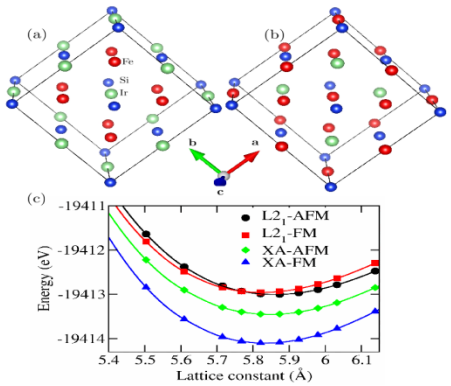

Fig.1: The crystal structure of regular (a) and inverse (b) full-Heusler Fe_2IrSi. (c) Relative energy per unit cell versus lattice constant profile of the various magnetic configurations

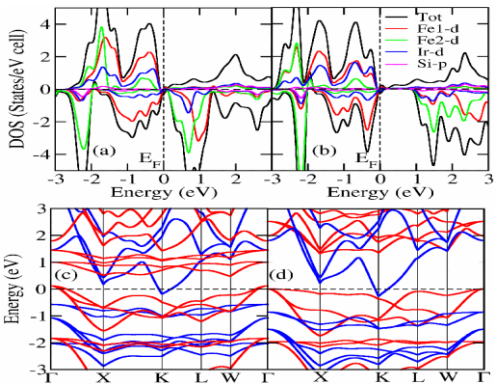

Fig.2: Calculated TDOS and PDOS and band structure from: 1.GGA[(a)&(b)], 2. GGA+U [(c)&(d)] respectively.

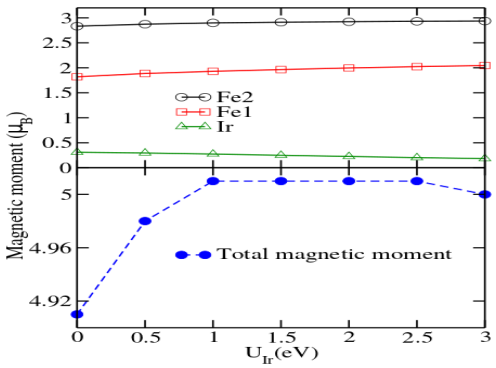

Fig.3: Variation of the partial and total magnetic moment obtained using GGA+U (U_{Fe} = 3.52 eV, U_{Ir} = 0.0 eV to 3.0 eV) for the XA phase of full-Heulser Fe_2IrSi.

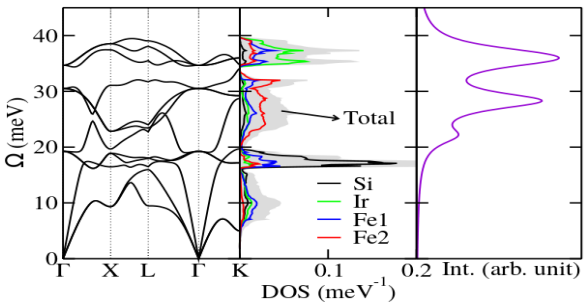

Fig.4: Calculated phonon band structure along the various high symmetry points in the first Brillouin zone, the density and the projected phonon density of states, and the Raman spectra.

REFERENCES

[1]. A. Fert, Thin Solid Films. **517** (2) 2008.
[2]. S. Wurmehl *et al*, Appl. Phys. Lett. **88** (3-032503) 2006.

P57

The study of in-plane and out-of-plane magnetostrictive stress for $CoFe_2O_4$/Si composite

Suman Guchhait[1], H. Aireddy[2] and A. K. Das[1]

[1]Indian Institute of Technology Kharagpur, Department of Physics, Kharagpur, 721302, India.
[2]Alliance College of Engineering and Design, Department of Electronics and Communication Engineering, Bengaluru, 560076, India.
Email: sumanguchhait4@gmail.com

Abstract: We have studied the in-plane and out of-plane magnetostrictive stress at room temperature (300 K) for a $CoFe_2O_4$ (CFO) film deposited on a Si cantilever substrate. The stress measurement has been performed by optical cantilever beam magnetometer set-up. When the film is magnetized along the length, the nature of the developed stress is compressive. But for other two mutually perpendicular directions (when magnetized along the width and thickness), the developed magnetostrictive stress is tensile in nature.

1. INTRODUCTION

The phenomenon of change in physical dimension of a magnetic material in presence of magnetic field is called magnetostriction [1,2]. The material could be either elongated or contracted depending on the nature of the magnetostrictive stress developed inside the material.

Among all the spinel ferrite, CFO is one of the most promising spinel to study the magnetostrictive stress (σ) as it shows high value of magnetostriction coefficient (λ).

2. RESULTS AND DISCUSSION

2.1. Structural and Morphological Study

For the structural analysis of the CFO film prepared through pulsed laser deposition (PLD) system, we have carried out grazing-incidence X-ray diffraction (GI-XRD) technique using Cu K_α radiation. The X-ray data confirms the formation of cubic spinel phase for the CFO film. The GI-XRD characteristic is shown in figure 1.

To identify the growth of the CFO film over the Si-substrate, we have performed the cross-sectional scanning electron microscopy (SEM). From the data, it is confirmed that the growth of the film has been taken place over the substrate. The corresponding figure is represented at the inset of figure 1.

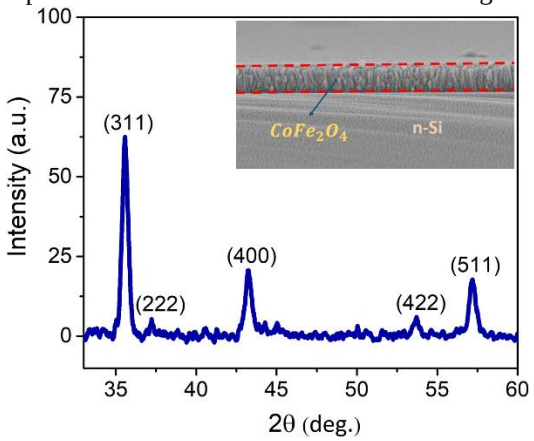

Fig. 1. GI-XRD pattern of the CFO film. Inset shows the cross-sectional view of SEM image.

2.2. Magnetostrictive stress study

Here, we have performed the in-plane and out-of-plane magnetic stress of the CFO film at room temperature by applying bi-polar magnetic field (B). The in-plane stress has been measured by magnetizing the sample along the length as well as along the width separately. The corresponding stress are denoted as σ_m^l *and* σ_m^w respectively. The out-of-plane magnetic stress (σ_m^t) is measured by applying the field along the thickness of the film. It is the converse piezomagnetic effect which is responsible for the origin of magnetic stress in the film. The variation of magnetic stress with the applied bi-polar magnetic field has been shown in figure 2.

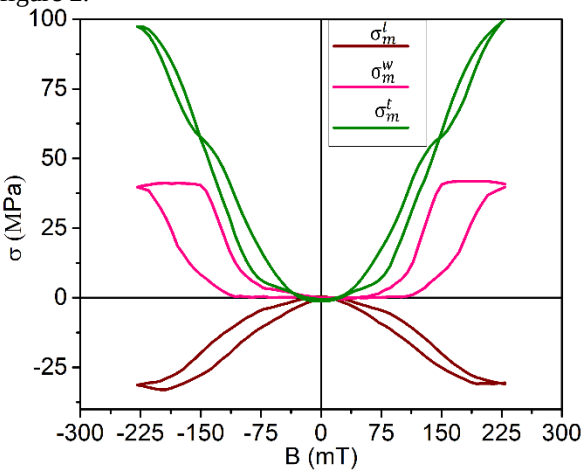

Fig. 2. The variation of magnetostrictive stress with magnetic field in in-plane and out-of-plane geometry.

ACKNOWLEDGEMENT

Suman Guchhait acknowledges DST-ISPIRE for providing the fellowship during the work.

REFERENCES

[1]. T. I. Richardson et al, J. Appl. Phys. **128,** 055109 (2020).
[2]. A. K. Das et al, Rev. Sci. Instrum. **90**, 103905 (2019).

P58

Electronic structure calculation of $DyVO_4$

Rajnikant Upadhyay and Chandan Upadhyay
School of Materials Science and Technology, Indian Institute of Technology (Banaras Hindu University), Varanasi, 221005
Email: rajnikantupadhyay.rs.mst18@itbhu.ac.in

Abstract: Ab-initio calculations of $DyVO_4$ have been performed to determine the electronic structure (band structure and density of states) with the help of a plane-wave pseudopotential technique within the local density approximation (LDA) as implemented in the PWscf code of quantum Espresso Simulation Package. The Electronic band structure has been discussed in this paper. The electronic structure classifies $DyVO_4$ as a direct bandgap insulator with a band gap value of 3.3294. Bandgap is correlated to the orbital overlapping of the oxygen atom and the transition atom, i.e., O-2p: V-3d orbitals.

1. INTRODUCTION

$DyVO_4$ crystallizes in zircon type structure with space group $14_1/amd$. The crystal structure consists of alternating VO_4 distorted tetrahedra, and DyO_8 triangulated dodecahedra with eight oxygen atoms coordinated with the central Dy atom.

It has been studied extensively because of its interesting crystallographic and magnetic properties at low temperatures. It undergoes two successive phase transitions a cooperative Jahn teller phase transition around 14 K from tetragonal phase to orthorhombic phase followed by antiferromagnetic magnetic ordering around 3 K.[1]

COMPUTATIONAL DETAILS

First principle calculations have been performed to investigate the electronic structure based on density functional theory (DFT) using a plane-wave basis set and pseudopotential as implemented in the Quantum-ESPRESSO software package.[2] The exchange-correlation (XC) potential is approximated by the local density approximation (LDA) approximation with the Perdew–Burke–Ernzerhof functional. Amongst all pseudopotentials, the Rappe-Rabe-Kaxiras-Joannopoulos (RRKJ) flavour of ultra-soft pseudopotentials was used to represent the interaction between the ion cores and the valence electrons

RESULTS AND DISCUSSION

Band structure for tetragonal $DyVO_4$ is shown in Fig. 1. The calculated band gap is 3.3294 eV which corresponds to direct transition involving Z symmetry point as mapped from the Brillouin zone for space group $14_1/amd$. Significant contribution for the valence band comes from the p orbital of oxygen and a small contribution from its s orbital along with the s and p orbitals of vanadium and dysprosium too. The top of the valence band (VB) comprises Dy-5d orbital with a certain level of hybridization to O-2p and V- 3d orbital hybridized with O-2p orbital. Lower CB involves the hybridization of V-3d unfilled states and O-2p states and Dy-5d & O-2p hybridized states. Ligand to metal charge transfer involving all symmetry points corresponds to the electronic transition between the derived states hybridized from V-3d & O-2p orbitals and Dy-5d & O-2p orbitals. But the bandgap is correlated to the orbital overlapping of the oxygen atom and the transition atom, i.e., O-2p: V-3d state. V-3d orbital is relatively lower than the Dy-5d orbital in energy and has a stronger hybridization affinity with the O-2p orbital near the Fermi surface. Hence, $DyVO_4$ belongs to the direct bandgap insulator class of magnetic systems.[3] Since the band gap lies in the visible region (3-4 eV), we possibly expect its absorption and emission spectra to be in visible region that will essentially facilitates its applications as scintillator material.

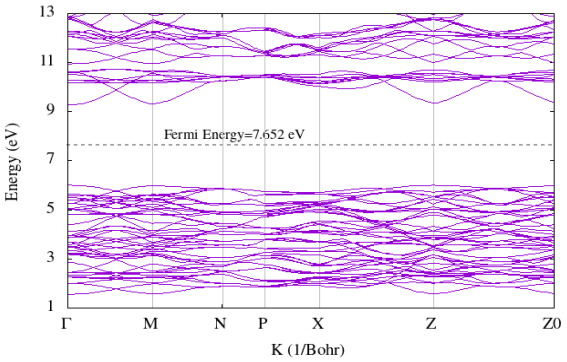

Fig. 1. Band Structure for $DyVO_4$.

CONCLUSION

We have investigated the electronic structure of $DyVO_4$ within the framework of DFT calculations using LDA approximations. Theoretical analysis shows that $DyVO_4$ is a direct band gap insulator with a bandgap value of 3.3294 eV.

ACKNOWLEDGEMENT

The author would like to acknowledge the PARAM Shivay facility under the National Supercomputing Mission, Government of India at the Indian Institute of Technology, Varanasi, for computational work

REFERENCES

[1]. A. Kasten, Condens. Matter **76**, 65 (1980).
[2]. M.B. P Giannozzi et. al, J. Phys. Condens. Matter **29**, 1 (2017)
[3]. G. Shwetha et al, Mater. Chem. Phys. **163**, 376 (2015).

P60

Study of Effect of Bi^{3+} Concentration and Particle Size Reduction on the Structural and Magnetic Properties of $Pr_{0.6}Sr_{0.4}MnO_3$

Anita D Souza[1], Mamatha D. Daivajna[2*], Megha Vagadia[3]

[1]*Department of Physics, Manipal Institute of Technology, Manipal Academy of Higher Education, Manipal, Karnataka - 576104, INDIA*

[2] *Department of Physics, Manipal Institute of Technology Bengaluru, Manipal Academy of Higher Education, Manipal, India*

[3]*Indian Institute of Science Education and Research, Bhopal, Madhya Pradesh – 462066, INDIA*

[*]Corresponding/Presenting author: mamata.shet@yahoo.com

Abstract

$Pr_{0.6}Sr_{0.4}MnO_3$ (PSMO) has been subjected simultaneous partial Bi^{3+} substitution (10 at %) and particle size reduction to understand the mechanism controlling the magnetic properties. PSMO is a room temperature ferromagnet with T_C = 308 K and undergoes an orthorhombic (space group: Pnma) to monoclinic (space group: I2/a) structural transition at T_S = 88 K. Partial Bi^{3+} substitution (x = 0.10) reduces T_C to 290 K and completely suppress the structural transition. However, a close look at the FC curve for x = 0.10 shows hump at T < 200 K which could be attributed to the disordered weak AFM interactions in the system. Nanoparticles of the same prepared by *top-down* approach in a high energy planetary ball mill show a direct impact of particle size reduction on the magnetism of the system. The T_C drops drastically from 308 K to 246 K for PSMO and 290 K to 257 K for 10 at% Bi^{3+} substituted PSMO. Also, the net magnetization drops both with Bi^{3+} substitution as well as particle size reduction. The decrease in magnetization with Bi^{3+} content can be explained considering the dominant *6s* lone pair character of Bi^{3+} while the core-shell model for the nanoparticles is considered to the account for the magnetic properties of the nanoparticles. Detailed analysis of X-ray diffraction and magnetization study has been presented and discussed here.

Keywords: Manganites, Magnetic Properties, X-ray diffraction, Particle Size reduction

Structural and thermal studies of Fe_2MnSn Heusler alloys

Naveen Kumar R[1], Uma Mahendra Kumar Koppolu[1], Senthur Pandi Rajasabai[1]
[1] Department of Physics, School of Advanced Sciences, Vellore Institute of Technology, Vellore, India.
Email: senthur.pandi@vit.ac.in

Abstract: The $Fe_{50}Mn_{35}Sn_{15}$ alloy is prepared by a vacuum arc melting furnace. As casted sample is annealed, polished, and characterized for structural and thermal properties. The annealed alloys exhibited a dominant hexagonal phase with modest tetragonal and cubic phases. Phase formation, crystallization, and melting point of the alloy are determined after the X-ray diffraction (XRD) and calculated differential scanning calorimetry (DSC) analysis. The dominant hexagonal phase confirms this alloy would be useful for various magnetocrystalline anisotropy-based applications.

1. INTRODUCTION

Heusler alloys with various compositions have been attracted for magnetocaloric, magneto-resistance, spintronics, and ferromagnetic shape memory (FSMA) applications owing to their magnetic ordering, magnetic exchange interaction, enthalpy (H), Curie temperature (T_C), and high magnetic resistance [1]. Fe_2-based Heusler alloys are known for the magnetic shape memory effect because of their High T_C and magnetic moment (μ_B). Tuning Mn/Sn composition will be a feasible approach to increase the magnetocaloric effect for magnetic refrigeration applications.

V.K. Jain *et. al*, reported the experimental and theoretical studies[1] of Fe_2MnSn. Dahal *et. al*. and Kratochvílov´a *et. al*. have reported that Fe_2MnSn alloy stabilizes in the hexagonal phase. As well they have mentioned the formation of cubic phase is difficult. It is observed that the corresponding T_C would be above the room temperature[2]. In the present work, we have studied the effect of Mn/Sn composition in the various phase formations in Fe_2MnSn.

2 MATERIAL PREPARATION

The non-stoichiometric composition of $Fe_{50}Mn_{35}Sn_{15}$ (>99.99% purity of metals) alloy is prepared in the vacuum arc furnace. To achieve good homogeneity the alloy is melted multiple times. The as-casted ingot is vacuum-sealed into a quartz tube and annealed at 1123K for 72 hours. Then it is quenched in cold water to obtain a required stable phase. The prepared ingot was polished using a mechanical disk polishing machine with different grid sheets till we achieve a mirror finish. In Philips X'Pert diffractometer (Cu Kα: 1.54056Å), we have measured the diffraction patterns in reflection mode.

3. RESULTS AND DISCUSSION

Figure 1. shows the formation of cubic, tetragonal, and hexagonal mixed phases. The hexagonal phase is more dominant than the other phases. Non-cubic Heusler alloys are commonly used in hard magnetic applications due to their high magnetocrystalline anisotropy[3]. Fe_2MnSn alloy is stabilized in the hexagonal phase ($P6_3/mmc$, #194 space group) with lattice parameter, a=5.5731Å, c=4.3584Å, and α=β=90°, γ=120°. The mixed phases contain Fe_3Sn and Fe_5Sn_3 which are ferromagnetic in nature.

The left inset depicts the annealing effect and micron-size grains, found in scanning electron microscopy (SEM) and the right inset shows elemental composition (EDAX). The computed DSC is shown in figure 2. It is evident that Fe_3Sn/Fe_5Sn_3 and Fe_2MnSn phases are formed between 400-850°C and the deformation of Fe_2MnSn phase started at 936°C.

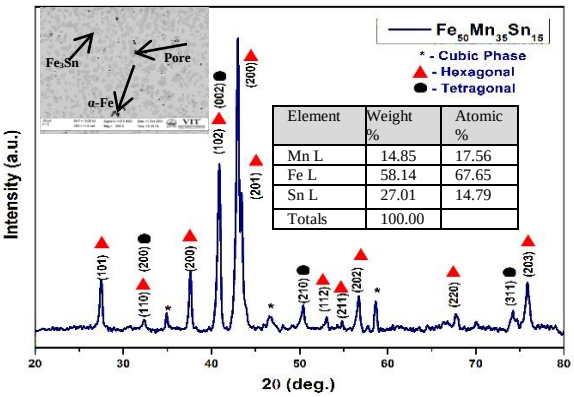

Fig.1.X-ray powder diffraction pattern of the $Fe_{50}Mn_{35}Sn_{15}$ with mixed phases (left-inset shows backscattered SEM image and right-inset-elemental composition of an alloy using EDAX)

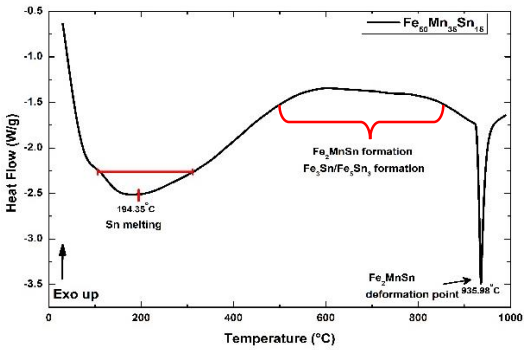

(Fig.2. DSC analysis for $Fe_{50}Mn_{35}Sn_{15}$ alloy)

4. CONCLUSION

We have synthesized the $Fe_{50}Mn_{35}Sn_{15}$ Heusler alloy, which has mixed phases of hexagonal ($P6_3/mmc$), tetragonal ($P4_2/mmc$), and cubic (Fm-3m). Annealing effect and grain size on the surface is studied using SEM and different phase formation temperature is confirmed by computed DSC.

ACKNOWLEDGEMENTS

The authors thank VIT for providing 'VIT SEED GRANT' for carrying out this research work.

REFERENCES

[1]. Wilber Pach`ın, et al,MOMENTO,**62**,43–62 (2021).
[2]. M. Kratochvílov´a et al, Intermetallics **131** 107073 (2021)
[3]. Dahal et al, AIP Advances **10**, 015118 (2020)

P62

Effect of Polymorphous Transformation of Dy doped Sm_2O_3 Nanoparticles from Cubic to Monoclinic phase on the Optical Properties

Rachana Sain[a,b] and Kamlesh Yadav[a, *]

Department of Physics, School of Basic Sciences, Central University of Punjab, Bathinda-151401, Punjab, India.

[b]SMST, Indian Institute of Technology Banaras, Varanasi-221005, UP, India.

[*]E-mail Address: kamlesh.yadav@cup.edu.in

Abstract: Dy-doped samarium oxide nanoparticles ($Sm_{2-x}Dy_xO_3$ where, x= 0.00, 0.03, 0.06, 0.09, and 0.12) are synthesized by sol-gel route. As prepared nanoparticles are characterized by X-ray diffraction (XRD), Field emission scanning electron microscope (FESEM), Energy dispersive X-ray (EDX) spectroscopy, Fourier transform infrared (FTIR) and, Ultraviolet–visible (UV-Vis) spectroscopy techniques to evaluate their structural and optical properties. XRD analysis reveals that the Dy-doped samples comprise polymorphic phases i.e., cubic and monoclinic. The fraction of monoclinic phase and Band gap increase with the increase of Dy-doping concentration while crystallite size and average particle size decrease with the increase of Dy-doping.

1. INTRODUCTION

Samarium oxide (Sm_2O_3) has attracted much attention from the viewpoint of its outstanding physical, chemical and optical properties for the fabrication of luminescent materials, nanosized phosphors, glasses, ceramics, catalysts, magnets, sensors and, optoelectronic devices. Sm_2O_3 exists in the most common monoclinic structure at ambient conditions, but modification has led to the formation of the cubic and hexagonal structure as well as the mixed polymorphic phases of these phases. Sm_2O_3 exhibits a wide bandgap of 4.33 eV (cubic), 4.7 eV (monoclinic) and 5.1 eV (hexagonal).

2. SYNTHESIS AND RESULTS

The preparation of $Sm_{2-x}Dy_xO_3$ where, x= 0.00, 0.03, 0.06, 0.09, and 0.12 nanoparticles was carried out through a low temperature, environmentally friendly sol-gel chemical synthesis method [1].

2.1. XRD Analysis

XRD of $Sm_{2-x}Dy_xO_3$ nanoparticles reveals the simultaneous formation of polymorphic cubic and monoclinic crystal structures in the doped samples. With Dy-doping, a polymorphous transformation has been observed and the fraction of the monoclinic phase increases with an increase in Dy-dopant content [1]. This result further indicates that the Dy- substitution stabilizes the formation of the monoclinic Dy-doped Sm_2O_3 phase.

2.2. FESEM Analysis

The FESEM micrograph reveals that the average particle size decreases from 55 nm to 32 nm with the increase of Dy-content. EDX spectra of Dy-doped Sm_2O_3 nanoparticles confirm Dy, Sm and, O atoms in the required ratio and the absence of any other impurity atom [1, 2].

2.3. FTIR and UV-Vis Analysis

FTIR spectra confirm the formation of crystalline Sm_2O_3 nanoparticles. Band gap increases with the increase in the Dy-doping content (w.r.t. decrease in the average particle size). The reduction in the bandgap may be attributed to the quantum confinement effect. The result shows an inverse relation between Urbach energy and band gap energy.

3. FIGURES AND IMAGES

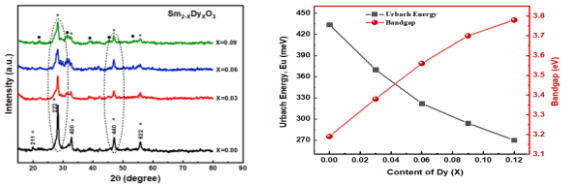

Fig.1 (a): Shows the XRD pattern of $Sm_{2-x}Dy_xO_3$ (where, x=0.0, 0.03, 0.06 and 0.09). The symbol ⋆ and ● show the cubic and monoclinic phases. Fig. 1(b) shows the nearly linear variation of bandgap and Urbach energy as a function of Dy-doping content.

4. TABLES

Table1: The variation in the optical properties (Direct bandgap, Refractive index and Urbach energy) as a function of Dy content.

Content of Dy (x)	Band Gap (eV)	Refractive Index (n)	Urbach Energy (Eu) (meV)
0.00	3.19	2.41	434
0.03	3.38	2.37	370
0.06	3.56	2.34	322
0.09	3.70	2.32	294
0.12	3.78	2.31	270

ACKNOWLEDGEMENT

We are grateful to acknowledge the Central Instrumentation Laboratory (CIL) and Department of Physics, Central University of Punjab, Bathinda, for providing the research facilities.

REFERENCES

[1]. Antoinette, M. M., & Israel, S., *Journal of Engineering and Technology*, 4, 276-9, 2017.

[2]. Srinivasan et al, *Journal of Alloys and Compounds*, 496 (1-2), 472-477, 2010.

P63

A Comparative study on the inter-relation between Structural, Magnetic and Dielectric Properties of Cobalt Ferrites on a low and high concentration of Magnesium Substitution

Sikha Sarmah[1], S. Ravi[2], P.K Maji[3], Tribedi Bora[1]

[1]*Department of Physics, National Institute of Technology Meghalaya, Shillong-793003, India*
[2]*Department of Physics, Indian Institute of Technology Guwahati, Guwahati-781039, India*
[3]*Department of Polymer & Process Engineering, Indian Institute of Technology Roorkee, Saharanpur Campus, Saharanpur, Uttar Pradesh, 247001, India*
Email: (sikhasarmah@nitm.ac.in)

Abstract: Polycrystalline samples of $Co_{1-x}Mg_xFe_2O_4$ (x = 0.00, 0.02, 0.07, 0.12 and 0.30) were composed by sol-gel Method. FT-IR, Raman, and Room Temperature M-H measurements were recorded. Surface morphology and compositional analysis were performed by FE-SEM and EDS. Temperature variation Impedance, Dielectric, and Modulus spectroscopy were studied.

1. INTRODUCTION

Ferro-spinels have grasped the interest of researchers due to their fascinating magnetic, electrical, magneto-dielectric, magneto-optical properties and their ease of preparation and high chemical stability. Amongst the spinel ferrites, the beguiling properties of Cobalt ferrites have grabbed researchers' attention due to its possibility of opening a door for the development of numerous devices. Substituting Magnesium in cobalt ferrites is said to tailor physical properties without degrading other properties [1].

2. RESULTS AND DISCUSSIONS

The XRD patterns were analyzed using Rietveld Refinement Method. The lattice parameters did not vary much with substitution due to the similar ionic radii of Co^{2+} and Mg^{2+}. FT-IR vibration band shifted slightly to the high wavenumber side, whereas, for x = 0.30, it shifted to the low-frequency side owed to the effect of Force constant. Raman spectroscopy showed the presence of five vibrational peaks, but it could be fitted well to eight peaks confirming it to be a mixed type of spinel ferrites [2]. The M_s value at Room temperature was found to decrease with an increase in Mg^{2+} substitution due to the replacement of magnetic Co^{2+} (3 μ_B) by non-magnetic Mg^{2+}. The XRD patterns, FT-IR and Raman Spectra, Room Temperature MH, Dielectric constant at 323 K are displayed in Fig.1

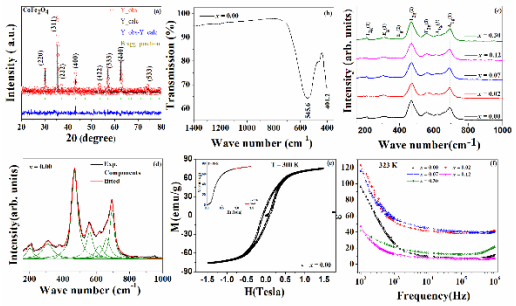

Fig.1. (a) XRD patterns (b) FT-IR spectra for x = 0.00 (c) Raman spectra for all samples (d) Deconvoluted Raman Spectra (e) M-H loop for x = 0.00 (f) Dielectric constant of all samples at 323 K

Enriched values of dielectric constants were obtained at both high and low-frequency regions for a low percentage of Mg^{2+} substitution. It could be explained by the presence of comparatively more $Fe^{2+} \Leftrightarrow Fe^{3+}$ networks at octahedral sites. FESEM analysis showed the formation of well-defined grain and grain boundaries. EDS analysis confirmed the formation of the samples in aspected ratios as that was targeted.

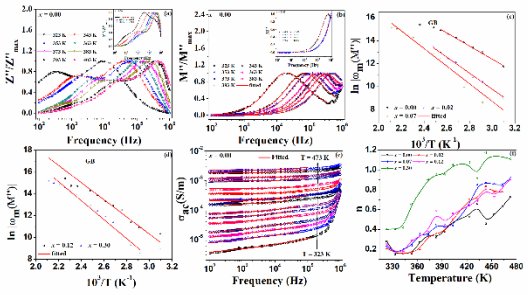

Fig.2. (a) Normalized Z'' vs. frequency (b) Normalized M'' vs. frequency at different temperatures data (c), (d) Arrhenius Plots (e) ac conductivity vs. frequency at different temperatures (f) n – T plots.

The comparison between Normalized Z'' and M'' vs. frequency at different temperatures suggests the presence of three electroactive regions for x = 0.00, 0.02 samples, absence of grain contribution for x = 0.02, 0.07 and absence of electrode effect for x = 0.30 sample. The activation energy was found to increase with increase in substitution owing to the reduction of $Fe^{2+} \Leftrightarrow Fe^{3+}$ networks, which hinders the conduction mechanism. The variation of ac conductivity was explained by Jonscher's Power Law, and the variation of frequency exponent term with temperature suggests the conduction mechanism to be a small polaron hopping type.

REFERENCES

[1] Nlebedim et al., in: Key Eng. Mater., Trans Tech Publ, 2014: pp. 287–289.

[2] Anantharamaiah et al., Phys. Chem. Chem. Phys. **18** (2016) 10516–10527.

P64

Tuning of Electrical and Magnetic properties of Samarium iron garnet by Holmium substitution

Shalini Verma, S. Ravi
Department of Physics, Indian Institute of Technology Guwahati, Guwahati - 781039
Email: sravi@iitg.ac.in

Abstract: Holmium substituted Samarium iron garnet i.e., $Sm_{3-x}Ho_xFe_5O_{12}$ (x = 0.0, 0.2, 0.5) were synthesized using solid-state reaction route. There structural, magnetic and impedance data is analyzed. XRD data reveals that the sample is formed in single phase with cubic crystal structure and Ia-3d space group. Room temperature magnetic hysteresis loops were recorded using vibrating sample magnetometer (VSM). The detailed analysis of impedance data would be presented.

1. INTRODUCTION

In the last 50 years, Rare Earth Iron Garnets (RIG) were studied and lead to many interesting theories, complementing models and new materials for applications. RIGs have the general formula $R_3Fe_5O_{12}$ (R = Rare Earth element) and show ferrimagnetic transitions at 500K to 600K along with magnetic compensation also for some materials. RIGs show many properties such as magneto-electric (ME) effect, magneto-dielectric effect, magnetization reversal, multiferroicity, magnetocaloric effect, magneto-optic properties, etc [1,2]. Such properties have a significant role in many technological applications like oscillators, optical isolators, sensors, bio-antennas, microwave devices, spintronic devices, phase shifters, and electrochemical devices, etc [3]. In this work, to tune the magnetic and electrical properties, we have prepared Ho substituted $Sm_{3-x}Ho_xFe_5O_{12}$.

2. EXPERIMENTAL DETAILS

The proposed series was synthesized by solid-state reaction method which is briefly described in ref. 4. The sample was finally sintered at 1300°C for 24 hours.

3. RESULTS AND DISCUSSION

Typical room temperature XRD patterns along with Rietveld refinements are shown in Figure1 for x=0 and 0.5. This data reveals the single-phase formation and cubic structure having Ia-3d space group. The lattice constant is decreasing from 12.53Å (x=0) to 12.45Å (x=0.5) with Ho doping.

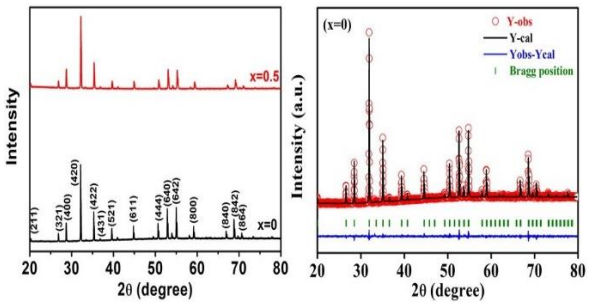

Figure1. XRD patterns for x=0 and 0.5 along with Rietveld refinement.

Room temperature magnetic hysteresis loop is shown in Figure 2 which shows that saturation magnetization is decreasing with increase in Holmium concentration from almost 20 to 10 emu/g.

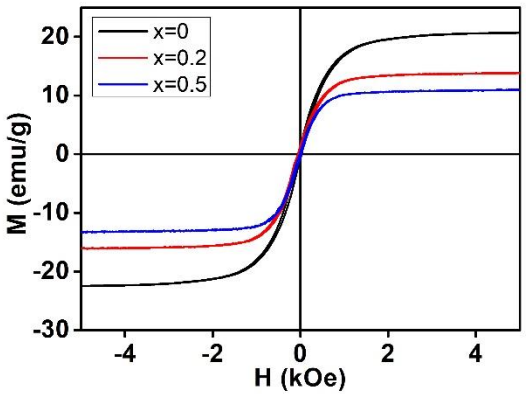

Figure 2: Room temperature M-H loop.

Impedance data are recorded at room temperature and it is found that both Z' (the real part of impedance) and Z'' (imaginary part of impedance) are decreasing with increase in frequency. The large value of impedance at low frequencies is due to space charge polarization. In addition to this, Z' and Z'' are decreasing on the substitution of Holmium. The detailed analysis will be presented.

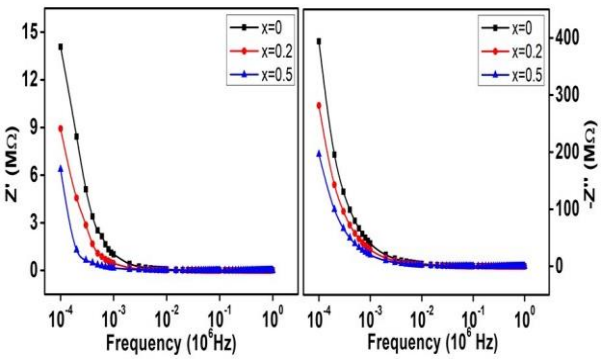

Figure 3: Variations of real and imaginary parts of impedance vs. frequency.

REFERENCES

[1]. Xiaobo Wu et al, Appl. Phys. Lett. **87** (2005) 042901.
[2]. Canglong Li et al,Ceramics International **46** (2020) 18758–18762.
[3]. Ankush B.Bhosale, Ceramics International **46**, (2020) 15372-15378.
[4]. Jie Su et al, Ferroelectrics, **448**, (2013) 71-76.

P65

Nonmonotonic magneto electric coupling in reduced-graphene-oxide-$BiFeO_3$ nano composite

Tania Chatterjee*, Arnab Mukherjee, Dipten Bhattacharya
SRF, CSIR-Central Glass and Ceramic Research Institute,Kolkata 700032, India
Email: (t31chat@yahoo.in)

Abstract: In a nanocomposite of reduced graphene oxide (RGO) and BiFeO3 (BFO), the remanent ferroelectric polarization is found to follow nonmonotonic magnetic field dependence at room temperature as the applied magnetic field is swept across 0-20 kOe on a pristine sample. The remanent ferroelectric polarization is determined both from direct electrical measurements on an assembly of nanoparticles and powder neutron diffraction patterns recorded under 0-20 kOe field. The nanosized (~20 nm) particles of BFO are anchored onto the graphene sheets of RGO via Fe-C bonds with concomitant rise in covalency in the Fe-O bonds. This creates a new way of tuning the magnetoelectric properties via reconstruction of interfaces in nanocomposites or heterostructures of graphene/single-phase-multiferroic systems.

1. INTRODUCTION

The reconstruction of crystallographic, magnetic, and electronic structures at the interface turns out to be quite an effective way of preserving the multiferroic orders and augmenting the coupling among the order parameters in multiferroics based heterostructures/ composites [1]. Among different heterostructures or composites, graphene/$BiFeO_3$ or reduced-graphene-oxide-BiFeO3 systems have attracted a lot of attention [2,3]. Large exchange field B_{ex} in graphene/$BiFeO_3$ heterostructure induces proximity effect driven magnetism [3]. Following all these results, it is important to examine how reconstruction of magnetic and electronic structures by exchange coupled surface atoms of graphene and nanoscale $BiFeO_3$ influences the multiferroicity in $BiFeO_3$.

2. RESULTS & DISCUSSIONS

The hydrothermally synthesized reduced graphene oxide and $BiFeO_3$ nano composite (Com-H) were thoroughly characterized using XRD, RAMAN, FTIR, TGA, XPS and Neutron. The ferroelectric polarization examined using two different protocols exhibit the similar observations as we have obtained after calculating the crystallographic polarization from refinement of Neutron diffraction data under different fields as shown in The Figure1. The schematic is as shown in Figure.2 is of the bonded and non-bonded $BiFeO_3$ particles with reduced graphene oxide layers; the bonded particles because of the presence of Fe-C bonds and exchange coupling interactions across them could offer positive magnetostrictive magnetoelectric coupling; the nonbonded ones, on the other hand, would exhibit negative magnetoelectric coupling; field-dependent competition between these two fractions is eventually yielding the nonmonotonic variation of P_R with H. Tuning of the volume fractions of the bonded and nonbonded $BiFeO_3$ particles, therefore, offer a pathway to tune the swithcing of magnetoelectric coupling – from purely negative to mixed positive and negative to purely positive.

The emergence of Fe-C bonds and consequent change in the magnetic and electronic structure of the interface region has influenced the coupling between ferroelectric and magnetic properties remarkably.

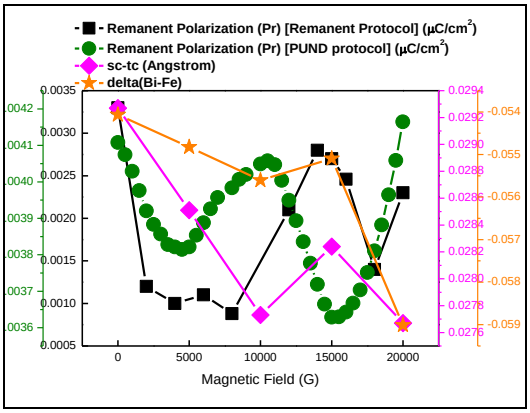

Figure 1 variation of PR with H obtained from remanent hysteresis loops (inner left axis) and PUND (outer left axis); unit cell off-centered displacement - sc-tc (inner right axis) and net off-centering with respect to the oxygen cages (outer right axis) - obtained from refinement of powder neutron diffraction data

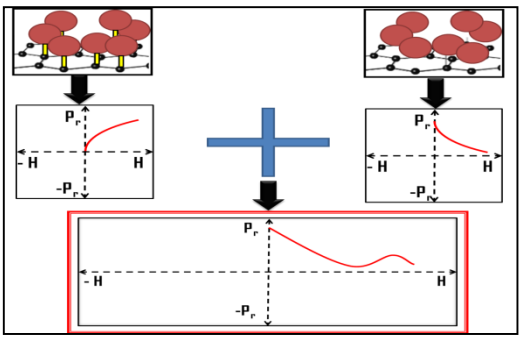

Figure 2 The schematic of result

This observation of competition between negative and positive magnetostriction and hence between negative and positive magnetoelectric coupling in the reduced-graphene oxide-BiFeO3 nanocomposite reveals the significant role played by the Fe-C bonds.

REFERENCES

[1] Huang, W.et al Appl. Phys. Rev. **5** (2018) 041110.
[2] Zanolli, Z. Sci. Rep. **6** (2018) 31346.
[3] Song, H-D. et al., Nano Lett. **18** (2018) 2435.

P66

Electrical properties of $In_{(2-x)}Nd_xO_3$ dilute magnetic semiconductor nanoparticles

Kapil. Y. Salkar [1*], R.B Tangsali [2], R.S Gad [3]
[1] Department of Physics, DCT's Dhempe College of Arts and Science, Miramar Panjim, Goa, India
[2,3] School of Physical and Applied Sciences, Goa University, Taleigao Plateau, Goa, India
Email: *salkarkapil22@gmail.com

Abstract: $In_{(2-x)}Nd_xO_3$ nanoparticles with (x = 0, 0.10, 0.15 and 0.20) were prepared by combustion method. Here we report our outcomes on electrical properties carried out on these materials from room temperature to 500^{o}C. Thermopower studies carried out on the materials resulted in Seebeck coefficient showing negative values with 'x' dependent enhancements. The material exhibits n-type semiconductor character from room temperature to higher temperatures without any first order transition in the seebeck coefficient. Electrical resistivity and the activation energy being related are seen to decrease with rising temperature due to increase in charge carrier concentration. Dielectric constant (ε) and dielectric loss (tan δ) examined as a function of frequency displayed nearly exponential decline in their values with increasing frequency for all the samples. However temperature dependent 'ε' and 'tan δ' show a peaking behaviour at lower temperatures with increasing trend at higher temperature as a result of increase in dielectric polarization. The DMS materials being ferromagnetic at room temperature are good temperature dependent semiconductors with high dielectric constant.

Keywords – Nanoparticle, Ferromagnetism, Dielectric Constant, Activation Energy, Seebeck coefficient.

P67

Unconventional Hall effect and its modification in 2D van der Waals ferromagnet Fe_3GeTe_2

Rajeswari Roy Chowdhury[1*], Samik DuttaGupta[2-4], Chandan Patra[1], Oleg A. Tretiakov[5], Sudarshan Sharma[1], Shunsuke Fukami[2-4,6,7], Hideo Ohno[2-4,6,7] and Ravi Prakash Singh[1]

[1] Department of Physics, Indian Institute of Science Education and Research, Bhopal, India

[2] Center for Science and Innovation in Spintronics (CSIS), Tohoku University, Japan

[3] Center for Spintronics Research Network (CSRN), Tohoku University, Japan

[4] Research Institute of Electrical Communication (RIEC), Tohoku University, Japan

[5] The University of New South Wales, Australia

[6] Center for Innovative Integrated Electronic Systems (CIES), Tohoku University, Japan

[7] WPI Advanced Institute for Materials Research, Tohoku University, Japan

Email: rajeswari@iiserb.ac.in

Abstract: van der Waals uniaxial ferromagnet Fe_3GeTe_2 has attracted immense attention due to its unique properties. Fe_3GeTe_2 shows ferromagnetism with a Curie temperature (T_C) ~ 220 K. Cobalt doping results in reduction of T_C. Magnetotransport studies reveal existence of non-trivial spin textures in FGT which is significantly modified with Co doping.

1. INTRODUCTION

Topological magnetic textures provide an attractive platform for the realization of future spintronic [1] and quantum information processing [2] devices. The discovery of 2D layered van der Waals (vdW) magnetic materials have enunciated the possibility for the realization of a variety of unconventional non-collinear spin textures, down to the monolayer limit. Among the family of quasi-2D vdW ferromagnets (FMs), metallic Fe_3GeTe_2 (FGT, hereafter) is promising owing to its high Curie temperature [3], large magnetic anisotropy, and stabilization of skyrmion and chiral spin-spiral structures [4,5]. However, an understanding of the physics responsible for the generation of these exotic spin textures and associated magnetoresistive manifestations have remained elusive. Here, we clarify the underlying factors responsible for the stabilization of these spin textures by investigating the impact of doping at the transition metal (Fe) site of 2D FM FGT.

2. RESULTS AND DISCUSSIONS

Single crystalline $(Co_xFe_{1-x})_3GeTe_2$ (x = 0, 0.05, 0.45, 0.55) samples and a reference sample (FGT) were grown by chemical vapor transport method. Magnetotransport measurements under applied $H \parallel c$-axis result in a sizeable anomalous Hall effect, possibly originating from the topological nodal lines in the band structure. On the other hand, transverse resistivity under applied $H \perp c$-axis results in an unconventional behavior with a prominent cusp-like feature, shifting to lower field values with increasing x. Concomitant magneto-optical Kerr effect measurements indicate the emergence of an aggregate of skyrmion-bubble-like lattice structures along with trivial circular or stripe domain patterns. Angle-dependent magnetotransport measurements (at constant H) confirms the 2D nature of these non-trivial spin configurations. A separation of the various magnetoresistive effects indicates a significant contribution originating from an unconventional topological Hall effect behavior [6], much larger than that previously observed either in vdW material [3] or other skyrmion-hosting material systems [7,8]. These results provide a deeper understanding of magnetoresistive responses originating from complex spin textures and offer a route towards the realization of non-collinear spin texture-based spintronic devices using vdW FMs (Fig.1)

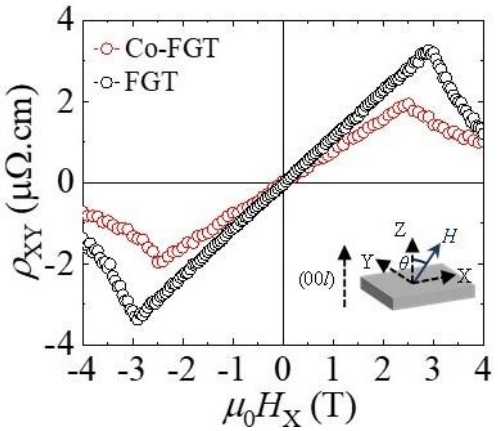

Fig.1. Transverse Hall resistivity versus magnetic field (along x direction).

ACKNOWLEDGEMENT

RRC acknowledges DST, for financial support (Grant no. DST/INSPIRE/04/2018/001755). RPS acknowledges SERB, for Core Research Grant CRG/2019/001028.

REFERENCES

[1] X. Lin *et al.*, Nature Elec. **2**, 274 (2019).
[2] D. M. Kennes *et al.*, Nature Phys. **17**, 155 (2021).
[3] Y. Wang *et al.*, Phys. Rev. B. **96**, 134428 (2017).
[4] B. Ding *et al.*, Nano Lett. **20**, 868 (2020).
[5] M. J. Meijer *et al.*, Nano Lett. **20**, 8563 (2020).
[6] R. Roy Chowdhury *et al.*, Scientific Reports **11**, 14121 (2021).
[7] S. Seki *et al.*, Science **336**, 198 (2012).
[8] N. Kanazawa *et al.*, Adv. Mater. **29**, 1603227 (2017).

P68

Intrinsic and field-induced magnetic ordering in Ni_5Al_3/NiO nanoparticle compacts

Pavan Venu Prakash Madduri[1] and Sharika Nandan Kaul[2]
[1]Department of Sciences, Indian Institute of Information Technology Design and Manufacturing Kurnool Kurnool-518007, Andhra Pradesh, India.
[2]School of Physics, University of Hyderabad, Central University P.O., Hyderabad-500046, Telangana, India
Email: prakash.madduri@iiitk.ac.in

Abstract: First synthesis of the intermetallic Ni_5Al_3 in the nanocrystalline form using inert gas condensation technique is reported. Microstructural characterization as well as the compositional analysis indicate the presence of Ni_5Al_3/NiO, core/shell nanoparticles with mean crystallite size $d \approx 6$ nm, with composition $Ni_{5+x}Al_{3-x}$/NiO ($x = 0.014$), $Ni_{5-x}Al_{3+x}$/NiO ($x = 0.038$) for the samples S_1 and S_2 respectively. Temperature dependent "Zero-dc field" ($H = 0$) linear (χ_1) and nonlinear (χ_n with $n = 2, 3, 4, 5$) ac-magnetic susceptibilities provided a conclusive evidence for the existence of two spin glass (SG) thermodynamic phase transitions: one at T_i ($H = 0$) ≈ 138 K and the other at a lower temperature $T_p(H = 0) \approx 108$ K in both S_1 and S_2. Linear ac-susceptibility in finite H, demonstrates that the thermodynamic nature of these transitions is preserved in finite low-fields (< 100 Oe). A detailed comparison of the H-T phase diagram between theory and experiment unambiguously identifies the two SG phase transitions as (i) the simultaneous paramagnetic (PM): chiral-spin glass (CG) and PM-SG phase transitions at T_i (H) and (ii) the replica symmetry-breaking SG transition at $T_p(H)$. For $H \geq 3$ kOe, the above mentioned 'SG' transitions transform into a single PM-ferromagnetic (FM) phase transition.

1. INTRODUCTION

Among the family of Transition-metal aluminides (TM_xAl_y with TM = Fe, Co, Ni), the Ni-rich nickel aluminides [1,2], namely Ni_3Al, Ni_5Al_3 and NiAl, offer a rare opportunity to study the effects of off-stoichiometry since they have homogeneity ranges around the stoichiometric compositions as wide as ≃14 at% Ni. Out of these intermetallic compounds, Ni_3Al has attracted maximum attention because it exhibits novel physical phenomena such as the weak itinerant-electron magnetism, pressure-induced or compositional and/or site disorder-induced non-Fermi liquid (NFL) behavior, depending on the average crystallite size, exchange-enhanced Pauli spin paramagnetism, anti-ferromagnetic spin fluctuation-mediated super-conductivity and NFL behavior close to the quantum critical point, chirality-driven intrinsic spin-glass ordering in nanocrystalline Ni_3Al. In sharp contrast, hardly anything is known about the physical properties of Ni_5Al_3 owing to the difficulty in synthesizing pure Ni_5Al_3 compound. Here we report the first synthesis of the intermetallic Ni_5Al_3 in the nanocrystalline form using inert gas condensation technique (IGC) and the intrinsic and field-induced magnetic ground states are explored.

2. EXPERIMENTAL DETAILS AND RESULTS

A thorough structural, microstructural and compositional characterization of IGC synthesized nc-Ni_5Al_3 was performed using x-ray diffraction, transmission electron microscopy, and wavelength dispersion x-ray spectroscopy. To unravel the true nature of the intrinsic magnetic ordering, the first five harmonics of the ac magnetic response (*linear,* χ_1 as well as *nonlinear,* χ_2–χ_5 magnetic susceptibilities) of the nc-Ni_5Al_3/NiO samples were measured over the temperature range 1.8–320 K at zero and finite magnetic fields, using Quantum Design PPMS-ACMS. The experimentally obtained H-T phase transitions from the linear ac-susceptibility in superposed dc magnetic fields for the samples S_1 and S_2 (see Fig.1) matches quite well with the H-T phase diagram predicted by the *chirality-driven* spin glass (SG) ordering model for a 3D nearest-neighbor Heisenberg SG system with *weak* random anisotropy.

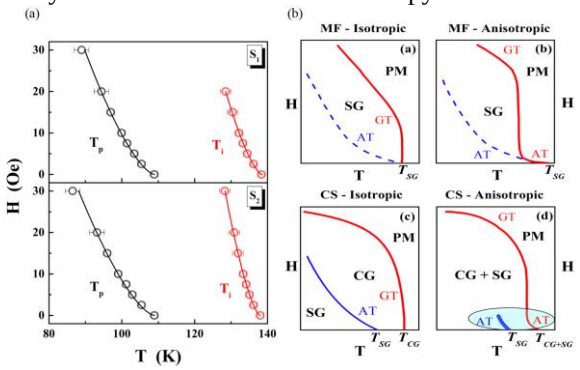

Fig.1. (a) H-T phase diagrams for the samples S_1 and S_2. (b) Schematic sketches of the H − T phase diagrams predicted by the mean-field (MF) and chiral-spin (CS) models for the isotropic and anisotropic cases. The notations SG, CG, PM, AT and GT refer to spin glass, chiral glass, paramagnetic phases, Almeida-Thouless, Gabay-Toulouse transition lines respectively.

ACKNOWLEDGEMENT

P.V.P.M. thanks the Center for Nanotechnology, University of Hyderabad, for permitting the use of the PPMS-VSM/ACMS facility for the measurement of ac magnetic response.

REFERENCES

[1]. P V Prakash Madduri, S N Kaul, Phys. Rev. Mater. **2** (2020) 126003, and references cited there-in.
[2]. P V Prakash Madduri, S N Kaul, J. Alloy Compd. **870** (2021) 159388, and references cited there-in.

P69

Evolution of antiskyrmion phase in tetragonal ferrimagnetic Heusler Mn-Pt(Pd)-Sn-In system

Bimalesh Giri [1], Dola Chakrabartty[1], Amitabh das[2], Ajaya K. Nayak[1]
[1]School of Physical Sciences, National Institute of Science Education and Research (NISER), Bhubaneswar, Jatni -752050, India;
[2]Solid State Physics Division, Bhabha Atomic Research Centre, Mumbai 400 085, India;
Email: bimalesh.giri@niser.ac.in

Abstract: The present study contains the evolution of antiskyrmion phase and its related phenomena in D_{2d} symmetry-based Mn-Pt(Pd)-Sn-In systems. The change in the underlying exchange strength and Dzyloshinkii-Moriya interaction (DMI) along with the magnetic anisotropy have a great potential to tune the antiskyrmion size.

1. INTRODUCTION

The non-collinear magnets provide a fertile ground to harbor the smaller, faster, and energy-efficient storage media. In particular, magnetic skyrmions (Skx)/antiskyrmions (a-Skx), which are localized topological objects with swirling spin textures, are considered as potential candidates to be implemented as a bit of information [1]. These topological objects are in general stabilized by Dzyaloshinskii–Moriya interaction (DMI) in non-centrosymmetric bulk magnets. In this regard, tetragonal Heusler compound $Mn_{1.4}Pt_{0.9}Pd_{0.1}Sn$ has been reported to host a-Skx [2]. The Heisenberg exchange interaction along with DMI governed the helical ground states which transform into an a-Skx phase under the application of external magnetic fields. The size of the a-Skx is related to the modulation length of the helical state which depends on the ratio of the Heisenberg exchange constant to the strength of the DMI. Furthermore, the dipolar energy associated with the large magnetic moment of the system also plays a vital role in controlling the shape and size of the a-Skx. Therefore, flexible tuning of these parameters can pave the way towards the realization of high-density race track memory devices.

2. RESULTS AND DISCUSSIONS

To achieve the goal of showcasing high density and small size a-Skx, we have synthesized a series of Heusler compounds $Mn_{1.4}Pt(Pd)Sn_{1-x}In_x$. Room temperature powder X-ray diffraction analysis reveals that the present compounds crystallize in the non-centrosymmetric inverse tetragonal structure belongs to the space group $I\bar{4}2m$. The D_{2d} symmetry confirms the presence of DMI interaction. The low-temperature isothermal magnetization measurement suggests a decrease in the saturation magnetization with the decrease in Sn composition. The deep/kink kind of signature in the real part of ac-susceptibility versus DC magnetic field measurement indicates the presence of a-Skx phase over a certain temperature range which is verified by the Lorentz transmission Electron Microscopy (LTEM) measurements. Powder neutron diffraction study performed at Dhruva reactor, BARC, Mumbai, reveals a ferromagnetic structure [Fig. 1(a)] in the temperature range (125-300 K) where we observe the presence of a-Skx using LTEM imaging. In the low temperature region a large release of in-plane components of the magnetic sub-lattices forming a non-collinear ferrimagnetic structure [Fig. 1(b)].

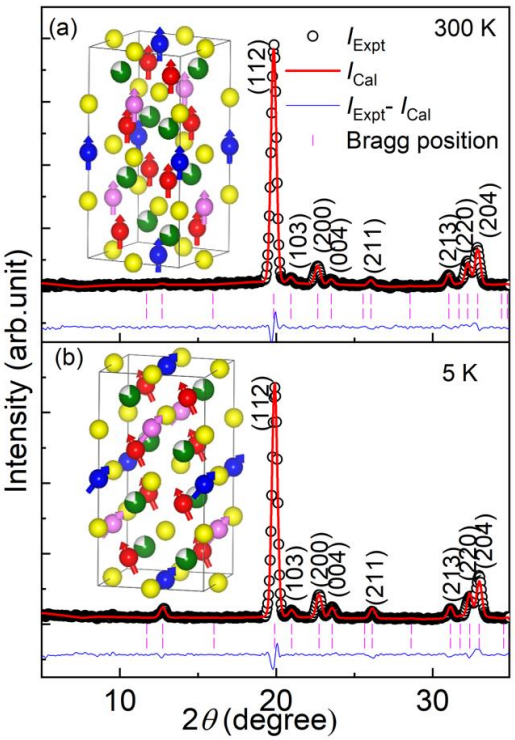

Fig. 1(a), (b) Represents the Reitveld refinement of the powder neutron diffraction data taken at 300 K and 5 K temperature for the $Mn_{1.4}PtSn_{0.8}In_{0.2}$. The insets show the corresponding magnetic structure.

REFERENCES

[1]. F. Jonietz *et al*, *Science* **330**, (2010) 1648-1651.

[2]. A. K. Nayak *et al*, *Nature* **548**, (2017) 561-566.
.

P70

Dual magnetic order and corresponding large anomalous Hall response in a Kagome magnet

Charanpreet Singh, Ashis Nandy and Ajaya K. Nayak
National Institute of Science Education and Research, HBNI, Jatni-752050, India
Email: charanpreet.singh@niser.ac.in

Abstract: The nature of magnetic ordering in a magnetic system define its properties. Usually, a single order parameter is observed in magnetic systems, which control its response to external stimuli. Here we show the existence of dual order parameter in the kagome lattice system Mn-Fe-Sn. We have utilized the Hall effect measurements to characterize this unprecedented phenomenon. To understand the experimental result, we theoretically show that an interplay of Heisenberg exchange and higher order exchange stabilizes present ground state.

1. INTRODUCTION

Ordered state in magnetic systems leads to many interesting effects such as spin polarization, magnetoresistance and anomalous Hall effect (AHE). The anomalous Hall signal, observed for the first time in ferromagnetically ordered materials, was found to scale with the magnetization of the sample. The modern theories attribute the intrinsic AHE to the Berry phase arising in the momentum space band structure. The band structure picture of the AHE has been studied extensively and the role of band topology is found to be very important. Furthermore, a large AHE has been found in a non-collinear antiferromagnetic Mn_3Sn due to breaking of time reversal symmetry by octupole order [1]. These complex ground states are mostly stabilized due to the exchange/geometrical frustration present in systems. Apart from this, the higher order exchange interaction can also lead to new ground states which cannot be stabilized by Heisenberg exchange interaction. We have studied the interplay of higher order exchange with Heisenberg on a Kagome lattice in the present report.

2. RESULTS

Mn_3Sn crystallizes in a layered kagome lattice structure with in-plane inverse triangular spin structure as ground state. Due to the shifted kagome layer structure, this in-plane spin configuration leads to an octupole order, reprted both experimentally and theoretically [2-4]. Here, we have studied the ground state of Mn-Fe-Sn Kagome lattice samples. We show that at low temperatures, the non collinear in-plane magnetic ground state is canted along *c*-axis. This canted state leads an additional non coplanar dipole order to stabilize on top of the octupole order already present. These orders manifests in Hall measurement as separate anomalous Hall signal as shown in figure 1. The octupole order of in-plane non-collinear spins breaks the time reversal symmetry which leads to stabilization of Weyl nodes. The momentum space Berry curvature of these Weyl points generate the ρ_{xz} component of Hall resistivity. On the other hand, the out of plane canting leads to a ground state with finite scalar spin chirality. The scalar spin chirality leads to a real space Berry curvature and generate a Hall signal (ρ_{xy}) even larger than the one observed due to Weyl nodes. We further confirmed the ground state using neutron diffraction measurements. The canted state discussed here is similar to the *3Q* state found in the triangular lattice in Mn/Cu(111) monolayer system [5]. Using DFT calculations we reveal the stabilization mechanism of *3Q* like canted state to be an interplay of 4-spin and 6-spin interactions with the 2-spin Heisenberg exchange.

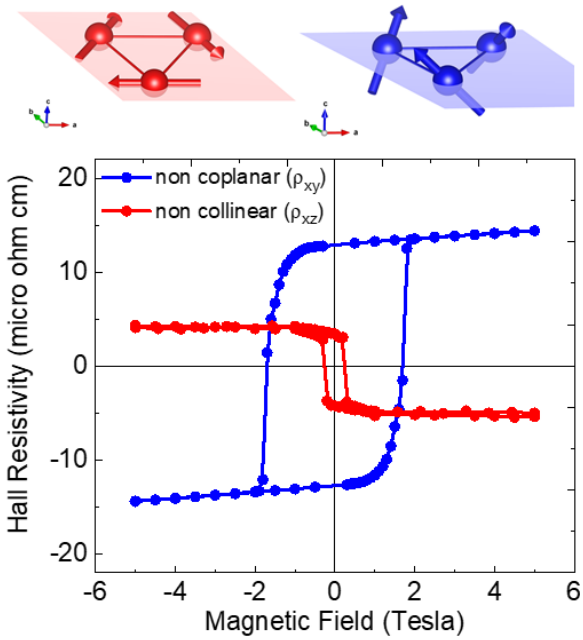

Fig.1. Hall data as recorded at 3K with magnetic field applied along different direction for Mn-Fe-Sn single crystal sample.

REFERENCES

[1]. S. Nakatsuji, et al. Nature 527, 212 (2015).
[2]. M-T. Suzuki, et al. Physical Review B 95.9 094406(2017).
[3]. T. Higo, et al. Nature Photonics 12, 73 (2018).
[4]. Motoi Kimata, et al. Nature communications 12, no. 1: 1-8(2021).
[5]. P. Kurz, et al. Phys. Rev. Lett. 86, 1106 (2001).

P71

Ni grafted RGO - a nanocomposite with tunable magnetic properties

S. Goswami[1*], M. Chakraborty[1] and D. De[1,2]
[1]Material Science Research Lab, The Neotia University, Sarisa, 24 Pgs (South) WB 743368, India
[2]Department of Physics, Sukumar Sengupta Mahavidyalaya, Keshpur, Medinipur 721150, WB, India
Email: (suchandra.goswami@tnu.in)

Abstract: A comparative study based on magnetic properties of three Ni nanoparticles grafted reduced graphene oxide (RGO) composites with different volume fractions is performed. Composite with high Ni concentration shows ferromagnetic characteristics whereas the composite with dilute Ni concentration reveals superparamagnetic (SPM) behaviour. A composite with ambient Ni concentration exhibits memory effect and another mixed phase (Ni-NiO) nanoparticles grafted RGO nanocomposite depicts exchange bias (EB) effect. Grafting of metal (Ni) nanoparticles on RGO sheets with different volume fractions introduces tunable magnetic properties along with ferromagnetism at room temperature, suitable for possible spintronic applications.

1. INTRODUCTION

In this aticle, we are motivated to report a simple method of one step synthesis of Ni nanoparticle grafted RGO nanocomposites through solvothermal synthesis via autoclave. Three samples with the same composition but with different volume fractions (ϕ=1%, 5% and 15%) of Ni in RGO are prepared with mean crystallite sizes varying from 27−29 nm by changing the stoichiometric amount of Ni chloride only. This provides the platform to perform a comparative study of the magnetic properties with a variation of interparticle interaction. These three samples are named after their volume fractions as Ni-1@RGO, Ni-5@RGO and Ni-15@RGO. Another sample Ni-NiO-10@RGO (with ϕ=10%) is synthesized following the same route where core shell Ni-NiO nanoparticles are embedded in RGO sheets.

2. RESULT AND DISCUSSION

Thermal variation of magnetization ($M(T)$) in FC and ZFC protocols reveal, for Ni-15@RGO, Ni-5@RGO and Ni-1@RGO, bifurcation temperatures between zero field cooled (ZFC) and field cooled (FC) are not reached till room temperature. FC magnetization curves for Ni-15@RGO and Ni-5@RGO follow a slow increasing trend with cooling as seen generally for interacting and dense nanoparticles systems having superspin-glass (SSG) like characteristics [1]. Low temperature $M(T)$ in ZFC and FC modes for Ni-1@RGO depicts a Curie tail like behaviour as generally evident in case of very dilute nanoparticle systems possessing superparamagnetic nature. Detailed analysis of the magnetic hysteresis ($M-H$) loops confirms that for all the samples, saturation moment (M_S) and coercivity (H_C) are higher at 2 K than the same at 300 K. In case of ferromagnetic dense nanoparticle assemblies, collective behaviour is generally observed resulting in SSG like characteristics as evident by the memory effect observed in Ni-15@RGO. In dilute nanoparticle systems, where the particle sizes are small enough to have single domain nature, SPM like behaviour is generally observed originating from anisotropic behaviour of individual nanoparticles [2].

$M-H$ loops of the composite Ni-NiO-10@RGO (where both FM metal-AFM metal oxide phases coexist) are recorded after cooling the sample in FC mode (H_{cool}=10 kOe). Figure 1 depicts a loop shift along the field axis followed by increase in coercivity as a footprint of exchange interaction revealing an application-oriented phenomenon – exchange bias [3].

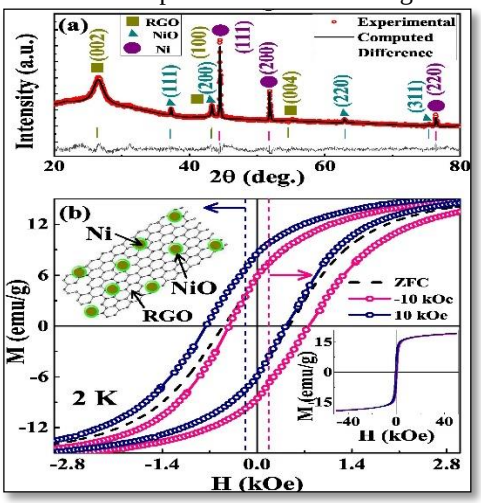

Fig.1. X-ray diffraction pattern (symbols) at 300 K of Ni-NiO-10@RGO. (b) Low field region of the $M-H$ loops at 2 K in ZFC and FC (H_{cool}=±10 kOe) modes.

3. CONCLUSION

A variation of volume fraction of Ni in RGO from 15 to 1% leads to change into SPM like behaviour from ferromagnetic SSGs. Application based phenomenon like exchange bias and memory effect are observed in a composite where nanoparticles pretend to have an overlapping domain of Ni-NiO.

ACKNOWLEDGEMENT

D. De, M. Chakraborty and S.Goswami thank SERB Project EMR/2017/001195 and TNU Project R&D/2020/F1 for financial support.

REFERENCES

[1]. D. De et al, J. Magn. Magn. Mater. **394** (2015) 448.
[2]. D. De et al, J. Appl. Phys. **111** (2012) 033919.
[3]. S. Goswami et al, J. Alloys Compd. **890** (2021) 161916.

P72

Electronic structure and magnetic properties of iron selenide KFe_2Se_2: A first principle study

Smrutirekha Hota, G. Panda, J. Das, A. V. Korumelli, A. Kar, S. Jata and K. L. Mohanta*
Department of Physics, Faculty of Engineering and Technology (ITER),
Siksha 'O' Anusandhan Deemed to be University, Bhubaneswar-751030, Odisha, India
***Corresponding author, E-mail: kamalmohanta@soa.ac.in**

Abstract: By the first principle electronic structure calculations, we study the electronic structure and magnetic properties of KFe_2Se_2. Here KFe_2Se_2 is an example of iron selenide family of 122 type iron based superconductors which show superconducting critical temperature above 30 K. Here we use density function theory (DFT) simulation package to study the magnetic properties of this iron based compounds. The self-consistent field (Scf) calculation has been done by using Quantum ESPRESSO software. Here we test the convergence of plane wave cutoff and Brillouin Zone sampling and using the optimized cell parameters we study the band structure and density of state (DOS) of this KFe_2Se_2 system.

1. INTRODUCTION

The discoveries of high temperature superconductivity in iron based materials [1] bring enthusiasm to study the superconducting and physical properties of these materials and triggered to search for new high temperature superconductors. Mainly these iron based superconductors are classified into iron pnictide and iron chalcogenide. They include different type of structure like 1111, 111, 11, 122, 32225 and 42226-type. The 122 type materials are the most studied system as compare to other class. KFe_2Se_2 is an example of this 122-type family and was reported to have transition temperature of 30 K [2]. This compound show a similar type of structure as $BaFe_2As_2$, but chemically close to FeSe i.e, 11-type iron based superconductors. So it is important to study the structure and physical properties of this KFe_2Se_2 compound. Here we study the electronic structure and magnetic properties of this material.

2. COMPUTATIONAL APPROACH

The crystal structure and the electronic structure properties are computed and analysed using density functional theory (DFT) approach [3, 4]. Here the DFT calculation for KFe_2Se_2 has been done using Quantum ESPRESSO Ab Initio Simulation Package [5, 6]. We first test the convergence of plane wave cutoff and Brillouin Zone (BZ) sampling for KFe_2Se_2 and using the optimized cell parameters, the self-consistent field (scf) calculation have been performed. The band structure and the density of state (DOS) calculations have been also studied for this system.

3. RESULTS

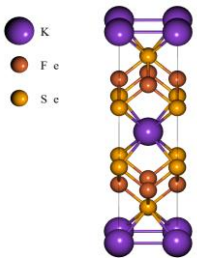

Fig1: Crystal Structure of KFe_2Se_2

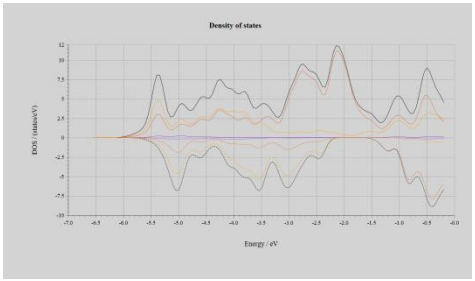

Fig2: Total density of states of KFe_2Se_2.

ACKNOLOWLEDGEMENT

The authors would like to gracefully acknowledge the research facility offered by the Institute of Physics, Bhubaneswar, India.

REFERENCE

[1] Y. Kamihara, et. al., J. Am. Chem. Soc., 130, (2008), 3296.
[2] J. Guo, et al., Phys. Rev. B., 82, (2010), 180520(R)
[3] P. Hohenberg, W. Kohn, Phys. Rev., 136, (3B), (1964), B864-B871.
[4] W. Kohn, L. J. Sham, Phy. Rev., 140 (4A), (1965), A1133-A1138.
[5] P. Giannozzi, S. Baroni, et al., J. Phys: Condens. Matter, 21, (2009), 395502.
[6] P. Giannozzi, et al. J. Chem. Phys, 152, (2020), 154105.

P73

Structural, Magneto-dielectric properties of 0.9$BiFeO_3$-0.1 $CaTiO_3$ nanocomposite

Manoj K. Singh[1], Bushra Khan[1]
[1]*Centre of Material Sciences, Institute of Interdisciplinary Studies (IIDS), University of Allahabad, Allahabad-211002, India*
Email: mksingh100@allduniv.ac.in

Abstract: In this work, 0.9 $BiFeO_3$-0.1 $CaTiO_3$ nanocomposites were synthesized using sol-gel method. The dielectric permittivity (ε) and tangent loss (tan δ) decreases with increasing frequency and show dielectric anomalies (as a hump) at different temperatures for different compositions. The frequency-dependent ac conductivity obeys Jonscher's power law with large ac conductivity dispersion for higher frequencies with increasing CTO concentration. The sample shows anomalous magneto-capacitance effect with frequency and and positive and negative magneto-dielectric effect at room temperature.

1. INTRODUCTION

Magnetoelectric multiferroics are the materials with coexistence of the electric and the magnetic order parameters in the same phase. Multiferroic materials potentially offer a whole range of new applications, including the emerging field of spintronics, new data-storage media, and multiple-state memories. In addition, they also exhibit the phenomenon called the magnetoelectric (ME) effect; magnetization induced by an electric field and electric polarization by a magnetic field. There has been much interest in recent years in artificially engineered nanostructured materials with novel physical properties. One of particular interest is super lattice and nano composite hetrostructures of functional oxides, such as multiferroics (MF), ferroelectric (FE), CMR manganites, ferromagnetic (FM) and antiferromagnetic (AFM) and other different order materials[1,2]. $BiFeO_3$ (BFO) is known to be the only material that exhibits multiferroism at room temperature. It is a rhombohedrally distorted ferroelectric perovskite (Tc ≈1100 K) with the space group R3cand shows G-type antiferromagnetism up to 643K (T_N).The quantum paraelectrics (or incipient ferroelectrics) such as $CaTiO_3$ has been attracted huge attention due to their polar soft modes but do not show a ferroelectric phase transition (T_C) ..$CaTiO_3$ exhibit orthorhombic structure with space group Pbnm up to 1380K. In this work, 0.9$BiFeO_3$-0.1$CaTiO_3$ nanocomposites were synthesized using sol-gel method.

2. RESULT AND DISCUSSION

2.1STRUCTURALPROPERTIES

The XRD pattern is in good agreement with the rhombohedral perovskite structure with space group *R3c*. All the observed diffraction peaks of $BiFeO_3$ is indexed by using JCPDS Card No: 01-071-2494.

2.2DIELECTRICAND ANALYSIS

The dielectric permittivity decreases monotonically with increasing frequencies for all the compositions. The low-frequency dispersion may be recognized due to space charge formation causing interfacial polarization due to the A-site vacancies whereas, at high frequencies, these space charges find very little time to align in the applied field direction and thus incapable of experiencing the relaxation process [3]. It is observed that the tangent loss decreases with an increase in frequency from 1 kHz to 1MHz for all the synthesized samples. The high value of ε and low value of tan δ makes the composite useful for capacitors, transducer and microwave application.

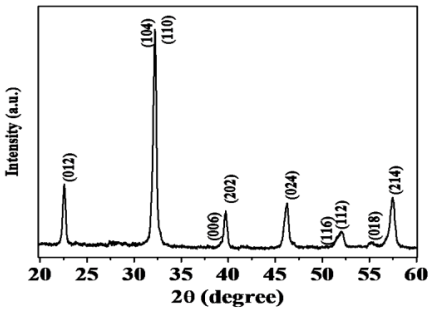

Fig. 1. X- ray diffraction (XRD) pattern of 0.9$BiFeO_3$-0.1 $CaTiO_3$

2.3. MAGNETO - CAPACITANCE ANALYSIS

Magneto-capacitance (MC) measure the strength of magneto - dielectric coupling (MD) in which the dielectric/capacitance parameters are measured with varying magnetic fields described by the equation given below:

$$MC\ (\%) = \frac{(C_H - C_0)}{C_0} \times 100\%\ \ \&\ MD\ (\%) = \frac{(\varepsilon_H - \varepsilon_0)}{\varepsilon_0} \times 100\%$$

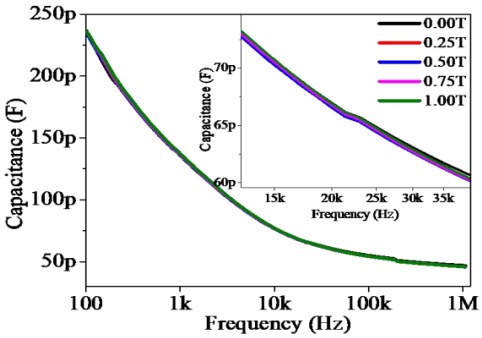

Fig.2 Magneto-capacitance (MC) versus frequencies

Fig. 2 and inset reveals the anomalous change in magneto capacitance was observed ~18 kHz and we also observed that the positive magneto-dielectric effect below and negative magneto-dielectric effect above 18 kHz.

ACKNOWLEDGEMENT

We acknowledge FIST programme (Grant No. SR/FST/PSI-216/2016).

REFERENCES

[1] J Ma et. al. Adv. Mater. 23 (2011) 1062–1087
[2] W Eerenstein et. al. Nature442 (2006) 759–765
[3]M. Rawat et. al. J. Alloys Comp. 597 (2014)188-1999

Tuning the anomalous Hall effect in MnPt(Ir)Sn Heusler system

Sk Jamaluddin, Ajaya Kumar Nayak
School of Physical Sciences, National Institute of Science Education and Research, HBNI, Jatni-752050, India
jamaluddin.sl@niser.ac.in

Abstract: In a ferromagnetic system, in addition to ordinary Hall voltage, an extra Hall contribution appears which is known as anomalous Hall effect (AHE). The AHE has two types of microscopic origin, such as (i) scattering independent intrinsic contribution and (ii) scattering dependent extrinsic contribution. In the present work, we have studied the AHE in MnPt(Ir)Sn Heusler system. We observe a large enhancement of the AHE with increasing the iridium concentration in place of platinum while the saturation magnetization decreases considerably. Experimentally, we have calculated the scaling factor α from the relation $\rho^{A}_{xy} \propto \rho^{\alpha}_{xx,}$ where $\rho^{A}_{xy,}$ ρ_{xx} are the anomalous Hall resistivity and longitudinal resistivity, respectively. We found that the scaling factor increases with iridium concentration which signifies that the intrinsic contribution is dominant over the extrinsic one.

1. INTRODUCTION

The emergence of anomalous Hall effect (AHE) owing to the combined effect of spin orbit coupling (SOC) and band topology of a broken time reversal symmetry system has been received much attention for the understanding of microscopic spin transport phenomena as well as for application in advanced spintronic devices. Recent studies have shown that the AHE mainly originates due to two different microscopic mechanisms, one is scattering independent intrinsic mechanism and another is scattering dependent extrinsic mechanism. The scattering independent intrinsic mechanism occurs due to the anomalous velocity of charge carriers caused by the electronic band structure in presence of SOC. The extrinsic contribution occurs due to the scattering of charge carriers by impurities has two types of scattering mechanism first one is skew scattering and the second one is the side jump. These different microscopic mechanisms of anomalous Hall effect has been understood in terms of power law relation between anomalous Hall resistivity (ρ^{A}_{xy}) and the longitudinal resistivity (ρ_{xx}).

$$\rho^{A}_{xy} \propto \rho^{\alpha}_{xx} \qquad (1)$$

With α = 2 the dominant contribution will be intrinsic [1] or side jump and for α = 1 the skew scattering [2] will be dominant. For the ferromagnetic metallic sample, the side jump contributions is in the order of 10^{-2} which is usually very small compared to other contributions. Here we have studied the magnetic and electronic transport properties of MnPt(Ir)Sn system. We have observed the enhancement of anomalous Hall effect in higher doped iridium samples. Further, we have separated out the different contribution using the equation [3].

$$\rho^{A}_{xy} = a\,\rho_{xx0} + b\rho^{2}_{xx} \qquad (2)$$

Where the first term is the skew scattering contribution and the second term is intrinsic contribution.

2. RESULT AND DISSCUSSION

Polycrystalline compounds $MnPt_{(1-x)}Ir_xSn$ (x=0, 0.1, 0.2, 0.3, 0.5) were prepared by arc melting technique. The longitudinal resistivity of all the alloys are shown in Fig. 1a. We observe that the magnetization decreases whereas the Hall resistivity increases with increasing iridium concentration shown in Fig. 1b. To identify the dominant mechanism of AHE we have used the scaling relation (equ. 1) form where it is found that the value of the scaling factor α increases with increasing iridium concentration shown in Fig. 1c. This signifies that the intrinsic contribution increases with increasing iridium concentration. Further, we have separated out the different contributions of AHE using (equ 2). Here also, we have observed that with increasing iridium concentration the extrinsic parameter 'a' decreases whereas the intrinsic parameter 'b' increases. The increment of intrinsic contribution with increasing iridium concentration is possibly due to the enhancement of spin orbit coupling with iridium doping.

Fig.1. (a-b) Isothermal magnetization and Hall resistivity at 5 K (c) Variation of Hall Resistivity (red

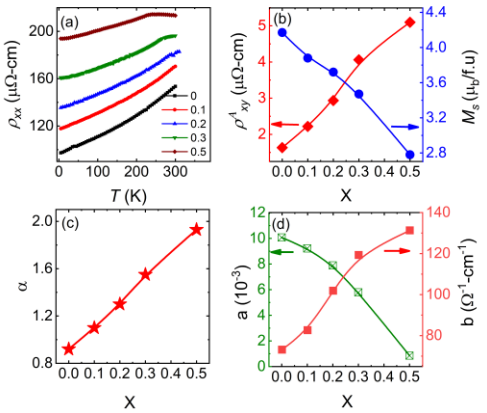

curve) and saturation magnetization with iridium concentration (blue curve) at 5 K. (d) Scaling factor α as a function iridium concentration (X).

REFERENCES

[1]. Q. Wang *et. al.*, Nat. commmun 9, 3681 (2018).
[2]. Yu Liu *et. al.*, Phys. Rev. B 103, 045106 (2021).
[3]. Y. Tian *et. al,* Phys. Rev. Lett. 103, 087206 (2009)

P75

Structural, Multiferroic and Magneto-Impedance Characteristic of $KBiFe_2O_5$

Bushra Khan[1], Manoj K. Singh[1]
[1]*Centre of Material Sciences, University of Allahabad, Prayagraj-211002, India*
Email: bushra@allduniv.ac.in

Abstract: In this work, $KBiFe_2O_5$ (KBFO) is synthesized using a sol-gel technique. XRD pattern confirms the presence of monoclinic crystal structure with space group *P*2/*c*. KBFO shows negative magneto-capacitance (MC%) and positive magneto-impedance (MI%) coupling with the increasing magnetic field. Impedance spectroscopy is performed to analyze the intrinsic and extrinsic effects in MD coupling. The Nyquist plot shows positive magneto-resistance and negative magneto-capacitance which represent strong MD coupling in KBFO. It also reveals that intrinsic effect dominates over the extrinsic effect in the sample.

1. INTRODUCTION

In recent year, a lot of work is being carried out on the development of multiferroic materials, which shows the co-existence of ferroelectric and ferromagnetic ordering in the same phase [1, 2]. This coupling generates a lot of recent properties such as magneto-electric (ME), magneto-dielectric (MD), magneto-optic properties and these properties make the multiferroics materials valuable for different applications such as dynamic random access memory (DRAM). $KBiFe_2O_5$ (KBFO) is an interesting multiferroic compound with brownmillerites structure having band gap ~1.6eV and Curie temperature (T_C) ~780K. The band gap of KBFO has an excellent match with solar spectra and it is distinct from the conventional semi-conductor photocatalyst because the separation of charges takes place in the occurrence of internal electric field [2]. According to B. Mettout et. al. [3], the photovoltaic effect in ferroelectric material is enhanced by electric polarization and ferroelectric domains which separated the photo-generated charge carriers. The magnetic properties facilitate the flow of photo-current due to spin orbit interaction and magnetic domain arrangement. Recently, directional magneto-photovoltaic effect is predicted, which reflect the magneto-electric properties on photo-current, and reveals KBFO could well be a promising material for next-generation photovoltaic and optoelectronic devices [2]. Hence, the present work provides a detailed investigation magneto-dielectric property of brownmillerite structured polycrystalline KBFO by using sol-gel method.

2. RESULT AND DISCUSSION

2.1STRUCTURAL ANALYSIS

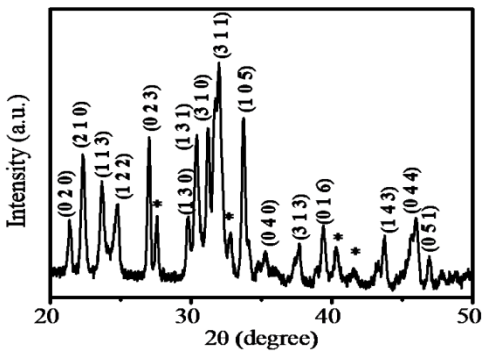

Fig. 1. X-ray diffraction pattern of KBFO sample.

The X-ray diffraction of KBFO powder calcined at 973K is shown in Fig. 1. All diffraction peaks are well-matched with the XRD pattern of KBFO reported for a monoclinic crystal structure under the space group $P2/c$ [1]. The broadening observed in XRD peaks indicates a smaller crystallite size. The crystallite size has been calculated by using Scherrer's formula for the most intense peak (311) [2], which is:

$$L = \frac{k\lambda}{\beta cos\theta}$$

The calculated crystallite size found is 28.93 nm.

2.2.MAGNETO-ELECTRIC ANALYSIS

Magneto-dielectric (MD) measure the strength of MD coupling in which the dielectric parameters are measured with varying magnetic fields described by the given below equation:

$$MC\ (\%) = \frac{(C_H - C_0)}{C_0} \times 100\%\ \ \&\ MI\ (\%) = \frac{(Z_H - Z_0)}{Z_0} \times 100\%$$

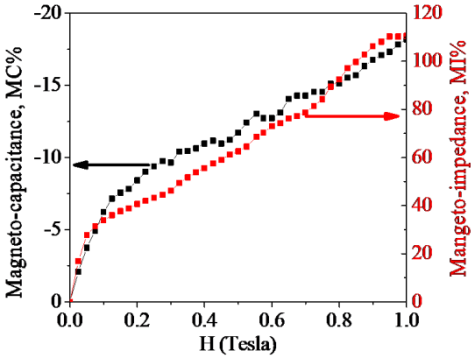

Fig.2. MC% and MI% with varying field of KBFO

Fig. 2 shows negative magneto-capacitance and positive magneto-impedance. The grain resistance and capacitance dominate over grain boundary resistance and capacitance. Hence, it is observed that the MI effect at room temperature is considered as an interface driven effect that is attributed to the interaction between the accumulated charge carriers and magnetic field and also the bulk property (intrinsic effect) dominates over extrinsic effects in the sample [4].

ACKNOWLEDGEMENT

WeacknowledgeFIST Programme (Grant No. SR/FST/PSI-216/2016).

REFERENCES

[1] H. T. Huang, Nat. Photonics 4 (2010) 134-135.
[2] B. Khan et. al. J. Alloy Compd. 893 (2021) 162225.
[3]B. Mettoutet. al. Phys. Rev. B 93 (2016) 195123
[4]Md. F. Abdullah et. al. J. Phys.: Condens. Matter32 (2020) 135701

P76

Structural and optical properties of $Bi_{1-x}Ca_xFeO_3$ nanoparticles synthesized by sol-gel method

Preeti Yadav[1], Manoj K Singh[1]
Centre of Material Science, University of Allahabad, Prayagraj, 211002
Email : preetiawe@allduniv.ac.in

Abstract Bismuth ferrite (BiFeO3) and Ca-doped BiFeO3 nanoparticles has synthesized by sol-gel technique and then annealed at 800ºC for well crystallinity. X-ray diffraction (XRD) analysis demonstrated rhombohedral crystal structure with R3c lattice space group and obtained the crystallite size is calculated by Scherrer's formula. The FTIR spectroscopy confirms the formation of BiFeO3 compound.

1. INTRODUCTION

Multiferroic materials have attracted enormous attention because their extra degrees of freedom in device applications such as new data storage media, random access memory, spintronics, sensors, and photovoltaic devices [1]. But it is really hard to find satisfactory materials, because the single phase magnetoelectric materials are reported so far have too weak coupling at room temperature [2]. Among the known multiferroics, $BiFeO_3$ (BFO) has received much attention, primarily because both the ferroelectric and the antiferromagnetic orders are quite robust at room temperature, and hence it has been reported to hold immense potential applications in multiple state memory elements, actuator and intelligent equipment [3]. In present work, Bisumth Ferrite nanoparticles is synthesized by sol-gel method and Ca-is used as dopant to enhance its properties. The structural analysis is done by using XRD and FTIR spectroscopy used for the chemical information about BFO samples.

2. Result and Discussion

2.1 XRD ANALYSIS

XRD pattern of synthesized $Bi_{1-x}Ca_xFeO_3$ (0%,10%) is given in figure 1

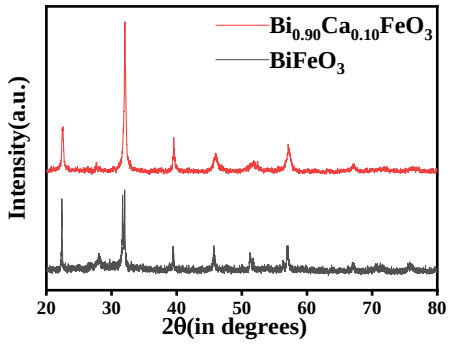

The average particle size of nanoparticles is calculated by Scherrer's formula,

D = □□□□□cos□

□he particle size of BFO sample is found 250 nm and and for 10% Ca doping it is found 192 nm.

2.2 FTIR ANALYSIS

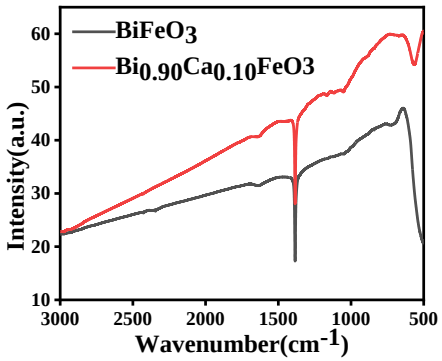

The FTIR spectra of BFO samples are recorded in the wavenumber range of 500-3000 cm^{-1} and shown in fig.2. The absorption peaks at around 1385 is assigned to C-H vibrations, the other band appeared at 1635 cm^{-1} is attributed to the C=O vibrations. The absorption highlights at 562 cm^{-1} is ascribed to the Fe-O stretching and bending vibrations that represent characteristics of the octahedral FeO6 group in the perovskite structure. The formation of a perovskite structure is confirmed by the presence of metal-oxygen bands [4].

ACKNOWLEDMENTS

Preeti Yadav is grateful to the Department of Science & Technology for providing financial support under the DST INSPIRE Programme.

REFERENCES

1. S.Z. Xu, J.R. Qiu, T.Q. Jia, C.B. Li, H.Y. Sun, Z.Z. Xu, Optic Commun. 274 (2007) 163-166.
2. M. Alam, K. Mandal, G.G. Khan RSC Adv. 6 (2016) 62545-62549.
3.P. Chen, X.S. Xu, C. Koenigsmann, A.C. Santulli, S.S. Wong, J.L. Musfeldt, Nano Lett. 10 (2010) 4526-4532.
4. Anju, Ashish Agrawal, Parveen Aghamkar, Bhajan Lal, Magn. Magn. Mater. (2017) 426 800–5.

P77

Structural properties of the hydrothermally synthesized multifunctional CZTS nanoparticles.

Arushi Pandey[1], Manoj K. Singh[1*]

[1]Centre of Material Sciences, University of Allahabad, Prayagraj-211002, India

Email: *arushi.pandey2911@gmail.com*

Abstract: In this work, pure phase CZTS nanoparticles using Cu (II), Zn (II), Sn (II) inorganic metal salts and thiourea as Sulphur source in distilled water solution as precursor is synthesized using green hydrothermal technique. The synthesized sample is characterized by X-Ray diffraction (XRD), which confirms the presence of tetragonal crystal structure with space group *I -4 2 m*. The vibrational stretching of different bonds present in CZTS was further investigated using an FTIR spectrophotometer.

1. INTRODUCTION

Kesterite Cu_2ZnSnS_4 (CZTS) is a multifunctional compound that has attracted attention as a new absorber material for photovoltaics because of its earth-abundant, non-toxic and highly stable nature. In this work, phase pure CZTS nanoparticles using Cu (II), Zn (II), Sn (II) inorganic metal salts and thiourea as Sulphur source in distilled water solution as precursor is synthesized using a low-cost, environment-friendly facile hydrothermal technique. The changes in structural and morphological properties are studied by means of X-ray diffraction (XRD), Fourier transform infrared (FT-IR). The band gap of synthesized sample is calculated to be 1.78eV which indicates that the synthesized material has good applicability in visible range. The synthesized CZTS nanocrystals could be used as absorber layer material in photovoltaic device for various applications.

2. RESULT AND DISCUSSION

2.1 X-RAY DIFFRACTION ANALYSIS

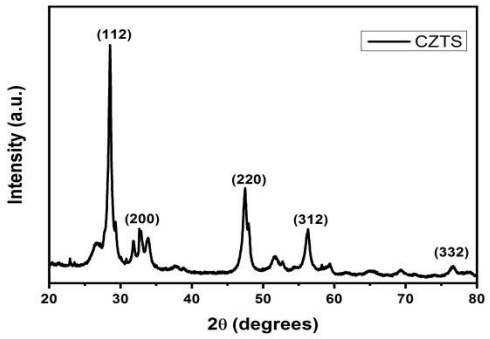

Fig. 1.X-ray diffraction pattern of CZTS sample.

The X-ray diffraction of hydrothermally synthesized CZTS powder is shown in Fig. 1. It exhibits prominent peaks at the positions 2θ = 27.90°, 31.72°, 37.83°, 45.64°, 54.63°, 73.93° assigned to the orientation of (112), (200), (220), (312) and (332) diffraction planes corresponds to the kesterite phase of CZTS respectively. All diffraction peaks are well-matched with the XRD pattern of CZTS reported for a tetragonal crystal structure under the space group I -4 2 m [1].

2.2 FTIR ANALYSIS

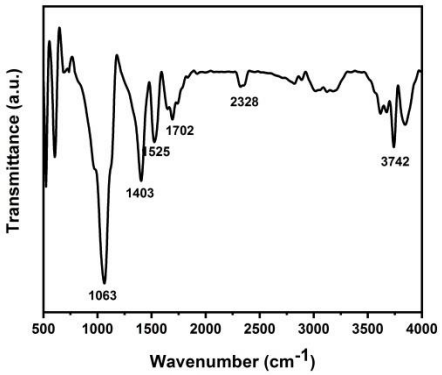

Fig. 2. FTIR spectra of CZTS sample.

FTIR investigation was undertaken and has revealed the presence of various peaks with peak maxima at 1063, 1403, 1525, 1702, 2328 and 3742 cm−1. In addition to the usual signature of water as well as thiourea (3742 cm−1)[2], peaks are observed between 1000 and 1700 cm−1 are attributed to metal–thiourea complexes [3]. In addition, it is evident that there are no additional peaks related to the presence of other compounds, which means that the single-phase CZTS films are obtained[4].

ACKNOWLEDGEMENT

We acknowledge FIST programme (Grant No. SR/FST/PSI-216/2016). Arushi acknowledge the University Grant Commission (UGC) for support through a University Research Fellowship.

REFERENCES

[1] S Das et. al. 2018 IOP Conf. Ser.: Mater. Sci. Eng. 338 012062

[2] M Patel et. al. 2012 J. Phys. D: Appl. Phys. 45 445103 162225.

[3] O Zeberca et. al. 2012 Nanotechnology 23 185402

[4] C D Lokhande et. al. 2011 Invertis journal of renewable energy 3 (1)

P78

Tetramer orbital-ordering induced lattice-chirality in ferrimagnetic, polar $MnTi_2O_4$

A. Rahaman[1,2 *], M. Chakraborty[3], T. Paramanik[1], R. K. Maurya[4], S. Mahana[5], R. Bindu[4], D. Topwal[5], P. Mahadevan[6] and D. Choudhury[1]

[1]Department Of Physics, Indian Institute of Technology Kharagpur, Kharagpur – 721302, India
[2]Department Of Physics, Yogoda Satsanga Palpara Mahavidyalaya, Palpara – 721458, India
[3]Centre of Theoretical studies, Indian Institute of Technology Kharagpur, Kharagpur – 721302, India
[4]School of Basic Sciences, Indian Institute of Mandi – Kamand, Himachal Pradesh – 175005, India
[5]Institute of Physics, Sachivalaya Marg, Bhubaneswar – 751005, India
[6]S.N. Bose National centre for Basic Sciences, Block JD, Salt Lake, Kolkata – 700098, India
Email: aminur.physics@gmail.com

Abstract: Using ab-initio density functional theory calculations and a combination of several experimental techniques, we have elucidated a unique $P4_1$ tetragonal ground state of $MnTi_2O_4$, which hosts a unique combination of tetramer orbital ordering, lattice-chirality and ferroelectricity. We find that a combination of superexchange interactions among Mn and Ti spins and the minimization of cooperative Jahn-Teller effect related strain energy become instrumental for the stabilization of the unique ground state in $MnTi_2O_4$.

1. INTRODUCTION

The transition metal oxides with orbital degrees of freedom constitute one of the most exciting fields of research in condensed matter physics. Exotic physics ensue when such localized electrons also possess orbital degrees of freedom, i.e. electrons can choose to occupy between a set of equivalent and energy-degenerate atomic orbitals and forms a regular pattern in atomic sites named as orbital ordering. Mostly, in these transition metal systems, either a ferro-orbital ordering state (similar occupied orbital at all ionic sites) or an antiferro-orbital ordering state (with alternate ions occupied by similar orbitals), or a combination of the two along different directions is realized. The presence of higher-order orbital ordering has very few examples, such as $CuIr_2S_4$, $MgTi_2O_4$ and Fe_3O_4, and unlike the simpler examples, the forces driving the orbital ordering still remain a puzzle. However, for the first time, not only do we identify an unusual higher order orbital ordering in $MnTi_2O_4$, we also identify the microscopic considerations that drive it.

2. GROUND STATE AND ORBITAL ORDERING

using a combination of first principle calculations and various experimental investigations, we explore a unique ground state for a orbital degenerate Ti^{3+} ($3d^1$) containing spinel, $MnTi_2O_4$ [1]. The system shows an exotic combination of a rare higher order tetramer orbital (associated with Ti^{3+} $3d^1$ electron)-ordering along equivalent <111> directions which involves all three t_{2g} orbitals (as shown in Fig. 1(a)) due to the Mn spins in its ferrimagnetic ground state. combination of Jahn-Teller-effect related strain-energy-optimization (as seen in Fig. 1(b)) and spin-orbital superexchange provides a microscopic understanding for the stabilization of the unique ground state. The tetramer orbital-ordering in $MnTi_2O_4$ induces Ti-Ti bond length modulations, which form helices with alternate short-long bond lengths around the crystallographic c-axis with a particular winding direction to become spatial-chiral (as shown in Fig. 1(c)).

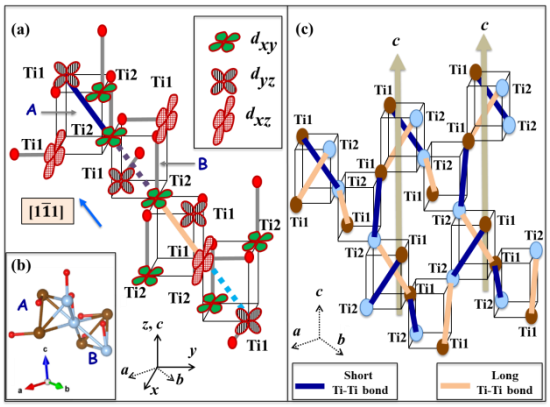

Fig. 1(a) Illustration showing the Ti d-level: d_{yz} -d_{xz} - d_{xy}-d_{xy} tetramer orbital ordering along <111> direction of the crystal unit cell of $MnTi_2O_4$. The obtained Ti d orbital-ordering is accompanied with Ti-Ti bond-length modulations (the solid dark blue, dashed blue, solid light-brown and dashed sky blue colored Ti-Ti bond lengths are 3.010 Å (short), 3.13 Å, 3.14 Å (long), and 3.03 Å, respectively.) (b) The spatial-distribution of the shortest Ti-O bond distances in the corner-shared Ti tetrahedral network of $MnTi_2O_4$. (c) Short and long Ti-Ti bonds, when joined, form helices around the crystallographic c-axis of $MnTi_2O_4$.

3. SUMMARY

In summary, we elucidate a unique higher-order tetramer orbital-ordering and the driving mechanism of such ordering in a titanate spinel $MnTi_2O_4$.

ACKNOWLEDGEMENT

Authors would like to acknowledge Swastika Chatterjee, Poonam Kumari, Partha Pratim Jana, Arghya Taraphder, and Dibyendu Dey for support and various fruitful discussions.

REFERENCES

[1]. A. Rahaman et al, Phys. Rev. B **100** (2019) 115162.

P79

Structural and magnetic properties of aluminium doped Y-type barium hexaferrites

Mukesh Suthar*; P. K. Roy
Department of Ceramic Engineering, IIT (BHU), Varanasi – 221005, (U.P.), India
mukeshs.rs.cer16@itbhu.ac.in

Abstract:

A series of aluminium doped Y-type barium hexaferrite having chemical composition of $Ba_2Co_2Fe_{12-x}Al_xO_{22}$ (x = 0.0, 0.1, 0.2, 0.3, 0.4, and 0.5) samples were synthesized using sol-gel auto combustion method. The prepared samples were calcined at 1200◦C for 2 hrs in a muffle furnace to obtain homogenized aluminium-doped barium hexaferrite powder. The prepared hexagonal ferrite powder samples were analyzed using X-ray diffraction (XRD) and SQUID-vibrating sample magnetometer (MPMS) techniques in order to study the effect of aluminium substitution on structural and thermomagnetic properties between the temperature range of 2K to 350K. The XRD analysis confirmed the formation of single phase of Y-Type barium hexaferrite within all synthesized samples. The prepared powders showed to be multi-domain in nature.

Keywords: Y-*type Barium hexaferrite, sol-gel auto combustion, Thermomagnetic properties*

Reference:

- G.Mukhtar *et al.* , Investigation of crystal structure, dielectric response and magnetic properties of Tb^{3+}substituted Co_2 Y-type barium hexaferrites, Solid State Sciences Volume 113, March 2021, 106549

- Rukhanov Alex, Panina Larisa, Trukhanov Sergei, TurchenkoVitalii, Salem Mohamed. Evolution of structure and physical properties in Al-substituted Ba-hexaferrites. *Chinese Physics B* , 2016, 25(1): 016102

P80

Quasi-one-dimensional magnetism in the spin-1/2 antiferromagnet $BaNa_2Cu(VO_4)_2$.

Sebin J. Sebastian[1], K. Somesh[1], M. Nandi[2], N. Ahmed[1], M. Baenitz[3], B. Koo[3], J. Sichelschmidt[3], A. A. Tsirlin[4*], Y. Furukawa[2], R. Nath[1+]

[1] *School of Physics, Indian Institute of Science Education and Research Thiruvananthapuram-695551, India*

[2] *Ames Laboratory and Department of Physics and Astronomy, Iowa State University, Ames, Iowa 50011, USA*

[3] *Max Planck Institute for Chemical Physics of Solids, Nöthnitzer Strasse 40, 01187 Dresden, Germany*

[4] *Experimental Physics VI, Center for Electronic Correlations and Magnetism, University of Augsburg, 86135 Augsburg, Germany*

We report synthesis and magnetic properties of quasi-one-dimensional spin-1/2 Heisenberg antiferromagnetic chain compound $BaNa_2Cu(VO_4)_2$. This orthovanadate has a centrosymmetric crystal structure, *C2/c*, where the magnetic Cu^{2+} ions form spin chains. These chains are arranged in layers, with the chain direction changing by 62^o between the two successive layers. Alternatively, the spin lattice can be viewed as anisotropic triangular layers upon taking the inter-chain interactions into consideration. Despite this potential structural complexity, temperature-dependent magnetic susceptibility, heat capacity, ESR intensity, and NMR shift agree well with the uniform spin-1/2 Heisenberg chain model with an intrachain coupling of $J/k_B \approx 5.6$ K. The saturation field obtained from the magnetic isotherm measurement consistently reproduces the value of J/k_B. Further, the ^{51}V NMR spin- lattice relaxation rate mimics the 1D character in the intermediate temperature range, whereas magnetic long-range order sets in below $T_N \approx 0.25$ K. The effective interchain coupling is estimated to be $J_\perp / k_B \approx 0.1$ K. The theoretical estimation of exchange couplings using band-structure calculations reciprocate our experimental findings and unambiguously establish the 1D character of the compound. Finally, the spin lattice of $BaNa_2Cu(VO_4)_2$ is compared with the chemically similar but not isostructural compound $BaAg_2Cu(VO_4)_2$ [2].

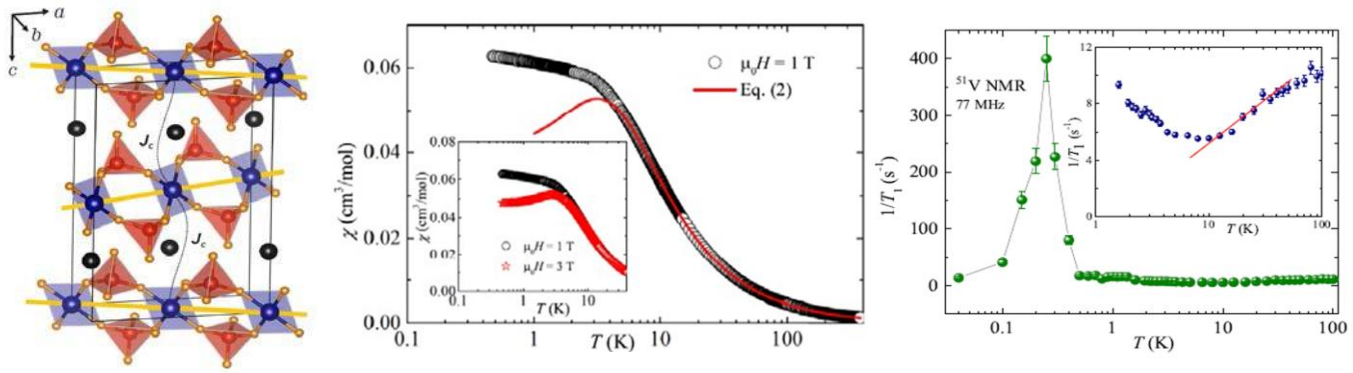

Left panel: Crystal structure of $BaNa_2Cu(VO_4)_2$ shown in a different orientation to visualize the spin chains. Middle panel: χ of polycrystalline $BaNa_2Cu(VO_4)_2$ sample as a function of temperature in an applied fields. Right panel: $1/T_1$ as a function of temperature measured on the ^{51}V nuclei down to 0.044 K.

[1] Sebin J. Sebastian, K. Somesh, M. Nandi, N. Ahmed, P. Bag, M. Baenitz, B. Koo, J. Sichelschmidt, A. A. Tsirlin, Y. Furukawa, and R. Nath, Phys. Rev. **B** 103, 064413 (2021).

[2] A. A. Tsirlin, A. Möller, B. Lorenz, Y. Skourski, and H. Rosner Phys. Rev. **B** 85, 014401 (2012).

*altsirlin@gmail.com, +rnath@iisertvm.ac.in

P81

Enhanced static and spin dynamic magnetic properties of annealed $CoFe_2O_4$ nanoparticles

Prashant Kumar[1,2,*], Saurabh Pathak[1,2,3], Arjun Singh[2,4], H. Khanduri[1],G.A.Basheed[1,2], R.P.Pant[1,2,]

[1]*CSIR-National Physical Laboratory, New Delhi, India-110012*
[2]*Academy of Scientific and Innovative Research, CSIR-NPL Campus, New Delhi, India*
[3]*School of Engineering, RMIT University, Australia*
[4]*Department of physics, Indian Institution of Technology, Jammu-181221*
**Corresponding Authors-prashantkhichi92@gmail.com*

Abstract: Cobalt ferrite nanoparticles with single domain nature have potential applications in the development of the high-density memory devices, EMI shielding and biomedicine. The effects of post process annealing (300 - 900ºC) on structural, magnetic and spin dynamic magnetic properties of the cobalt ferrite nanoparticles synthesized by wet chemical co-precipitation method, has been investigated and reported in present study.

1. INTRODUCTION

Cobalt ferrite is one of the most versatile magnetic materials with broad applications in biomedical, magnetic recording and EMI shielding because of high chemical & physical stability, high Curie temperature, large magnetocrystalline anisotropy, moderate magnetization and high coercivity [1-3]. To achieve higher figure of merit in these applications, properties of MNPs needs to be optimized for relevant application. The orientation of magnetic spins plays a very important role in the magnetization reversal phenomenon in storage devices. The magnetocrystalline anisotropy should be very high for the magnetic films (it does not affected by external parameters like temperature). The $CoFe_2O_4$ NPs have very large magnetocrystalline anisotropy of the order of (with anisotropy constant (K) = 2.2-3.8 X 10^6 erg/cc). In the past decade, there has been widespread interest in the fabrication of magnetic nanocomposites, because they exhibit high flexibility, non-brittle and bio-compatibility in nature [1,2].

2. EXPERMINETAL

$CoFe_2O_4$ ferrite MNPs were synthesized by wet chemical co-precipitation method. The0.25 M iron chloride and 0.18 M of cobalt chloride solutions were prepared in DI water and heated to 80ºC under constant stirring for 90 minute and pH was maintained to 10-12 using 8M ammonium hydroxide (28%) solution. The precipitated particles were centrifuged at 8000 rpm followed by several washings with ethanol and DI water, to obtain a uniform and narrow size distribution of particles. Finally, the black powder of $CoFe_2O_4$ were grinded to fine powder and annealed at four different temperatures: 300ºC, 500ºC, 700ºC, 900ºC, in argon (Ar) gas atmosphere for 3 hours with slow heating rate of 5ºC/minute

3. Result and Discussion

3.1 XRD-The X-ray diffraction (XRD) patterns of the powder samples of MNPs have been performed with multipurpose X-ray diffractometer (Rigaku Ultima-IV). The diffraction pattern was recorded at a tube voltage and current of 40kV and 30mA, respectively, using Cu-Kα (λ = 1.54056Å). The average crystalline size was estimated by Debye-Scherrer equation and Williamson-Hall method.[2]

3.2 HRTEM-The shape and size distribution of the annealed MNPs weredetermined by HRTEM. In all the samples, the particles were found to be spherical in shapewith uniform size distribution.

3.3 VSM- The room temperature static magnetic measurements of all the samples were carried out with a magnetic field up to 20kOe. The magnetic hysteresis curves confirmed the ferromagnetic behaviour in all the annealed $CoFe_2O_4$ MNPs samples.[1]

3.4 FMR-The spin dynamics of the MNPs have also been studied by performing ferromagnetic resonance (FMR) measurement. The resonance field increased with the increase in annealing temperature, which could be due to the change in super-exchange interaction between metallic ions through oxygen ion.[3]

4.Figure & Images-

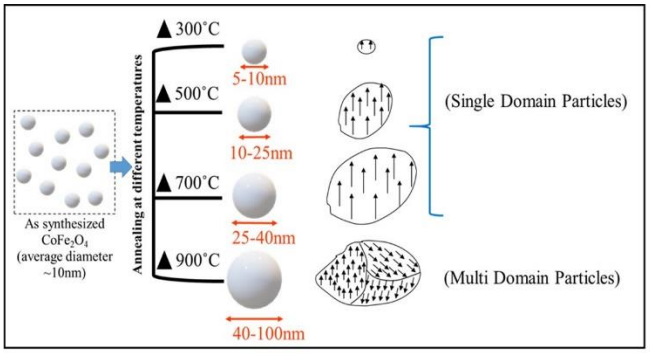

Fig.1.Annealing effects on domain structure of MNPs.

ACKNOWLEDGEMENT—
Authors are thankful to Director CSIR-NPL for his encouragement to carry out this work. One of the author Prashant Kumar is grateful to University Grant Commission (UGC), India for Senior Research Fellowship (SRF), Ref No-(19/06/2016(i) EU-V) to carry out this research.

REFERENCES

[1]. K. Usadel Phys. Rev. B. 73 (2006).
[2].E. De Biasi, E. Lima, C.A. Ramos, A. Butera, R.D. Zysler, J. Magn. Magn. Mater. 326 (2013) 138–146.
[3]. A. Sukhov, K.D. Usadel, U. Nowak, J. Magn. Magn. Mater. 320 (2008) 31–35.

P82

A correlation between the structural and magnetic properties of $Sr_{2-x}La_xCoNbO_6$

Ajay Kumar[1], B. Schwarz[2], H. Ehrenberg[2], and Rajendra S. Dhaka[1,*]

[1] Department of Physics, Indian Institute of Technology Delhi, Hauz Khas, New Delhi, 110016, India
[2]Karlsruhe Institute of Technology (KIT), 76344, Eggenstein-Leopoldshafen, Germany

Email: rsdhaka@physics.iitd.ac.in

Abstract: The magnetic properties of the $Sr_{2-x}La_xCoNbO_6$ has been studied, where substitution of the non-magnetic Sr^{2+} at La^{3+} site transform Co^{3+} into Co^{2+} and result in the evolution of AFM interactions in the samples for $x \geq 0.6$. A strong correlation between the valence state of Co, degree of B-site ordering, change in the density of the states near the Fermi level, and evolution of AFM ordering has been established in the samples. The specific heat measurements evident the presence of free-ion-like discrete energy states in the samples.

The understanding of crystal field strength and hence the resulting energy levels/ bands in the complex oxides is the most challenging problem in the condensed matter physics. A weaker crystal field give rise to the free-ion-like discrete energy states and the resulting effect can be successfully reproduced using the crystal field theory, whereas a strong crystal field lead to the orbital hybridization and can be suitably explained using the molecular orbital theory. For example, perovskite oxide (ABO_3; A: rare earth/alkali earth metals, B: transition metals) $LaCoO_3$ is the most studied member in this family due to its somewhat peculiar spin-state transitions around 80-100 K from the insulating and non-magnetic low-spin (LS: $t_{2g}^6e_g^0$) sate to the insulating magnetic state, and further into bad metallic magnetic state around 400-600 K due to a delicate competition between the Hund's exchange energy and crystal field strength. Further, a 50% substitution of the Co by another element results in the double perovskite oxides ($A_2BB'O_6$), which gives an extra degree of freedom to manipulate the chemical pressure exerted on the Co ions by the substitution of different cations at A and/or B-site(s) and flexibility to systematically investigate the evolution of the resulting valence and spin-states of Co ions in the octahedral coordination [1,2]. However, presence of another magnetic cation at B-site makes it difficult to study the complex spin-states of Co ions from the magnetizations like macroscopic measurements.

In order to understand this, we synthesize and investigate the $Sr_{2-x}La_xCoNbO_6$ (x=0-1) series of samples, where substitution of non-magnetic La^{3+} at Sr^{2+} site is expected to completely transform the Co^{3+} (in x=0) in to Co^{2+} (in x=1) across the series. Rietveld refinement of the X-ray diffraction (XRD) data shows the transformation from the tetragonal to monoclinic phase for $x \geq 0.6$. Temperature dependent magnetization measurements indicate the conversion from the weak ferromagnetic (FM) to the antiferromagnetic (AFM) ordering for $x \geq 0.6$ due to evolution of the Co-O-Nb-O-Co exchange path resulting from the increased B-site ordering with the La substitution [3]. Here, it is important to understand that the strength of the crystal field can be manipulated by the formal charge on the B-site transition metal cations. For example, in the present case, the crystal field is expected to be stronger for x=0 (Sr_2CoNbO_6) sample as compared to x=1 ($LaSrCoNbO_6$) sample due to an additional unit charge on the Co ions in the former and hence much stronger Co3d—O2p hybridization. Thus, Co is more likely to preserve the HS state in the x=1 sample as compared to the x=0 sample. Further, the effective magnetic moment extracted from the temperature dependent magnetization measurements show its significantly higher value (5.62 μ_B/f.u.) than the spin only moment for x=1 sample (S=3/2; 3.87 μ_B/Co^{2+}), which indicate the persistence of the triply degenerate (orbital) free ion like $^4T_1$ ground state and hence significant contribution of the orbital magnetic moment [3].

We observe the low temperature Schottky anomaly in the specific heat curves in case of the $x \leq 0.4$ samples due to the transition between the low lying energy levels of Co^{3+}, resulting from the spin-orbit coupling and octahedral distortion [4]. Strong crystal field split the 5-fold degenerate (orbital) 3*d* levels into 3-fold degenerate ground t_{2g} levels with effective orbital moment (L_{eff})=1, and 2-fold degenerate excited e_g levels. Further, spin-orbit coupling split the t_{2g} levels into low lying state with J=1, and first and second excited states with J=2 and 3, respectively. Presence of this low lying spin-orbit triplet has been observed in the several experimental as well as theoretical studies on $LaCoO_3$. Further, octahedral distortion split this ground state triplet into a singlet and a doublet, whose relative position depends on the type of the distortion, i.e., compression or elongation. In the present case, we observe the 3-level Schottky anomaly in the low temperature specific heat, with ground and first excited singlet and second excited doublet. This, indicate the presence of the LS state close to this spin-orbit triplet of the HS state in these compounds. Further, applied magnetic field lift the degeneracy of the excited doublet and the field dependent separation of which gives Landé g-factor =3.2 (2) and 2.7(1) for x=0.2 and 0.4 samples, respectively [4]. This, further indicate the presence of the HS state above the LS state and discard the possibility of the IS state of Co^{3+} as expected from the magnetization measurements. Moreover, the ac-susceptibility and thermoremanent magnetization (TRM) measurements for the $x \leq 0.4$ samples show the low temperature cluster-glass-like behavior resulting from the B-site disorders, where inter-cluster interactions and spin-spin interaction strength decreases with the La substitution [4].

REFERENCES

[1]. S. Vasala and M. Karppinen, Prog. in solid st. Chem **43** (2015) 1.
[2]. C. Frontera and J. Fontcuberta, *Phys. Rev. B* **69** (2004) 014406.
[3]. A. Kumar and R. S. Dhaka, *Phys. Rev. B* **101** (2020) 094434.
[4]. A. Kumar et al., *Phys. Rev. B* **102** (2020) 184414.

P83

Synthesis, Crystal Structure and Magnetic Properties of a new series of Cobalt-Iron Bimetallic Hybrid-Framework

Malaya K. Sahoo [a b], J. N. Behera [a, b*]
a National Institute of Science Education and Research, Khurda-752050, Odisha, India
b Homi Bhabha National Institute, Mumbai-400094, Maharashtra, India
Email: malaya.sahoo@niser.ac.in

Abstract: A series of Cobalt-Iron bimetallic Hybrid-Framework has been synthesized by one-step hydrothermal synthetic method. The Single-Crystal X-ray studies reveal the formula of the as-synthesized MOFs has chemical formula **$[Co_xFe_{1-x}(C_4H_4N_2)(SO_4)_{0.5}F]$**. The magnetic properties studies predict that the Co-MOF exhibits antiferromagnetic interaction with T_N = 30 K, Fe-MOF exhibits ferrimagnetic interaction with T_C = 20 K; However, by integrating 25% of Fe into the Co-MOF shifts the antiferromagnetic coupling between the paramagnetic centers into ferrimagnetic coupling with a higher T_C value of 58 K.

1. INTRODUCTION

The self-assembly of metal ions and inorganic/organic linkers leads to the formation of multidimensional Frameworks. There are a lot of reports that have been published in recent years because of the versatile application of such materials in the field of catalysis, Gas-sorption, Magnetism, sensors, etc.[1] Among the others, transitional metal and halide/pyrazine-based Metal-Organic Framework are the most studied because of the potential of magnetic coupling through super-exchange interaction and the redox-active nature of the pyrazine ligand. However, pyrazine-based MOFs are limited to one and two-dimensionality[2].

Herein, by taking pyrazine, sulfate, and fluorine as linkers we have synthesized a series of cobalt-iron bimetallic hybrid-framework having a general formula **$[Co_xFe_{1-x}(C_4H_4N_2)(SO_4)_{0.5}F]$** and studied their magnetic properties. The Co-MOF has nano-Rods like morphology, Fe-MOF has nano-plate-like morphology and Co0.75fe0.25-MOF has nano-strip Like morphology. Besides this, we have presented the magnetic properties of these MOFs.

2. RESULT AND DISCUSSION

2.1. Crystal Structure

All the MOFs has identical crystal structure thus we have only presented for The Co-MOF. The Co octahedral are bridged together via bridging pyrazine linkers along the crystallographic a-direction. Similarly, these are further linked via bridging fluorides along the b-direction resulting in grid-like layers. Further, these layers are joined together via sulfate tetrahedral to construct a network of 3D-Framework.

2.2. Magnetic Properties

The temperature-dependent susceptibility measurements predict an antiferromagnetic coupling for the Co-MOF with T_N of 30 K. it also exhibits a giant magnetic hysteresis at 2 K Since Co MOFs are known for exhibiting long-range antiferromagnetic super-exchange interaction[3]. Unlike Co-MOF the Fe-MOF exhibits ferrimagnetic coupling with TC of 20 K. The integration of Fe into the Co-MOF initiates lattice defects. In addition, there is an extra electron because Co d^7 and Fe d^5 Have the chance to induce double-exchange interaction leading to ferrimagnetic coupling with a higher T_C Value of 58 K.

3. FIGURES AND IMAGES

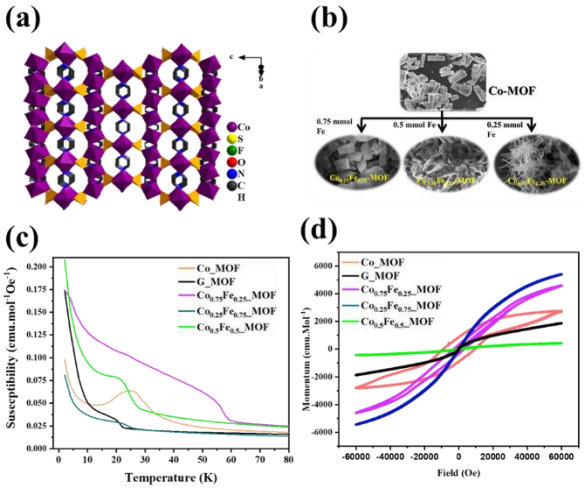

Fig.1. (a) three-dimensional Co-MOF, (b) FESEM morphology, (c) temperature-dependent susceptibility at 100 Oe, (d) isothermal magnetization at 2 K.

ACKNOWLEDGEMENT

We thank the Center for Interdisciplinary Science (CIS), NISER for providing FESEM. We greatly acknowledge Dr. Subhankar Bedant for providing access to the PPMS3-SQUID magnetometer.

REFERENCES

1 D. Maspoch, D. Ruiz-Molina and J. Veciana, *Chem. Soc. Rev.*, 2007, **36**, 770–818.

2 M. Kurmoo, *Chem. Soc. Rev.*, 2009, **38**, 1353–1379.

3 E. A. de Campos, N. J. O. Silva, F.-N. Shi and J. Rocha, *CrystEngComm*, 2014, **16**, 10439–10444.

P84

Comparative Study of magnetic Properties of Ni doped Nd Orthoferrites

Mohmad Asif Khan[1,2], Abida[1]

1. Government Degree College for Women Anantnag J&K
2. J S University U.P

maksphysics141093@gmail.com.

Abstract:

The general representation of perovskite oxides is by the ABO_3 where (A belongs to the class of rare earth and B is transition metal ion), their charming properties, have developed a keen interest in the field of research and technology. Metal ion forms the basis for the naming culture of such kind of compounds at B site e.g. Cobalites, Manganites, Orthoferrites, Ortho chromites etc. Transition metal oxides execute Ortho rhombic structure and because of the difference in the outer electronic shell structure gives rise to the magnetic behavior in such type of ions. Because of the multiferroic behavior, more and more interest is developed in this field as compared to the other materials. Forestier and Guillian in 1950 were the first who discovered the rare earth orthoferrites ($ReFeO_3$). [1-6]. In this study we have calculated the behavior of sample in Zero field cooled and Field Cooled at the temperature of 50, 500 and 1000K,up to 500 K the sample shows antiferromagnetic behavior up to transition temperature. However at 1000 K the samples show ferromagnetic transition to paramagnetic which is backed by the spin glass behavior. We have also calculated the M vs H and find out the values of corecivity, remnant field and the saturation values.

References:

1. C.N.R. Rao, V.G. Bhide, and N.F. Mott. Philos Mag;32, (1975). p.1277.
2. C.N.R. Rao, and O.M. Parkash. Philos. Mag.;35, (1977). p. 1111.
3. A. Casalot, P. Dougieret, and P. Hagenmuller. J PhysChem Solids;32, (1971). p.407.
4. D.S. Rajoria, V.G. Bhide, G.R. Rama, and C.N.R. Rao. J. Chem. Soc., Faraday Trans; 70, (1973). p. 512.
5. G. Thornton, F.C. Morrison, S. Partington, B.C. Tofield, and D.E. Williams. J Phys C: Solid State Phys.; 21, (1988). P. 2871.
6. Y. Tokura, Y. Okimoto, S. Yamaguchi, H. Taniguchi, T. Kimura, and H. Takagi Phys. Rev B;58, (1998). p. 1699.

P85

Anomalous Hall effect from gapped nodal line in the Co_2FeGe Heusler compound

Gaurav K. Shukla[1], Jyotirmoy Sau[2], Nisha Shahi[1], Anupam K. Singh[1], Manoranjan Kumar[2] and Sanjay Singh[1]

[1]School of Materials Science and Technology, Indian Institute of Technology (Banaras Hindu University), Varanasi 221005, India

[2]S. N. Bose National Centre for Basic Sciences, Kolkata 700098, West Bengal, India

Email: ssingh.mst@iitbhu.ac.in

Abstract: Full Heusler compounds with cobalt as a primary element show anomalous transport properties owing to the Weyl fermions and broken time-reversal symmetry. We present here the study of anomalous Hall effect (AHE) in the Co_2FeGe Heusler compound. The experiment reveals anomalous Hall conductivity (AHC) ~ 100 S/cm at room temperature with an intrinsic contribution of ~ 78 S/cm. The analysis of anomalous Hall resistivity suggests the scattering independent intrinsic mechanism dominates the overall behavior of anomalous Hall resistivity. The first principles calculation reveals that the Berry curvature originated by a gapped nodal line near E_F is the main source of AHE in the Co_2FeGe Heusler compound.

1. INTRODUCTION

The additional contribution in the Hall resistivity in the ferromagnetic materials known as anomalous Hall effect (AHE) [1]. The AHE originates due to interplay between the magnetism and spin-orbit coupling.
Weyl semimetals host fascinating transport properties due to their non-trivial topological band structure [2]. The Weyl nodes are possible in systems with broken time-reversal symmetry or inversion symmetry. The Weyl nodes creates large Berry curvature; a fictitious magnetic field in momentum space and creates large anomalous Hall effect [3]. The crossing of two bands along closed curve form nodal line and in the presence of spin orbit coupling nodal lines gap out. The gapped nodal lines also act as source of Berry curvature and creates large anomalous Hall effect [4].

2. METHODS

The polycrystalline sample of Co_2FeGe was prepared by arc melting using high pure elements. Cryogen free measurement system (CFMS) was used for transport measurement. Density functional theory using VASP package was employed for first principles calculation.

3. RESULTS AND DISCUSSION

Sample crystallizes in cubic Fm-3m space group with lattice parameter 5.74 Å. The magnetic moment was found 5.38 μ_B/f.u. The longitudinal resistivity indicates the metallic behavior of sample. The scaling of anomalous Hall resistivity suggests the intrinsic origin of anomalous Hall. The anomalous Hall conductivity (AHC) was found ~ 100 S/cm with intrinsic AHC ~ 78 S/cm. The Berry curvature calculation gives intrinsic AHC ~ 77.29 S/cm due to gapped nodal line, which is in well agreement with experiment.

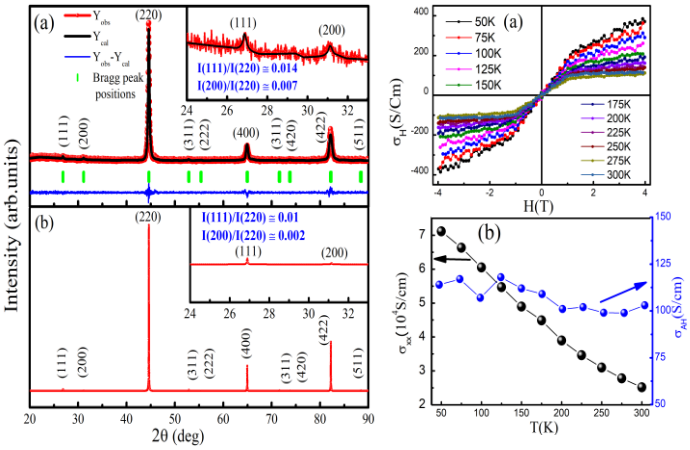

Figure. Left: (a) Rietveld refinement of X-ray diffraction pattern. (b) Simulated XRD pattern. Right: The Hall conductivity isotherms as function of magnetic field. (b) Temperature dependent longitudinal and anomalous Hall conductivity.

*This work is published in Phys. Rev. B **104**, 195108 (2021).

References:

[1]. N. Nagaosa et al, Rev. Mod. Phys. 82, 1539 (2010)

[2]. N. Nagosa et al, Nat. Rev. Mater. **5**, 621 (2020)

[3]. K. Manna et al, Nat. Rev. Mater. **3**, 244 (2018).

[4]. P. Li et al, Nat. Commun. **11**, 3476 (2020).

P86

Experimental and Theoretical Insights into the Magnetic Exchange, Geometry and Electronic Structure Affecting the Slow-Magnetic Relaxation Behaviours of 3d, 4f and 3d-4f Based Molecular Magnets

Naushad Ahmed[a,b,c] Maheswaran Shanmugam[a]*, Vadapalli Chandrasekhar [b]* and Ganesan Prabusankar [c]*

[a] Department of Chemistry, Indian Institute of Technology Bombay (India 400076), [b] Tata Institute of Fundamental Research Hyderabad (India 500046), [c] Department of Chemistry, Indian Institute of Technology Hyderabad (India 502285, current address)

Email. naushad.chem@gmail.com, cy21pdf15@iith.ac.in (NA), eswar@chem.iitb.ac.in (MS), vc@tifrh.res.in (VC), prabu@chy.iith.ac.in (GP)

Abstract: The slow magnetic relaxation behaviour is a signature of a typical single-molecule magnet (SMM) that shows the magnetic bi-stability below magnetic blocking temperature (blocking temperature T_B defined as the maximum temperature at which magnetization maintained for 100 s).[1] SMMs are proposed for various technological applications in high-dense storage devices, spintronics, quantum computing, etc.[2] The thermal energy barrier to the reversal of magnetization (U_{eff}) and the magnetic blocking temperature (T_B) are used to compare the effectiveness of SMMs.[1, 3] Under-barrier magnetic relaxation processes such as Raman, direct, and quantum tunnelling (QTM) are a few drawbacks that suppress the thermal energy barrier.[4] Here we present a few 3d, 4f, and 3d-4f based molecular magnets, which are synthesized, experimentally characterized, and investigated using state-of-the-art computational studies. We will discuss the various factors such as magnetic exchange, geometry, electronic structure, etc., governing the slow-magnetic relaxations behaviour and hence thermal energy barrier for these complexes. In the line of magnetic exchange interaction, we have recently investigated the origin of 3d-4f magnetic exchange interaction (ferro/antiferro) using the precise HF-EPR experimental technique and theoretically established the mechanism and correlation of extent of magnetic exchange coupling $J_{3d\text{-}4f}$ and occupancy of lanthanide 4f orbitals.

Acknowledgment

NA thanks Prof. Maheswaran Shanmugam (Ph.D. supervisor), IITB., Prof. V. Chandrasekhar (former postdoctoral supervisor 2019-2021), TIFRH., and Prof. Ganesan Prabusankar (current supervisor, NPDF-2021) IITH.

References

[1] *D. Gatteschi, et al.,* Molecular Nanomagnets, *Oxford University Press, Oxford,* 2006.

[2] a) M. Mannini *et al., Nature* **2010,** *468*, 417; b) *R. Vincent et al., Nature **2012**, 488, 357;* c) *L. Bogani et al., Nature Materials* **2008,** *7* (3), 179-186.

[3] a) Ishikawa *et al., J. Am. Chem. Soc*. **2003**, *125*, 8694; b) C.A.P. Goodwin *et al., Nature* **2017**, *548*, 439.

[4] a) N.F. Chilton *et al., Nat. Commun.* **2018,** 3134; b) D. Aravena *et al., Inorg. Chem. Front.*, **2020**, 7, 2478.